Institute of Electronic Systems
Aalborg University

Tuneable DVB-H Antenna in a Small Handheld Device

Master Thesis

MOB 10th Semester, June 2006
Group 06gr1113

Institute of Electronic Systems
Aalborg University

Title:

Tuneable DVB-H Antenna in a Small Handheld Device

Project period:

January, 2006 - June, 2006

Project group:

Mobile Communications
06gr1113

Group members:

Mauro Pelosi

Supervisor:

Gert Frølund Pedersen

Number of reports printed: 7
Number of pages in prologue:19
Number of pages in report:118
Number of pages in appendix:48
Total number of pages:185

ABSTRACT

Digital Video Broadcasting for Handheld devices (DVB-H) is a feature that will be introduced to the consumers during 2006. With DVB-H it will be possible to watch TV with a mobile phone. However, since the typical size of a mobile phone is small compared to the wavelength of the transmitted DVB-H signals (470 MHz to 702 MHz), the internal antenna design is a very challenging topic.

In this Master Thesis we focused our attention on tuneable antennas, which simulation and evaluation was possible thanks to a new lumped components tool, that we added to the FDTD simulation package developed by the Center for Person Kommunikation (CPK), Aalborg University, Denmark.

The lumped components tool has been validated with a comparasion with the commercial software CST Microwave Studio.

Simple antenna tendencies were derived during the simulation part, allowing us to address to the most promising solutions.

We proposed two different tuneable antenna configurations: the meandered pifa and the meandered monopole respectively with a small part related to switchable antennas.

We conlcluded that is it possible to obtain acceptable performances at the expense of increasing complexity in the antenna design trying at the same time to keep the antenna volume as small as possible.

Preface

This report has been written as a project for the 10th semester final Master Thesis within the specialization in Mobile Communication in the Department of Communication Technology at Aalborg University by the group 1113, during the period January, 2006 - June, 2006.
The literature references are marked by numbers in square brackets, for example [4.7] and the equations are marked in brackets, for example (2.8). Numerations are made by chapters but all the literature references are listed at the beginning of the report.
In a similar way, regarding tables and figures, expressions like (4.11) are used.
We want to thank our supervisor Gert Frølund Perdersen for his maieutic guidance through the project and for the time he spent with us. We also would like to thank all the people in Siemens-BenQ and in the Antenna and Propagation Department at Aalborg University who helped us during this project.
This report about "Tuneable DVB-H antenna in a small handheld device" can be found on our web page at:

http://kom.aau.dk/group/06gr1113/report.pdf

Author

Mauro Pelosi

Table of Contents

List of Figures

List of Tables

List of Abbreviations

ATSC	Advanced Television System Committee
AVC/H264	Advanced Video Coding/H264
CIF	Common Intermediate Format
DVB	Digital Video Broadcasting
DVB-C	Digital Video Broadcasting-Cable
DVB-S	Digital Video Broadcasting-Satellite
ELG	European Launching Group
FBW	Fractional Bandwith
FDTD	Finite Difference Time Domain
GSM	Global System for Mobile communications
GSM-900	Global System for Mobile communications 900MHZ
IFA	Inverted F Antenna
IP	Internet Protocol
ISDB-T	Integrated Services Digital Broadcasting-Terrestrial
MOM	Method OF Moments
MPE-FEC	Multi Protocol Encapsulation-Forward Error Correction
MPEG-2	Moving Picture Experts Group-2
MUX	Multiplexer
OFDM	Orthogonal frequency Division Multiplexing
PAL	Phase-Alternating Line
PDA	Personal Digital Assistant
PEC	Perfect Electric Conductor
PIFA	Planar Inveted F Antenna
QCIF	Quarter Common Intermediate Format
RF	Radio Frequency
SC-MSA	Short Circuit-Microstrip Antenna
SFN	Single Frequency Network
SNR	Signal to Noise Ratio
TM-H	Technical Module-Handheld group
TPS	Transmission Parameter Signaling
TV	Television
UHF	Ultra High Frequency
US	United States
VSWR	Voltage Standing Wave Ratio

List of Symbols

G	Reflection coefficent
Δd	unit cell size
Δf	bandwidth
Δu	generic space increment
Δx	x-directed space increment
Δy	y-directed space increment
Δz	z-directed space increment
ε	electric permittivity
λ	wavelength
λ_0	wavelength at resonance
μ	magnetic permeability
ζ_1	generic point of a Taylor expansion
ζ_2	generic point of a Taylor expansion
$O\left[(\Delta t)^2\right]$	higher order spatial remainder term of a Taylor expansion
$O\left[(\Delta x)^2\right]$	higher order temporal remainder term of a Taylor expansion
ρ'	equivalent magnetic resistivity
σ	electric conductivity
ω	$2\pi f$
2k	2048 OFDM carriers
4k	4096 OFDM carriers
8k	8192 OFDM carriers
B	susceptance
$\vec{B}$	magnetic flux density
c	speed of light in vacuum
C	capacity
$\vec{D}$	electric flux density
$d\vec{l}$	unit path length vector of the curve C
$d\vec{S}$	normal vector of surface S
$\vec{E}$	electric field
emh	electrical meander height
eml	electrical meander length
esurf	electrical surface
etwl	electrical total wire length
f	frequency
feed1	x-oriented offset of the feed
feed2	y-oriented offset of the feed
frperr	resonance frequency percentage error
frsim	resonance frequency obtained by simulation
frth	theoretical resonance frequency
f_r	resonance frequency when 0<W/L1<1
f_{r1}	resonance frequency when W = L1
f_{r2}	resonance frequency when W = 0
H	short circuit plate height of the pifa

$\vec{H}$	magnetic field
hb	height of the metal chassis box
hb1	height of the upper box element
hg	height of the ground plane
hgr	height of the meander over the ground plane
hme	height of the meander over the chassis
ho	height of the meander horizontal section
hpm	height of the meandered plate
hsc	height of the short circuit plate
hv	height of the meander vertical section.
i	integer spatial index related to the x direction
I_{eff}	root mean square current value
I_L	total element current
Im(Zin):	imaginary part of the antenna input impedance
index	dummy index to describe the elements of the lumped components arrays
j	integer spatial index related to the y direction
$\vec{J_e}$	electric conduction current density
$\vec{J_m}$	magnetic conduction current density
k	integer spatial index related to the z direction
$\tilde{k}$	wave number
K	ratio between L1 and L2
l	closed curve bounding the surface S
L	inductance
L_{refl}	reflection loss
L_{retn}	return loss
lambda	wavelength
lb	length of the metal chassis box
lboff	offset of the meander along lb
lb1	length of the upper box element
lg	length of the ground plane
los	length of meander horizontal section
lvs	length of meander vertical section
lum	binary variable to enable or disable the lumped components
lumax	max number of lumped components used in the simulation
lumdir(index)	orientation of the cell corresponding to the $(index)^{th}$ lumped component
lumimped(index)	define the value of the impedance of the $(index)^{th}$ lumped component
lumtype(index)	type of the $(index)^{th}$ lumped component
lumx(index)	x location of the cell corresponding to the $(index)^{th}$ lumped component
lumy(index)	y location of the cell corresponding to the $(index)^{th}$ lumped component
lumz(index)	z location of the cell corresponding to the $(index)^{th}$ lumped component
lum1	x-oriented offset of the lumped element
lum2	y-oriented offset of the lumped element
L1	not short circuit length of the pifa
L1off	x-oriented offset of the pifa
L1pm	length of the meandered section

L2	short circuit length of the pifa
L2off	y-oriented offset of the pifa
L2pm	width of the meandered section
n	integer temporal index
nfb	number of near field boundaries cells
nos	number of meander horizontal sections
nvs	number of meander vertical sections
off1	y-oriented feed offset
off2	x-oriented feed offset
Q	antenna quality factor
Q_{meas}	measured Q
Q_{ohmic}	ohmic losses Q
Q_{rad}	radiation Q
R_L	load resistance
Re(Zin)	real part of the antenna input impedance
S	arbitrary three-dimensional surface
t_n	fixed time instant of a Taylor expansion
TM	Transverse Magnetic
twl	total wire length
u	generic function
u_i^n	quantity evaluated at $x_i = i\Delta x$ in space and at $t_n = n\Delta t$ in time
V	electric potential
$v_{\max}$	maximum velocity of propagation
vol	antenna volume
W	short circuit plate width of the pifa
W_e	electric energy
W_m	magnetic energy
wb	width of the metal chassis box
wboff	offset of the meander along wb
wsc	width of the short circuit plate
x_i	starting point of a Taylor expansion
X	reactance
X_L	load reactance
Z_L	load impedance
Z_0	characteristic impedance
Zin	antenna input impedance

List of References

[1.1]Walter Fischer: "*Digital Television: A Practical Guide for Engineers*" Rohde & Schwarz, Springer 2004.

[1.2]DVB – History of the DVB Project http://www.dvb.org/.

[1.3]Almgren, Hanna and Vestin, Johanna – "*Scalable Services Distributed over DAB and DVB-T from a Receiver Point of View*", Mar 2002.

[1.4]G. Faria, J. A. Henriksson, E. Stare, and P. Talmola, "*DVB-H: Digital Broadcast Services to Handheld Devices*" Proc. IEEE, vol. 94, no. 1, pp. 194-209, Jan. 2006.

[1.5]Michael Kornfeld and Ulrich Reimers: "DVB-*H:The Emerging Standard for Mobile Data Communication* "Institute for Communications Technology, Technische Universität Braunschweig.

[1.6]ETSI EN 302 304 V1.1.1 (2004-11) "*Digital Video Broadcasting (DVB); Transmission System for HandHeld Terminals (DVB-H)*".

[1.7]TR 102 377 V1.2.1 "*Implementation Guidelines*".

[1.8]TR 102 401 V1.1.1 "*Validation Task Force Report*".

[2.1]K. Fujimoto, A. Henderson, K. Hirasawa and J. R. James, "*Small Antennas*", Research Studies Press, 1987.

[2.2]L.J. Chu, "*Physical Limitations on Omni-Directional Antennas*" *J. Appl. Phys.*, vol. 19, Dec. 1948, pp.1163-1175.

[2.3]R.F. Harrington, "*Effect of Antenna Size on Gain, Bandwidth, and Efficiency*" *J. Res. Nat. Bur. Stand.*, vol64-D, Jan/Feb 1960, pp. 1-12.

[2.4]R.C. Hansen, "*Fundamental Limitations in Antennas*" *Proc. IEEE*, vol. 69, Feb. 1981, pp. 170-182.

[2.5]Constantine A. Balanis *"Antenna theory analysis and design"* John Wiley & Sons, Inc., 1997.

[2.6]G. GouBau, "*Multi-element Monopole Antennas*" Proc. Workshop on Electrically Small Antennas ECOM, Ft. Monmouth, N. J., pp. 63-67, May 1976.

[2.7]R.Vaughan and J. B. Andersen "*Channels, propagation and antennas for mobile communications*" IEE London 2003.

[3.1]T. Taga, K. Tsunekawa, and A. Sasaki, "*Antennas for Detachable Mobile Radio Units*" Review of the ECL, NTT, Japan, Vol.35, No. 1, January 1987, pp. 59-65.

[3.2]R. W. P. King, C. W. Harrison, Jr., and D. H. Denton, Jr., "*Transmission-Line Missile Antennas*," IRE Trans. Antennas and propagation, Vol. 8, No. 1, January 1960, pp. 88-90.

[3.3]G. Dubost, "*Short- or Opened-Circuited Dipole Parallel to Perfect Reflector Plane and Embedded in Substrate and Acting at Resonance*" Electron. Lett., Vol. 17, No. 24, November 1981, pp 914-916.

[3.4]G. Sanford and L. Klein, "*Increasing the Beamwidth of a Microstrip Radiating Element*," IEEE AP-S Int. Symp. Digest, Seattle, June 1979, pp. 126-129.

[3.5]K. Hirisawa and M. Haneishi, "*Analysis, Design, and Measurement of small and Low-Profile Antennas"*, Artech House, Boston: 1992.

[3.6]H. Mishima and T. Taga, "*Mobile antennas and duplexer for 800 MHz Band Mobile Telephone System*," IEEE AP-S Int. Symp. Digest, Quebec, June 1980, pp. 508-511.

[3.7]Y. Yokoyama and N. Gotoh, "*Dual-Resonance Broadband Microstrip Antenna*" Proc. Int. Symp. Antennas and Propagation, Kyoto, Japan, Agoust 1985, pp 429-432.

[3.8]J.Rasinger, A. L. Scholtz, W. Picher, and E. Bonek, "*A new enhanced-Bandwidth Interval Antenna for Portable Communication Systems*" Proc. 40th IEEE Vehicular Technology Conf., Orlando, FL, May 1990, pp. 7-12.

[4.1]A. Taflove "*Computational electrodynamics: the finite-difference time-domain method*" Artech House 1995 first edition.

[4.2]A. Taflove, S. C. Hagness: "*Computational electrodynamics: the finite-difference time-domain method*" Artech House 2000 second edition.

[4.3]K. S. Kunz, R. J. Luebbers: "*The finite difference time domain method for electromagnetics*" CRC Press 1993.

[4.4]Sui, W., D. A. Christensen, and C H. Durney, "*Extending the Two-Dimensional FDTD Method to Hybrid Electromagnetic Systems with Active and Passive Lumped Elements*" IEEE Trans. Microwave Theory and Techniques, vol 40, 1992, pp. 724-730.

[4.5]Piket-May, M. J., A. Taflove, and J. Baron, "*FD-TD modelling of digital signal propagation in 3-D circuits with passive and active loads*"IEEE Trans. Microwave Theory and Techniques. Vol 42, 1994, pp1514-1523.

[4.6]Yee, K. S., "*Numerical solution of initial boundary value problems involving Maxwell's equations in isotropic media*", IEEE Trans. Antennas and propagation, vol14, 1966, pp.302-307.

[5.1]Meier, A.S., and Summers, W.P.: "*Measured impedance of vertical antennas and effects of finite ground planes*", Proc. IEEE, 1969, 37, pp.609–616.

[5.2]M.-C. Huynh and W. Stutzman, "*Ground plane effects on planar inverted-F antenna (PIFA) performance* ",IEEE Proc.-Microw. Antennas Propag., Vol. 150, No. 4, August 2003.

[5.3]Kathleen L. Virga, Yahya Rahmat-Samii, "*Low-Profile Enhanced-Bandwidth PIFA Antennas for Wireless Communications Packaging*" IEEE Transactions on microwave theory and techniques, Vol. 45, No. 10, Octber 1997.

[A.1]A. Taflove "*Computational electrodynamics: the finite-difference time-domain method*" Artech House 1995 first edition.

[B.1]Constantine A. Balanis, *"Antenna theory analysis and design"* John Wiley & Sons, Inc., 1997.

[B.2]R. E. Collin, "*Antennas and Radiowave Propagation*", McGraw-Hill Book Inc., 1985.

[B.3]R. E. Collin, "*Foundations for microwave engineering*" IEEE Press Wiley 2001.

[B.4]D. M. Pozar, "*Microwave Engineering*" Wiley 1998.

Introduction

Nowadays we are fast going towards the development of a universal telecommunication device, that would allow us to reach a real taste of ubiquity.
As we can see in our common life, the separation between devices thought for different purposes is getting more and more veiled.
The mobile phone development paved the way for this dream, and now it incorporates a lot of different services; on the same apparatus we can find a trial-band phone, an mp3 player, a radio, a digital camera, a gaming station and so on. The television will be the next obliged step.
In fact the market of television broadcasting is demanding more and more visibility, and new formulas have to be thought in order to reach a wide and heterogenous audience.
Why we have to limit our tv experience to an environment mainly confined to our houses?
We have now the technology to bring with us the most common and user-friendly form of entertainment.
This has been possible after the birth of the digital video broadcasting standard (DVB) that changed the television transmission from analogue to digital.
Digital Video Broadcasting–Handheld (DVB–H) is a standard that allows the delivering of live broadcast television to handheld terminals.
DVB-H was built on the DVB-T standard, and it was modified in order to be easily integrated in handheld devices.
Being this a brand new technology, it needs more study first to be delivered to the big public. In fact, because of the small size of handheld devices and the relatively large wavelength involved, the antenna design is a very challenging topic.
In this Master Thesis we decided to focus our attention on DVB-H antenna design, in order to propose solutions for small handheld devices.
Because of the relatively large impedance bandwidth involved, we had to study tuneable and switchable antennas.
In this Report we will use mainly the FDTD simulation package developed at Alborg University, that we modified in order to include in our investigations the modelling of lumped components.
We needed this new features to simulate tuneable antennas, that include elements like lumped capacitors and resistors.
The behavior of the simulated lumped components was validated comparing the obtained results with the commercial simulation package CST Microwave Studio.

Project delimitations

Because of the market request, we decided to study internal antennas.
We will consider DVB-H with GSM-900 interoperability, which means a frequency range between 470MHz and 702MHz.
Our antennas are thought to fit inside a handheld device which approximate reference dimensions are 120 mm x 80 mm x 20 mm (length x width x height).
This reference dimensions were derived by existing DVB-H concept phones, that because of the relatively large screen size, are still a hybrid between conventional mobile phones and PDAs.
Our performance metric will be mainly the mismatch efficiency, because of the fact we didn't include losses in the analysis.
We defined the impedance bandwidth that frequency range in which the absolute value of the reflection coefficient S11 is smaller than 0.7 in natural value or -3 in dB.
This threshold will be our reference, because it is very difficult to provide such a large impedance bandwidth with a small internal antenna.
We studied two different antenna topologies, the PIFA antenna and the meandered monopole antenna.
Simulating tuneable antennas, we didn't include in the analysis the biasing networks, because of the limited time at our disposal.

Report structure

- In Chapter 1 we introduce the DVB standard and its features.
- In Chapter 2 we provide information about small antenna theory.
- In Chapter 3 we study PIFA antennas.
- In Chapter 4 we introduce the FDTD technique.
- In Chapter 5 we proceed with the simulation part.
- In Appendix A we provide the FDTD lumped components documentation.
- In Appendix B we discuss impedance matching theory.
- In Appendix C we provide the modified Fotran77 code for the lumped components modelling in the FDTD Algorithm developed at Aalborg University.

Chapter 1: Digital Video Broadcasting.

1.1: Introduction.

We know that the conventional analogue TV system has been practically unchanged for decades, with the only one exemption of the color television launch [1.1].
A digitalization of the TV signal brings not only additional interactive features, but also implies a better video resolution respect to the conventional PAL System.
Though in the beginning of the 90th's it was thought that the digital television broadcasting would result impractical to implement, a leading group named European Launching Group (ELG), started to think about the unification of European standards proposals towards a common one. When in 1993 ELG changed to Digital Video Broadcasting (DVB), examples of experimental Digital Video Broadcasting-Cable (DVB-C) and Digital Video Broadcasting-Satellite (DVB-S) were yet a tangible reality.
The success was so big that DVB-standards turned to a worldwide digital television benchmark [1.2].
However it has to be remarked that DVB is not the only one existing standard in the world concerning digital broadcast, but as an example we can remind the Japanese Integrated Services Digital Broadcasting-Terrestrial (ISDB-T) and the US Advanced Television System Committee (ATSC) [1.3].

1.2: DVB-T.

DVB-T is the Digital Video Broadcasting operating mode adopted specifically for terrestrial signal transmission. This standard was definitely adopted in the end of 1995.
An usual way to compress DVB-T transmission is the use of the MPEG-2 coding, even if the standard provides an alternative choice like AVC/H264 [1.2].
DVB-T works dividing the original signal into a specific number of orthogonal subcarriers using OFDM.
In order to fulfill the requirements of the UHF frequency band, 6, 7 or 8 MHz wide spectra can be assigned to a single channel [1.1].
Depending on regional specific needs, for example some parameters such as the number of subcarriers, modulation scheme and error correction level can be properly adjusted.
If we consider the implications of the OFDM carrier number variation on the Doppler effect resistance [1.8], with the 2k and 8k modes we can handle different situations, in such a way to increase the tolerance of the system to signal echoes with variable guard intervals.
This attitude of the system towards the toleration of signal echoes, makes it possible the use of the so called spectrum efficient single frequency network (SFN), a network made up by several stations that transmit in broadcasting the same signal at the same time [1.1].
Though all the features of the DVB-T well fit a broad set of mobile configurations, such the reception in a car or in indoor environment, regarding the needs of a handheld device such as little power consumption, it reveals its intrinsic limits, fairly overlapped by its natural extension: the DVB-H.

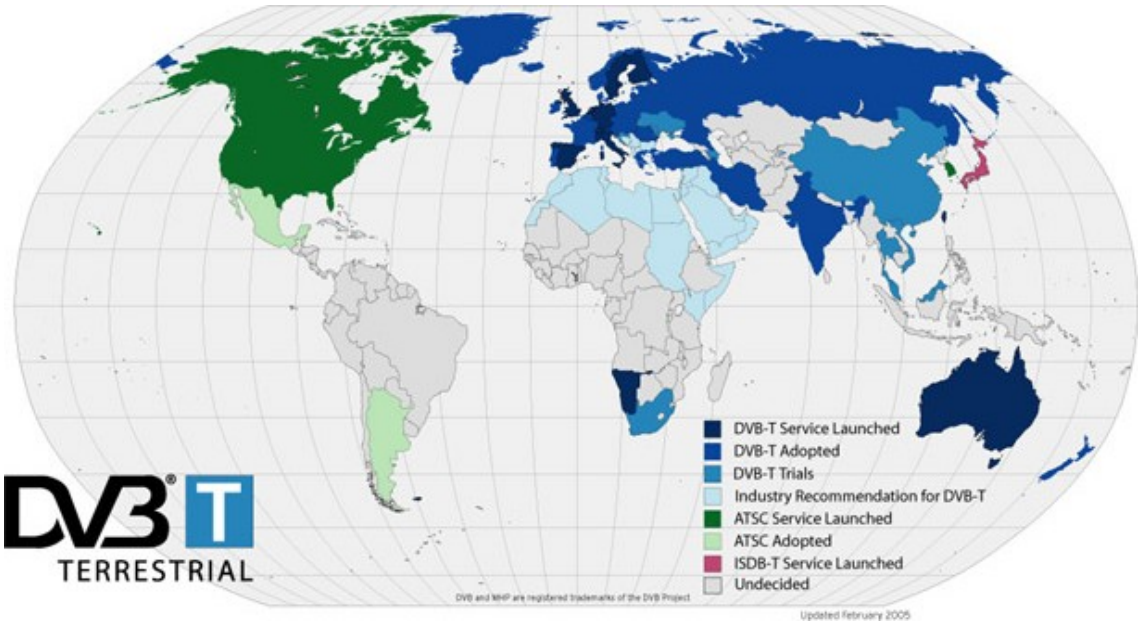

Figure 1.1: Digital tv standards in the world [1.2].

1.3: DVB-H.

DVB-H is the most recent standard defined by the Digital Video Broadcasting consortium [1.4].
This system deals with the distribution of multimediale services to mobile terminals in multicast and broadcast operating mode.
The DVB-H system has been developed by TM-H ad hoc group and it is not an alternative standard like DVB-S, DVB-C and DVB-T, but it was thought as a normal evolution of the DVB-T system, sharing with it the frequency range, adding new features to permit more robustness in mobile reception, and allowing a more efficient battery consuming together with a higher synergy with the internet world.

1.4: DVB-H Terminals.

The DVB-H system has been designed to work in different configurations of use:
mobile reception with fixed or low-speed receiver (“pedestrian”), mobile reception with external antennas, indoor reception in moving vehicles.
The use of conventional handheld terminals demands for limited size screens.
Even if the standard doesn’t prescribe it as mandatory, probably the video format will be the CIF (Common Intermediate Format), with a resolution of 352x288 pixel, that corresponds to ¼ of traditional tv, or the QCIF (Quarter CIF), with a resolution that corresponds to 1/16 of traditional tv [1.5].

The used frequency range will be a challenging problem for the manufacturers, being very hard to build a small integrated broadband antenna that has to operate in the UHF band.

Figure 1.2: Siemens DVB-H concept phone [1.2].

1.5: DVB-H add-ons

The add-ons of the DVB-H respect to the DVB-T are [1.5,1.6]:

- Time slicing: to increase the battery's life.
- IP DataCast: to increase flexibility in data transmission (audio video and file).
- MPE-FEC (Multi Protocol Encapsulation-Forward Error correction): to increase the robustness.
- 4k mode: to increase the system flexibility in network planning and management.
- Extended interleaver (2k and 4k modes): to achieve more interference immunity.
- TPS-bit: to send physical level signalling that identifies a DVB-H stream.

1.6: Time Slicing.

The main unsolved problem of all handheld devices has always been the battery life.
Because the DVB-T original data stream is broadband and with a high data rate, it is very hard to receive and decode it completely with a battery powered terminal.
Originally the power consumption of a DVB-T receiver was about 1 Watt, but though today it could be decreased, the desired target of 100 mW is still unreachable [1.7].
The main advantage in the DVB-H solution is that the receiver only has to receive and process a fraction of the complete data stream corresponding to the selected service.
To fulfill these requirements, the data stream has to be well organized.
In DVB-H we have a pure time division service multiplexing, in fact there is no continuous transmission of data, because this happens with periodical bursts.
The receiver is synchronized with only that service you want to receive, so that in the remainder of the time, the receiver can be shut down easily.
This way of dividing the signal is named time slicing [1.7].

Because of the need of a continuous video playing, the data stream has to be buffered, so that in each burst has to be indicated information about the turning off of the receiver.
A burst duration is about several hundred milliseconds, so the power saving is very efficient.
There is a synchronization issue, in fact the receiver has to be turned on slightly before it is time to receive.
Depending on the ratio of on-time / power-save-time, it is possible a resulting power saving of more than 90 % [1.5].

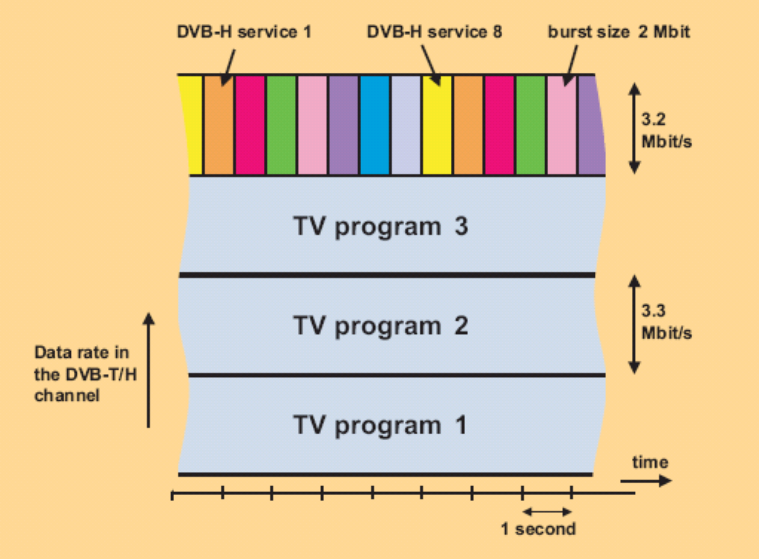

Figure 1.3: Time slicing technique [1.5].

1.7: Ip Datacast.

DVB-H is the first broadcast protocol with a full utilization of IP for data transportation.
This feature allows a fair synergy between different mobile technologies and internet world.
The IP Datacast on DVB-H is defined as a broadcast system end-to-end suitable for the distribution of digital metadata and services using IP-oriented features, optimized for limited resources (battery, computational power) [1.7].

1.8: MPE-FEC.

The MPE-FEC is an IP-level error correction code, that is added to those adopted in the DVB-T standard to ease the reception when the SNR at the receiver is low [1.7].
It has to be remarked that this is a possible option, in fact the data can be received also without the MPE-FEC implementation, because data packets are separated from redundancy ones with the forward error correction.

When we deal with a high packet loss, we can introduce redundancy packets thanks to an efficient algorithm of interleaving and protection based on the Reed Solomon parity code. With a wise choice of padding and puncturing in the MPE-FEC table, the level of protection can vary according to the channel condition.
The MPE-FEC processing is placed on the link layer to form with the MPE and the time slicing the DVB-H codec.

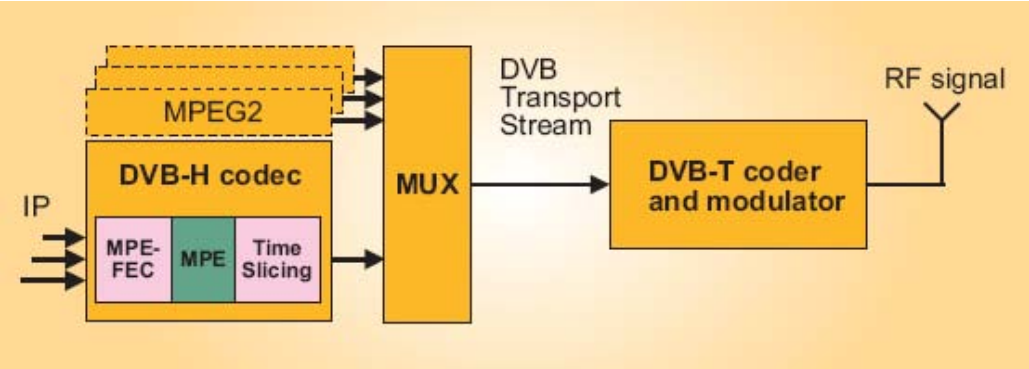

Figure 1.4: Schematic of DVB-H codec and transmitter [1.5]

1.9: 4k mode.

DVB-T and DVB-H both use a multicarrier modulation OFDM, but while DVB-T only includes 2k and 8k operating modes, DVB-H adds the 4k one, meaning that 4096 carriers are used for the signal transportation.
This modality allows a higher network planning flexibility, because a trade-off between network resources and mobile reception is needed.
In the DVB-T system the 2k modality has fair performances in mobile reception thanks to a good Doppler effect resilience.
With the 8k modality we have the best performances respect to spectral efficiency.
For all these reasons, the 4k modality allows a good trade-off between spectral efficiency and user mobility [1.5].

1.10: Extended interleaver.

To make possible the use of the 4k mode, a new interleaver was designed.
In fact the receiver must support all modalities, so a 8k symbol interleaver is needed.
This new symbol interleaver is able to process alternatively a single 8k OFDM symbol, two 4k OFDM symbols or four 2k OFDM symbols [1.7].
The adoption of this special interleaver allows the dispersion of impulsive noise power over more symbols.

1.11: TPS-bit.

TPS carriers (Transmission Parameter Signalling) are specified in the DVB-T standard and they carry information about the modulation scheme used in the transmission.
The transmission of TPS bits takes advantage of a very robust modulation scheme, in order to be received and demodulated also with a very low SNR [1.7].

1.12: DVB-H antenna specifications.

There are few antenna requirements for a DVB-H antenna mentioned in the standard.
However those requirements are strict and difficult to achieve with an internal antenna.
The specified frequency range in the DVB-H standard is between 470 and 862 MHz, but because of GSM-900 interoperability, the upper frequency is limited to channel 49 (corresponding to 702 MHz) [1.7].

So we have two different cases:

- DVB-H without GSM-900.
- DVB-H with GSM-900.

DVB-H without GSM-900

- Frequency range from 470 to 862 MHz.
- Bandwidth of 392 MHz.
- Central frequency equal to 666 MHz.
- Relative Bandwidth of 58.8%.
- Central frequency wavelength equal to 0.52 m.

DVB-H with GSM-900

- Frequency range from 470 to 702 MHz.
- Bandwidth of 232 MHz.
- Central frequency equal to 586 MHz.
- Relative Bandwidth of 39.5%.
- Central frequency wavelength equal to 0.45 m.

The specified antenna power gain is of -10 dBi at the lowest UHF-band frequencies, increasing to -5 dBi at the end of the UHF band [1.7].
All the others nominal antenna gain between these frequency bounds can be obtained by linear interpolation.

Frequency [MHz]	Gain [dBi]
474 [channel 21]	-10
698 [channel 49]	-7
858 [channel 69]	-5

Table 1.1: DVB-H power gain specifications [1.7].

Because of this kind of portable reception antenna, we don't expect any polarization discrimination, so that the antenna radiation pattern is omni-directional in the horizontal plane.
The volume of the antenna has to be as low as possible, in order to fit inside a receiver which approximate reference dimensions are:
120 mm x 80 mm x 20 mm (length x width x height) [1.2];
The previous dimensions are not mandatory, but they respect the actual requirements of the market, being adopted as a reference by several constructors [1.2].
The impedance matching technique is not specified in the DVB-H standard.

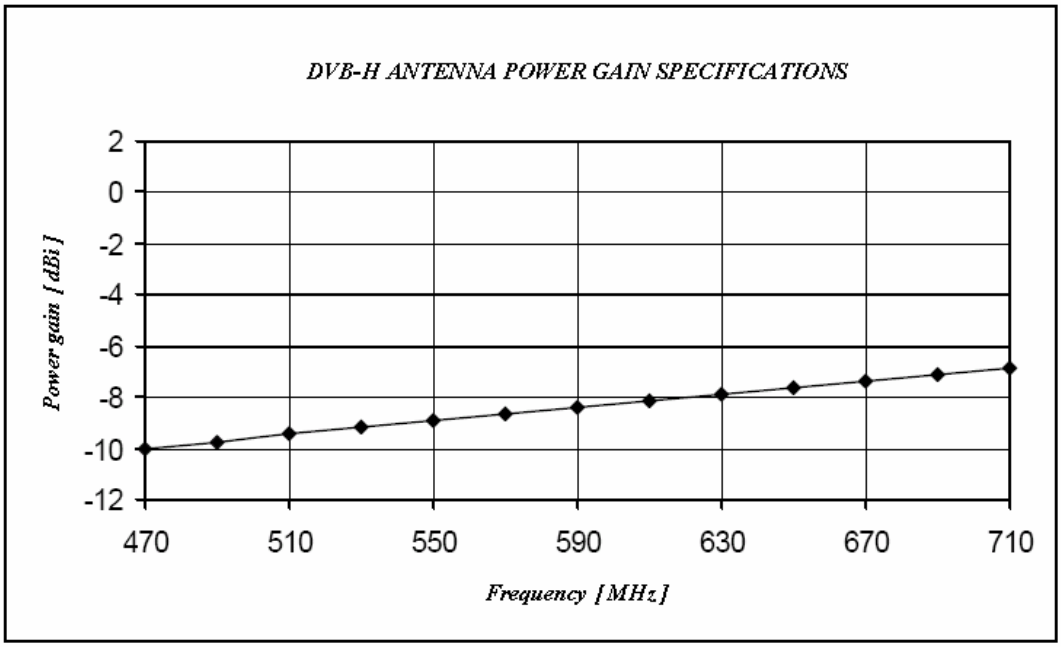

Figure 1.5: DVB-H antenna power gain specifications.

Chapter 2: Small antennas theory.

2.1: Small antennas

Antennas are today very common objects, and they will be more and more useful in our everyday life.
Because of the high success in electronic devices miniaturization, there is a large demand of small embedded antennas, one of the last space-consuming and bulky hardware components.
Some of the first examples of reduced height antennas can be traced back to the low frequency broadcast antennas [2.1], that because of the corresponding large wavelengths involved, needed the erection of expensive and massive transmitting towers.
This situation brought the introduction of L-shaped antennas and the utilization of capacitive top loading, in order to dramatically reduce the antenna size.
The second world war itself contributed to find the earliest wise antenna solution, because of the need of constrained antennas size, for both ease of transportation and enemy visibility.
There were several reasons for the increasing demand of small antennas, such as for example low aerodynamic profiles, reduction in the radar signature and so on.
Present day, it is a very rare situation to see external antennas over a handheld radio unit such as mobile phones.
Though if it would be technically possible to build a good external antenna, with a huge complexity reduction for the antenna designer point of view, the market demands for invisible solutions, that are more roboust and seem to make happy the final users.
This gives also more freedom to the equipment designers, that can fully use their artistic skills to catch the client attention.
We have to remark that not only aesthetic considerations leads to an internal antenna choice, because this continuous optimization gives us the opportunity to find more efficient solutions.
There are different ways to differentiate the characteristics of the general term “small antennas” [2.1]:

- An electrically small antenna can be physically bounded by aλ/2p radius sphere.
- A physically constrained antenna is not necessarily small electrically, but its shape configuration contributes to a considerable size reduction in given directions.
- Functionally small antennas summarize the previous two definitions with additional performance requirements without space consuming solutions.

2.2: Quality factor and its derivation.

The quality factor Q is a very useful parameter to describe, for example, the impedance bandwidth of one antenna in a rigorous manner, in order to compare easily the performances of various kind of antennas.
A classical definition of the Q of a general electric circuit is:

$$Q = 2\pi \cdot \frac{Energy\ stored}{Energy\ dissipated\ \ per\ \sec.} \tag{2.1}$$

When we deal with lossless antennas, the previously defined Q is named Q_u, which means Q unloaded.
The antenna can store two kinds of energy, respectively electric (W_e) and magnetic (W_m) energy, and these quantities can be obtained through an integration over the antenna volume, bounded by a proper surface that encloses the whole structure [2.7]:

$$W_e = \int \varepsilon |E|^2 dv \quad and \quad W_m = \int \mu |H|^2 dv \tag{2.2}$$

being E the peak electric field and H the peak magnetic field.
We know that W_e and W_m are related with the reactance in the following way [2.7]:

$$X = \frac{2(W_e + W_m)}{|I_{eff}|^2} \tag{2.3}$$

where I_{eff} is the root mean square current value in a current defined electric circuit.
If we take the derivative of the reactance, Foster's theorem says us that if we are in the case of a lossless network, the slope of the reactance is always positive:

$$\frac{\partial X}{\partial \omega} = \frac{2(W_m + W_e)}{I_{eff}} \tag{2.4}$$

Of course the slope of the reactance can also be negative if losses are included.
We can easily derive the following expression for the Q:

$$Q = \frac{\omega}{2R} \cdot \frac{\partial X}{\partial \omega}\Big|_{\omega=\omega_0} \tag{2.5}$$

where R is the resistance belonging to the real part of the input impedance of the antenna and ω_0 the resonance frequency.
This is a very useful relation, that allows us to derive directly the Q having at our disposal only the input impedance of the antenna.

However, when we have to measure the Q of one particular antenna, the value that we get accounts also for the ohmic and radiated losses [2.7]:

$$\frac{1}{Q_{meas}} = \frac{1}{Q_{rad}} + \frac{1}{Q_{ohmic}} \tag{2.6}$$

A large impedance bandwidth can also hide high losses in the antenna, that corresponds in a waste of radiated power.

2.3: Fundamental limits derivation of electrically small antennas.

In this Master Thesis we will concentrate on electrically small antennas, because of the relatively large wavelength involved respect to the dimensions of a handheld terminal mainly suitable for the DVB-H signal reception.
We can derive limits for an electrically small antenna by assuming that an apparatus consisting of antenna, transmission lines and transceiver devices could be bounded within a sphere of radius r, being 2r the largest linear dimension of the antenna structure.
Inside that sphere we can identify an arbitrary source or current distribution, so that we can express its radiated field with a complete set of orthogonal spherical modes, going this field towards the exterior of the sphere.
This method was introduced first by Chu [2.2], later studied by Harrington [2.3] and others.
Since we can determinate an infinite number of different sources within the sphere, Chu confined his studies to the most suitable source distribution, minimizing the amount of energy that was stored inside the sphere, in order to obtain a resistive input impedance at a given frequency.
The ideal orthogonality of the spherical modes outside the sphere makes possible to see the total energy flowing outside the sphere as the superposition of that energy corresponding to each single mode, without energy or power coupling between two distinct modes inside the sphere.
With the previous considerations, we can replace the space outside the sphere with independent equivalent circuits corresponding to each spherical mode.
While only the propagating modes contribute to the radiated power, the reactive power is dependent on all the modes.
We can conclude that when the sphere becomes smaller and smaller, the propagating modes fast disappear.
Being all the remaining modes evanescent, the quality factor Q becomes very large.
If we consider an antenna with radiation efficiency = 100%, we can see the total equivalent circuit of the antenna as a ladder L-C network, with a shunt resistive load in the end to represent the normalized antenna radiation resistance.

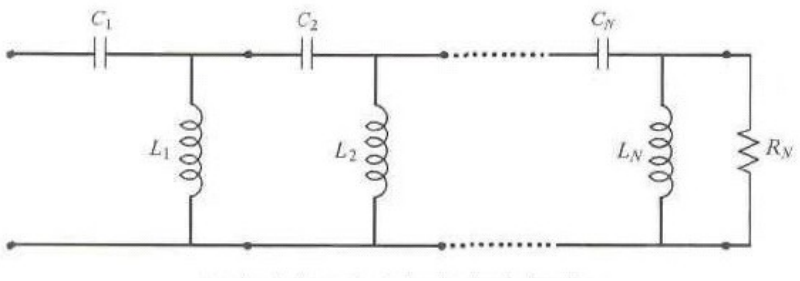

Figure 2.1: Equivalent circuit for N spherical modes [2.5].

The higher order modes experience cut-off when kr < 1, where k is the wave number.
It has been found by [2.4] that the Q of the system reduces to

$$Q = \frac{1+2\cdot(kr)^2}{(kr)^3\cdot[1+(kr)^2]} \simeq \frac{1}{(kr)^3}\Big|_{kr\ll 1} \tag{2.7}$$

The previous equation represents an unachievable lower bound on the electrical size of an antenna, that can be in practice only approached.
In figure 2.2 are shown computed values of Q versus kr, considering idealized antennas that are enclosed within a sphere of radius r with different radiation efficiencies.
An important parameter that can be derived from the Q is the fractional bandwidth FBW:

$$FBW = \frac{\Delta f}{f_0} \propto \frac{1}{Q} \tag{2.8}$$

where Δf is the bandwidth and f_0 the central frequency
Looking at the fig.2.2, we can see what kind of antenna better approaches the values of the 100% minimum Q curve, that corresponds to the highest FBW.
It is concluded that we can improve the bandwidth characteristics of one antenna of given maximum electrical dimension only if we do a wise use of the whole physical space at our disposal.
For example a dipole is a very poor volume utilizer because of its intrinsic 1-dimensional nature.
On the other hand, a Goubau antenna [2.6], that is a clover leaf dipole with coupling loops placed over a ground plane, better uses the 3-dimensional space.

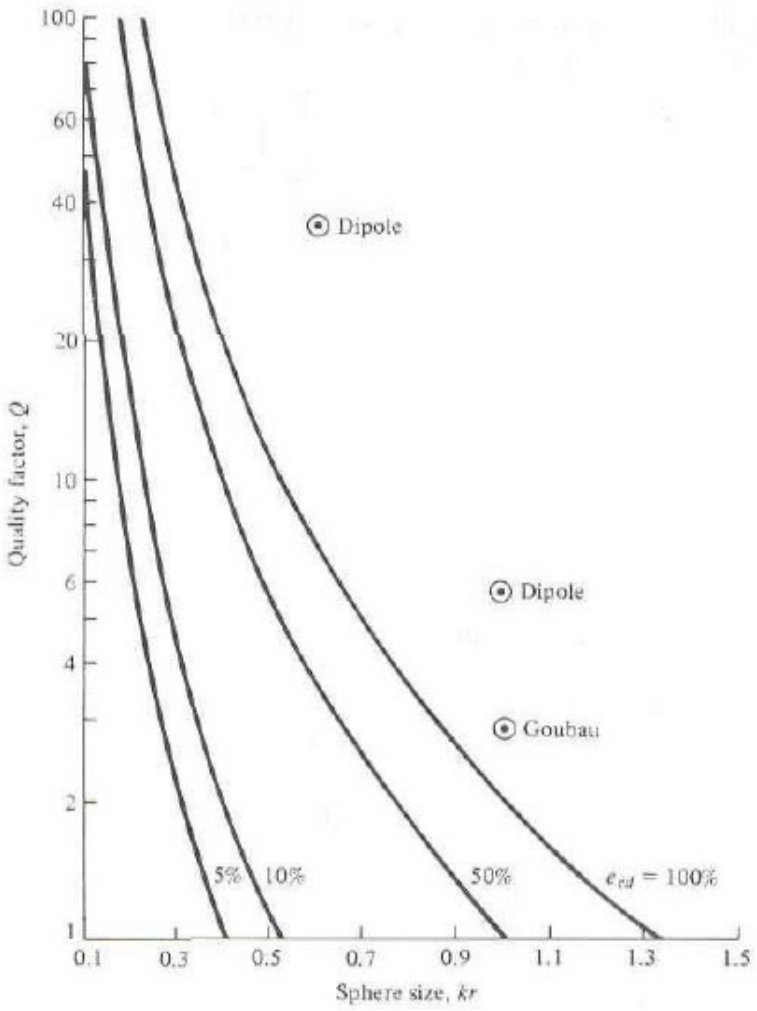

Figure 2.2: Fundamental limits of Q versus antenna size [2.4].

.

Chapter 3: Planar inverted-F antennas.

Among antennas respecting physical size constraints, suitable for the integration in handheld devices, we find the planar inverted-F antenna (PIFA) to be one of the most promising [3.1].
A PIFA is made up typically by a ground plane, a rectangular patch, and a short circuit plate of a width narrower than the shortened side of the patch.
On the one hand we can consider the PIFA as a sort of inverted-F antenna (IFA), where the thin wire has been replaced with a larger metallic patch in order to increase the bandwidth.
The IFA is a well known structure, and it is typically reported as a "shunt-driven inverted-L antenna-transmission line with an open end" [3.2].
On the other hand, the PIFA can be seen alternatively as a short circuit rectangular microstrip antenna (SC-MSA) resonating with the TM_{100} dominant mode.
We can reduce the dimension of the plate to one half of the length by inserting a short circuit in correspondence of the null of the electric field for the TM_{100} mode [3.3, 3.4].
We can drive the resonant frequency to a lower value increasing the effective inductance of the antenna, as a result of the progressive reduction of the width of the short circuit plate.
The previous ambiguous characteristics between the IFA and the SC-MSA make interesting the study of the behaviour of such a structure, not yet completely clarified.

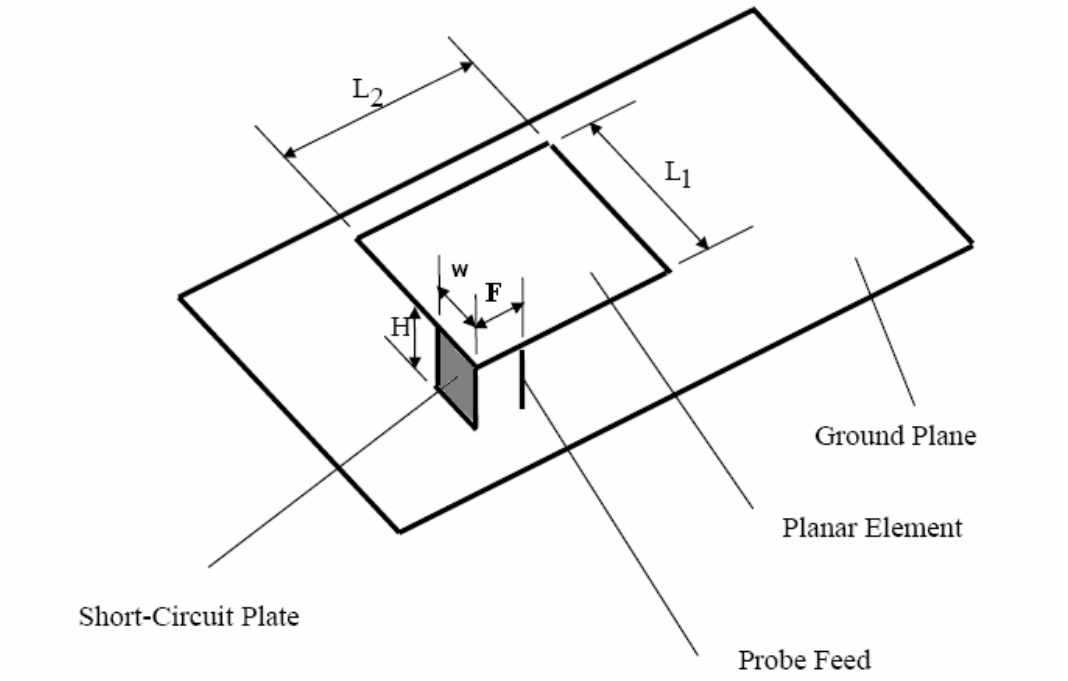

Figure 3.1: An example of PIFA.

The aforementioned dependence of the resonance frequency of the antenna from the width of the short circuit plate is also influenced by the size ratio of the patch element L_1 / L_2.

In fact this size ratio has to be as high as possible in order to have a low resonance frequency. So it is understood that the PIFA resonance frequency is proportional to the current distribution effective length.

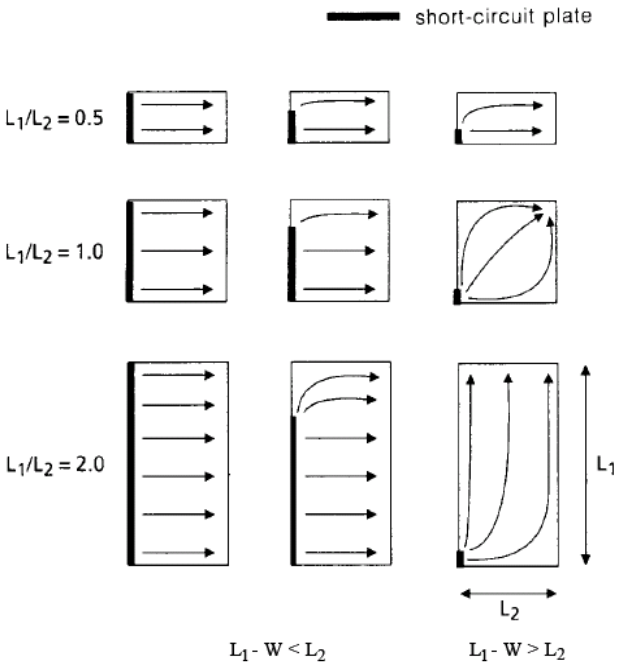

Figure 3.2: "Variation of surface current flow on planar element due to size ratio of planar element and width of short-circuit plate" [3.5].

To clarify the previous statement we will deal with two simple conditions.

The first situation is when the width of the short circuit plate W equals the whole length of the planar element L1, correspondent to the case of a SC-MSA , a λ/4 antenna.

Being W/L1 =1 the resonance frequency f_{r1} can be expressed as [3.5]:

$$L_2 + H = \frac{\lambda}{4} \tag{3.1}$$

that is

$$f_{r1} = \frac{c}{4(L_2 + H)} \tag{3.2}$$

With L2 + H the MSA effective length, c the speed of light and H the short-circuit plate height.

The other degenerate case where W=0, can be physically represented by an infinitesimal short circuit pin:

$$L_1 + L_2 + H = \frac{\lambda}{4} \tag{3.3}$$

that is:

$$f_{r2} = \frac{c}{4(L_1 + L_2 + H)} \tag{3.4}$$

When 0<W<L1:

$$f_{r2} = \frac{c}{4(L_1 + L_2 + H - W)} \tag{3.5}$$

As stated in [3.5], with a linear interpolation operation we can approximate the resonance frequency when 0<W/L1<1:

$$f_r = R \cdot f_{r1} + (1-R) \cdot f_{r2} \quad for \ \frac{L_1}{L_2} \le 1 \tag{3.6}$$

and

$$f_r = r^k \cdot f_{r1} + (1-r^k) \cdot f_{r2} \quad for \ \frac{L_1}{L_2} > 1 \tag{3.7}$$

where $R = \frac{W}{L_1}$ and k = $\frac{L_1}{L_2}$.

Concerning the bandwidth of the antenna, it increases according to the rise of H, the planar element size ratio $\frac{L_1}{L_2}$ and the ratio $\frac{W}{L_1}$, as we can see from the following figures 3.3, 3.4, where Δd is the unit cell size used in [3.5].

However the bandwidth of a PIFA installed over a handheld housing is wider than of the same PIFA placed on an infinite ground plane.

A suitable cause for this effect can be found in the surface current flow on the conductive housing. There are several ways to increase the bandwidth, such as the addition of parasitic elements like in [3.6], and the design of double-resonant PIFA's [3.7, 3.8].

Obviously a trade-off must be established in order to reduce the antenna volume.

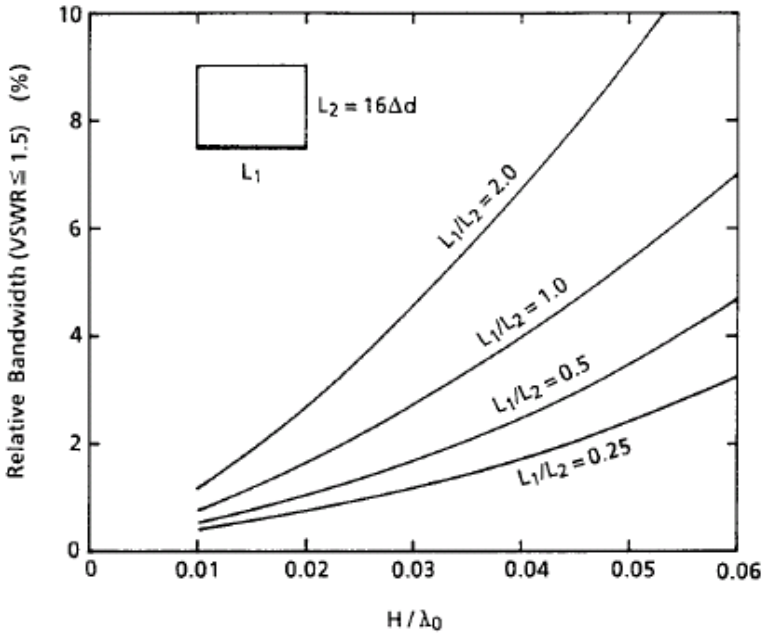

Figure 3.3:Bandwidth of the PIFA when short-circuit plate width is equal toL_1 (SC-MSA) [3.5].

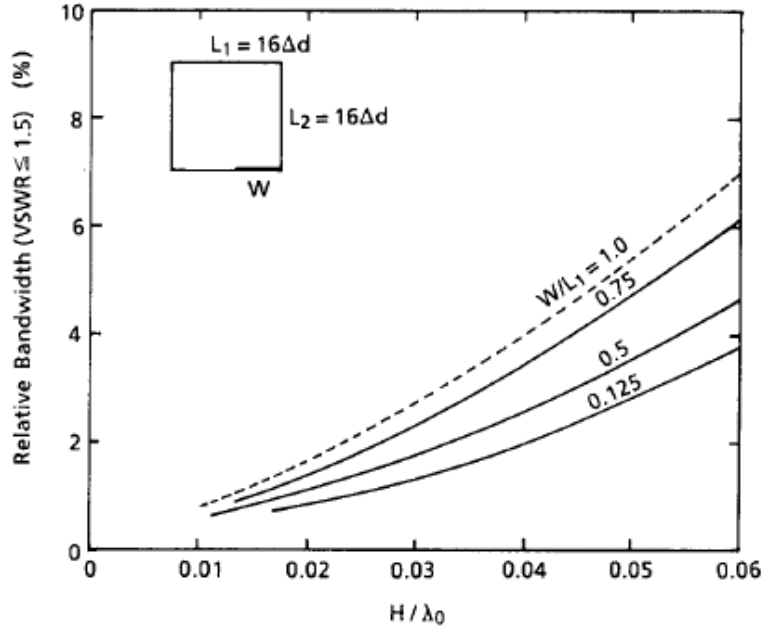

Figure 3.4: "Bandwidth of the PIFA when short circuit plate width is narrower thanL_1 "[3.5].

Chapter 4: FDTD theory.

4.1: The FDTD technique.

Finite-Difference Time-Domain (FDTD) is nowadays a leader techique in modelling and simulating a wide range of electromagnetic problems.
This has been possible thanks to the exponential growth of computers, that allowed the solution of complicate problems in a reasonable computational time.
As every field of engineering, the widespread of the FDTD traces back its origins to military applications, such as the reduction of the radar cross-section of airplanes and missiles [4.3].
FDTD works in time-domain, so a wide range of frequencies can be covered within a unique simulation run [4.1].
This method works modifying Maxwell's equations in differential form to central difference equations, that can be solved easily in software.
Because of the dependence between the electric and magnetic fields, Yee [4.6] proposed the so called leap-frog algorithm, described in section 4.6.
In order to use the FDTD algorithm, it is necessary to specify a computational domain, decribing properly all the geometrical objects inside the domain.
These objects are made up by specific materials, which properties need to be specified.
For example, a perfect conducting material (PEC) will be specifed by a proper choice of the boundary conditions.
The next step implies the modelization of the source, that for example can be an impinging plane wave or a current distribution.
Once that the simulation is finished, from the knowledge of the electric and magnetic field at each location, other information can be extrapolated with post-processing.
Antenna input impedence, surface currents and far field plots can be easily derived, depending on what is needed.

4.2: Advantages of the FDTD technique.

The FDTD technique, being a direct implementation of Maxwell's curl equations, doesn't need pre-processing.
Thanks to the fact that the entire procedure is carried out in the time domain, a broadband frequency response can easily be obtained with a proper excitation.
Complex three-dimensional systems can be modelled and analyzed, including microwave interaction with human body or non-linear components simulation.
The structure under analysis can be made up by constitutive materials with special features, such as lossy dielectrics, anisotropic media or magnetized ferrites.
It can be included also the dependence of permittivity and permeability respect to the variation of the frequency.
Because of the possibility of using the so called "near to far" transformations, the antenna far field pattern can be obtained, together with the derivation of currents and power flows.
The input impedance of the antenna can be calculated thanks to a broadband simulation, in order to study both impedance matching and antenna efficiency.
It is interesting to remember that we can also display real-time animations, that contributes to a deeper understanding of the physical behavior of the structure under simulation.

4.3: Weaknesses of the FDTD technique.

Depending on the wavelength of the electromagnetic waves under investigation, it is necessary to increase the lattice discretization, in order to be consistent with the Nyquist sampling theorem. More cells signifies more solving time, and often large computational domains have to be established.
To mitigate these situations, such as the modelization of thin wires, subcell gridding can be used instead of the conventional uniform one [4.3].
Because of the finite computational domain, we have to properly model artificial boundaries, trying to minimize the inherent error.

4.4: Maxwell's equations.

The two-hundred and more years old Maxwell's equations are still the milestone of modern engineering, because their elegant property to unify the electric and magnetic field, predicting electromagnetic wave propagation and interaction.
Now we present the Maxwell's equations in three dimensions in both differential and integral form. We suppose the absence of magnetic or electric current sources, with the possibility of absorbing materials in the space under investigation [4.1].

- Faraday's Law:

$$\frac{\partial \vec{B}}{\partial t} = -\nabla \times \vec{E} - \vec{J_m} \tag{4.1}$$

$$\frac{\partial}{\partial t}\iint_S \vec{B} \cdot d\hat{S} = -\oint_C \vec{E} \cdot d\hat{l} - \iint_S \vec{J_m} \cdot d\hat{S} \tag{4.2}$$

- Ampere's Law:

$$\frac{\partial \vec{D}}{\partial t} = \nabla \times \vec{H} - \vec{J_e} \tag{4.3}$$

$$\frac{\partial}{\partial t}\iint_S \vec{D} \cdot d\hat{S} = \oint_C \vec{H} \cdot d\hat{l} - \iint_S \vec{J_e} \cdot d\hat{S} \tag{4.4}$$

- Gauss's Law for the electric field:

$$\nabla \cdot \vec{D} = 0 \tag{4.5}$$

$$\oiint_S \vec{D} \cdot d\hat{S} = 0 \tag{4.6}$$

- Gauss's Law for the magnetic field:

$$\nabla \cdot \vec{B} = 0 \tag{4.7}$$

$$\oiint_S \vec{B} \cdot d\hat{S} = 0 \tag{4.8}$$

with the following symbols meaning in MKS units [4.2]:

- $\vec{E}$: electric field $\left(volts \cdot meter^{-1}\right)$
- $\vec{D}$: electric flux density $\left(coulombs \cdot meter^{-2}\right)$
- $\vec{H}$: magnetic field $\left(amperes \cdot meter^{-1}\right)$
- $\vec{B}$: magnetic flux density $\left(webers \cdot meter^{-2}\right)$
- S: arbitrary three-dimensional surface
- $d\vec{S}$: normal vector of surface S $\left(meter^{2}\right)$
- l : closed curve bounding the surface S
- $d\vec{l}$: unit path length vector of the curve C $\left(meter\right)$
- $\vec{J_e}$: electric conduction current density $\left(amperes \cdot meter^{-2}\right)$
- $\vec{J_m}$: magnetic conduction current density $\left(volts \cdot meter^{-2}\right)$

If we do hypotheses of linear, isotropic and non dispersive materials, we can do some simplifications, because of the scalar relation of $\vec{B}$ to $\vec{H}$, and $\vec{D}$ to $\vec{E}$ respectively:

$$\vec{B} = \mu \vec{H} \tag{4.9}$$

$$\vec{D} = \varepsilon \vec{E} \tag{4.10}$$

Where ε is the electric permittivity of the material $\left(farads \cdot meter^{-1}\right)$, and μ is the magnetic permeability of the material $\left(henrys \cdot meter^{-1}\right)$.

As stated in the beginning of the section, we allow both magnetic and electric losses in the materials, so that electromagnetic energy can be dissipated via Joule effect.

So we introduce two equivalent currents, the equivalent electric current $\vec{J_e}$ and the equivalent magnetic current $\vec{J_m}$:

$$\vec{J_e} = \sigma \vec{E} \tag{4.11}$$

$$\vec{J_m} = \rho' \vec{H} \tag{4.12}$$

where σ is the electric conductivity $\left(siemens \cdot meter^{-1}\right)$, and ρ' is the equivalent magnetic resistivity $\left(ohms \cdot meter^{-1}\right)$.

With the previous assumptions, we can easily obtain after some passages:

$$\frac{\partial \vec{H}}{\partial t} = -\frac{1}{\mu}\nabla \times \vec{E} - \frac{\rho'}{\mu}\vec{H} \tag{4.13}$$

$$\frac{\partial \vec{E}}{\partial t} = \frac{1}{\varepsilon}\nabla \times \vec{H} - \frac{\sigma}{\varepsilon}\vec{E} \tag{4.14}$$

Introducing for example a three-dimensional Cartesian coordinate system (x,y,z) in rectangular form, (4.13, 4.14) can be rewritten to form a system of six coupled scalar equations:

$$\frac{\partial H_x}{\partial t} = \frac{1}{\mu}\left(\frac{\partial E_y}{\partial z} - \frac{\partial E_z}{\partial y} - \rho' H_x\right) \tag{4.15}$$

$$\frac{\partial H_y}{\partial t} = \frac{1}{\mu}\left(\frac{\partial E_z}{\partial x} - \frac{\partial E_x}{\partial z} - \rho' H_y\right) \tag{4.16}$$

$$\frac{\partial H_z}{\partial t} = \frac{1}{\mu}\left(\frac{\partial E_x}{\partial y} - \frac{\partial E_y}{\partial x} - \rho' H_z\right) \tag{4.17}$$

$$\frac{\partial E_x}{\partial t} = \frac{1}{\varepsilon}\left(\frac{\partial H_z}{\partial y} - \frac{\partial H_y}{\partial z} - \sigma E_x\right) \tag{4.18}$$

$$\frac{\partial E_y}{\partial t} = \frac{1}{\varepsilon}\left(\frac{\partial H_x}{\partial z} - \frac{\partial H_z}{\partial x} - \sigma E_y\right) \tag{4.19}$$

$$\frac{\partial E_z}{\partial t} = \frac{1}{\varepsilon}\left(\frac{\partial H_y}{\partial x} - \frac{\partial H_x}{\partial y} - \sigma E_z\right) \tag{4.20}$$

This system of six coupled partial differential equations will be the basis of the following derivation of the FDTD algorithm.

4.5: The one-dimensional scalar wave equation.

The one-dimensional scalar wave equation is one of the constitutive bricks that allows us to investigate the FDTD method.
For this purpose, we will now introduce the finite differences, which properties will be useful in the next.
The following partial differential equation represents the simple one dimensional wave equation [4.1]:

$$\frac{\partial^2 u}{\partial t^2} = c^2 \frac{\partial^2 u}{\partial x^2} \tag{4.21}$$

where "u" is a function of both space and time u = u(x,t), and c is the speed of light, considering in this case a physical wave propagation in vacuum.
If now we do two Taylor's series expansions of $u(x,t_n)$ respect to the space, with starting point x_i at the fixed time instant t_n, both to the right and to the left of x_i, we get:

$$u(x_i+\Delta x)\big|_{t_n} = u\big|_{x_i,t_n} + \Delta x.\frac{\partial u}{\partial x}\bigg|_{x_i,t_n} + \frac{\Delta x^2}{2}.\frac{\partial^2 u}{\partial x^2}\bigg|_{x_i,t_n} + \frac{\Delta x^3}{6}.\frac{\partial^3 u}{\partial x^3}\bigg|_{x_i,t_n} + \frac{\Delta x^4}{24}.\frac{\partial^4 u}{\partial x^4}\bigg|_{\xi_1,t_n} \tag{4.22}$$

$$u(x_i-\Delta x)\big|_{t_n} = u\big|_{x_i,t_n} - \Delta x.\frac{\partial u}{\partial x}\bigg|_{x_i,t_n} + \frac{\Delta x^2}{2}.\frac{\partial^2 u}{\partial x^2}\bigg|_{x_i,t_n} - \frac{\Delta x^3}{6}.\frac{\partial^3 u}{\partial x^3}\bigg|_{x_i,t_n} + \frac{\Delta x^4}{24}.\frac{\partial^4 u}{\partial x^4}\bigg|_{\xi_2,t_n} \tag{4.23}$$

where ζ_1 and ζ_2 are located in the space interval $(x_i+\Delta x)$ and $(x_i-\Delta x)$ respectively.
After some simple passages, we obtain [4.1]:

$$\frac{\partial^2 u}{\partial x^2}\bigg|_{x_i,t_n} = \left[\frac{u(x_i+\Delta x)-2u(x_i)+u(x_i-\Delta x)}{(\Delta x)^2}\right]_{t_n} + O\left[(\Delta x)^2\right] \tag{4.24}$$

where $O\left[(\Delta x)^2\right]$ accounts for all the higher order remainder terms.
The previous equation is a second-order accurate approximation, central difference, of the second partial space derivative of u, that for ease of notation can be rewritten as:

$$\frac{\partial^2 u}{\partial x^2}\bigg|_{x_i,t_n} = \frac{u^n_{i+1}-2u^n_i+u^n_{i-1}}{(\Delta x)^2} + O\left[(\Delta x)^2\right] \tag{4.25}$$

where for the next u_i^n stands for a quantity evaluated at $x_i = i\Delta x$ in space and at $t_n = n\Delta t$ in time.

By simple analogy we can derive the correspondent expression for the second partial time derivative of u:

$$\left.\frac{\partial^2 u}{\partial t^2}\right|_{x_i,t_n} = \frac{u_i^{n+1} - 2u_i^n + u_i^{n-1}}{(\Delta t)^2} + O\left[(\Delta t)^2\right] \tag{4.26}$$

the previous formulas lead to the following approximation of the one dimensional scalar wave equation:

$$u_i^{n+1} = (c\Delta t)^2 \left[\frac{u^n_{i+1} - 2u_i^n + u^n_{i-1}}{(\Delta x)^2}\right] + 2u_i^n - u_i^{n-1} + O\left[(\Delta t)^2\right] + O\left[(\Delta x)^2\right] \tag{4.27}$$

We see that the equation is fully explicit, because of the fact that no simultaneous equation solution has to be found.
It exists a special case that reduces the equation to a very interesting form, called in the next magic time step, that is [4.2]:

$$c\frac{\Delta t}{\Delta x} = 1 \tag{4.28}$$

In this situation, the equation 4.27 reduces to:

$$u_i^{n+1} = u_{i+1}^n + u_{i-1}^n - u_i^{n-1} \tag{4.29}$$

where there is no remainder term accounting for the numerical error introduced in the discretization of the one-dimensional scalar wave equation.
This is because for this particular step choice, all the approximations in the Taylor's series expansion simply cancel out each other, leading to an exact solution.

4.6: Yee's algorithm.

We can trace the origin of finite-difference time domain technique (FDTD) back to 1966, when Kane Yee wrote his paper about solving Maxwell's equations in isotropic media thanks to a brand new numerical method [4.6].
Yee's basic idea was to develop a powerful but simple algorithm to solve both electric and magnetic fields in space and time using the aforementioned Maxwell's equations, which form is coupled and interlinked.
When we have at our disposal information about both electric and magnetic field, we get a more robust solution.
This algorithm also allows to model field singularities, such as structures with thin wires or sharp edges.
As we can see from the next figure, Yee's algorithm places its $\vec{E}$ and $\vec{H}$ components in a wise way in the three-dimensional space, so that "every $\vec{E}$ component is surrounded by four circulating $\vec{H}$ components, and every $\vec{H}$ component is surrounded by four circulating $\vec{E}$ components" [4.1].

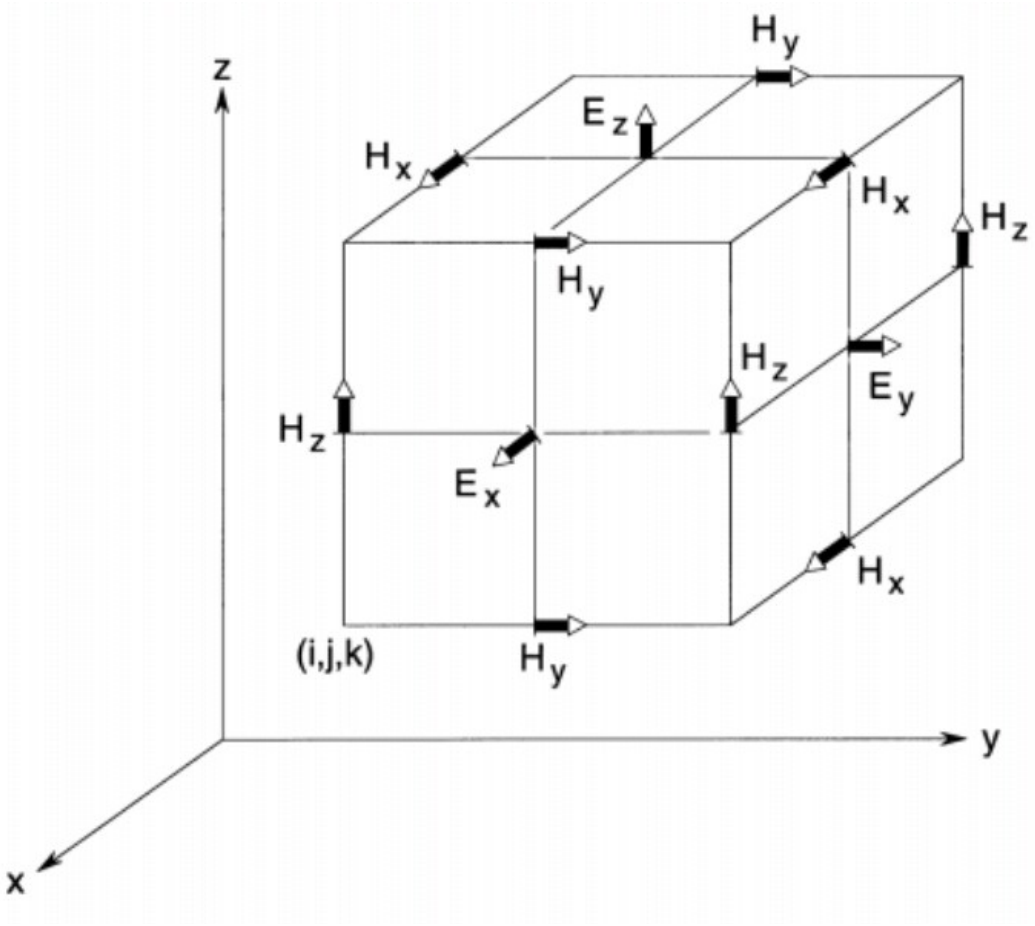

Figure 4.1: Allocation of the electric and magnetic field vector components respect to a single unit cell of the Yee space lattice [4.1].

We can recognize in fig. 4.1 an interlinked array of contours dealing with both Faraday's and Ampere's laws.
This configuration can be seen simultaneously as a pointwise differential form or a macroscopic integral form of Maxwell's equations [4.1].
Another interesting feature of this algorithm is that the space derivatives belonging to the curl operators are central-difference in nature and second order accurate.
If we specify at each location in the lattice appropriate values for permittivity, permeability and conductivity, we don't have to enforce boundary conditions, because they are automatically enforced by the algorithm.
However the total structure geometry has to be approximated with a finite space resolution depending on the dimension of the lattice unit cell.
If we don't have electric or magnetic charges, the Yee algorithm becomes divergence-free for both $\vec{E}$ and $\vec{H}$ field components, because of an automatic enforcement of the two Gauss' laws.

With the ulterior centring of both $\vec{E}$ and $\vec{H}$ field components in time, we reach the famous Yee's leap-frog algorithm.

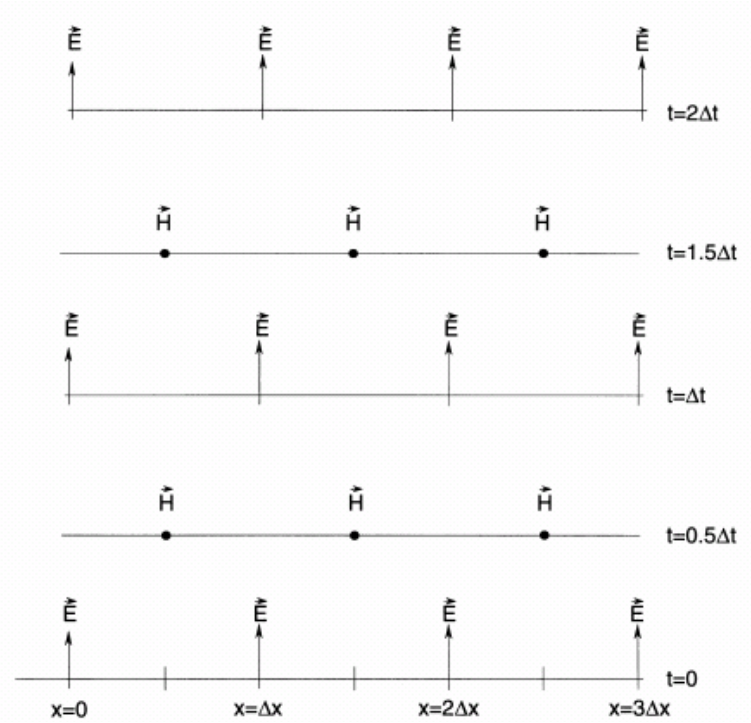

Figure 4.2: leap-frog algorithm in both space and time [4.1].

In fact the computations of the electrical field at each lattice point is done using the previously stored magnetic field values, with a reciprocal behaviour at the next time step.
This is an explicit method, because no matrix inversion is needed, a problem occurring for example in the numerical technique method of moments (MOM), because of the high number of simultaneous equations to be solved.
An interesting feature of the Yee algorithm is also the absence of dissipation, that results in a physical propagation of the wave in the lattice, without any spurious decay.
In order to be consistent with the original paper of Yee, we keep the same notation in the next, generalizing to the three-dimensional case.
A space point in a rectangular Cartesian coordinate system will be represented in a three-dimensional lattice as:

$$(i, j, k) = (i \cdot \Delta x, j \cdot \Delta y, k \cdot \Delta z) \tag{4.30}$$

where Δx, Δy, and Δz are space increments in x, y, z directions respectively, being i, j, and k integer indexes.

If we want to describe a function "u" of both space and time at some discrete point, calling Δt a uniform time increment, we have:

$$u(i\Delta x, j\Delta y, k\Delta z, n\Delta t) = u^n_{i,j,k} \tag{4.31}$$

where n is an integer.
Yee wanted to design his algorithm in such a way to have both electric and magnetic field components interleaved in space at intervals of $\frac{\Delta x}{2}$, leading for example to the following expression of finite differences in space:

$$\frac{\partial u}{\partial x}(i\Delta x, j\Delta y, k\Delta z, n\Delta t) = \frac{u^n_{i+1/2,j,k} - u^n_{i-1/2,j,k}}{\Delta x} + O\left[(\Delta x)^2\right] \tag{4.32}$$

where we are considering the x-directed first partial space derivative of u, evaluated when the time is fixed to $t_n = n \cdot \Delta t$.
Yee made an analogous choice for the expression of the first time partial derivative of u, keeping the space point fixed to (i, j, k). In fact, this will lead to the completion of the so called leap-frog algorithm, with the ulterior interleaving of both electric and magnetic field components in time at intervals of $\frac{\Delta t}{2}$.

4.7: Finite difference Maxwell's equations in three dimensions.

Recalling equations (4.13, 4.14), we can now derive their correspondent formulation in finite differences through the Yee algorithm.

$$\frac{\partial \vec{H}}{\partial t} = -\frac{1}{\mu}\nabla \times \vec{E} - \frac{\rho'}{\mu}\vec{H} \tag{4.33}$$

$$\frac{\partial \vec{E}}{\partial t} = \frac{1}{\varepsilon}\nabla \times \vec{H} - \frac{\sigma}{\varepsilon}\vec{E} \tag{4.34}$$

If we use a Cartesian three-dimensional coordinate system in rectangular form, after some manipulations equations (4.33, 4.34) lead to a system of six coupled scalar difference equations [4.1]:

$$H_x\Big|_{i,j,k}^{n+1/2} = \left(\frac{1-\frac{\rho'_{i,j,k}\Delta t}{2\mu_{i,j,k}}}{1+\frac{\rho'_{i,j,k}\Delta t}{2\mu_{i,j,k}}}\right) H_x\Big|_{i,j,k}^{n-1/2} + \left(\frac{\frac{\Delta t}{\mu_{i,j,k}}}{1+\frac{\rho'_{i,j,k}\Delta t}{2\mu_{i,j,k}}}\right)\left(\frac{E_y\Big|_{i,j,k+1/2}^{n} - E_y\Big|_{i,j,k-1/2}^{n}}{\Delta z} - \frac{E_z\Big|_{i,j+1/2,k}^{n} - E_z\Big|_{i,j-1/2,k}^{n}}{\Delta y}\right)$$

(4.35)

$$H_y\Big|_{i,j,k}^{n+1/2} = \left(\frac{1-\frac{\rho'_{i,j,k}\Delta t}{2\mu_{i,j,k}}}{1+\frac{\rho'_{i,j,k}\Delta t}{2\mu_{i,j,k}}}\right) H_y\Big|_{i,j,k}^{n-1/2} + \left(\frac{\frac{\Delta t}{\mu_{i,j,k}}}{1+\frac{\rho'_{i,j,k}\Delta t}{2\mu_{i,j,k}}}\right)\left(\frac{E_z\Big|_{i+1/2,j,k}^{n} - E_z\Big|_{i-1/2,j,k}^{n}}{\Delta x} - \frac{E_x\Big|_{i,j,k+1/2}^{n} - E_x\Big|_{i,j,k-1/2}^{n}}{\Delta z}\right)$$

(4.36)

$$H_z\Big|_{i,j,k}^{n+1/2} = \left(\frac{1-\frac{\rho'_{i,j,k}\Delta t}{2\mu_{i,j,k}}}{1+\frac{\rho'_{i,j,k}\Delta t}{2\mu_{i,j,k}}}\right) H_z\Big|_{i,j,k}^{n-1/2} + \left(\frac{\frac{\Delta t}{\mu_{i,j,k}}}{1+\frac{\rho'_{i,j,k}\Delta t}{2\mu_{i,j,k}}}\right)\left(\frac{E_x\Big|_{i,j+1/2,k}^{n} - E_x\Big|_{i,j-1/2,k}^{n}}{\Delta y} - \frac{E_y\Big|_{i+1/2,j,k}^{n} - E_y\Big|_{i-1/2,j,k}^{n}}{\Delta x}\right)$$

(4.37)

$$E_x\Big|_{i,j,k}^{n+1} = \left(\frac{1-\frac{\sigma_{i,j,k}\Delta t}{2\varepsilon_{i,j,k}}}{1+\frac{\sigma_{i,j,k}\Delta t}{2\varepsilon_{i,j,k}}}\right) E_x\Big|_{i,j,k}^{n} + \left(\frac{\frac{\Delta t}{\varepsilon_{i,j,k}}}{1+\frac{\sigma_{i,j,k}\Delta t}{2\varepsilon_{i,j,k}}}\right)\left(\frac{H_z\Big|_{i,j+1/2,k}^{n+1/2} - H_z\Big|_{i,j-1/2,k}^{n+1/2}}{\Delta y} - \frac{H_y\Big|_{i,j,k+1/2}^{n+1/2} - H_y\Big|_{i,j,k-1/2}^{n+1/2}}{\Delta z}\right)$$

(4.38)

$$E_y\Big|_{i,j,k}^{n+1} = \left(\frac{1-\frac{\sigma_{i,j,k}\Delta t}{2\varepsilon_{i,j,k}}}{1+\frac{\sigma_{i,j,k}\Delta t}{2\varepsilon_{i,j,k}}}\right) E_y\Big|_{i,j,k}^{n} + \left(\frac{\frac{\Delta t}{\varepsilon_{i,j,k}}}{1+\frac{\sigma_{i,j,k}\Delta t}{2\varepsilon_{i,j,k}}}\right)\left(\frac{H_x\Big|_{i,j,k+1/2}^{n+1/2} - H_x\Big|_{i,j,k-1/2}^{n+1/2}}{\Delta z} - \frac{H_z\Big|_{i+1/2,j,k}^{n+1/2} - H_z\Big|_{i-1/2,j,k}^{n+1/2}}{\Delta x}\right)$$

(4.39)

$$E_z\Big|_{i,j,k}^{n+1} = \left(\frac{1-\frac{\sigma_{i,j,k}\Delta t}{2\varepsilon_{i,j,k}}}{1+\frac{\sigma_{i,j,k}\Delta t}{2\varepsilon_{i,j,k}}}\right) E_z\Big|_{i,j,k}^{n} + \left(\frac{\frac{\Delta t}{\varepsilon_{i,j,k}}}{1+\frac{\sigma_{i,j,k}\Delta t}{2\varepsilon_{i,j,k}}}\right)\left(\frac{H_y\Big|_{i+1/2,j,k}^{n+1/2} - H_y\Big|_{i+1/2,j,k}^{n+1/2}}{\Delta x} - \frac{H_x\Big|_{i,j+1/2,k}^{n+1/2} - H_x\Big|_{i,j-1/2,k}^{n+1/2}}{\Delta y}\right)$$

(4.40)

Though the previous equations may seem difficult, there are some constant parts than can be easily grouped, in order to store them in a computer memory unit before the beginning of the time-stepping.

In fact, supposing the presence of a cubic lattice ($\Delta x = \Delta y = \Delta z = \Delta u$) , we can define the following coefficients, which ulterior simplifications are possible depending to the material properties [4.1]:

$$C_a\Big|_{i,j,k} = \left(\frac{1 - \frac{\sigma_{i,j,k}\Delta t}{2\varepsilon_{i,j,k}}}{1 + \frac{\sigma_{i,j,k}\Delta t}{2\varepsilon_{i,j,k}}} \right) \tag{4.41}$$

$$C_b\Big|_{i,j,k} = \left(\frac{\frac{\Delta t}{\Delta u \cdot \varepsilon_{i,j,k}}}{1 + \frac{\sigma_{i,j,k}\Delta t}{2\varepsilon_{i,j,k}}} \right) \tag{4.42}$$

$$D_a\Big|_{i,j,k} = \left(\frac{1 - \frac{\rho'_{i,j,k}\Delta t}{2\mu_{i,j,k}}}{1 + \frac{\rho'_{i,j,k}\Delta t}{2\mu_{i,j,k}}} \right) \tag{4.43}$$

$$D_b\Big|_{i,j,k} = \left(\frac{\frac{\Delta t}{\Delta u \cdot \mu_{i,j,k}}}{1 + \frac{\rho'_{i,j,k}\Delta t}{2\mu_{i,j,k}}} \right) \tag{4.44}$$

4.8: FDTD lumped elements modelling.

The FDTD method can be easily extended to allow the modelling of both linear and non-linear lumped circuit elements [4.4].
However, in those lattice cells that identify the space location of lumped elements, some modifications in the time-stepping algorithm are needed.
In order to modify the equations belonging to the conventional Yee algorithm, we recall here the Maxwell's curl $\vec{H}$ equation, from which we can obtain the electric field $\vec{E}$ via conventional time-stepping [4.1]:

$$\nabla \times \vec{H} = \vec{J_c} + \frac{\partial \vec{D}}{\partial t} \tag{4.45}$$

using the well-known relations $\vec{J_c} = \sigma \vec{E}$ and $\vec{D} = \varepsilon \vec{E}$, because of linearity, nondispersivity and isotropy hypotheses for used materials, after central differencing of (4.45) we get [4.1]:

$$E_z\Big|_{i,j,k}^{n+1} = \left(\frac{1-\frac{\sigma_{i,j,k}\Delta t}{2\varepsilon_{i,j,k}}}{1+\frac{\sigma_{i,j,k}\Delta t}{2\varepsilon_{i,j,k}}}\right) E_z\Big|_{i,j,k}^{n} + \left(\frac{\frac{\Delta t}{\varepsilon_{i,j,k}}}{1+\frac{\sigma_{i,j,k}\Delta t}{2\varepsilon_{i,j,k}}}\right)\left(\frac{H_y\Big|_{i+1/2,j,k}^{n+1/2} - H_y\Big|_{i-1/2,j,k}^{n+1/2}}{\Delta x} + \frac{H_x\Big|_{i,j-1/2,k}^{n+1/2} - H_x\Big|_{i,j+1/2,k}^{n+1/2}}{\Delta y}\right)$$

(4.46)

we suppose to evaluate $\vec{J_c}$ at the time step n+1/2, so we are dealing with a semi-implicit formulation, still keeping the algorithm numerical stability for values of $\sigma \geq 0$:

$$J_c\Big|_{i,j,k}^{n+1/2} = \frac{\sigma_{i,j,k}}{2}\left(E_z\Big|_{i,j,k}^{n} + E_z\Big|_{i,j,k}^{n+1}\right) \tag{4.47}$$

If we consider the lumped circuit elements placed in free space, we can simplify the notation assuming respectively $\varepsilon = \varepsilon_0$, $\sigma = 0$ and $\vec{J_c} = 0$.
If we express the curl of $\vec{H}$ with finite differences:

$$\nabla \times H_{i,j,k}^{n+1/2} = \frac{H_y\Big|_{i+1/2,j,k}^{n+1/2} - H_y\Big|_{i-1/2,j,k}^{n+1/2}}{\Delta x} + \frac{H_x\Big|_{i,j-1/2,k}^{n+1/2} - H_x\Big|_{i,j-1/2,k}^{n+1/2}}{\Delta y} \tag{4.48}$$

we obtain after trivial passages a simple expression for equation (4.46):

$$E_z\Big|_{i,j,k}^{n+1} = E_z\Big|_{i,j,k}^{n} + \frac{\Delta t}{\varepsilon_0} \nabla \times H_{i,j,k}^{n+1/2} \tag{4.49}$$

Thanks to the papers of Sui et al. [4.4], and [4.5], it has been shown that modifying Maxwell's equations with the addition of a lumped current density term $\vec{J_L}$ makes possible the introduction of lumped circuit elements in the FDTD algorithm:

$$\nabla \times \vec{H} = \vec{J_c} + \frac{\partial \vec{D}}{\partial t} + \vec{J_L} \tag{4.50}$$

If I_L is the total element current, related also to the electric potential V, we have:

$$J_L = \frac{I_L}{\Delta x \Delta y} \tag{4.51}$$

$$V = E_z\big|_{i,j,k} \Delta z \tag{4.52}$$

Beside these assumptions we have to specify other geometrical features, such as the orientation of the lumped element along the z axis of the grid, without loss of generality.
In fact permuting indexes properly we can derive the other cases for arbitrary alignment of the lumped circuit element respect to the reference axes.
After some passages we get [4.1]:

$$E_z\Big|_{i,j,k}^{n+1} = E_z\Big|_{i,j,k}^{n} + \frac{\Delta t}{\varepsilon_0} \nabla \times H_{i,j,k}^{n+1/2} - \frac{\Delta t}{\varepsilon_0 \Delta x \Delta y} I_L^{n+1/2} \tag{4.53}$$

4.9: The numerical resistor.

If we want to model a numerical linear resistor aligned along the z axis at the field component $E_z\big|_{i,j,k}$, we find [4.5]:

$$I_z\Big|_{i,j,k}^{n+1/2} = \frac{\Delta z}{2R}\left(E_z\Big|_{i,j,k}^{n+1} + E_z\Big|_{i,j,k}^{n}\right) \tag{4.54}$$

and

$$J_L = \frac{I_z\Big|_{i,j,k}^{n+1/2}}{\Delta x \Delta y} \tag{4.55}$$

Finally we get the following time-stepping equation:

$$E_z\Big|_{i,j,k}^{n+1} = \left(\frac{1 - \frac{\Delta t \Delta z}{2R\varepsilon_0 \Delta x \Delta y}}{1 + \frac{\Delta t \Delta z}{2R\varepsilon_0 \Delta x \Delta y}}\right) E_z\Big|_{i,j,k}^{n} + \left(\frac{\frac{\Delta t}{\varepsilon_0}}{1 + \frac{\Delta t \Delta z}{2R\varepsilon_0 \Delta x \Delta y}}\right) \nabla \times H_{i,j,k}^{n+1/2} \tag{4.56}$$

The previous equation may seem difficult to implement in practice, but if we look carefully, only constant parameters have to be modified, so it is necessary only changing properly the definition of the coefficients mentioned in equations (4.41-4.44).
In literature [4.5] it has been found a good agreement between the impedance matching using the numerical resistor and the conventional physical resistor made up of one cell filled by a material chosen properly to account for the resistive behaviour.

4.10: The numerical capacitor.

Now we proceed to the description of the numerical capacitor, aligned along the z axis like before and placed at $E_z\big|_{i,j,k}$ in free space.

Recalling the well known relation for the current I flowing in a capacitor which terminals insists a voltage difference V:

$$I = C\frac{dV}{dt} \tag{4.57}$$

we obtain as before a semi-implicit relation:

$$I_z\Big|_{i,j,k}^{n+1/2} = \frac{C\Delta z}{\Delta t}\left(E_z\Big|_{i,j,k}^{n+1} - E_z\Big|_{i,j,k}^{n}\right) \tag{4.58}$$

$$J_L = \frac{I_z\Big|_{i,j,k}^{n+1/2}}{\Delta x \Delta y} \tag{4.59}$$

The resulting modified time-stepping relation is [4.5]:

$$E_z\Big|_{i,j,k}^{n+1} = E_z\Big|_{i,j,k}^{n} + \left(\frac{\frac{\Delta t}{\varepsilon_0}}{1+\frac{C\Delta z}{\varepsilon_0 \Delta x \Delta y}}\right)\nabla \times H_{i,j,k}^{n+1/2} \tag{4.60}$$

Also here the only modification to introduce in the conventional Yee time-stepping algorithm is the reformulation of constant parameters.
It has been demonstrated in [4.5] a good agreement between this numerical capacitive load implementation and theory.

4.11: The numerical inductor.

Similarly, if we want to model a numerical linear inductor aligned along the z axis at the field component $E_z\big|_{i,j,k}$, we have to impose the following conditions:

$$I_z\Big|_{i,j,k}^{n+1/2} = \frac{\Delta z \Delta t}{L}\sum_{m=1}^{n} E_z\Big|_{i,j,k}^{m} \tag{4.61}$$

$$J_L = \frac{I_z\Big|_{i,j,k}^{n+1/2}}{\Delta x \Delta y} \tag{4.62}$$

where L is the value of the inductance
The resulting modified time-stepping relation is [4.5]:

$$E_z\Big|_{i,j,k}^{n+1} = E_z\Big|_{i,j,k}^{n} + \frac{\Delta t}{\varepsilon_0}\nabla \times H_{i,j,k}^{n+1/2} - \frac{\Delta z(\Delta t)^2}{\varepsilon_0 L \Delta x \Delta y}\sum_{m=1}^{n} E_z\Big|_{i,j,k}^{m} \tag{4.63}$$

4.11: Cell size considerations.

In order to sample properly the structure to be simulated with the FDTD algorithm, the unit cells must be small compared to one wavelength, as a consequence of the general Nyquist criterion.

With these constraints to satisfy, the side of each cell should be $\frac{\lambda}{10}$ or less [4.3].

Sometimes it is better to use smaller cells, such as in the case of thin wire modelling, being the antenna impedance very sensitive to small modifications in the radius of the wire, so that also sub-cell gridding can be included.

4.12 Numerical stability criteria

When we define the input parameters of a FDTD problem, we have to pay particular attention to choose the right time and space increments, in order to ensure both accuracy and numerical stability.
Having determined the spatial cell size, thanks to the Courant condition, we can derive the maximum allowed time step Δt [4.1]:

$$v_{\max} \cdot \Delta t \le \frac{1}{\sqrt{\frac{1}{\Delta x^2} + \frac{1}{\Delta y^2} + \frac{1}{\Delta z^2}}} \tag{4.64}$$

where $v_{\max}$ is the maximum velocity of propagation, with $v_{\max}$ = c in free space.
When we are in the special case where $\Delta x = \Delta y = \Delta z = \Delta u$, the aforementioned condition becomes:

$$v_{\max} \cdot \Delta t \le \frac{\Delta u}{\sqrt{3}} \tag{4.65}$$

4.13: Numerical dispersion.

The constitutive equations that rule the FDTD technique imply a non-physical numerical dispersion of the waves as they travel in the simulated computational free-space lattice.
Parameters like grid discretization, relative direction of propagation or wavelength variation, contribute to change the phase velocity of the numerical waves that travel in the lattice, so that it differs from the speed of light c.

This phenomenon can be the cause of several problems, such as numerical anisotropy, accumulation of delays, phase errors and broadening of pulses.
Numerical dispersion can be analyzed through the derivation of dispersion relations for a plane wave [4.1]:

$$\left[\frac{1}{c\Delta t}\sin\left(\frac{\omega\Delta t}{2}\right)\right]^2=\left[\frac{1}{\Delta x}\sin\left(\frac{\tilde{k}_x\Delta x}{2}\right)\right]^2+\left[\frac{1}{\Delta y}\sin\left(\frac{\tilde{k}_y\Delta y}{2}\right)\right]^2+\left[\frac{1}{\Delta z}\sin\left(\frac{\tilde{k}_z\Delta z}{2}\right)\right]^2 \qquad (4.66)$$

where the ideal dispersion relation for a plane wave in a lossless homogeneous medium is given by:

$$\frac{\omega^2}{c^2}=k_x^{\,2}+k_y^{\,2}+k_z^{\,2} \qquad (4.67)$$

It can be easily shown that the two relations in the limit as Δx, Δy, Δz, and Δt approach to zero are equal.
This behaviour suggests that if we want to reduce numerical dispersion below a defined threshold, we only need to increase the spatial gridding properly.

4.14: Absorbing Boundary Conditions (ABC).

Several electromagnetic problems deal with propagation in unbounded media, such as open space regions.
In theory such a problem would require an infinite amount of both memory and processing time for a calculator. Because of this problem it is necessary to truncate the computational domain trying to minimize the truncation error.
We divide the whole domain in two regions called respectively interior and exterior region, the first accounting for the structure delimitation, and the second to simulate infinite space. The exterior region is bounded by perfect electric conductor (PEC).
When the outward propagation coming from the interior region approaches the PEC in the exterior region, reflections occur.
Being this reflection the non-physical result of the truncation error, we must reduce their effect, trying to avoid them if possible [4.3].
We can simulate in two different ways the open space surrounding the interior region.
The first method is to assign appropriate equivalent currents to the surface of the interior region, deriving later the exterior region's field using the Green functions.
The second approach uses specific absorbing boundary conditions to limit reflections from the truncation of the lattice mesh.

Chapter 5: Simulations.

5.1: Simulations outline.

In this section we summarize the steps we did to progressively propose and evaluate some antenna configurations suitable for implementation in small handheld terminals for DVB-H signals reception:

- **5.2: Pifa antenna investigations over a ground plane.**

Here we get started with the investigation of simple antenna configurations, in order to familiarize with the FDTD simulation package developed at Aalborg University.
Several pifa antennas mounted on ground planes are simulated, in order to derive tendencies that will be useful for the following design.

- **5.3: Effects of ground plane size variation for a pifa antenna.**

Here we study the influence of the ground plane size variation on the performances of a pifa antenna, in order to characterize the behaviour of this antenna in a rigorous manner, trying to find the accuracy limits of our simulations.

- **5.4: Tuning of a pifa antenna with lumped components investigations.**

In this section we introduce the chassis metal box in our simulations, because of the fact we want to model real handheld terminals, which antenna doesn't radiate over a large ground plane as before. Thanks to the lumped component tool we developed in this Master Thesis [App. A, C], we try to see if it is possible to obtain a tuneable pifa antenna, placing properly varying capacitors in the simulated structure. We also validate the behaviour of our lumped components comparing our code with the commercial simulation package CST Microwave Studio.

- **5.5: Tuning of a meandered pifa antenna.**

Here we continue our study, and we propose a new antenna configuration, that is a tuneable meandered pifa antenna. We will simulate the implementation of varactors through a proper choice of lumped components, to see the advantages and the limits of this approach.
We tried to do our investigations adding progressively degrees of realism, in the limit of the resources at our disposal.

- **5.6: Top meandered monopole antenna investigations.**

Now we decide to try a new kind of antenna, addressing our attention on meandered monopole antennas. As before, we first get started with this solution in order to derive simple tendencies, that will suggest the next choices.

- **5.7: Effects of the chassis metal box for meandered monopole antennas.**

In this section we continue our investigations with the meandered monopole antenna, to understand the implications of the coupling effects between the chassis metal box and the antenna.

- **5.8: Top meandered monopole antenna design.**

Here we do a proposal for a meandered monopole antenna, where we try to provide a tuning of the antenna resonance frequency to cover the whole band of interest.
As before we model a varactor with lumped components in the FDTD code, to see what are the advantages and drawbacks of this implementation.

- **5.9: Top meandered switched monopole antenna.**

In this section we reduce the dimension of the meandered monopole antenna thanks to the use of several matching circuits, that divide our frequency range in several sub-bandwidths.
We will do this with different L-section matching circuits, which selection can be done by a RF-switch. In order to reduce the number of reactive components involved, we find also a compromise between impedance bandwidth and absolute value of the reflection coefficient S11.

5.2: Pifa antenna investigations over a ground plane.

5.2.1: Introduction.

The aim of this set of simulations is to derive simple tendencies for pifa antennas mounted on a ground plane.
We will investigate the effect of the height of the pifa short circuit plate on the antenna quality factor.
Similarly, we will study the effect of the ratio between the linear dimensions of the pifa top plate on the antenna quality factor variation.
We simulate several pifa antennas, all placed in the middle of a ground plane which dimensions are progressively changed.

We define the following parameters:

- lg [mm]: length of the ground plane.
- hg [mm]: height of the ground plane.
- L1 [mm]: not short circuit length of the pifa.
- L2 [mm]: short circuit length of the pifa.
- feed1 [mm]: x-oriented offset of the feed.
- feed2 [mm]: y-oriented offset of the feed.
- vol [mm^3]: antenna volume.
- hsc [mm]: height of the short circuit plate.
- wsc [mm]: width of the short circuit plate.
- frth [MHz]: theoretical resonance frequency.
- frsim [MHz]: resonance frequency obtained by simulation.
- frperr: resonance frequency percentage error.
- Q: antenna quality factor.
- Zin [Ohm]: antenna input impedance.
- Re(Zin) [Ohm]: real part of Zin.
- Im(Zin) [Ohm]: imaginary part of Zin.

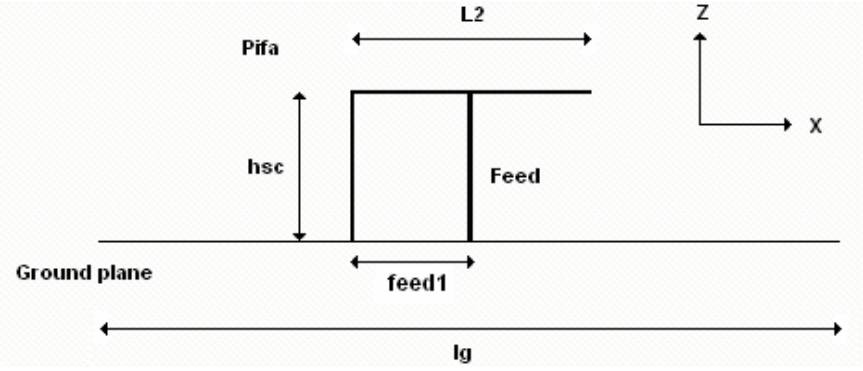

Figure 5.1: Pifa geometry in the XZ plane.

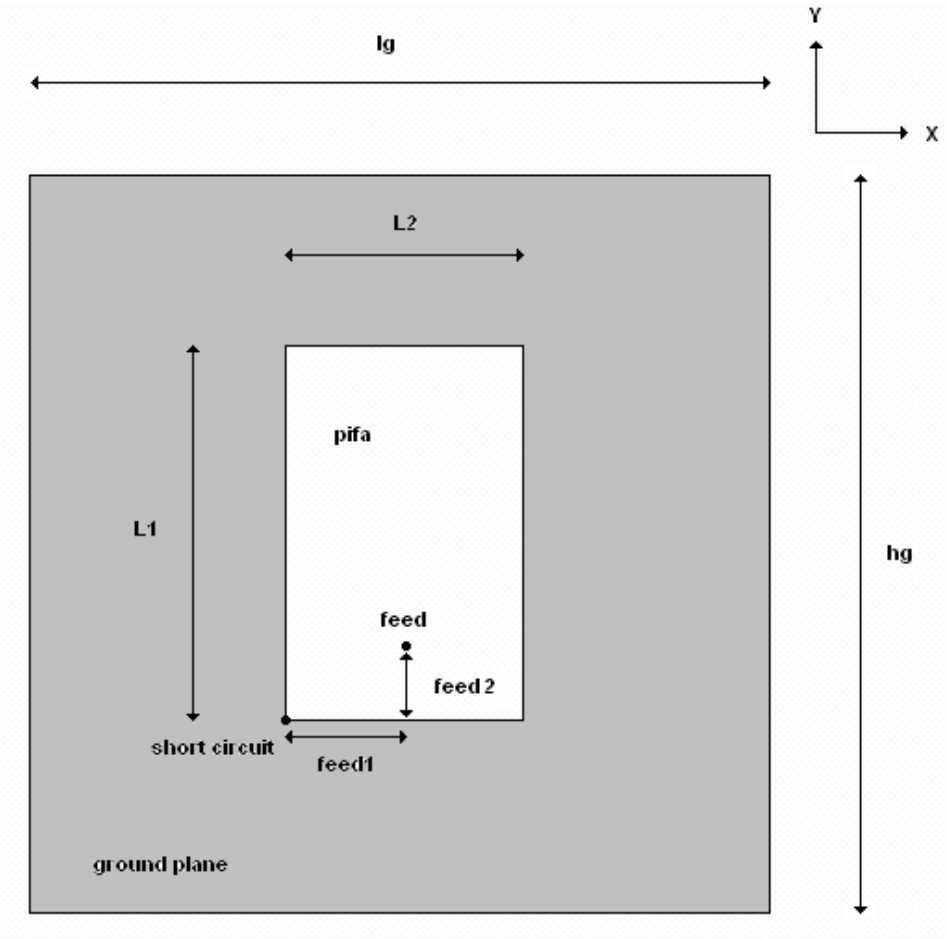

Figure 5.2: Pifa geometry in the XY plane.

5.2.2: Simulation of pifa antennas.

The ground plane will be adapted each time to the pifa antenna, and its dimensions will be $2L1 \cdot 2L2$. Even if a rigorous study would need the presence of a very large ground plane to be consistent with the infinite ground plane assumptions, we decided to scale each ground plane depending to the dimensions of the pifa, so that the antennas performances will be nearly affected in the same way. This choice was made because of the inherent large computational time needed in the simulations when the ground plane is too big.
This suggests that every time a trade-off between resources and accuracy in the results has to be established.
We decided to keep in all the simulations the same feed location (feed1 = 0.5L2mm, feed2 = 5mm) and the same wsc = 0mm, so that we can apply eq. 5.1.

In order to have always nearly the same resonance frequency of 586 MHz (central frequency of DVB-H with GSM900), we choose hsc, L1, and L2 properly, following the equation:

$$frth = \frac{c}{4(L1 + L2 + hsc)} \tag{5.1}$$

so that the sum (L1+L2+hsc) is constant.
We also calculate the antenna quality factor Q as:

$$Q = \frac{\omega}{2R} \cdot \frac{\partial X}{\partial \omega} \tag{5.2}$$

where R is the value of the real part of the input impedance of the antenna measured at resonance, while X is the reactance of the input impedance of the antenna at resonance.
The derivative of the reactance has to be calculated close to the resonance, but because we don't have an analytical expression for the reactance, we have to approximate that derivative.
So we calculate $\left.\frac{\partial X}{\partial \omega}\right|_{\omega=\omega_0}$ as:

$$\frac{\left|X(\omega_0 - \Delta\omega) - X(\omega_0 + \Delta\omega)\right|}{2\Delta\omega} \tag{5.3}$$

We have only discrete values of the input impedance of the antenna, so we choose two values that are close to the resonance.
In fact if we choose $\Delta\omega$ too big , we loose linearity and the values that we get are wrong.
We define resonance at the frequency point where the reactance of the input impedance of the antenna is equal to the mean of its maximum and minimum value.
Near resonance the reactance is linear, so that we can calculate an approximate derivative (fig. 5.3).
The size of one cell in the FDTD simulation is 5mm.
The antenna input impedance is calculated over a frequency range of 300 MHz centred on 586MHz, where 10 samples per MHz are taken, with a total of 3000 samples, and we will keep these assumption in the next of the report.
The following table is a summary of the simulated antenna (1-18) features and inherent results:

pifa	L1 [mm]	L2[mm]	L1/L2	hsc [mm]	frth [MHz]	frsim [MHz]	Q	frperr
1	60	60	1.00	5	586	596	297	1.68
2	70	50	1.40	5	586	598	364	2.01
3	80	40	2.00	5	586	600	250	2.33
4	90	30	3.00	5	586	604	129	2.98
5	100	20	5.00	5	586	603	32	2.82
6	105	15	7.00	5	586	599	21	2.17
7	55	60	0.92	10	586	593	121	1.18
8	65	50	1.30	10	586	593	112	1.18
9	75	40	1.88	10	586	596	83	1.68
10	85	30	2.83	10	586	597	40	1.84
11	95	20	4.75	10	586	592	22	1.01
12	100	15	6.67	10	586	585	19	0.17
13	50	60	0.83	15	586	591	64	0.85
14	60	50	1.20	15	586	588	47	0.34
15	70	40	1.75	15	586	589	47	0.51
16	80	30	2.67	15	586	589	31	0.51
17	90	20	4.50	15	586	586	23	0.00
18	95	15	6.33	15	586	578	17	1.38

Table 5.1: pifa antenna simulation summary (1-18).

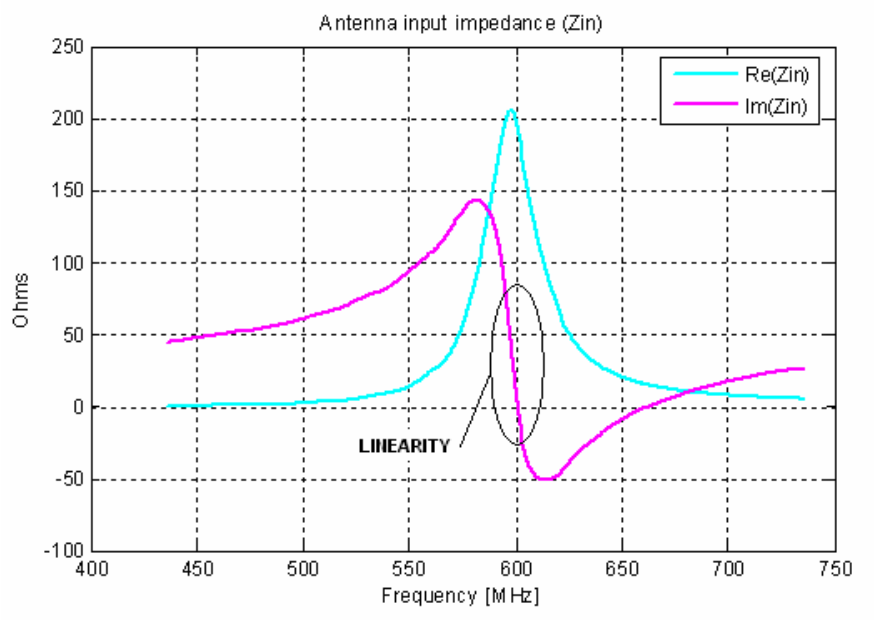

Figure 5.3: Example of antenna input impedance (Zin).

As we can see from fig. 5.4, the antenna quality factor Q is more influenced from the variation of the height of the short circuit plate hsc, and this is consistent with the theory; in fact the bandwidth grows as hsc grows. The mean percentage error on resonance frequency is 1.37%.

Theory state that the bandwidth has to increase as L1/L2 grows, and this is confirmed by all the simulations except for pifa2.
This may be explained by accuracy errors inherent both approximation of the Q and limited ground plane size.
The tendencies derived suggest for the next the choice of pifa antennas with a large ratio L1/L2, together with a high hsc.
However we will be limited by the dimensions of the chassis box and by the fact that the antenna volume has to be kept as small as possible.

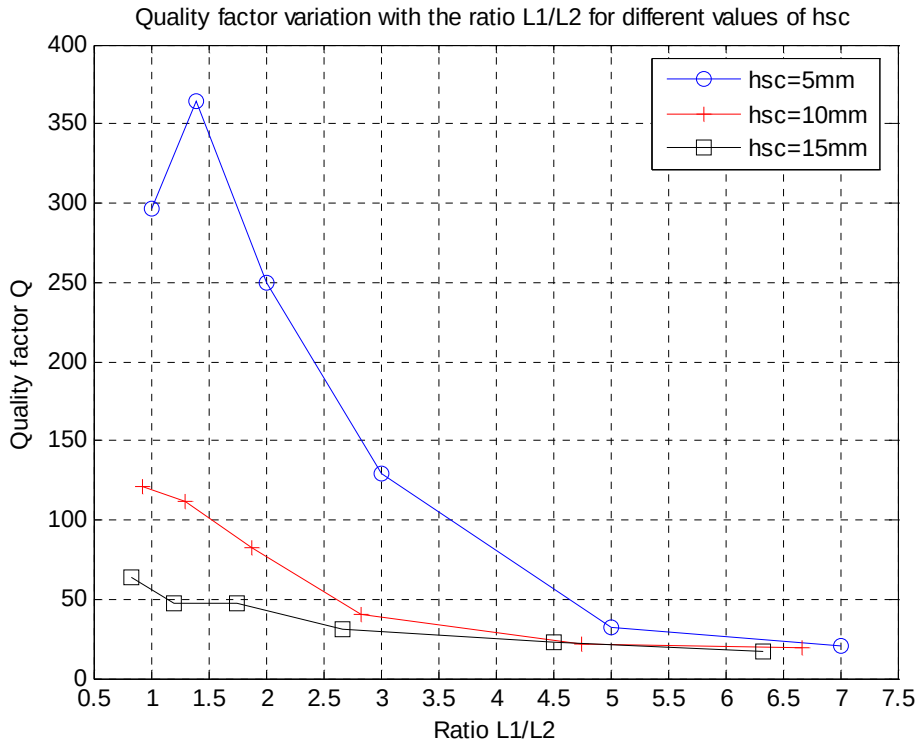

Figure 5.4: Quality factor variation with the ratio L1/L2 for different values of hsc (1-18).

5.2.3: Simulation of constant volume pifa antennas.

In the next simulation set we keep the volume of the antenna constant and equal to $3cm^3$, over a square ground plane with lg = hg = 140mm.
In fact it is important to compare antenna performances when the volume is fixed, because this will lead to a fair understanding of the antenna behaviour.
However, it is more difficult to do this when the antenna is mounted on its chassis, because we have to consider also physical constraints in our investigations.
As before we decide to keep in all the simulations the same feed location (feed1 = 0.5L2mm, feed2 = 5mm) and the same wsc = 0mm.
The following table is a summary of the simulated antenna (19-25) features and inherent results:

pifa	L1 [mm]	L2 [mm]	L1/L2	hsc [mm]	frth [MHz]
19	60	50	1.20	10	625
20	75	40	1.88	10	600
21	100	30	3.33	10	536
22	120	25	4.80	10	464
23	60	25	2.40	20	714
24	75	20	3.75	20	652
25	100	15	6.67	20	556

pifa	frsim [MHz]	Q	vol [mm3]	frperr
19	623	119	3000	0.32
20	597	87	3000	0.50
21	535	50	3000	0.19
22	481	27	3000	3.53
23	701	27	3000	1.85
24	634	26	3000	2.84
25	533	19	3000	4.32

Table 5.2: pifa antenna simulation summary (19-25)

As we can see from fig. 5.5, similar tendencies are derived for hsc and the ratio L1/L2. Also here the percentage error on resonance frequency is quite small.
The quality factor is more sensitive to the height of hsc, so that for a fixed volume, it seems better to choose that antenna configurations with the highest hsc, in the limit of our physical constraints.

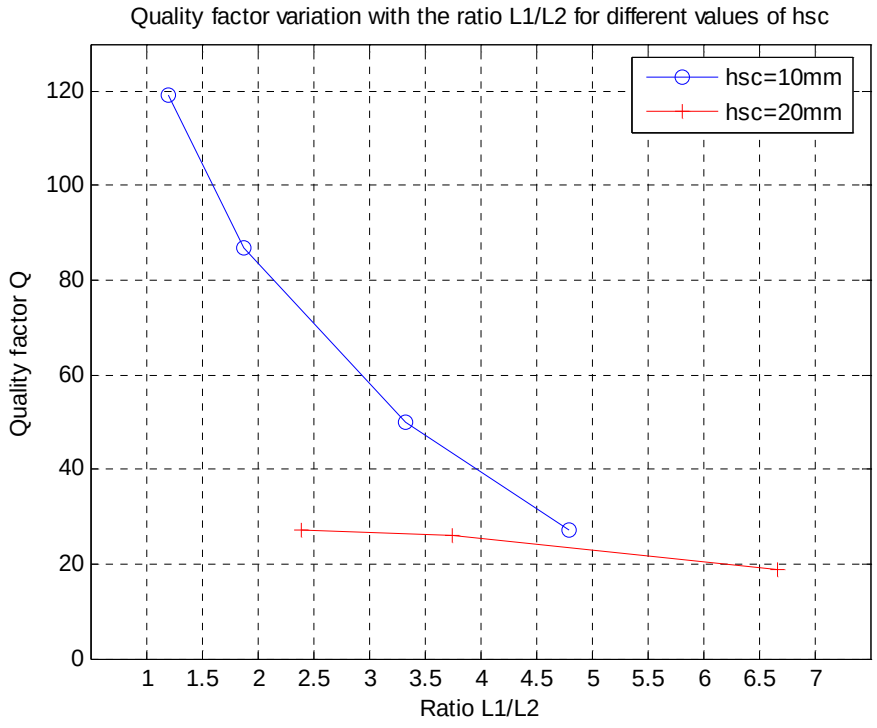

Figure 5.5: Quality factor variation with the ratio L1/L2 for different values of hsc (19-25).

5.3: Effects of ground plane size variation for a pifa antenna.

5.3.1: Introduction.

In this simulation set we investigate the effect of the ground plane size on both resonance frequency and quality factor of a pifa antenna.
We also look at the variation of the antenna input impedance calculated at resonance.
A popular antenna theory simplification states as a common hypothesis the perfect ground plane, that is in the ideal case perfectly conducting, planar, and infinite in extent.
This makes possible to apply image theory, in order to remove the ground plane from the analysis.
When we simulate real antennas, we deal with finite size ground planes, that deviate results from the ideal case.
It was shown in [5.1] that antenna input impedance oscillates about the value corresponding to the infinite ground plane as the size of the ground plane increases.
At some point this oscillation should converge to the perfect ground plane value.
The resonance frequency was reported to be less affected by the ground plane size [5.1].
The variation of the antenna input impedance with the ground plane size, implies a correspondent variation in the quality factor.
In [5.2] it was reported a lowering of the quality factor as the ground plane size increases, that corresponds to a wider relative impedance bandwidth.
We keep for all simulations the same pifa antenna, that will be centred each time on a larger ground plane. We define the following geometric parameters:

- lg [mm]: length of the ground plane.
- hg [mm]: height of the ground plane.
- L1 [mm]: not short circuit side of the pifa.
- L2 [mm]: short circuit side of the pifa.
- feed1 [mm]: x-oriented offset of the feed.
- feed2 [mm]: y-oriented offset of the feed.
- hsc [mm]: height of the short circuit plate.
- wsc [mm]: width of the short circuit plate.
- nfb [cells]: number of near field boundaries cells.

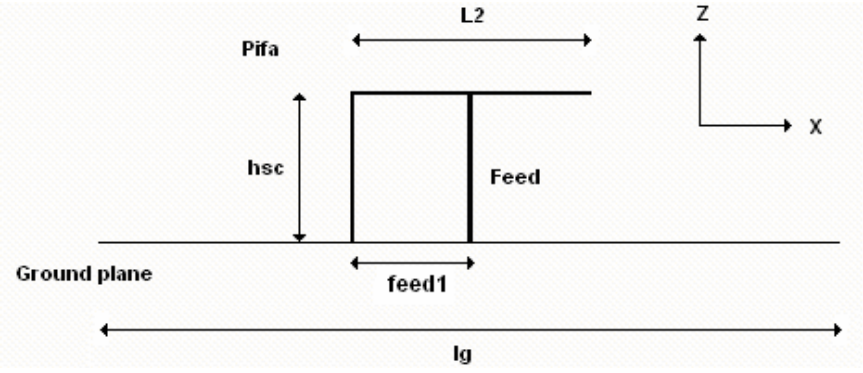

Figure 5.6: Pifa geometry in the XZ plane.

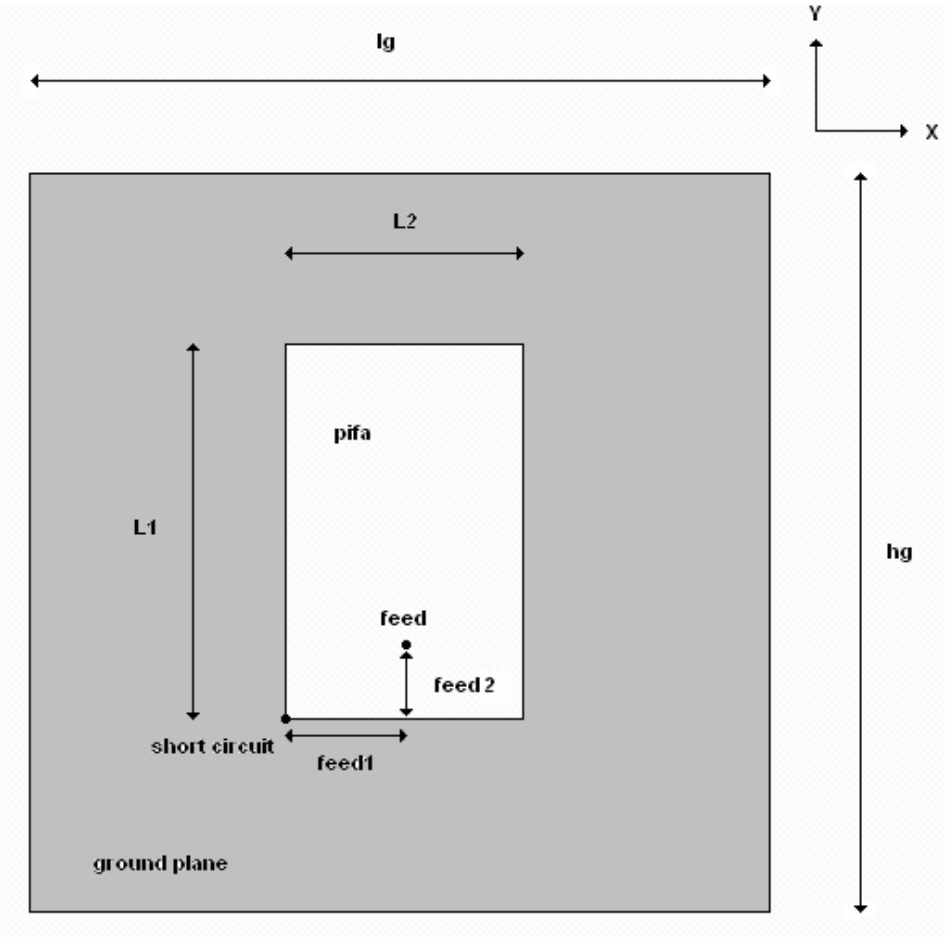

Figure 5.7: Pifa geometry in the XY plane.

L1 [mm]	L2 [mm]	hsc [mm]	wsc [mm]	feed1 [mm]	feed2[mm]
70	40	15	0	20	5

Table 5.3: pifa's geometric values.

5.3.2: Simulation.

We choose a square ground plane with lg = hg = L varying from 100mm to 670mm in 20 steps of 30mm.
The number of near field boundaries cells is a parameter to specify in the FDTD code, that dictates the size of the box where the FDTD boundaries conditions are enforced.
The FDTD cell size is 5mm, while the number of near field boundaries cells is set first to 10 cells and later to 20 cells.

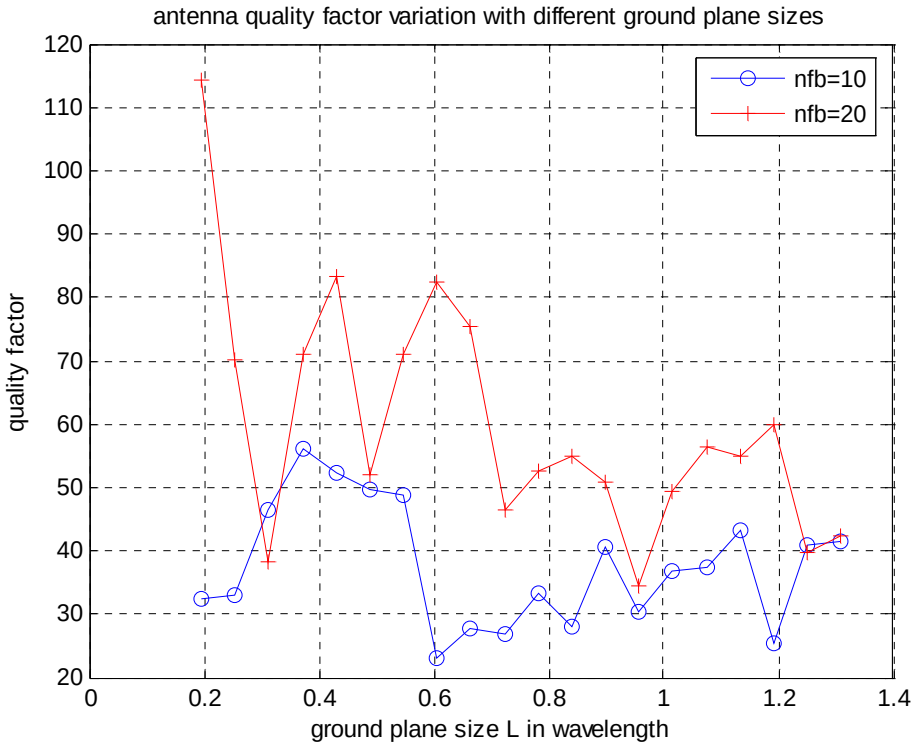

Figure 5.8: Antenna quality factor with different ground plane sizes.

Fig. 5.8 shows an oscillating trend for the antenna quality factor, which asymptotic behaviour is not clear.
This may be explained by the fact that only when the ground plane size is large compared to one wavelength we can expect a fair convergence.
Fig. 5.9 shows that the resonance frequency finally seems to converge to the perfect ground plane value as expected.

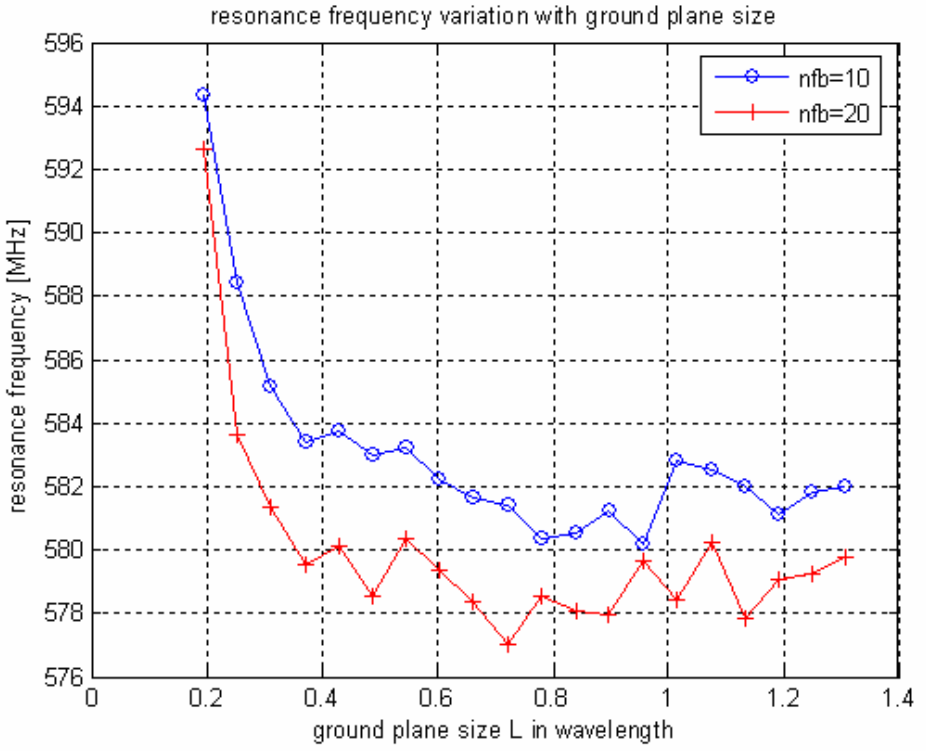

Figure 5.9: Antenna resonance frequency with different ground plane sizes.

Now we show the behaviour of both real and imaginary parts of the antenna input impedance, calculated in the correspondence of the resonance frequency.
We remind that we defined the resonance frequency that frequency value where the reactance is equal to the mean of the maximum and minimum reactance values.
A variation in the antenna input impedance implies a correspondent modification of the quality factor, that is influenced also by the slope of the reactance.
From fig. 5.10, 5.11 we see a sort of convergence in the impedance values, as the ground plane size increases.
The influence of the near field boundaries unit cells at this point is not clear.

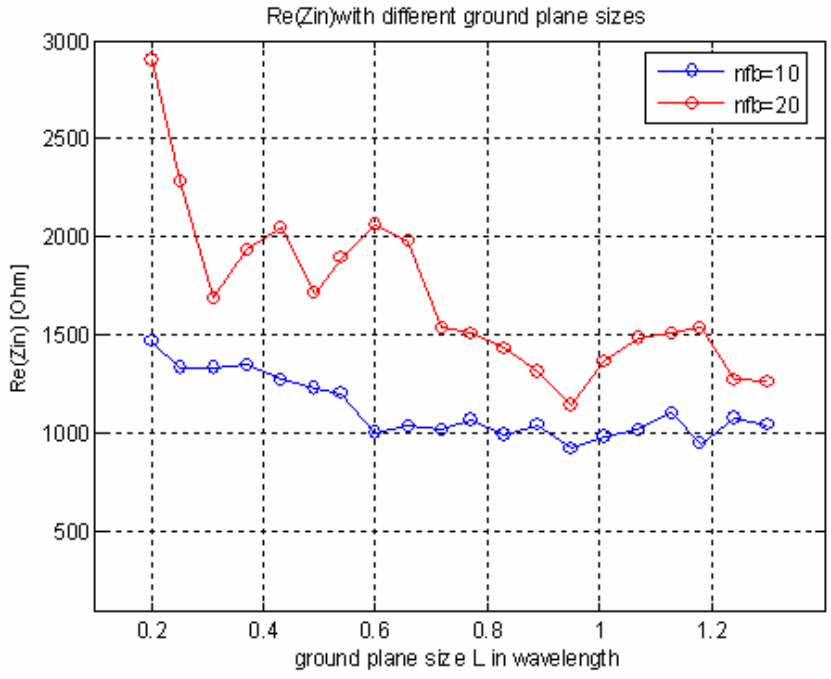

Figure 5.10: Re(Zin) with different ground plane sizes.

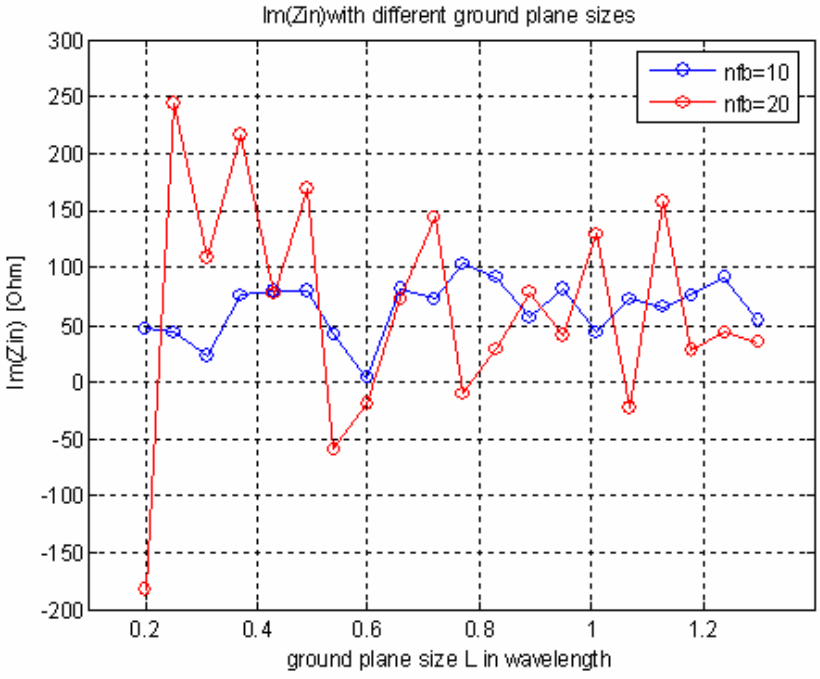

Figure 5.11: Im(Zin) with different ground plane sizes.

5.3.3: Effect of the variation of the number of near field boundaries cells.

In order to understand the necessary number of "nfb" cells to appreciate a fair convergence in the parameters investigated, we vary nfb from 15 to 50 cells, where the size of each cell is still 5mm.
In this investigation we use the same pifa geometry, with a ground plane size L =220mm.

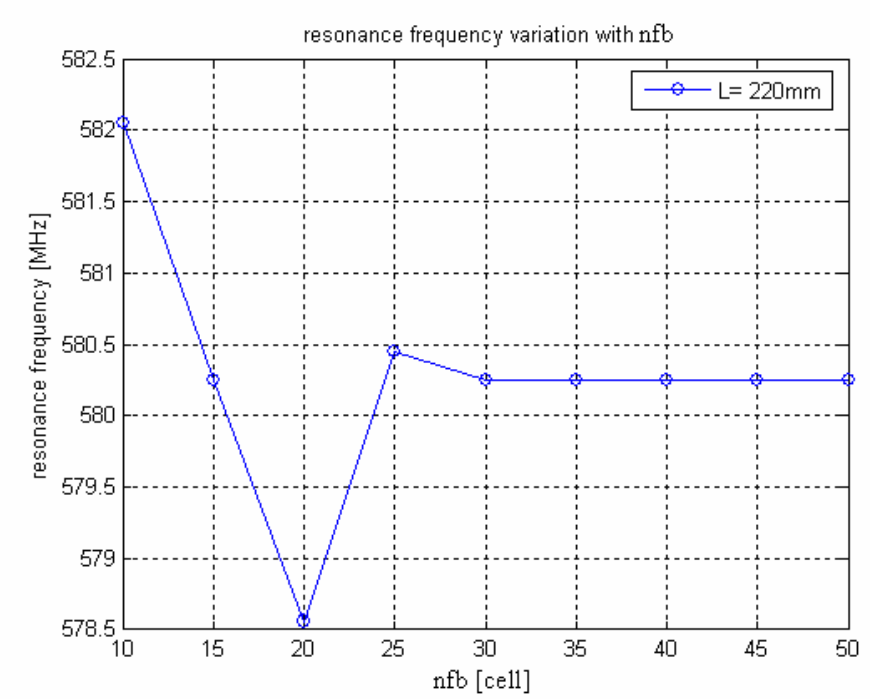

Figure 5.12: resonance frequency variation with nfb.

From fig. 5.12 we can see as the resonance frequency becomes stable when nfb approaches 30 cells.
Fig. 5.13 show that the quality factor converges after 40 unit cells.
Similarly, as we can see from fig. 5.14, 5.15, both real and imaginary parts of the antenna input impedance seem to converge after 40 unit cells.
The previous behaviour suggests to use in the next 40 "nfb" cells for the ground plane size variation. This would avoid unwanted oscillations in the results for different nfb values.

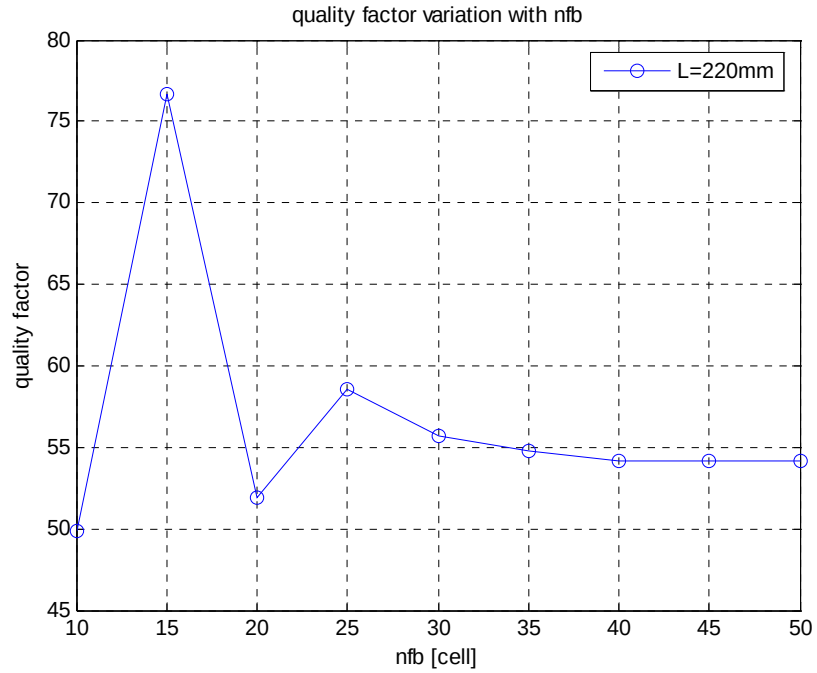

Figure 5.13: quality factor variation with nfb.

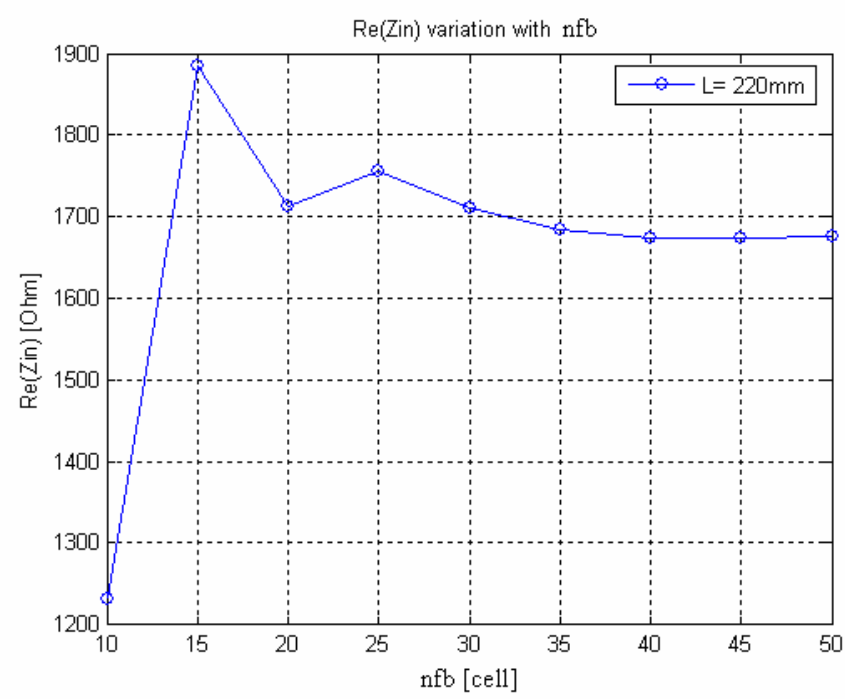

Figure 5.14: Re(Zin) variation with nfb.

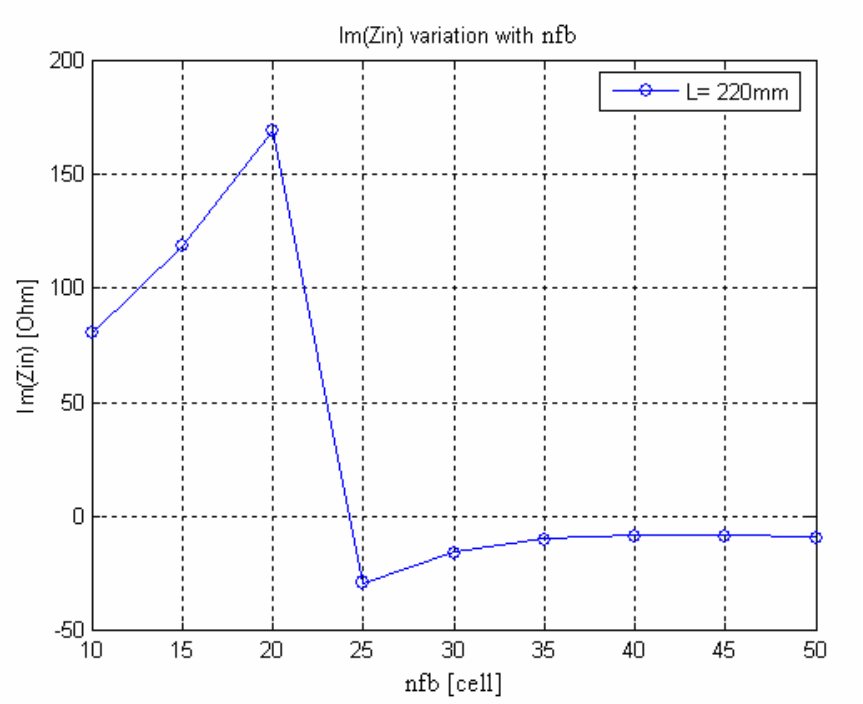

Figure 5.15: Im(Zin) variation with nfb.

Now, imposing a number of near field boundaries cells = 40, we derive tendencies for the antenna quality factor and the resonance frequency as before, varying at each step the ground plane size.

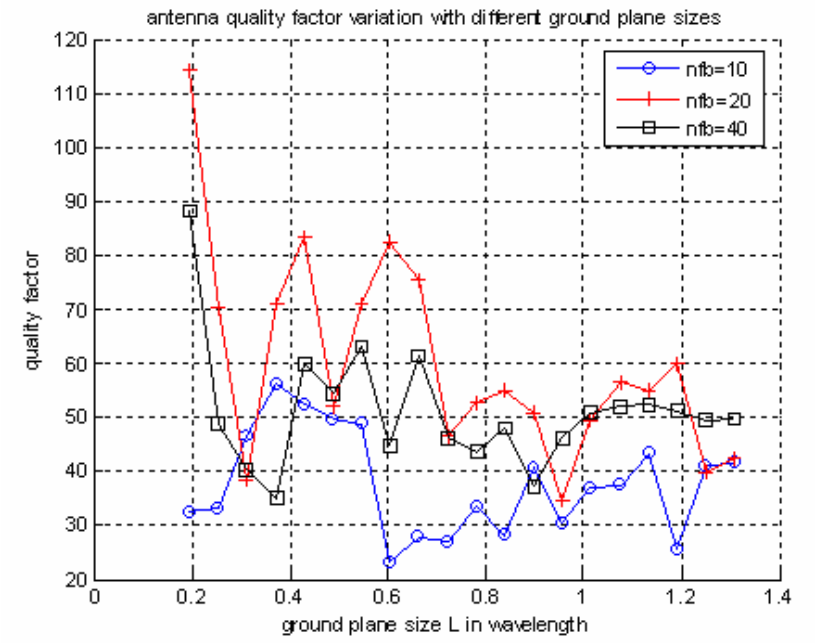

Figure 5.16: antenna quality factor variation with different ground plane sizes.

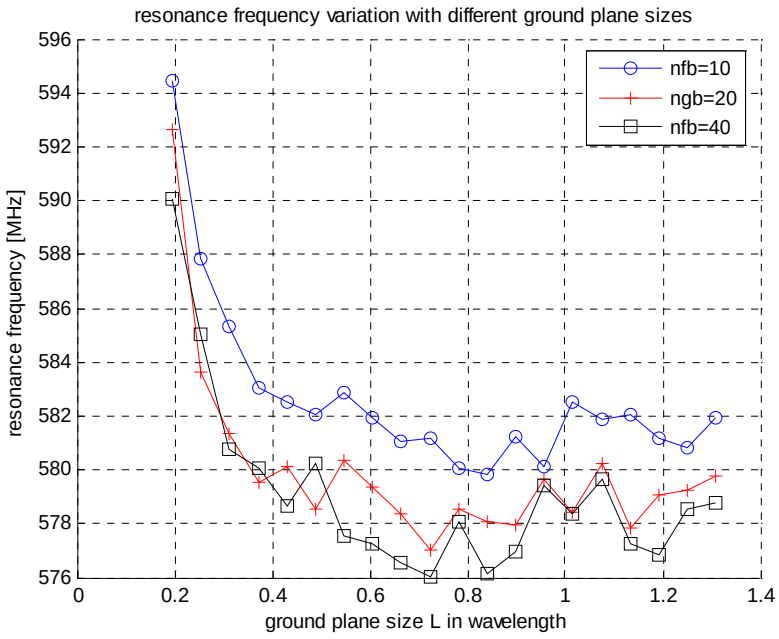

Figure 5.17: resonance frequency variation with different ground plane sizes.

As we can see from fig. 5.16 the quality factor really seems to converge with both ground plane size and number of "nfb" cells. The oscillation of the Q is clearly around 50.
Regarding the resonance frequency (fig. 5.17), we experience a similar behaviour as before, because of the fact that a convergence is fairly clear.

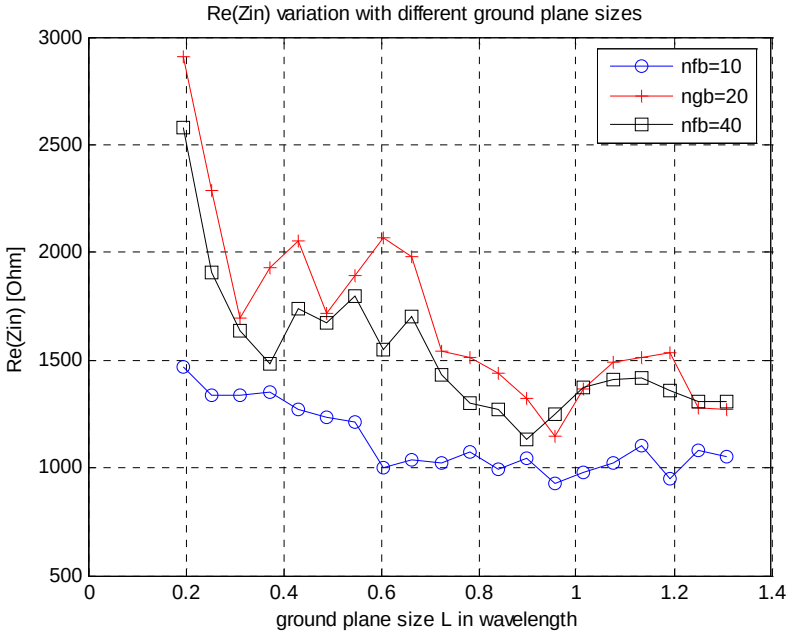

Figure 5.18: Re(Zin) variation with different ground plane sizes.

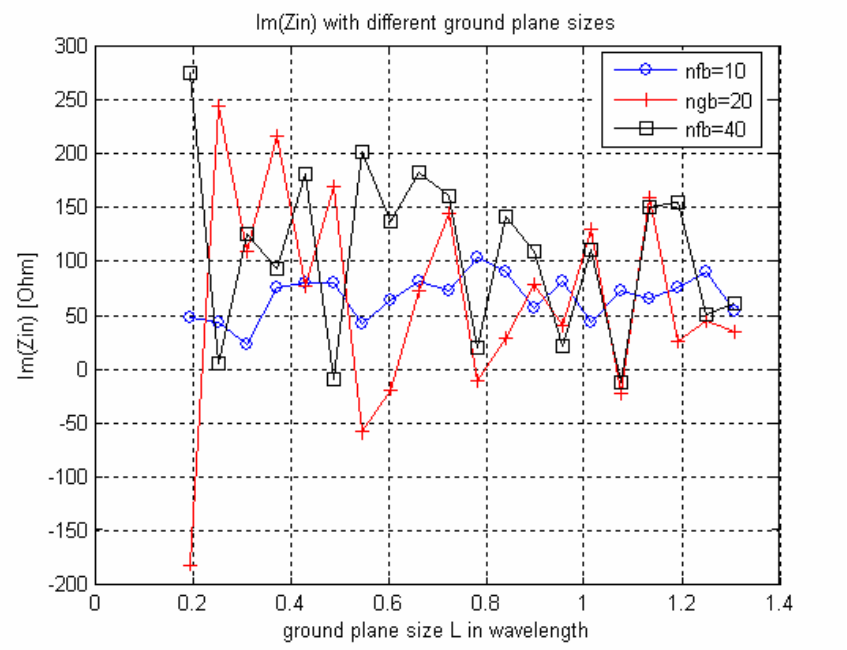

Figure 5.19: Im(Zin) variation with different ground plane sizes.

Fig. 5.18, 5.19 show the behaviour of the antenna input impedance, and even if its real part seems to finally converge, the imaginary one has more oscillations.
We conclude that when we deal with simulation of pifa antennas over a planar ground plane, it is very important to choose the size of this ground plane large enough to appreciate a convergence in the resonance frequency and the quality factor.
However, we have only limited computational resources, and sometime it is a very heavy burden for the calculator to simulate structures with a large number of FDTD cells, that results in a corresponding dramatic increase in simulation time.
Regarding the number of near field boundaries cells, it needs to be chosen properly, but it contributes to enlarge the computational domain too.
It is understood that a trade-off between accuracy of results and computational resources is necessary.

5.4: Tuning of a pifa antenna with lumped components investigations.

5.4.1: Introduction.

In this first simulation set we investigate the tuning capabilities of a lumped capacitor in a conventional pifa antenna. This capacitor will be modelled thanks to the algorithm developed during this Master Thesis [App. A, C].
We define the following parameters:

- lb [mm]: length of the metal chassis box.
- wb [mm]: width of the metal chassis box.
- hb [mm]: height of the metal chassis box.
- hsc [mm]: height of the short circuit plate.
- wsc [mm]: width of the short circuit plate.
- L1 [mm]: not short circuit side of the pifa.
- L2 [mm]: short circuit side of the pifa.
- L1off [mm]: x-oriented offset of the pifa.
- L2off [mm]: y-oriented offset of the pifa.
- feed1 [mm]: x-oriented offset of the feed.
- feed2 [mm]: y-oriented offset of the feed.
- lum1 [mm]: x-oriented offset of the lumped element.
- lum2 [mm]: y-oriented offset of the lumped element.

We have a structure composed by a chassis metal box and a pifa antenna with the following geometric parameters:

lb[mm]	wb [mm]	hb [mm]	hsc [mm]	wsc [mm]	L1 [mm]
100	20	70	15	0	80
L2 [mm]	L1off [mm]	L2off [mm]	feed1 [mm]	feed2 [mm]	
20	0	0	20	10	

Table 5.4: geometric parameters of the simulated pifa antenna.

The capacitor, with z-axis orientation, will be placed between the ground plane and the top plate element, with a capacity ranging from 0.1pF to 1pF.
The antenna without capacitor resonate at 614MHz with a quality factor of 19.
The following figures show the spatial representation of the simulated structure in the XY and XZ planes respectively.

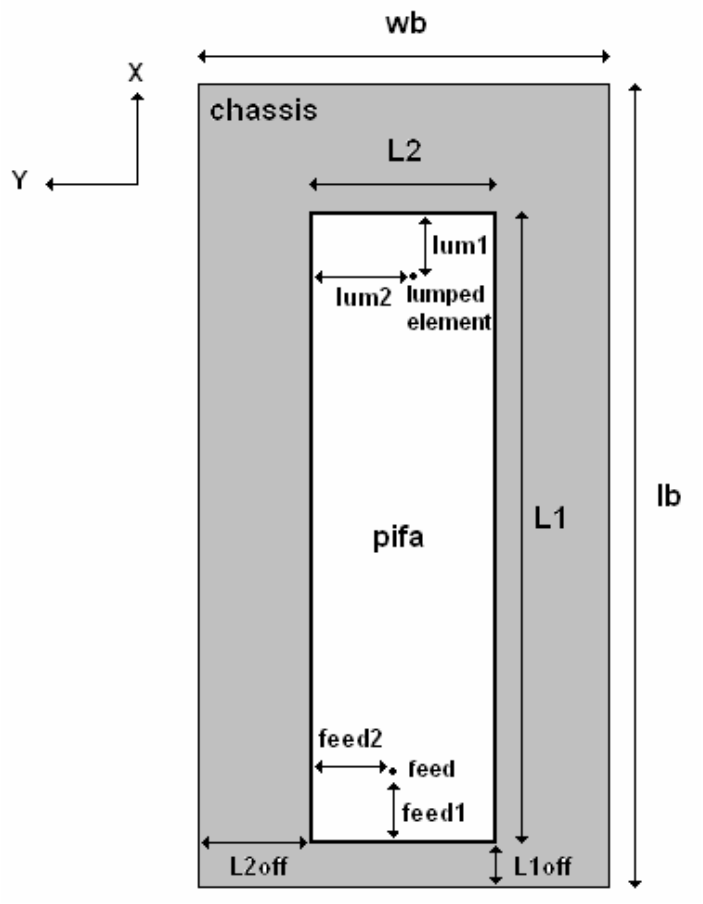

Figure 5.20: Pifa geometry in the XY plane.

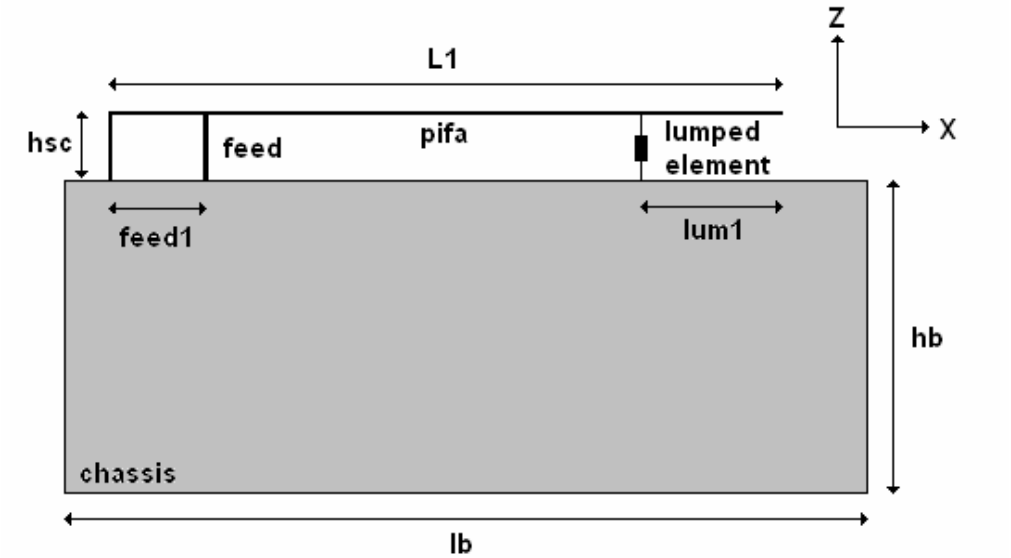

Figure 5.21: Pifa geometry in the XZ plane.

5.4.2: Capacity variation.

In this simulation set we keep fixed the position of the capacitor, and we vary only the capacity ranging progressively from 0.1pF to 1pF.
The capacitor will be placed in the z-direction, in the middle of the pifa's top plate, at a distance of one cell from the plate end, that is, looking at figures 5.20, 5.21:

- lum1=5mm.
- lum2=10mm.

We will demonstrate that it is possible to tune the resonance frequency of the antenna introducing a load capacity, that will vary the correspondent electrical length of the antenna and may excite higher order modes.
High values of capacity correspond to a short circuit behaviour, while low capacity values can be seen as an open circuit behaviour.
A proper choice of the capacity allows to tune the resonance frequency in a controlled way.
We will investigate also what happens to the antenna quality factor as the capacity varies, in order to better understand the tuning capabilities of this approach.

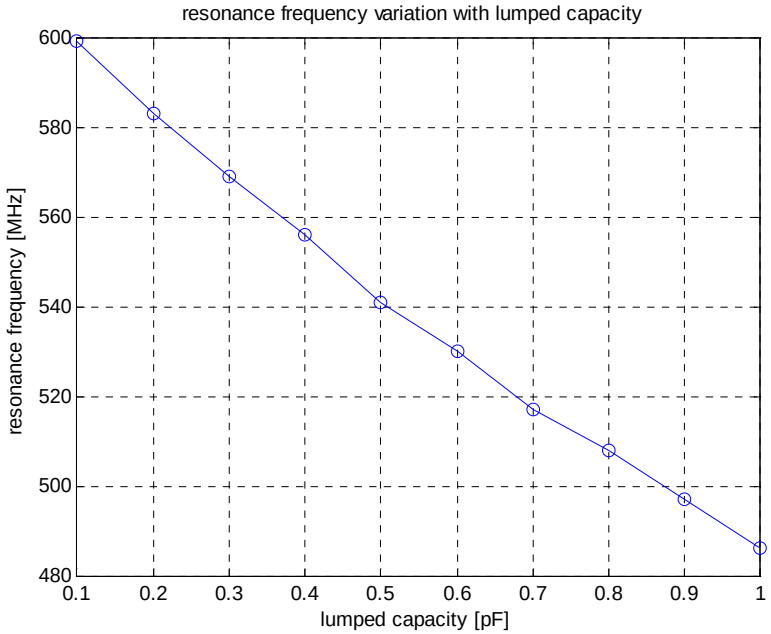

Figure 5.22: resonance frequency variation with lumped capacity.

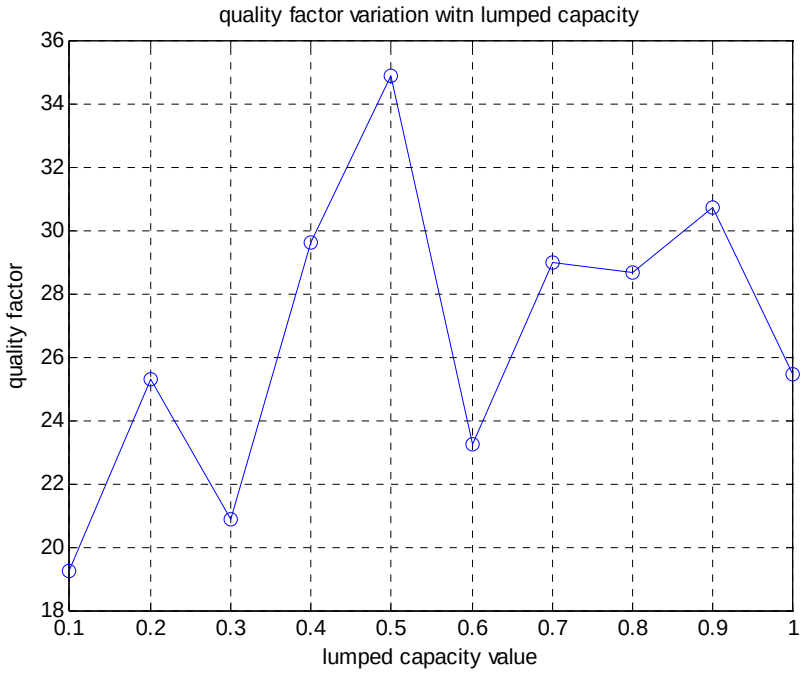

Figure 5.23: quality factor variation with lumped capacity.

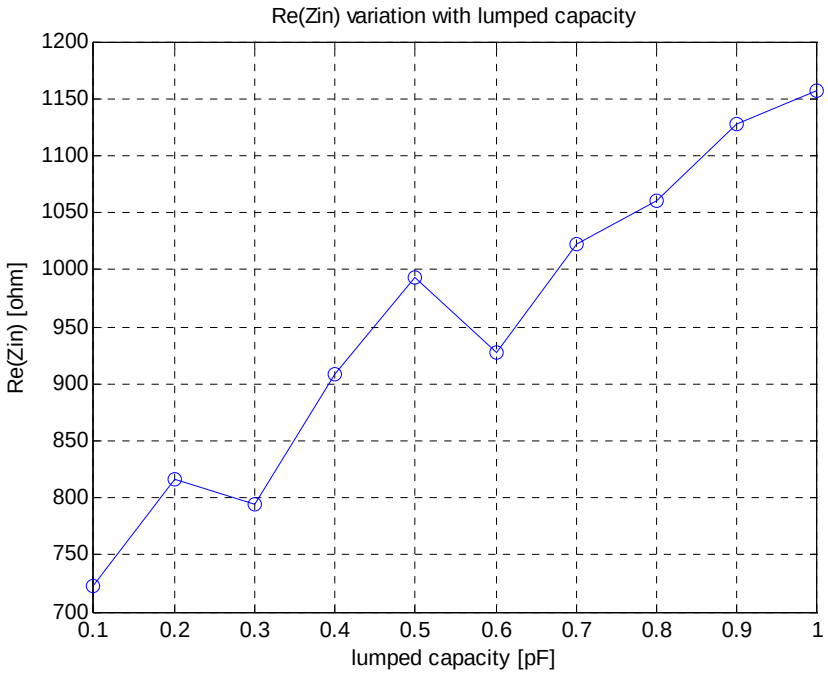

Figure 5.24: Re(Zin) variation with lumped capacity.

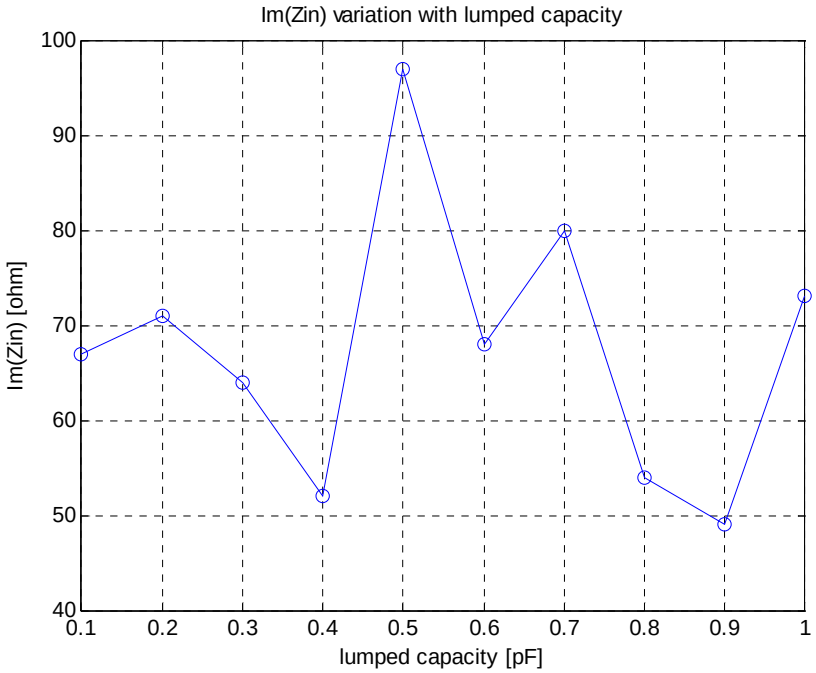

Figure 5.25: Im(Zin) variation with lumped capacity.

As we can see from fig. 5.22, the resonance frequency linearly decreases as the capacity increases, while looking at fig. 5.23, the quality factor seems to show a growing tendency, with a correspondent decrease in the relative bandwidth as the capacity increases.
Fig. 5.24 shows that the real part of the antenna input impedance increases as the capacity increases, while the imaginary part doesn't show a clear tendency.

5.4.3: Offset variation.

In the next simulation set we keep fixed the value of the capacity to 1pF, while we vary its position from the upper plate end towards the feeding point with steps of 5mm.
In the next we will rename lum1 "offset", for ease of notation.

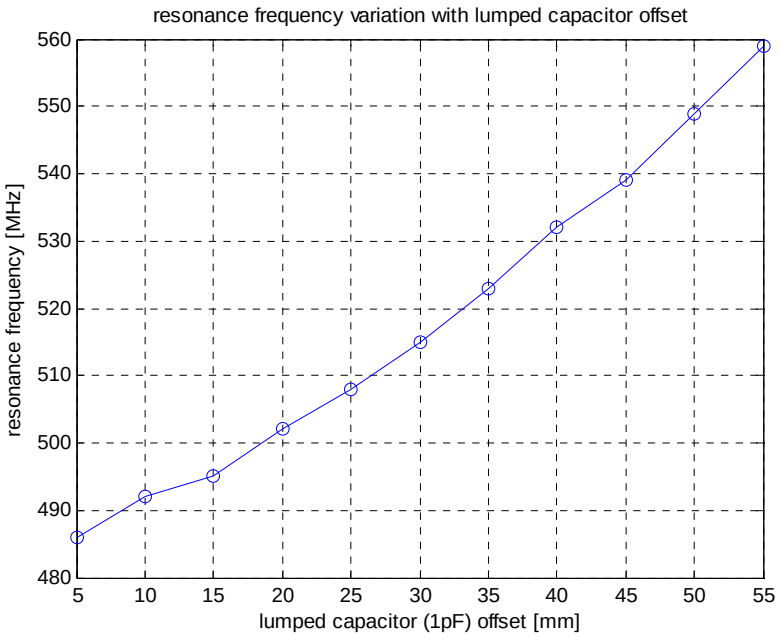

Figure 5.26: resonance frequency variation with lumped capacitor offset.

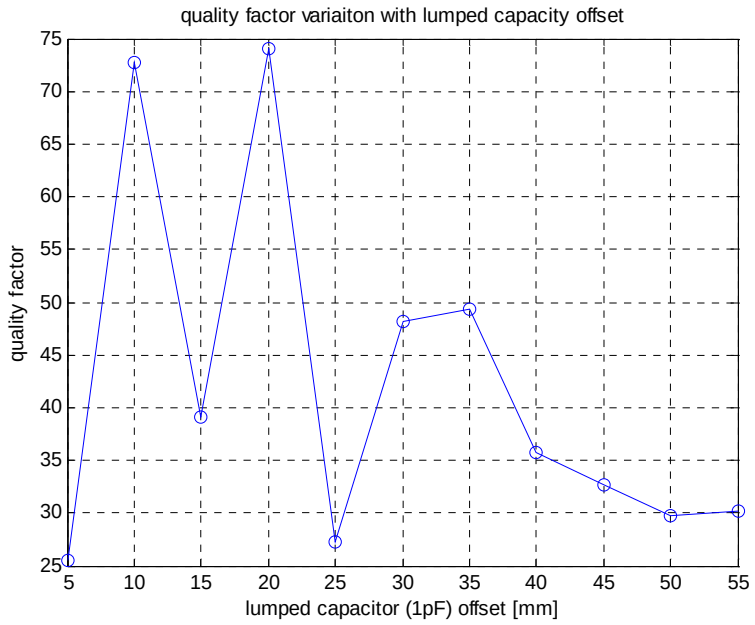

Figure 5.27: quality factor variation with lumped capacitor offset.

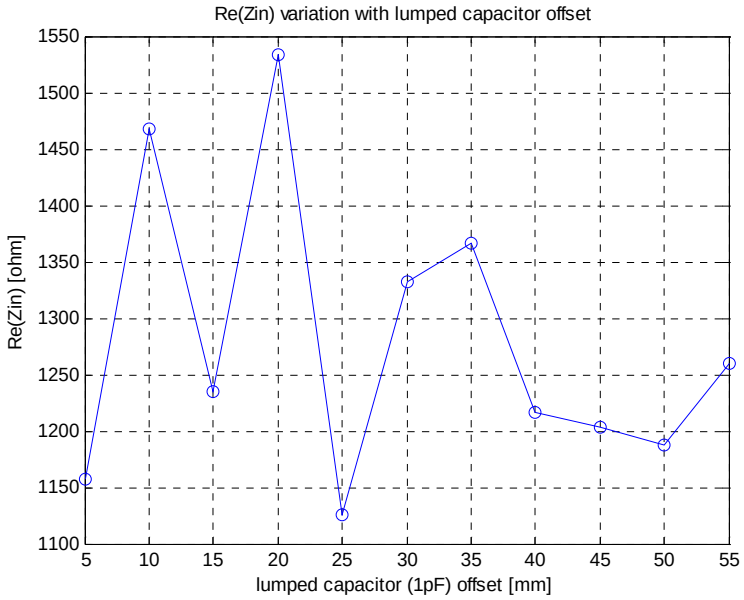

Figure 5.28: Re(Zin) variation with lumped capacitor offset.

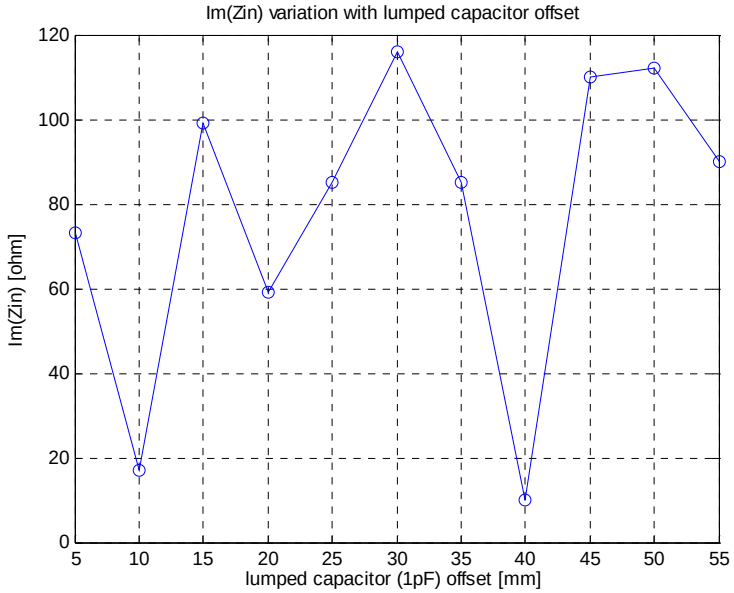

Figure 5.29: Im(Zin) variation with lumped capacitor offset.

Fig.5.26 shows that the resonance frequency increases as the offset increases.
We remind that a large offset corresponds to a location of the lumped capacitor near the feed. No tendencies can be derived for the antenna quality factor and input impedance.

5.4.4: Combined capacity and offset variation.

Now we combine the previous investigations varying the capacity between 0.1 pF and 1 pF and modifying the offset at the same time.
We do this in order to derive more clear tendencies; so we have 4 simulation sets, where in each set the offset is fixed and the capacity varies in 10 steps from 0.1pF to 1pF.
As we can see from fig.6.30, the resonance frequency decreases as the capacity increases.
The tendency is fairly linear, but with different slope depending on the offset.
When the offset is large, we are placing the capacitor near the feed, where we observe a reduction in the tuning range. The explanation of this behaviour may be the effective excitation of higher order modes as the offset is placing the capacitor near the feed.
Another effect we notice is that for large capacity values, the offset modification gives a high tuning range.
We can explain this by the fact that when the capacity is large, it looks electrically more like a short circuit than an open circuit.
If it looks more like a short circuit, it is more sensitive to the offset, because we are changing the electrical length of the top antenna plate and the excitation of higher order modes is more stressed.
To obtain the maximum tuning range, it seems that we have to choose the capacity location near the end of the plate.
However, if we want to use capacity levels greater than 1pF, we have to investigate in the next what happens if we choose the location of the lumped capacitor near the feed.

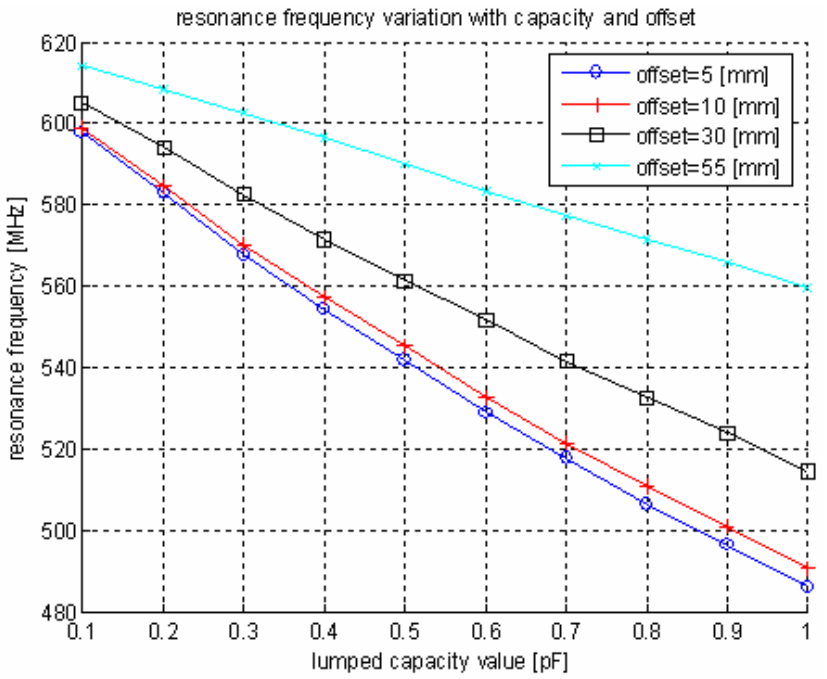

Figure 5.30: resonance frequency variation with capacity and offset.

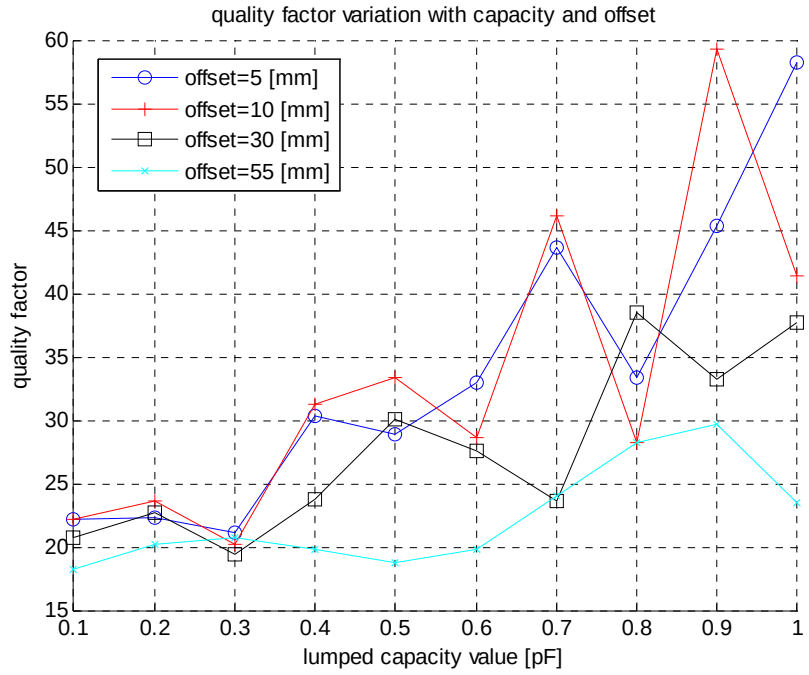

Figure 5.31: quality factor variation with capacity and offset.

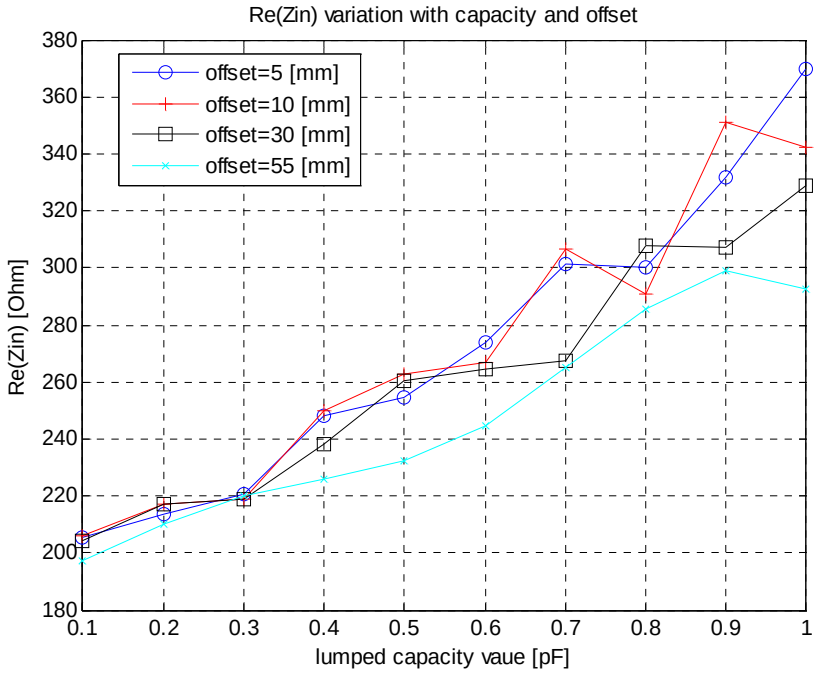

Figure 5.32: Re(Zin) variation with capacity and offset.

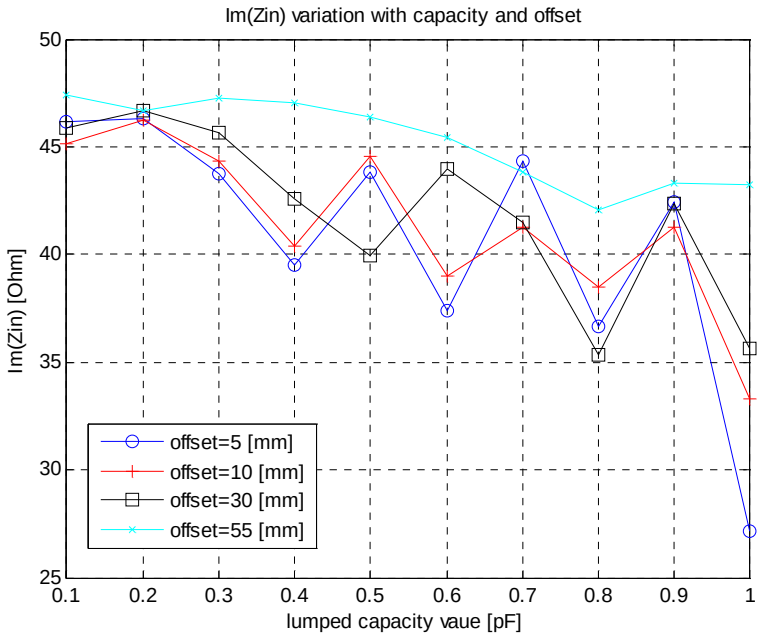

Figure 5.33: Im(Zin) variation with capacity and offset.

Fig. 5.31 describes the quality factor variation as the capacity and the offset change.
The quality factor seems to grow with capacity, and this tendency is less evident when the offset is large, that corresponds to a capacitor placed near the feed.
In fig. 5.32 it is shown the real part of the antenna input impedance, and we observe a clear growing tendency with the capacity.
When the offset is large, the resistance increase is reduced.
This behaviour of course influences the quality factor.
In fig. 5.33 the imaginary part of the antenna input impedance has quite similar behaviour as the offset varies, but regarding the capacity it oscillates, justifying the inherent small randomness in the quality factor.
The inherent problem of using small capacity values is that if we substitute the varying capacitor with a varactor, we will have some difficulties in finding such a component, because of both manufacturing limitations and parasitic effects.
For all these reasons, the next investigations will focus on the establishment of a proper trade-off between capacity values and antenna performances.

5.4.5: Capacity variation in a broader range.

In order to have a better understanding of the effects of a lumped capacitor placed between the pifa top plate and the chassis, we vary now the capacity value in a broader range. The lumped capacity will vary between 0.1pF and 3pF:

capacity	capacity1	capacity2	capacity3	capacity4
value [pF]	0.1	1	2	3

Table 5.5: lumped capacity variation.

Higher and smaller capacity values were tried, but the obtained results were out of our frequency band of interest (470MHz-702MHz).
Now the pifa is slightly different; only the feeding point is moved closer to the short circuit plate, in order to get a better impedance matching only with the feed positioning.
We did this also to make a larger capacity offset variation.
The offset is defined as before, and we vary its position from the upper plate end towards the feeding point with steps of 5mm.
We will have the following offset values:

offset	offset1	offset2	offset3	offset4	offset5	offset6	offset7
value[mm]	0	5	10	15	20	25	30
offset8	offset9	offset10	offset11	offset12	offset13	offset14	offset15
35	40	45	50	55	60	65	70

Table 5.6: offset variation starting from the upper plate end towards the feeding point (see fig. 5.20-5.21).

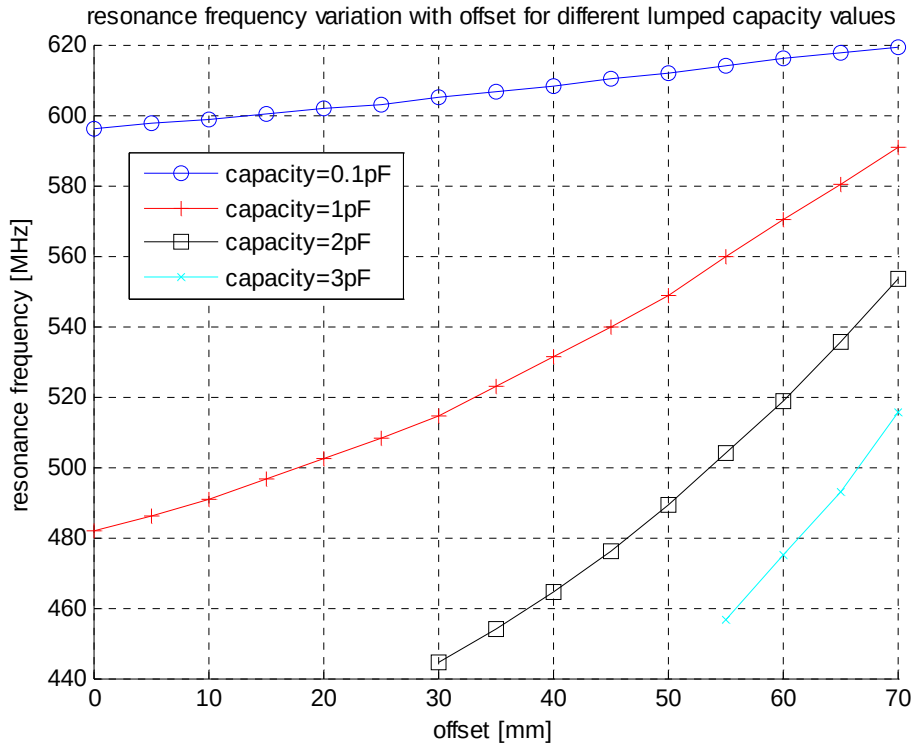

Figure 5.34: resonance frequency variation with offset for different lumped capacity values.

Fig. 5.34 shows what happens when both offset and capacity vary.
One clear tendency is that the resonance frequency increases when the offset grows, that simply mirrors the fact that we are moving closer and closer towards the feeding point.
However the curves with higher capacity values are steeper, because in this situation the lumped capacitor acts more like a short circuit.

At first glance it would be attractive to choose high capacity values and a small offset, because what we really want is a tuning of the antenna resonance frequency with a reduced capacity variation, but this will result in a deterioration in antenna performances, as is shown in the following.
In fact, if we look at the variation of the antenna quality factor with offset for different lumped capacity values in fig. 5.35, the Q decreases as both offset and lumped capacity increase.
This effect is more dramatic when the lumped capacity is greater than 1pF, so that a sort of trade-off between tuning range and antenna performances has to be found if possible.

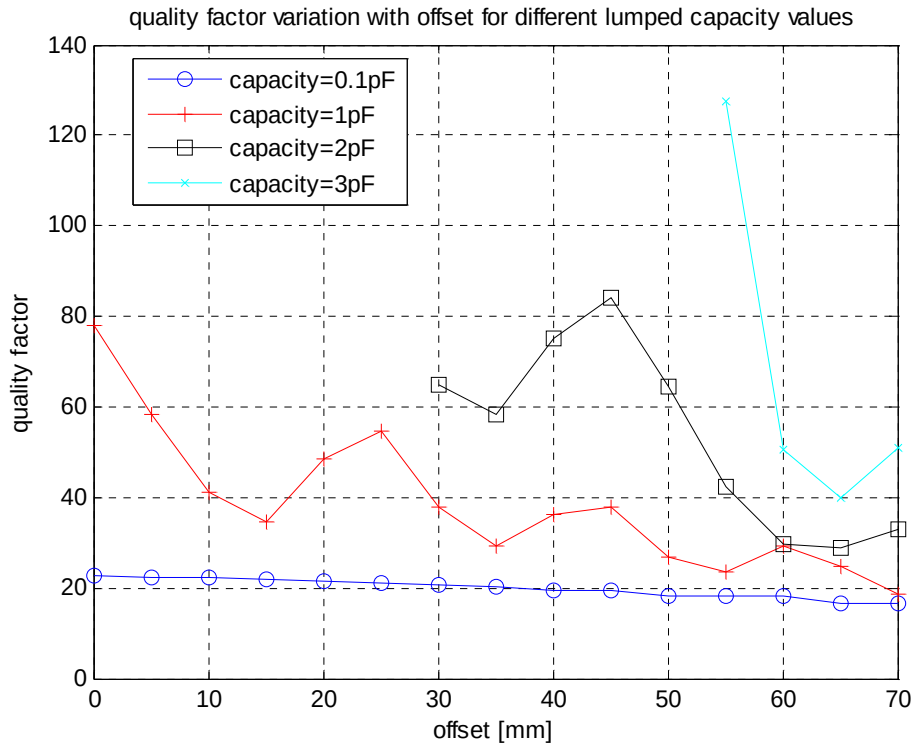

Figure 5.35: quality factor variation with offset for different lumped capacity values.

As we can see in fig. 5.36 the antenna impedance bandwidth, that we defined earlier in the project delimitations, is affected by both lumped capacity value and offset. A small offset and a high capacity value correspond to a dramatic deterioration in impedance bandwidth, that decreases fast to zero.
This will make it very difficult to establish the aforementioned trade-off between tuning range and antenna performances.
Fig. 5.37, 5.38 show the variation of the antenna input impedance, that affects the quality factor and then the impedance bandwidth. A possible impedance matching would be possible only for small capacity values, because in that cases the impedance variation over the desired frequency band is limited.

If this antenna configuration would be ok for a narrower frequency band, in our situation the drawbacks are larger than the advantages.
This lead us to migrate towards other antenna configurations, to see if it is possible to satisfy our requirements.

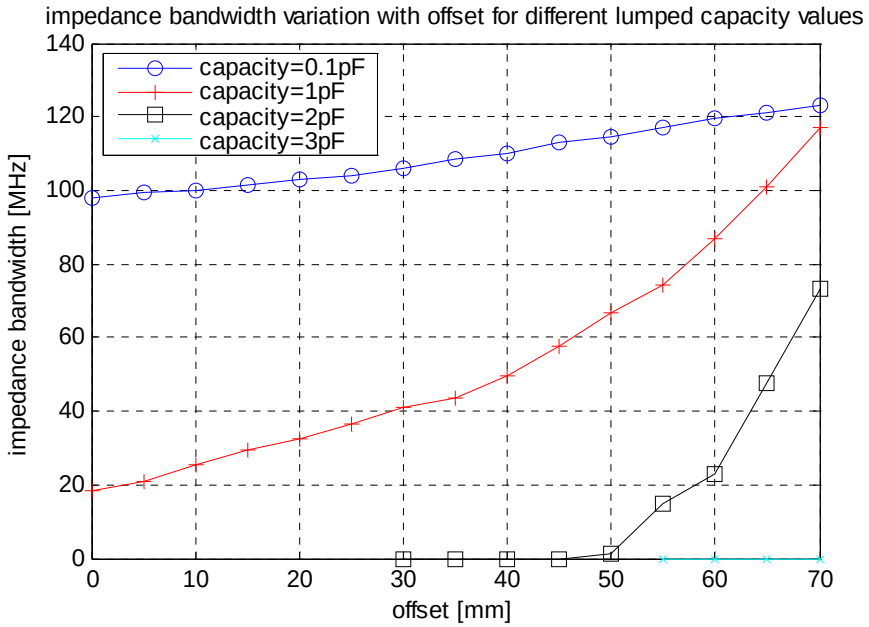

Figure 5.36: impedance bandwidth variation with offset for different lumped capacity values.

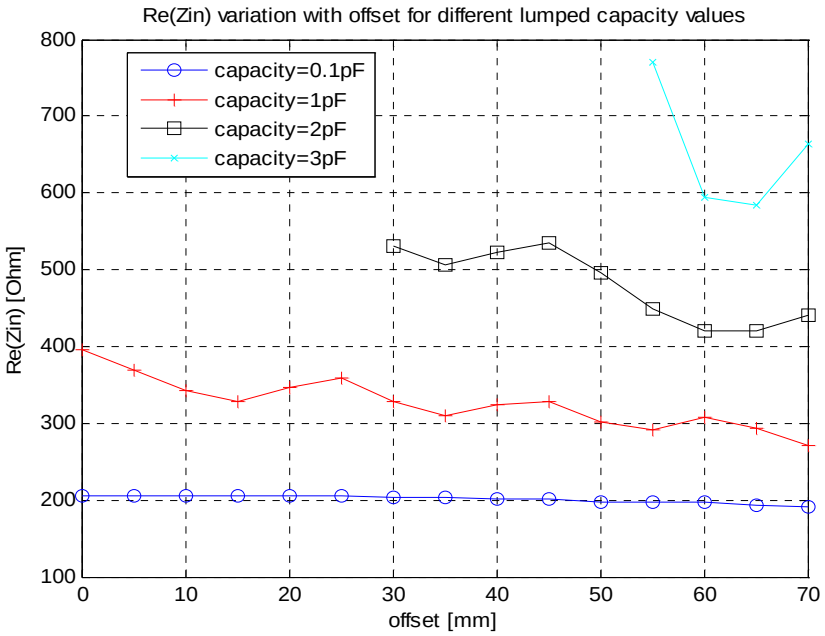

Figure 5.37: Re(Zin) variation with offset for different capacity values.

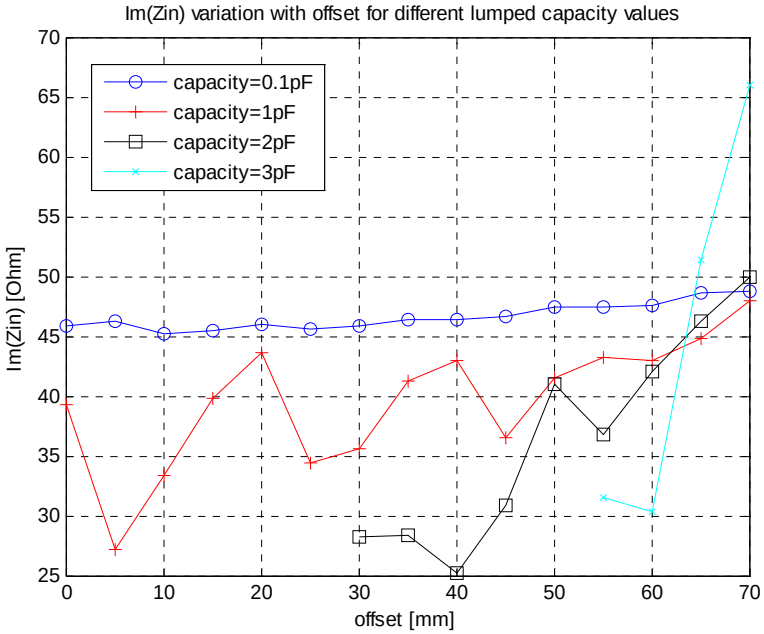

Figure 5.38: Im(Zin) variation with offset for different lumped capacity values.

5.4.6: Comparasion between two different simulators.

Now with one example we compare the results obtained with the FDTD program developed at Aalborg University (AAUFDTDP) with the commercial software CST Microwave Studio (CSTMS) regarding the implementation of lumped components.
We will have a capacitor with a series resistor, and we will vary progressively the resistance value from 1 Ω to 30 Ω, keeping the capacity fixed to 1pF.
The antenna geometry is similar to the previous simulations, so that now we will place between the ground plane and the top plate element a series made up by a resistor and a capacitor, with z-axis orientation.
The capacitor-resistor series will be placed in the z-direction, in the middle of the pifa top plate, at a distance of 20mm from the plate end, that is, looking at figure 5.20, 5.21:

- lum1=20mm.
- lum2=10mm.

We expect that the variation of the resistance will imply a corresponding modification of the real part of the antenna input impedance.
Figure 5.39 shows a decreasing trend for the real part of the antenna input impedance in both simulators.
It seems there is a quite good agreement between the two simulators, and the differences experienced may be explained by the intrinsic differences of the two approaches.
In a similar way, we put a coil in the same location as before, and we look at the resonance frequency variation as we modify the inductance value from 75nH to 300nH.

When the inductance is very high, a coil behaves like an open circuit, while when the inductance is very small, it behaves like a short circuit.
Fig. 5.40 shows that the resonance frequency decreases as the inductance grows in both simulators, and even if the two curves seems to differ because of an initial frequency shift, the tendencies are quite the same.

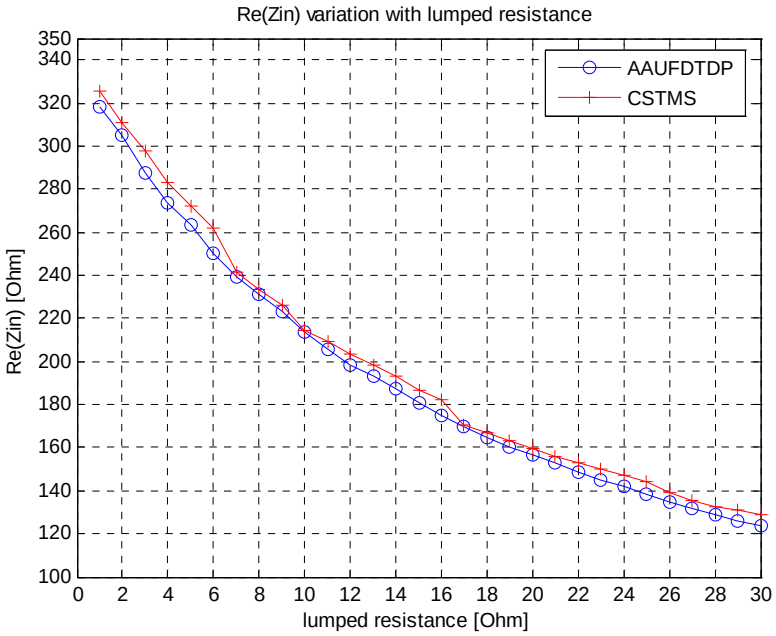

Figure 5.39: Re(Zin) variation with lumped resistance.

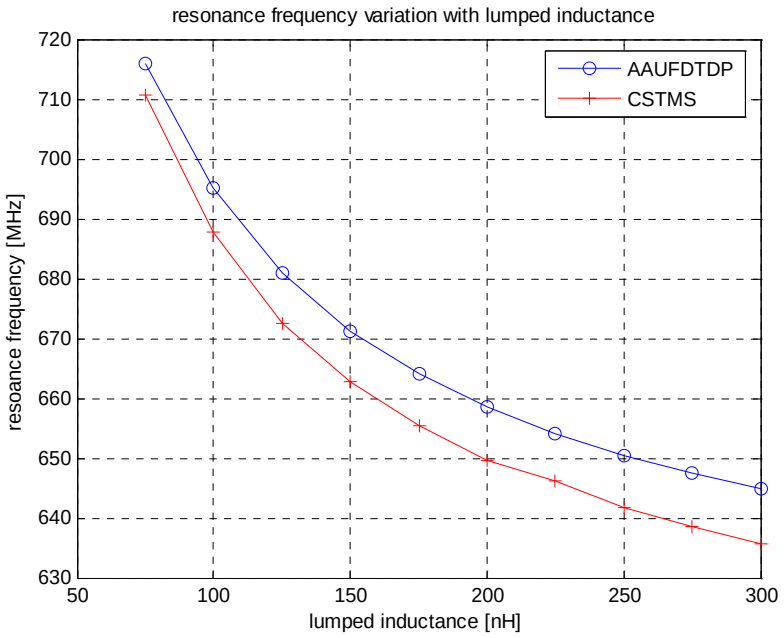

Figure 5.40: resonance frequency variation with lumped inductance.

5.5: Tuning of a meandered pifa antenna.

5.5.1: Introduction.

There are several ways to design pifa antennas which resonance frequency can be tuned.
Instead of placing a varactor between the metal chassis box (that act as a ground plane) and the pifa top plate as in section 5.4, thanks to the paper of Virga [5.3] we suggest a new configuration, where the top plate is meandered and divided properly in two parts, that will dictate the lower and higher resonance frequencies. These two parts will then be connected with one varactor, placed in correspondence of one of the two top plate side edges; in fact the current is stronger in those locations, and this allows a larger tuning range.
When the capacity provided by the varactor is very small (in the limit zero), it acts like an open circuit, disconnecting the two sections of the pifa.
This will correspond to the superior resonance frequency bound.
On the other hand, when the capacity is very high (in the limit infinite), the varactor acts like a short circuit, connecting the two sections of the pifa.
This will correspond to the inferior resonance frequency bound.
If we had the capability of a capacity variation over the whole capacity range $[0,\infty]$, we could in the ideal case have a higher tuning possibility.
Unfortunately, real varactors provides only a finite tuning range.
However, we will show that thanks to the asymptotic behaviour of the capacity variation, it is possible to tune the resonance frequency with a limited varactor tuning range.
One of the disadvantage of this configuration, is that the top plate has to be increased in length in order to provide a proper inferior frequency bound.
Because of this, we had to meander the pifa top plate, in order to reduce at minimum the volume occupation of the antenna.
The main advantage of this configuration is that the capacity range is in the order of several pF. In fact it is difficult to find commercial varactors with very small capacity values, because they are difficult to manufacture and more influenced by parasitic effects.

We define the following parameters:

- lb [mm]: length of the chassis metal box.
- hb [mm]: height of the chassis metal box.
- wb [mm]: width of the chassis metal box.
- L1 [mm]: not short circuit length of the pifa.
- L1pm [mm]: length of the meandered section.
- L2 [mm]: short circuit length of the pifa.
- L2pm [mm]: width of the meandered section.
- feed1 [mm]: x-oriented offset of the feed.
- feed2 [mm]: y-oriented offset of the feed.
- hsc [mm]: height of the short circuit plate.
- hpm [mm]: height of the meandered plate.
- wsc [mm]: width of the short circuit plate.
- frsim [MHz]: resonance frequency obtained by simulation.
- Q: antenna quality factor.
- Zin [Ohm]: antenna input impedance.
- Re(Zin) [Ohm]: real part of Zin.
- Im(Zin) [Ohm]: imaginary part of Zin.

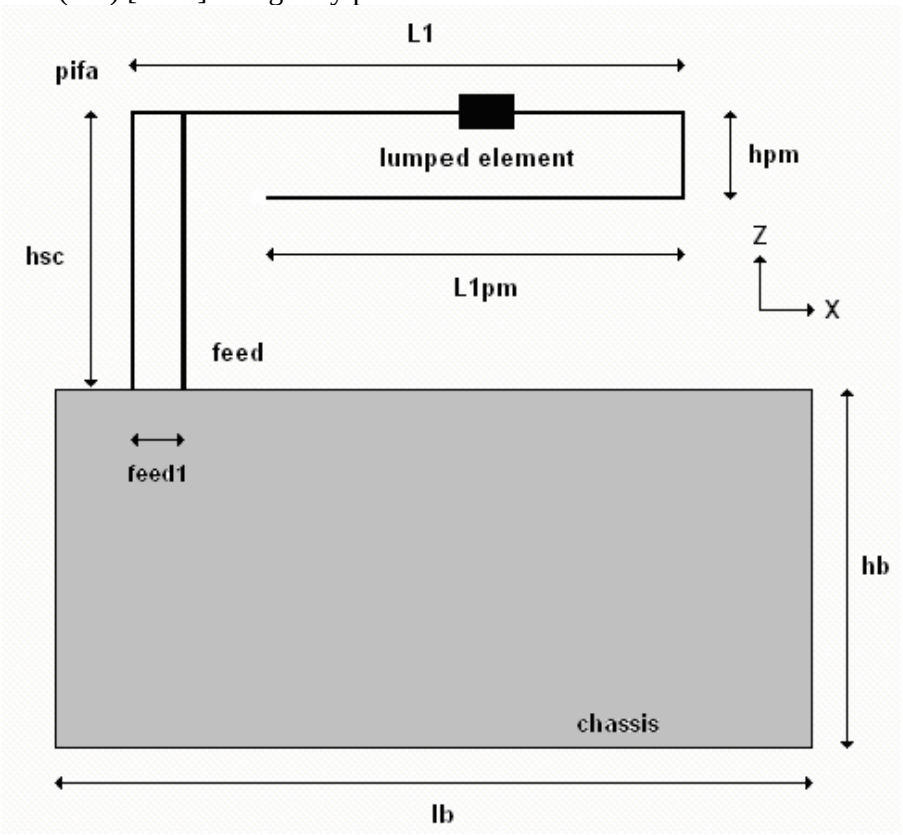

Figure 5.41: antenna geometry in the XZ plane (the drawing is not in scale to better display the meandered pifa antenna: for more details see fig. 5.61).

5.5.2: Simulation of a meandered pifa antenna.

So we specify in the next table the antenna geometric parameters:

lb [mm]	wb [mm]	hb [mm]	L1 [mm]	L2 [mm]	L1pm [mm]
100	20	70	90	20	70
L2pm [mm]	feed1 [mm]	feed2[mm]	hsc[mm]	hpm [mm]	wsc [mm]
20	5	5	15	5	0

Table 5.7: geometric parameters for the meandered pifa antenna.

We introduce a lumped capacitor, and varying its capacity we will see what sort of varactor is needed to perform the required tuning of the antenna resonance frequency.
Looking at fig. 5.41, we will place the lumped elements in the space of separation of the two plates of the meandered pifa antenna.
This space will be of 5mm that corresponds to one cell in the FDTD algorithm.
So the lumped capacitor will be placed after 80mm from the short circuit plate in the x direction, placed in correspondence of the top plate side edge located at y = 0.
We will have finally two plates, each of them 80mm long.
We will vary the capacity of these lumped elements doing a proper sampling of the capacity range $[0,\infty]$.
We will have eight capacity values:

c1 [pF]	c2 [pF]	c3 [pF]	c4 [pF]	c5 [pF]	c6 [pF]	c7 [pF]	c8 [pF]
0	0.1	1	5	10	20	100	∞

Table 5.8: tuning capacity values.

We will simulate the lumped capacitors thanks to the FDTD algorithm, but to model the case in which the capacity is zero or infinity, we will modify the structure disconnecting the lumped components in the first case, and adding a short circuit in the latter.
As we can see from fig. 5.42, varying the capacity between 1pF and 10pF it is possible to have an acceptable tuning of the antenna resonance frequency.
In fact what we observe is a saturation effect in the capacity variation, so that capacity values near to zero or infinity, lead to small variation in resonance frequency because of the experienced asymptotic behaviour.
This property seems to be promising, because of the necessity to deal with real varactors, which capacity tuning range is finite and limited.
Fig. 5.43 shows that the antenna quality factor grows with capacity, but its variation is not so high, so that the relative impedance bandwidth is similar nearly for all the tuning steps between 1pF and 20pF.
Fig. 5.44, 5.45 show the behaviour of the antenna input impedance, which variation over the tuning range is limited, so that it would be relatively easy to provide a possible impedance matching.

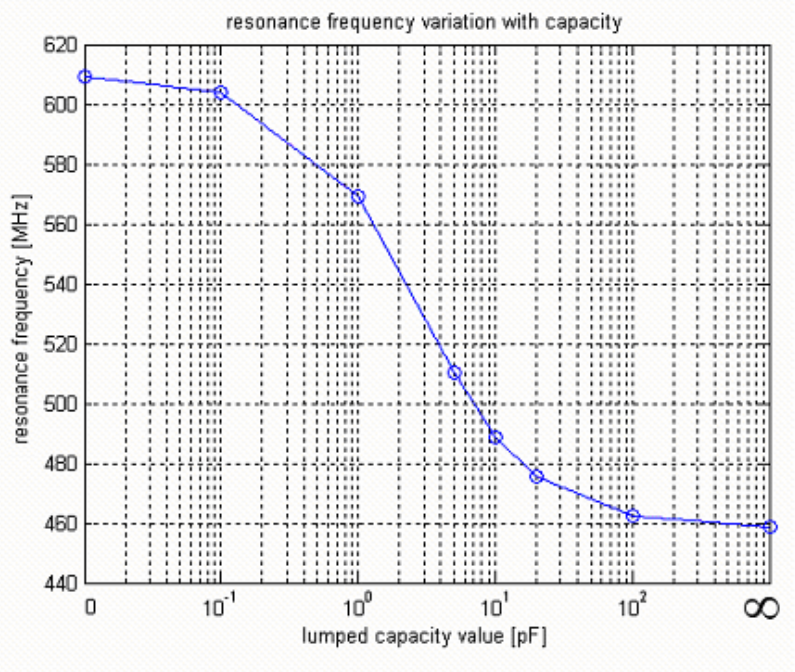

Figure 5.42: resonance frequency variation with capacity.

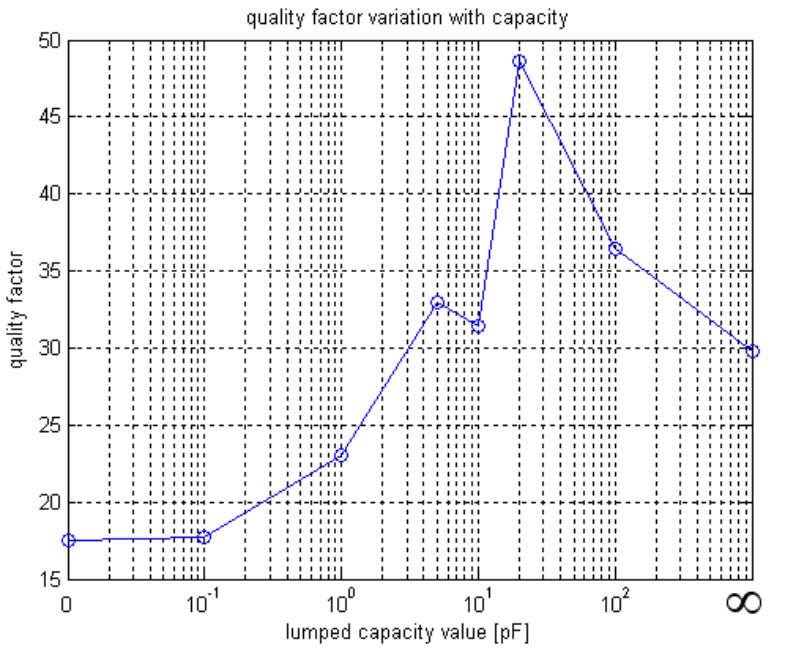

Figure 5.43: quality factor variation with capacity.

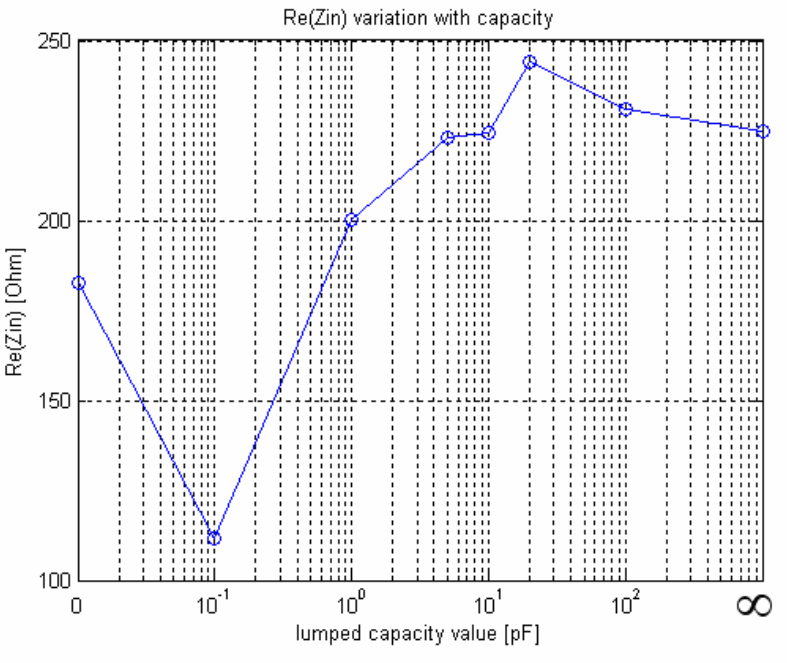

Figure 5.44: Re(Zin) variation with lumped capacity.

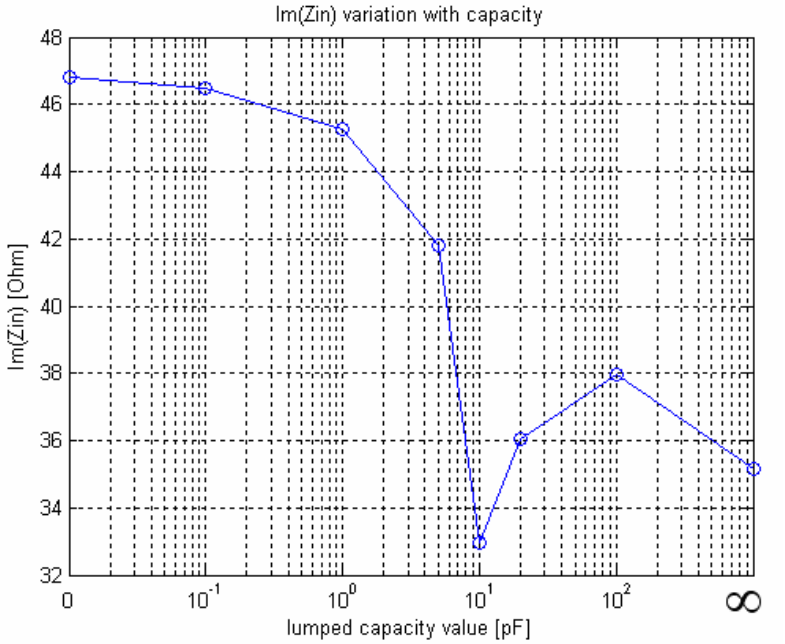

Figure 5.45: Im(Zin) variation with lumped capacity.

5.5.3: Antenna design and simulation.

Recalling our aim to provide a tuneable antenna working in the DVB-H frequency band (470MHz-702MHz), we start its design following the ideas provided by the previous simulations.
We defined as impedance bandwidth that frequency range in which the absolute value of the reflection coefficient S11 is smaller than 0.7 in natural value.
We suppose to have at our disposal a varactor than can provide a capacity range at least between 2pF and 20 pF.
The antenna will be a meandered pifa as before, with the top plate divided in two sections.
The first section is 40mm long, while the second one is 130mm long.
In the gap between the sections, that is 5mm long, we place properly one varactor.
The following table summarizes the antenna geometric features:

lb [mm]	wb [mm]	hb [mm]	L1 [mm]	L2 [mm]	L1pm [mm]
100	20	70	90	20	80
L2pm [mm]	feed1 [mm]	feed2[mm]	hsc[mm]	hpm [mm]	wsc [mm]
20	5	5	15	5	0

Table 5.9: antenna geometric features.

The antenna occupies a volume of $100mm \times 20mm \times 15mm = 30cm^3$, where we consider also the empty space to leave on the chassis for a good radiation.

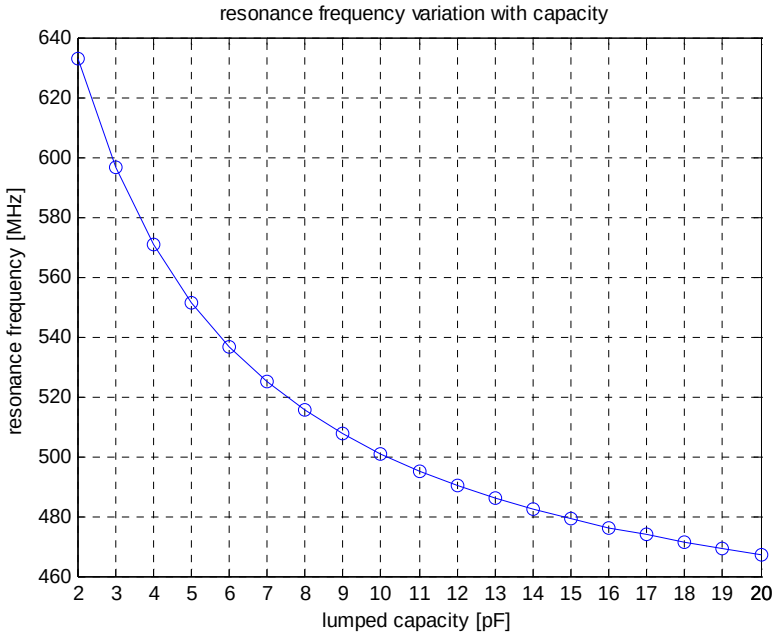

Figure 5.46: resonance frequency variation with capacity.

Now we show the results of our simulation, where we varied the capacity from 2pF to 20pF, to span the desired frequency range.
As we can see from fig.5.46, when the capacity increases the resonance frequency decreases as expected, even if the tuning capabilities are reduced in the higher capacity values because of saturation effects.

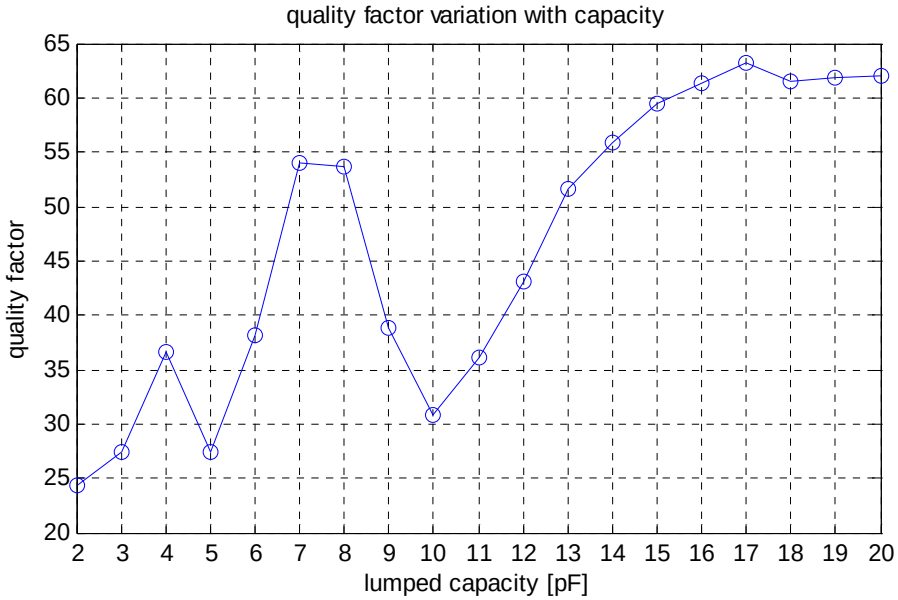

Figure 5.47: quality factor variation with capacity.

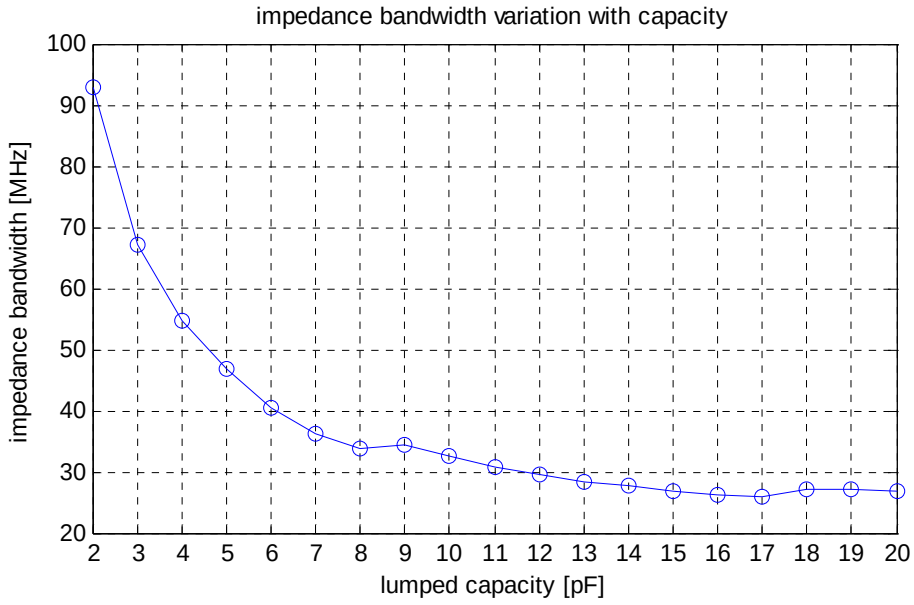

Figure 5.48: impedance bandwidth variation with capacity.

Fig. 5.47 shows a growing trend for the quality factor with some oscillations, while in fig. 5.48 we see that the impedance bandwidth decreases as the capacity grows.
Fig. 5.49 shows the achievements of our goals, because we can appreciate the tunability capabilities of the antenna.
In fig. 5.49 the observed ripples are only caused by numerical error inherent in the FDTD simulation, and even if they can be reduced increasing the accuracy of the FDTD simulation, they don't affect our conclusions.
All the frequency range (470MHz-702MHz) is then covered with a resulting relative bandwidth of more than 40%.

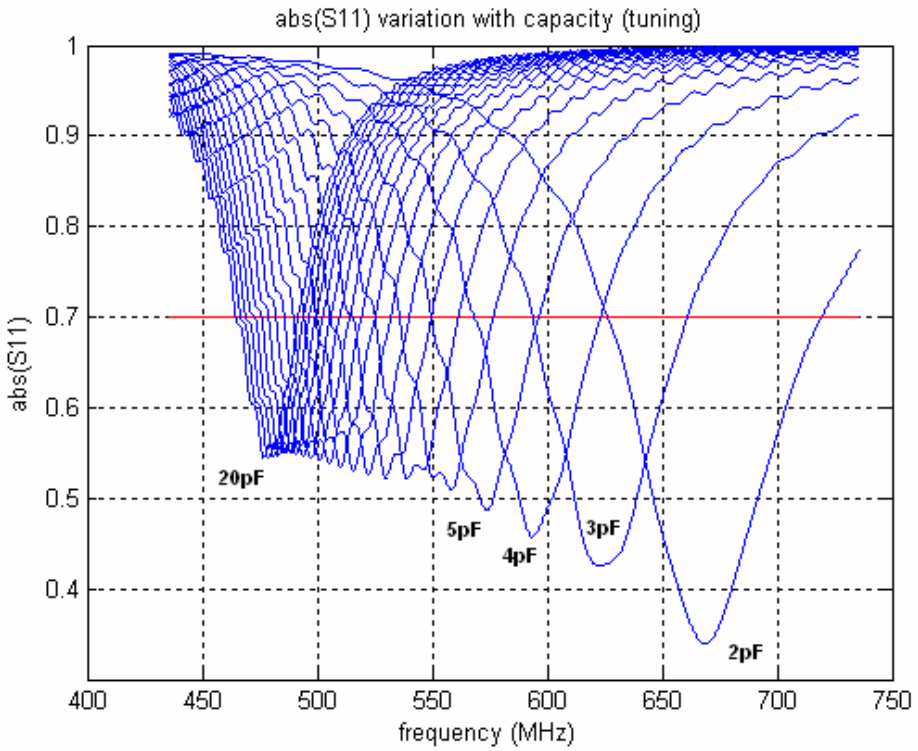

Figure 5.49: abs(S11) variation with capacity (tuning).

All this was obtained without impedance matching, but if we look at fig. 5.50, 5.51, the reduced variability of the antenna input impedance would suggest the introduction of a matching network, depending on the complexity we want to add in the design.
In order to have a complete understanding of the antenna behaviour, we show also the Smiths chart for each tuning step.
In fig. 5.52-5.56 we can see that we are far away the center of the Smith chart, that correspond to the perfect matching case. A more complete analysis would suggest further investigation to see if a better matching with the variation of the feeding could be achieved.

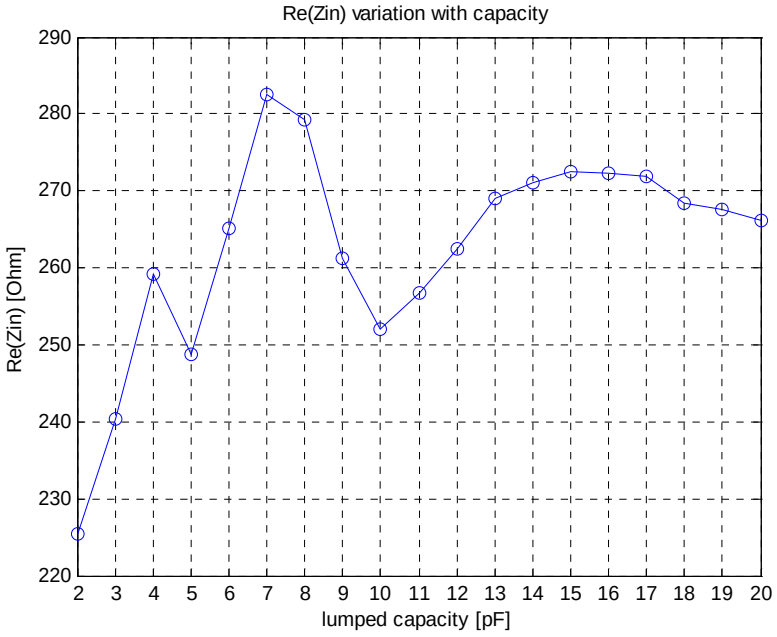

Figure 5.50: Re(Zin) variation with capacity.

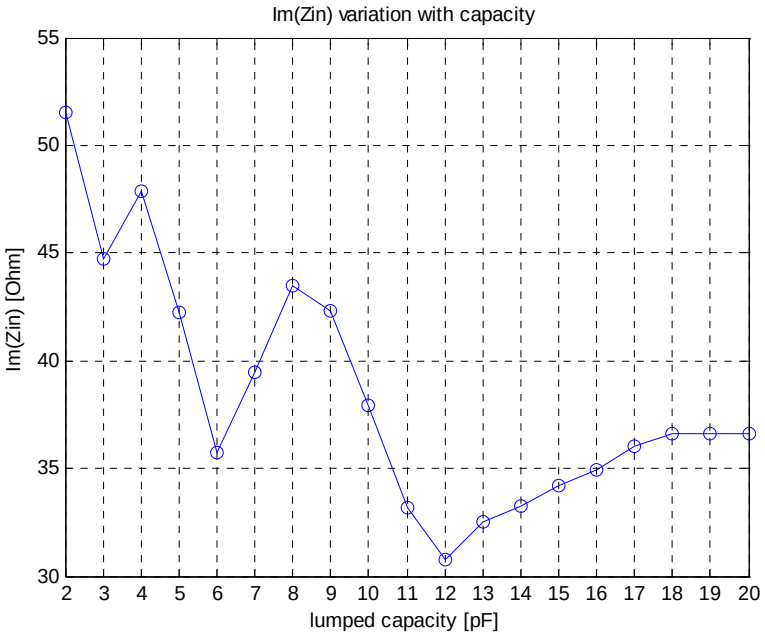

Figure 5.51: Im(Zin) variation with capacity.

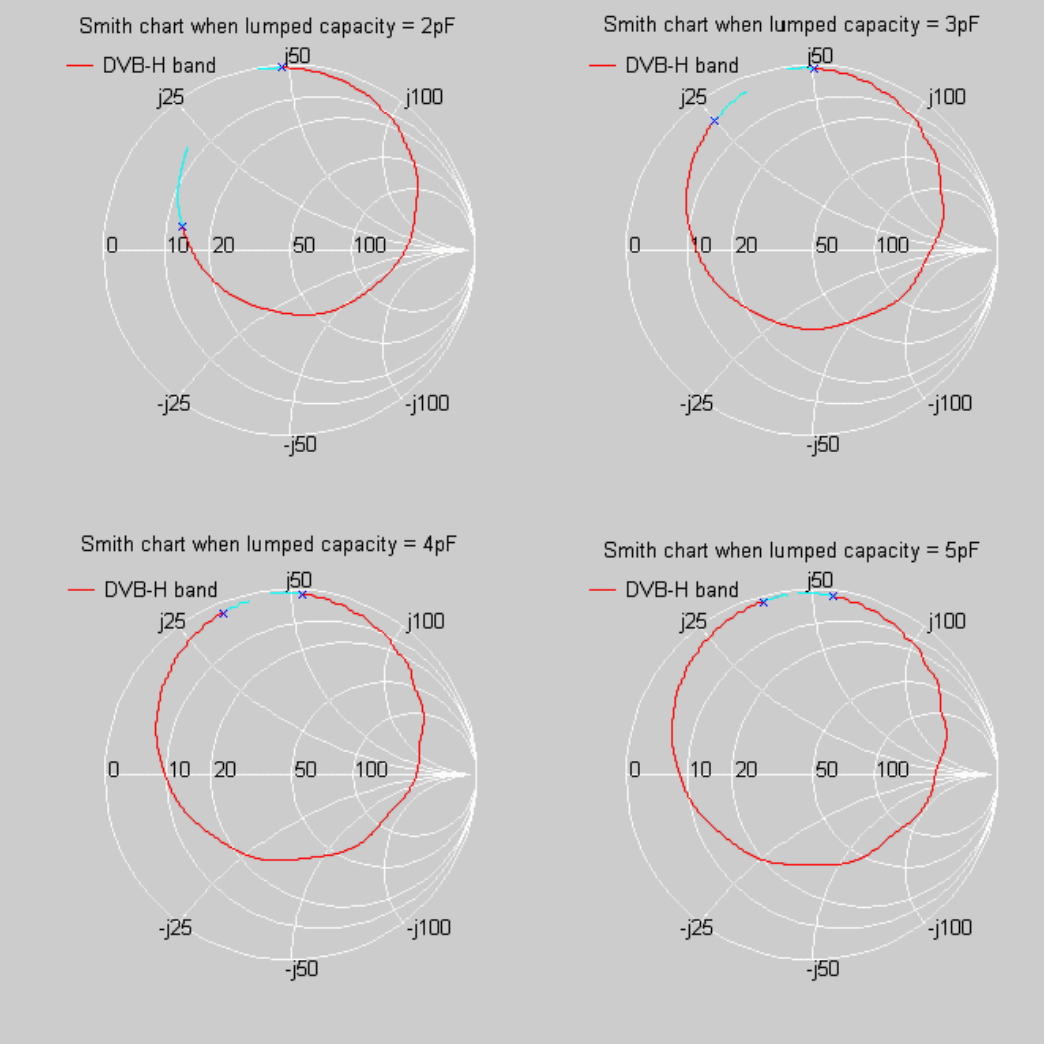

Figure 5.52: Smith charts corresponding to the meandered pifa antenna for different tuning steps (2pF-5pF).

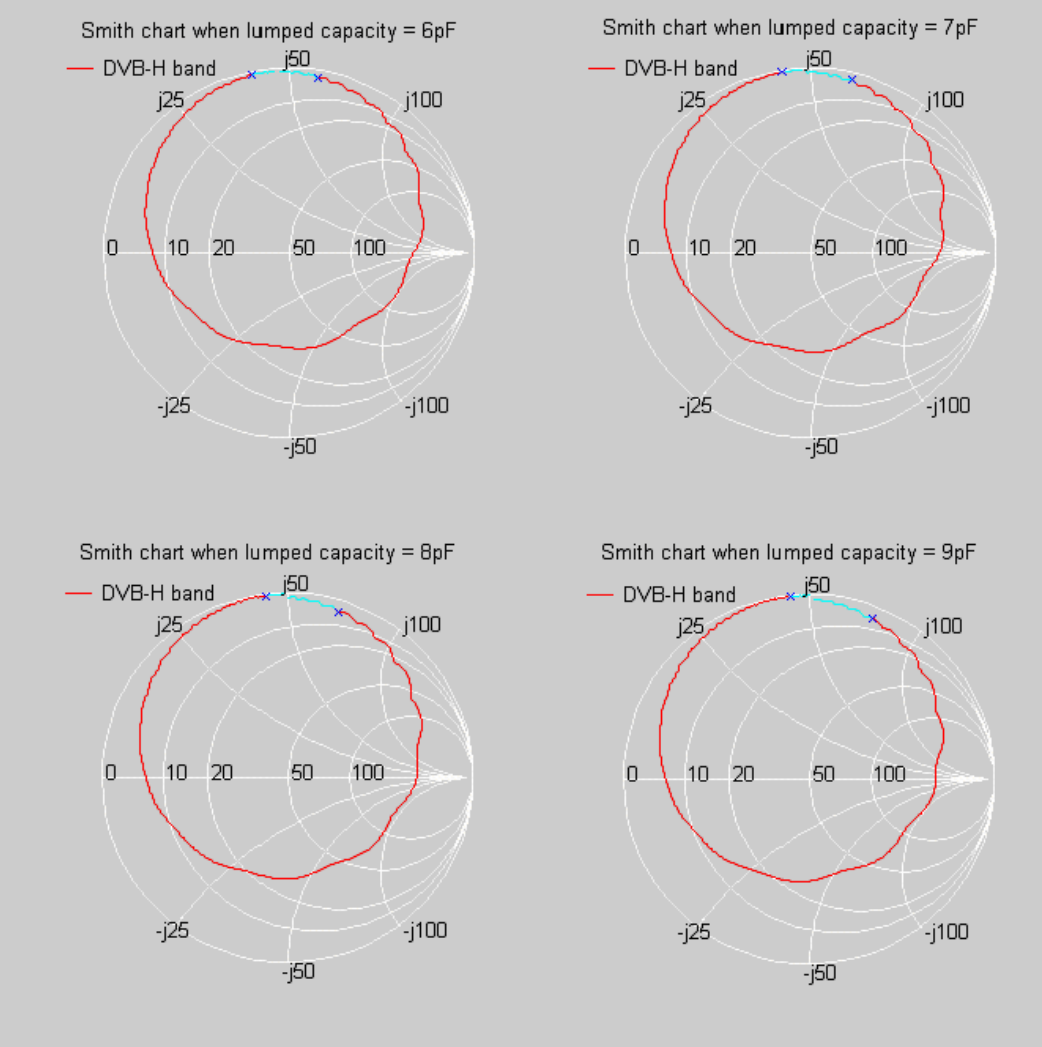

Figure 5.53: Smith charts corresponding to the meandered pifa antenna for different tuning steps (6pF-9pF).

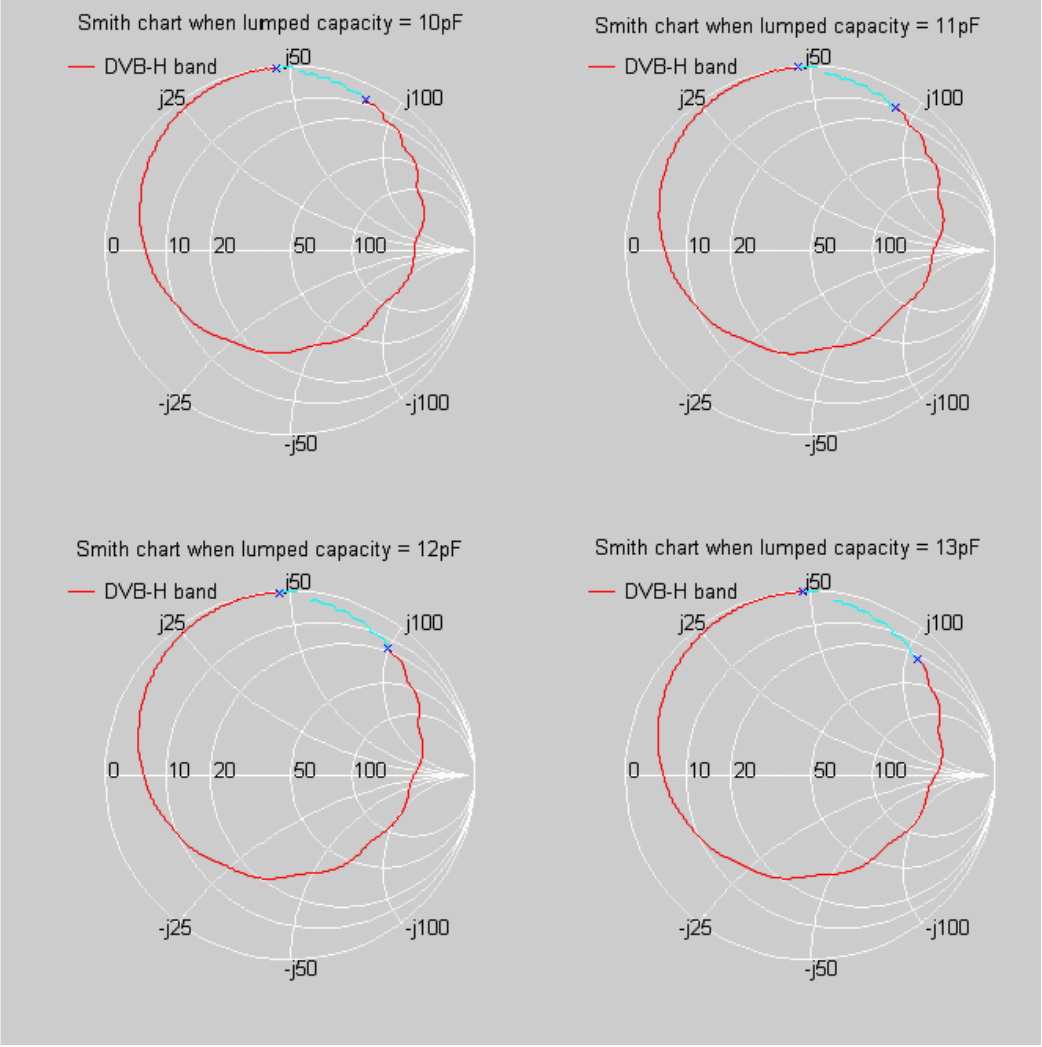

Figure 5.54: Smith charts corresponding to the meandered pifa antenna for different tuning steps (10pF-13pF).

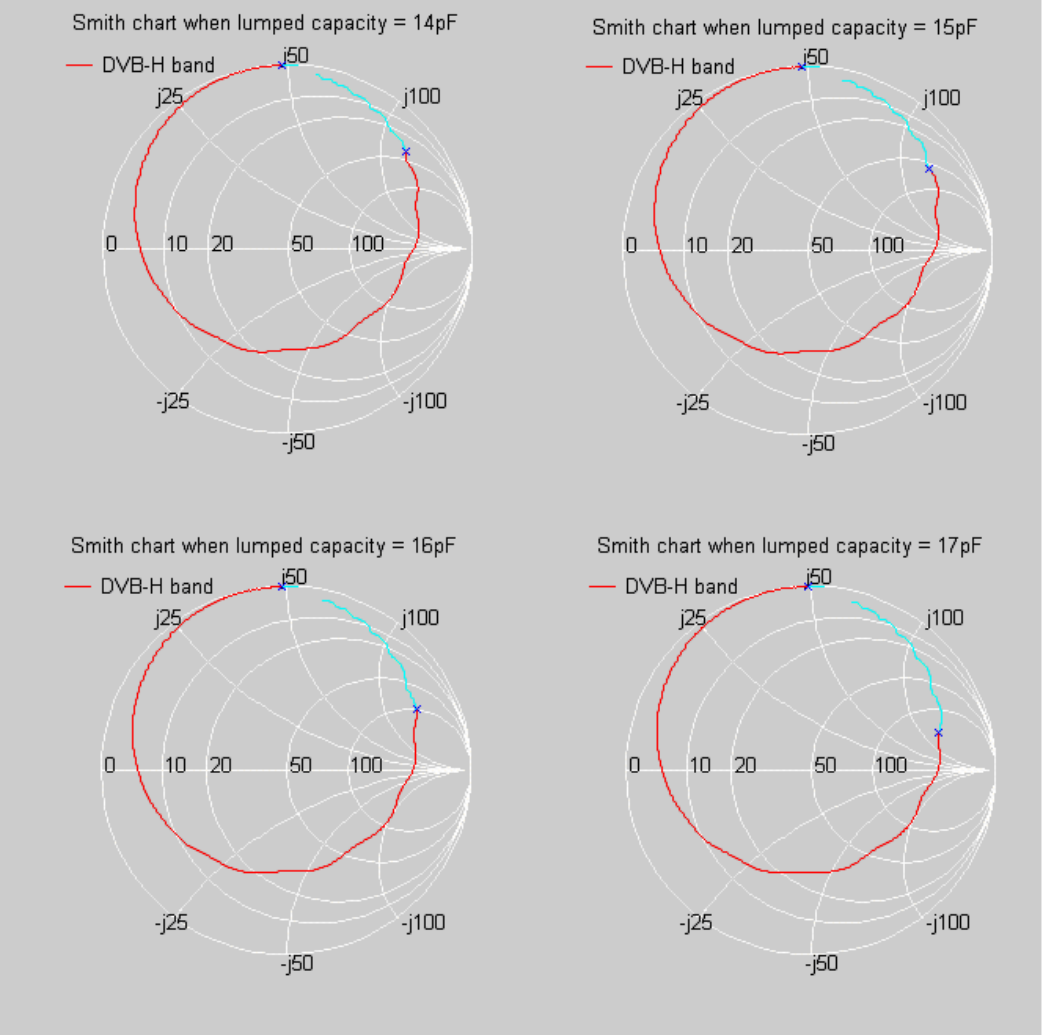

Figure 5.55: Smith charts corresponding to the meandered pifa antenna for different tuning steps (14pF-17pF).

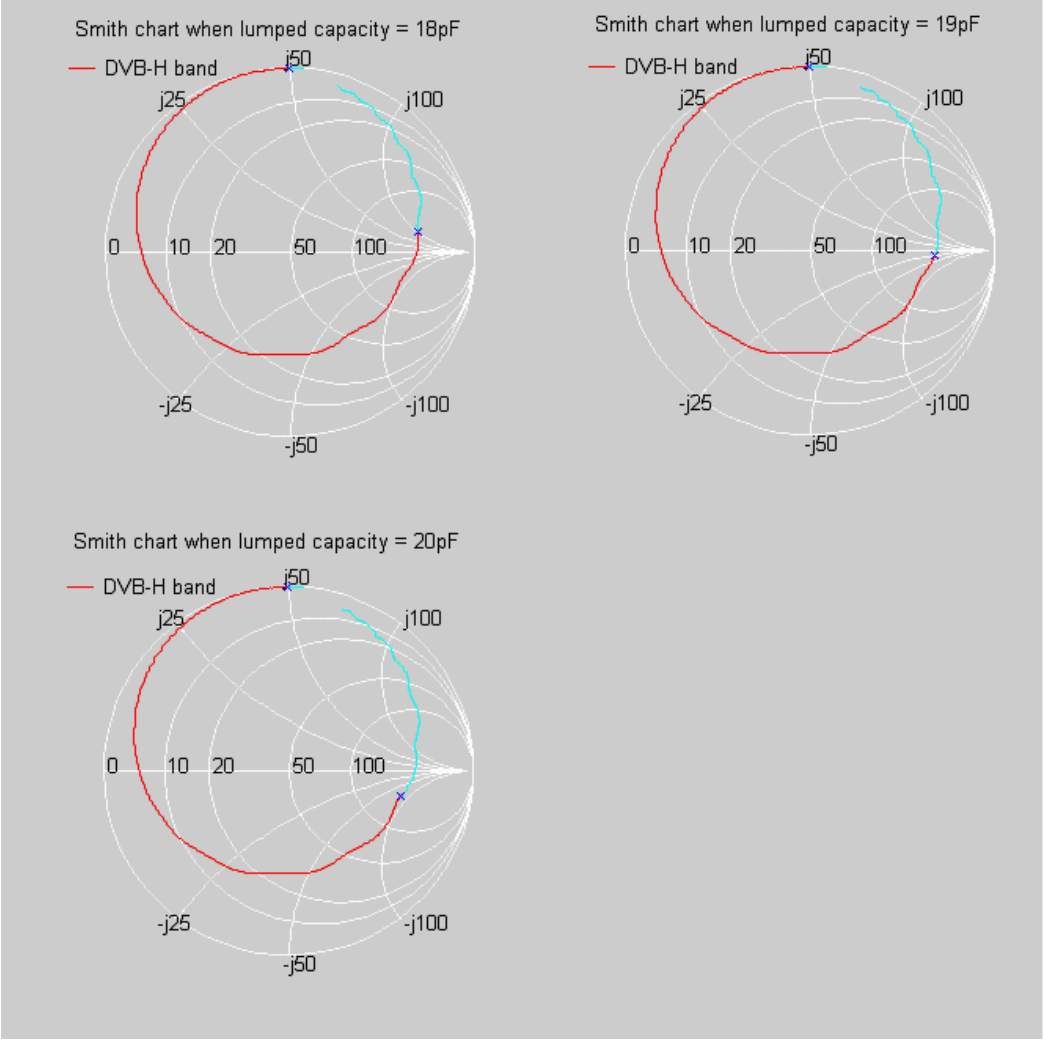

Figure 5.56: Smith charts corresponding to the meandered pifa antenna for different tuning steps (18pF-20pF).

5.5.4: Comparasion of the obtained results between two different simulators.

Now we compared the results obtained with the Aalborg University FDTD program (AAUFDTDP) with the commercial software CST Microwave Studio (CSTMS), in order to see if our implementation of the lumped capacitor in the FDTD code was correct.
We tried to recreate exactly the same geometrical antenna features in both simulators, but some differences are expected for the two different approaches.
As before, we varied the lumped capacity between 2pF and 20pF, in order to see if the resulting tuning of the antenna resonance frequency covers the desired frequency bandwidth.

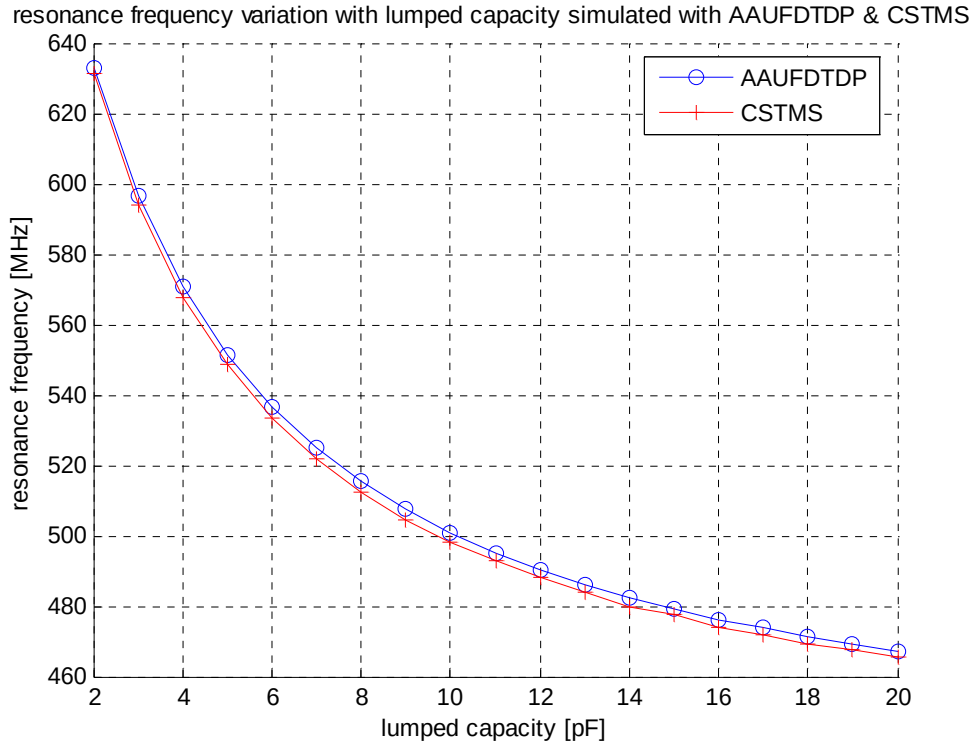

Figure 5.57: resonance frequency variation with lumped capacity simulated with AAUFDTDP & CSTMS.

As we can see from fig. 5.57, there is a good agreement between the two simulators respect to the resonance frequency variation with lumped capacity.
Fig. 5.58 shows the variation of the absolute value of the reflection coefficient S11 over the frequency band under investigation, so that also the simulation with the CSTMS confirms our tuning capability between 470MHz and 702MHz.

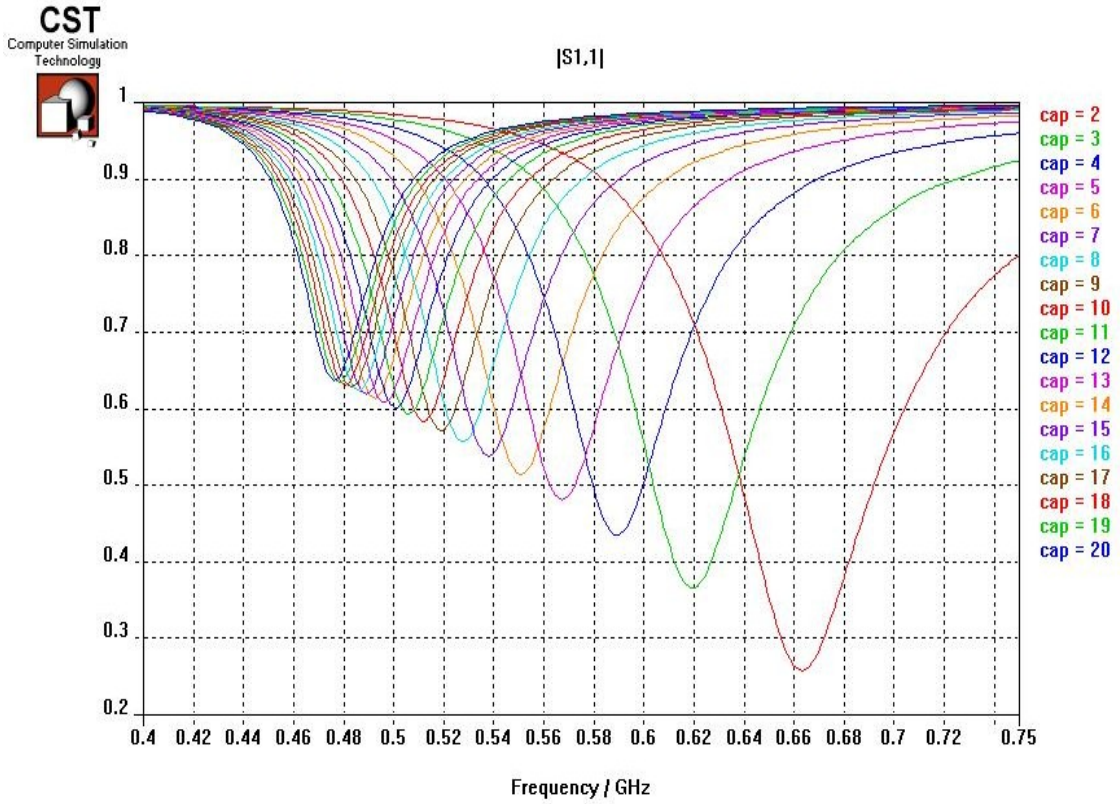

Figure 5.58: abs(S11) variation with capacity (tuning) for CSTMS.

5.5.5: More realistic model for the varactor.

Now we do a more realistic model for the varactor, that will be simulated by a simple equivalent circuit made up by a variable capacitor in series with a resistor.

In this investigation we kept the resistance fixed to 1Ω to see what happens to the antenna radiation efficiency.

The antenna geometry is now slightly different, because of the need to include a cell in the FDTD code corresponding to the series resistor.

In fact the two parts of the meandered pifa will now be separated by 2 FDTD cells, that corresponds to a distance of 10mm in the x direction.

In these two cells we will place the series of the varying capacitor and the resistor to simulate the behaviour of the more realistic varactor.

Being the antenna radiation efficiency defined as the ratio between the radiated power and the input power, is a very important parameter to consider.

However, because of the fact we are considering a receiving antenna, we may accept lower efficiency values.

The addition of a resistor is the reason of the efficiency deterioration, but we expect on the other hand a wider impedance bandwidth.

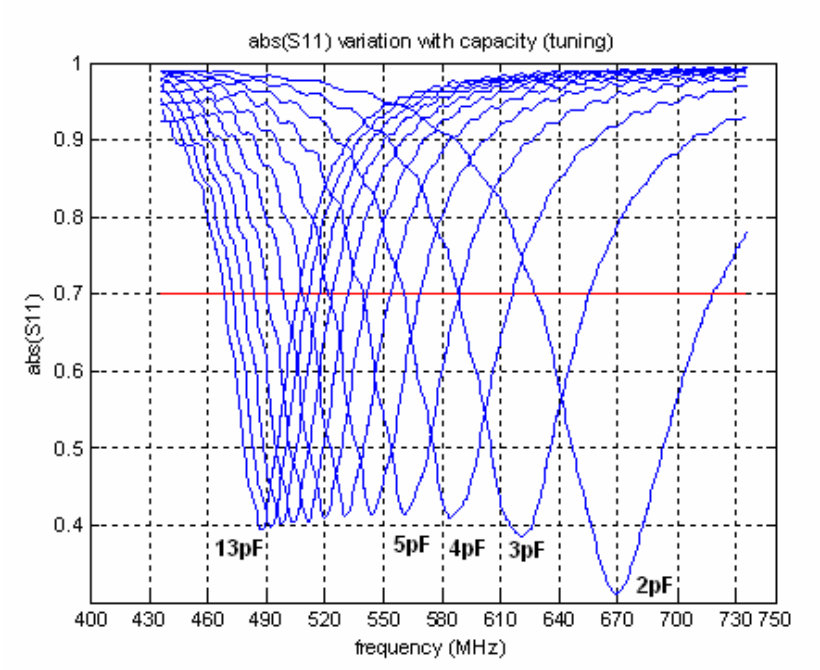

Figure 5.59: abs(S11) variation with capacity (tuning).

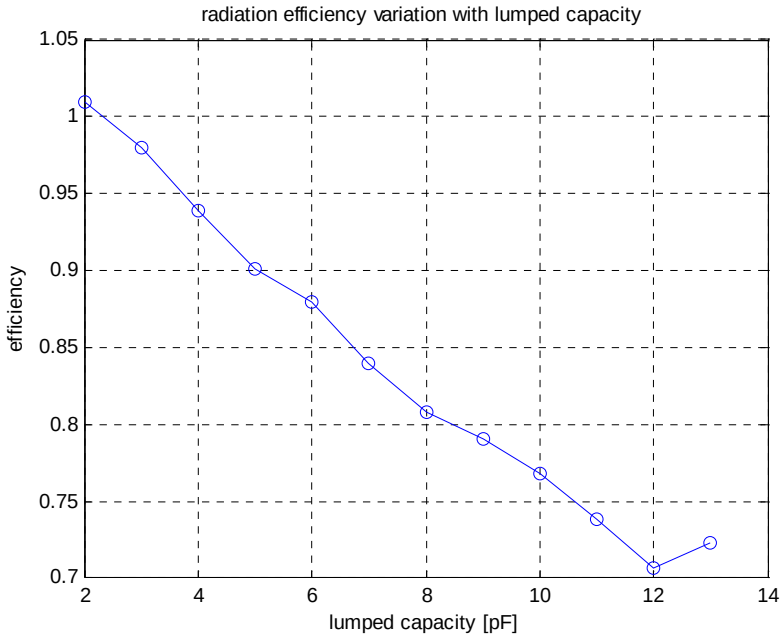

Figure 5.60: radiation efficiency variation with lumped capacity.

With this new antenna configuration, the impedance bandwidth was found slightly wider than before (fig. 5.59), so that we need to change the capacity value only between 2pF and 13pF.
As we can see in fig. 5.60, the antenna radiation efficiency decreases as the capacity grows.
The first value in fig. 5.60 is slightly greater than 1, being equal to 1.01, and the last one doesn't follow the same tendency which explanation may be a small numerical error in the simulation.
The radiation efficiency for the higher capacity values decreases till 0.7, a level that may not be acceptable depending to our performance requirements.
Also in this case we show the Smith chart for each tuning step.

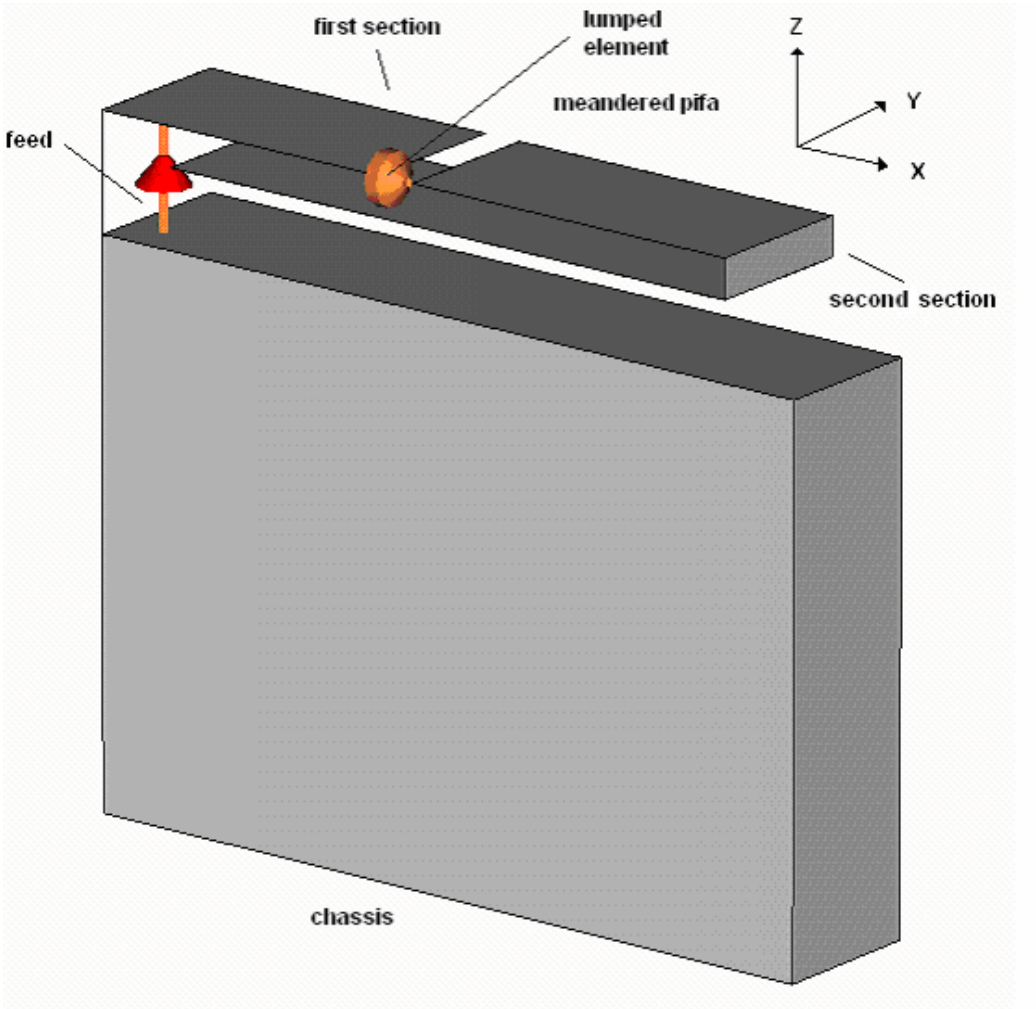

Figure 5.61: meandered pifa antenna 3-D view.

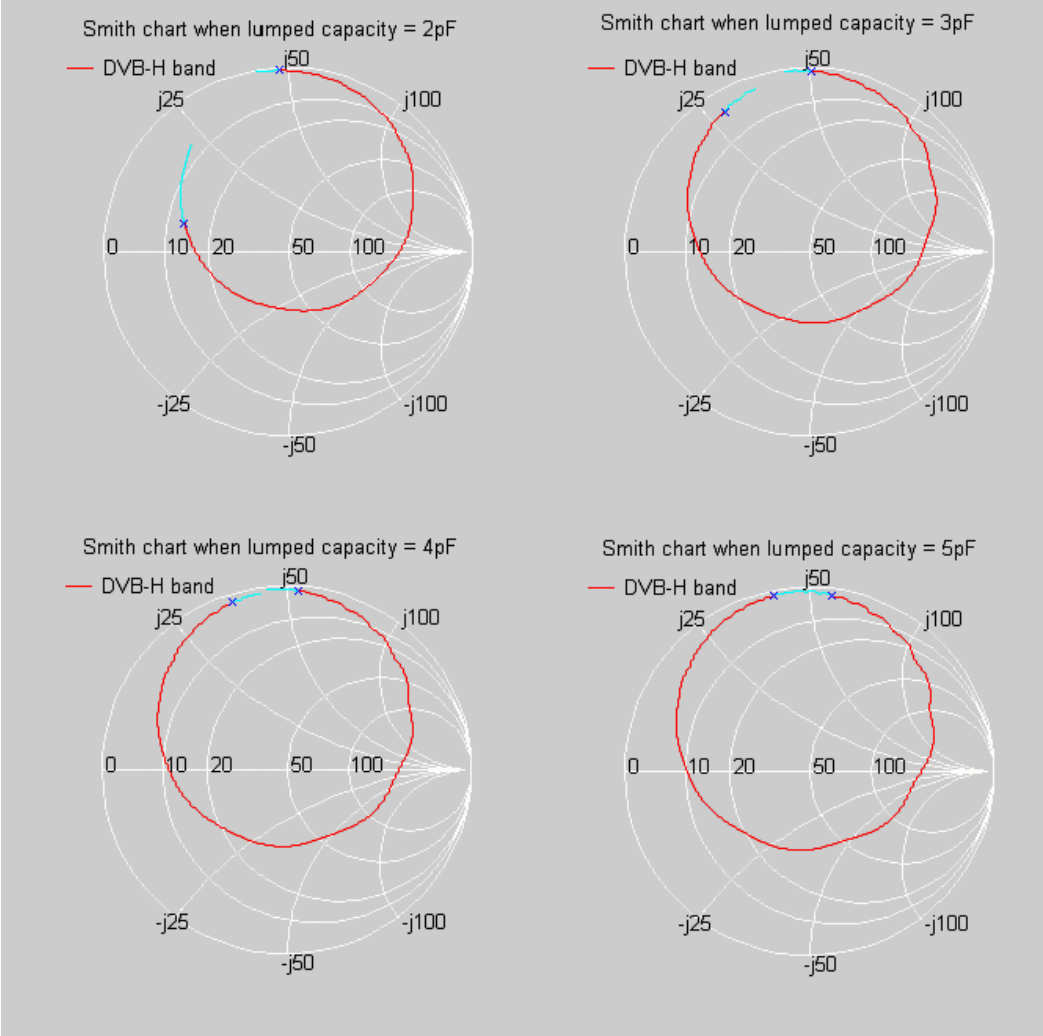

Figure 5.62: Smith charts corresponding to the meandered pifa antenna tuning when it is added a series resistor of 1Ω to model a more realistic varactor (2pF-5pF).

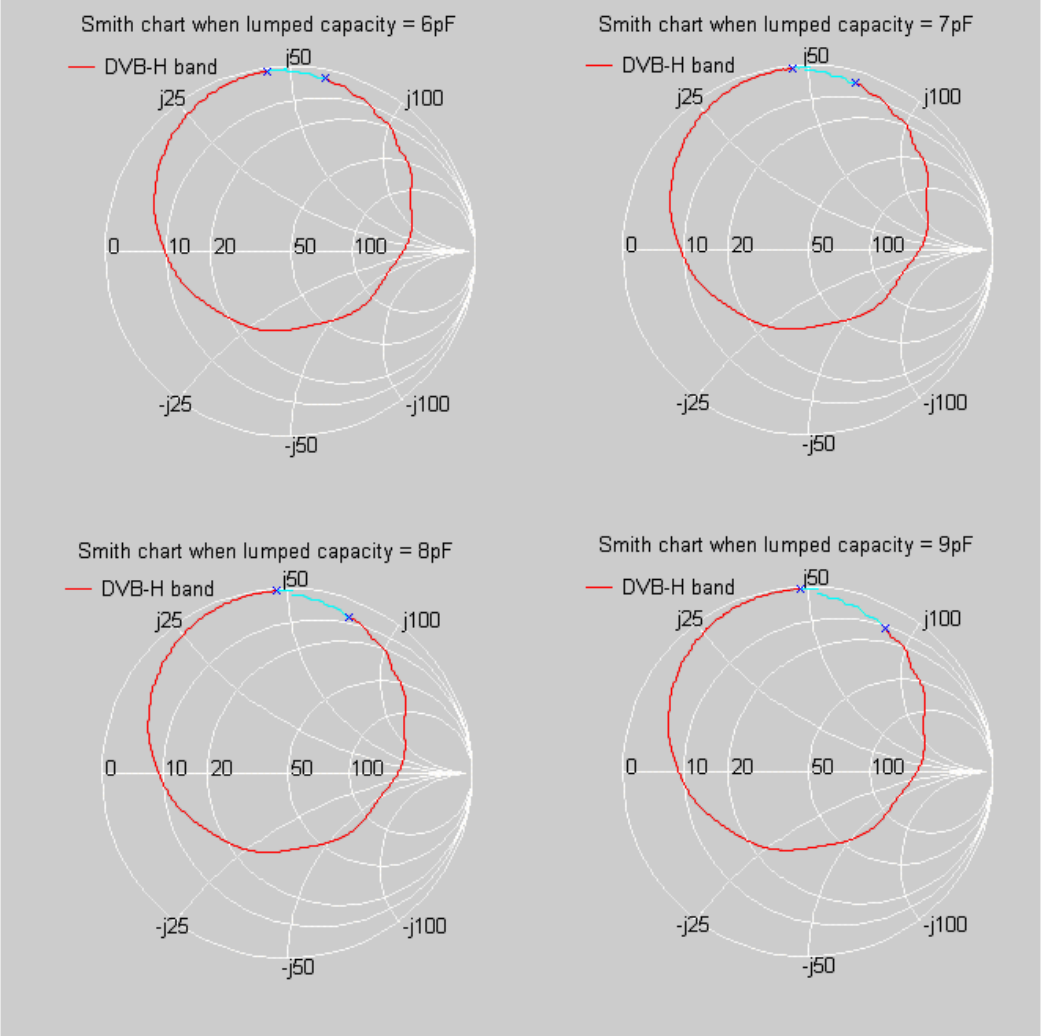

Figure 5.63: Smith charts corresponding to the meandered pifa antenna tuning when it is added a series resistor of 1Ω to model a more realistic varactor (6pF-9pF).

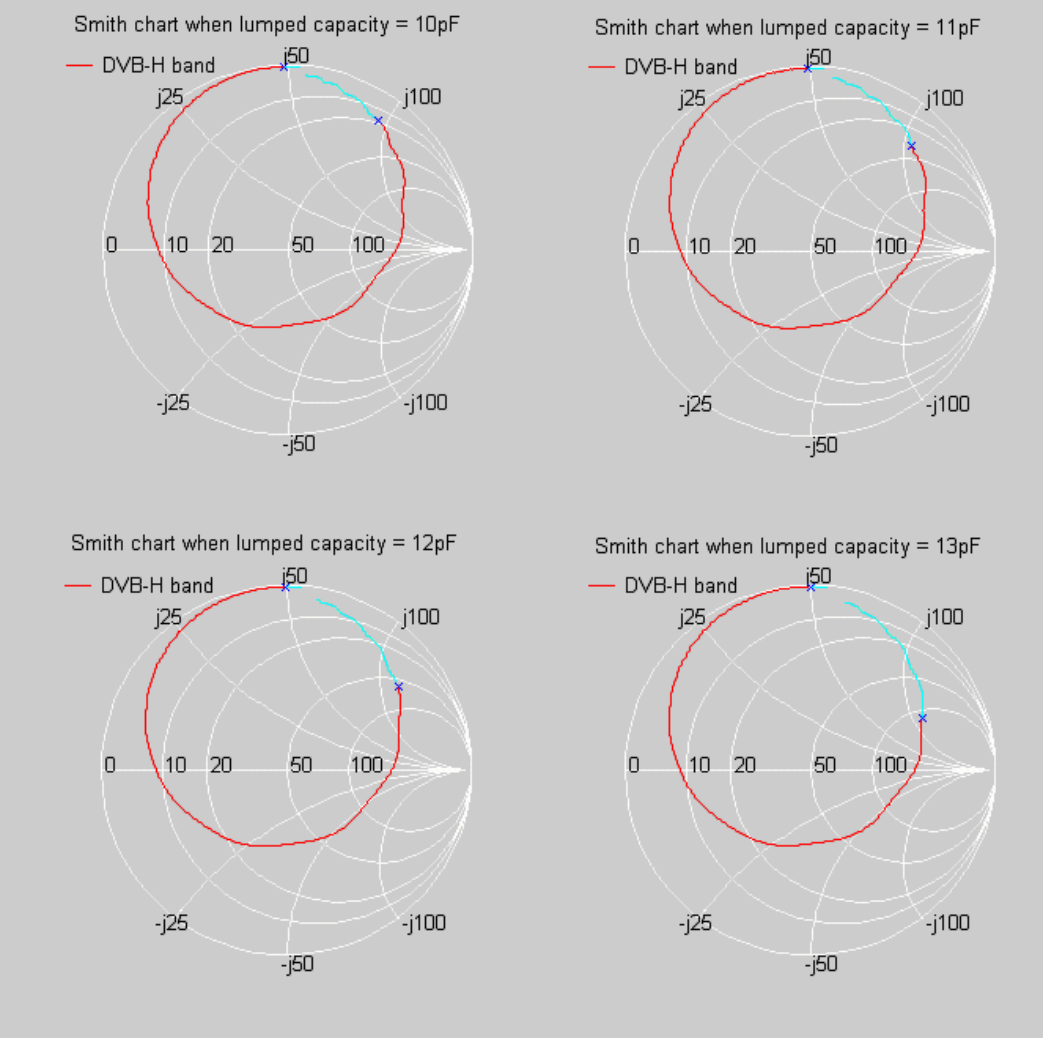

Figure 5.64: Smith charts corresponding to the meandered pifa antenna tuning when it is added a series resistor of 1Ω to model a more realistic varactor (10pF-13pF).

5.6: Top meandered monopole antenna investigations.

Now we begin the study of a new antenna configuration.
In this simulation set we investigate the behaviour of a meandered antenna placed on the top of a metallic chassis box. We define the following parameters:

- lb [mm]: length of the metal chassis box.
- wb [mm]: width of the metal chassis box.
- hb [mm]: height of the metal chassis box.
- hv [mm]: height of the meander vertical section.
- ho [mm]: height of the meander horizontal section.
- hgr [mm]: height of the meander over the ground plane.
- lboff [mm]: offset of the meander along lb.
- wboff [mm]: offset of the meander along wb.
- nvs: number of meander vertical sections.
- nos: number of meander horizontal sections.
- twl [mm]: total wire length.
- frsim [MHz]: resonance frequency obtained by simulation.
- Q: antenna quality factor obtained by simulation.
- lambda [λ]: wavelength.
- etwl [λ] = twl/lambda: electrical total wire length.
- emh [λ] = $(hgr + hv)/lambda$: electrical meander height.
- eml [λ] = $(nos \cdot ho)/lambda$: electrical meander length.
- esurf [λ^2] = $(emh \cdot eml)$: electrical surface.

All the meanders will have quite the same geometrical properties, with the exemption of the number of horizontal sections “nos” and the height of the meander vertical section “hv”.
We try to adapt “nos” and “hv” in order to have a resonance frequency in the neighbourhood of 586MHz.
We expect a smaller antenna quality factor as “hv” increases, because the height of the meander over the metallic chassis box, that acts as ground plane, is higher.

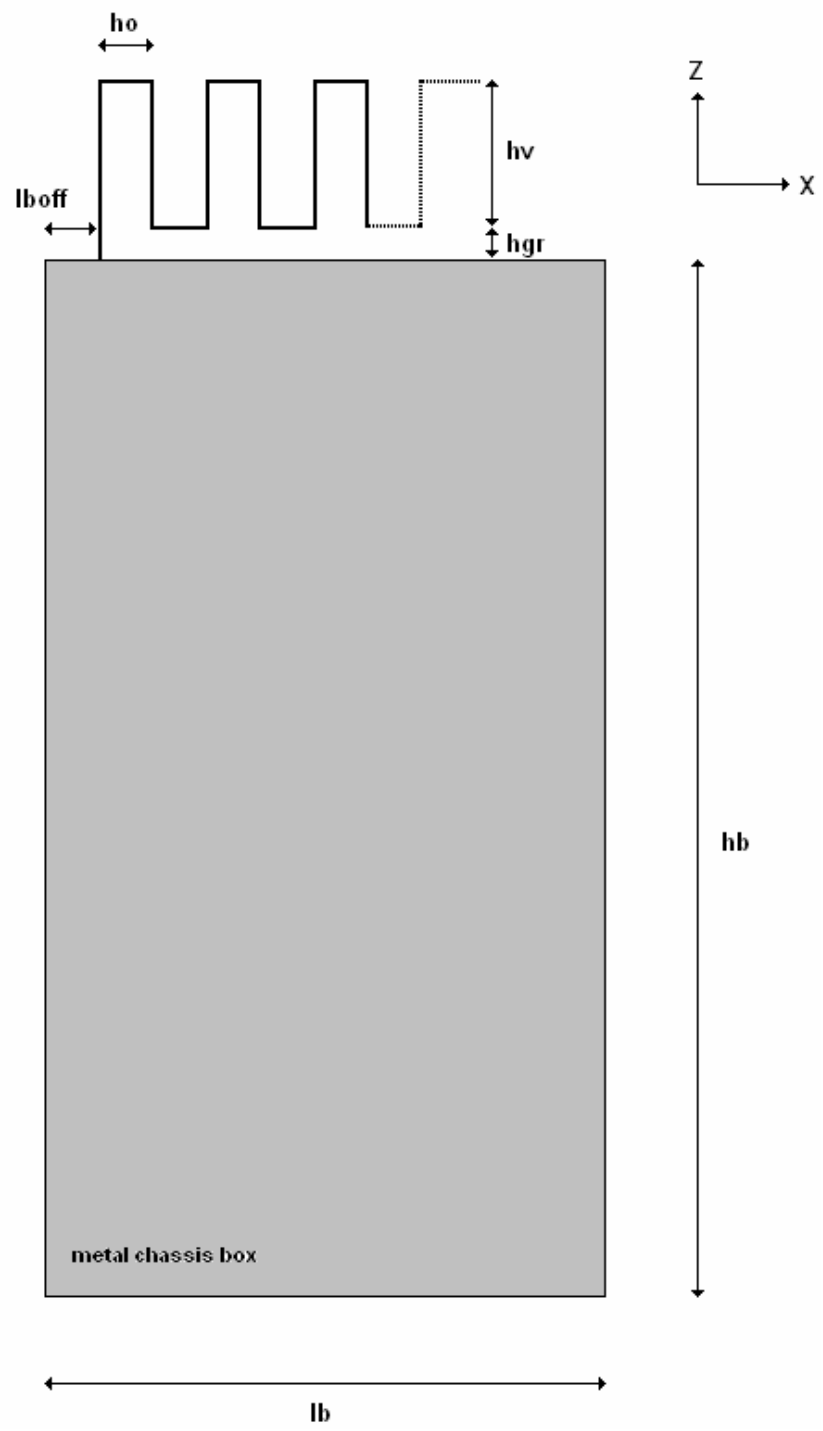

Figure 5.65: Antenna geometry in the XZ plane.

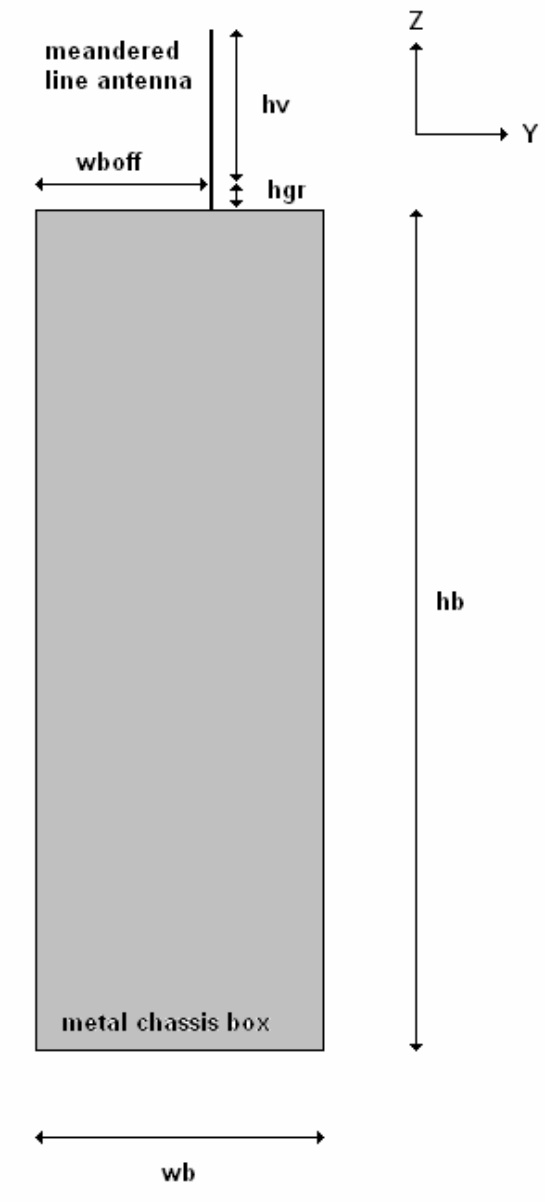

Figure 5.66: Antenna geometry in the YZ plane.

In the following tables we can see the geometric parameters and the results for all the simulations (1-6):

antenna	lb [mm]	wb [mm]	hb [mm]	hv [mm]	ho [mm]	hgr [mm]
1	70	30	100	40	5	5
2	70	30	100	35	5	5
3	70	30	100	30	5	5
4	70	30	100	25	5	5
5	70	30	100	20	5	5
6	70	30	100	15	5	5

antenna	lboff [mm]	wboff [mm]	nvs	nos	twl [mm]
1	5	10	5	4	230
2	5	10	6	5	245
3	5	10	7	6	250
4	5	10	8	7	245
5	5	10	9	8	230
6	5	10	11	10	225

antenna	fr [MHz]	Q	lambda [mm]	etwl $[\lambda]$
1	573	17	523.56	0.44
2	560	20	535.71	0.46
3	559	24	536.67	0.47
4	567	27	529.1	0.46
5	589	31	509.34	0.45
6	584	38	513.7	0.44

antenna	emh $[\lambda]$	eml $[\lambda]$	esurf $[\lambda^2]$
1	0.086	0.048	0.0041
2	0.075	0.056	0.0042
3	0.065	0.065	0.0043
4	0.057	0.076	0.0043
5	0.049	0.088	0.0043
6	0.039	0.107	0.0042

Table 5.10: geometric parameters and the results for simulations (1-6).

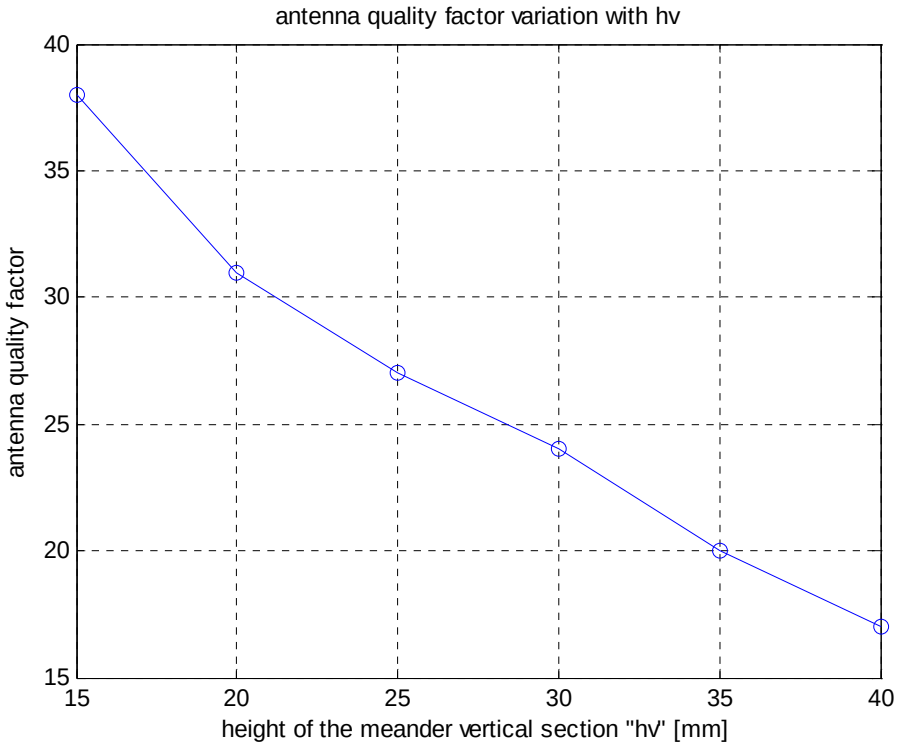

Figure 5.67: Antenna quality factor variation with "hv".

As we can see from fig. 5.67, the antenna quality factor Q decreases as the height of the meander vertical section "hv" increases, that corresponds to a larger impedance bandwidth, as expected from theory.
Because of mutual coupling between different meander sections, the effective wire electrical length is reduced, so the antenna doesn't resonate at lambda/4 but near to lambda/2.
Also the finite ground plane size contributes to this behaviour, because image theory cannot be applied as in the ideal case.
Unfortunately, we cannot allow the use of one antenna with a large value of "hv", because of the fact we have physical volume occupation constraints.
In the next we will try to limit the antenna size as much as possible, in order to deal with a suitable implementation of our design solutions.

5.7: Effects of the chassis metal box for meandered monopole antennas.

5.7.1: Introduction.

In this simulation set we investigate a meandered antenna placed on the top of a metallic chassis box. We want to characterize the meander when it is in free space and when it is surrounded by the metal chassis.
This distinction addresses to an external or internal antenna configuration respectively.
In fact when the antenna is internal, the space at our disposal is reduced, so the antenna volume is not only that occupied by the antenna itself, but we have to add a certain amount of volume to separate the meander from the chassis box because of mutual coupling. We define the following parameters:

- lb [mm]: length of the metal chassis box.
- lb1 [mm]:length of the upper box element
- wb [mm]: width of the metal chassis box.
- hb [mm]: height of the metal chassis box.
- hb1 [mm]: height of the upper box element.
- hv [mm]: height of the meander vertical section.
- ho [mm]: height of the meander horizontal section.
- hgr [mm]: height of the meander over the ground plane.
- lboff [mm]: offset of the meander along lb.
- wboff [mm]: offset of the meander along wb.
- nvs: number of meander vertical sections.
- nos: number of meander horizontal sections.
- twl [mm]: total wire length.
- frsim [MHz]: resonance frequency obtained by simulation.
- Q: antenna quality factor obtained by simulation.

All the simulated meandered antennas will share the following parameters:

lb [mm]	wb [mm]	hb [mm]	hv [mm]	ho [mm]	hgr [mm]
70	30	100	35	5	5
lboff [mm]	wboff [mm]	nvs	nos	twl [mm]	
5	15	5	4	205	

Table 5.11: parameters for the simulated meandered antenna.

5.7.2: Simulation.

We will vary the upper box element length, in order to estimate the coupling between the meandered antenna and the chassis metal box.
We will start with no upper element, that is lb1 = 0, and then we will increase lb1 starting from the right side of the chassis metal box (fig.5. 68).
When lb1 is maximum, we are very close to the meander, and we expect a higher coupling.

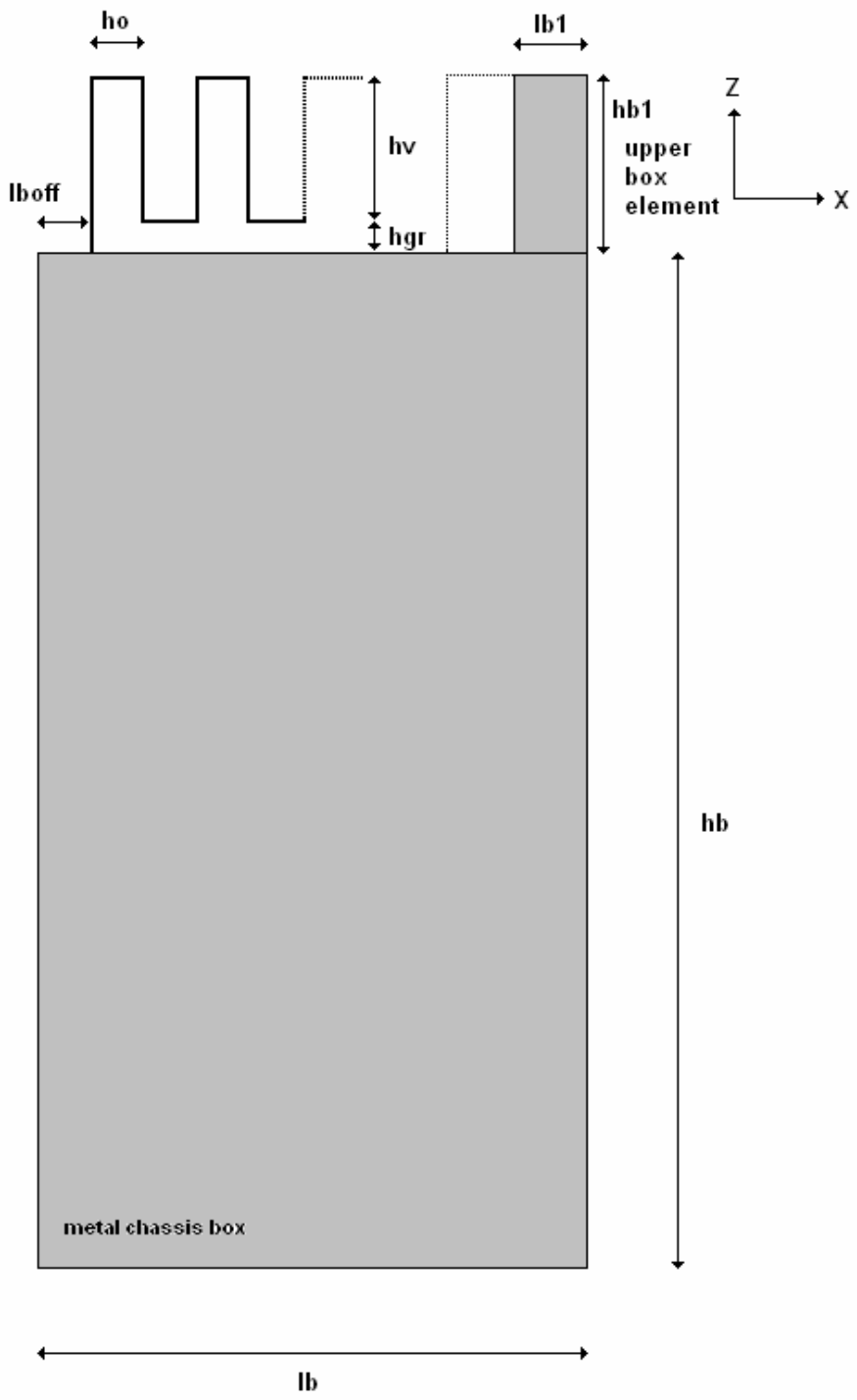

Figure 5.68: Antenna geometry in the XZ plane.

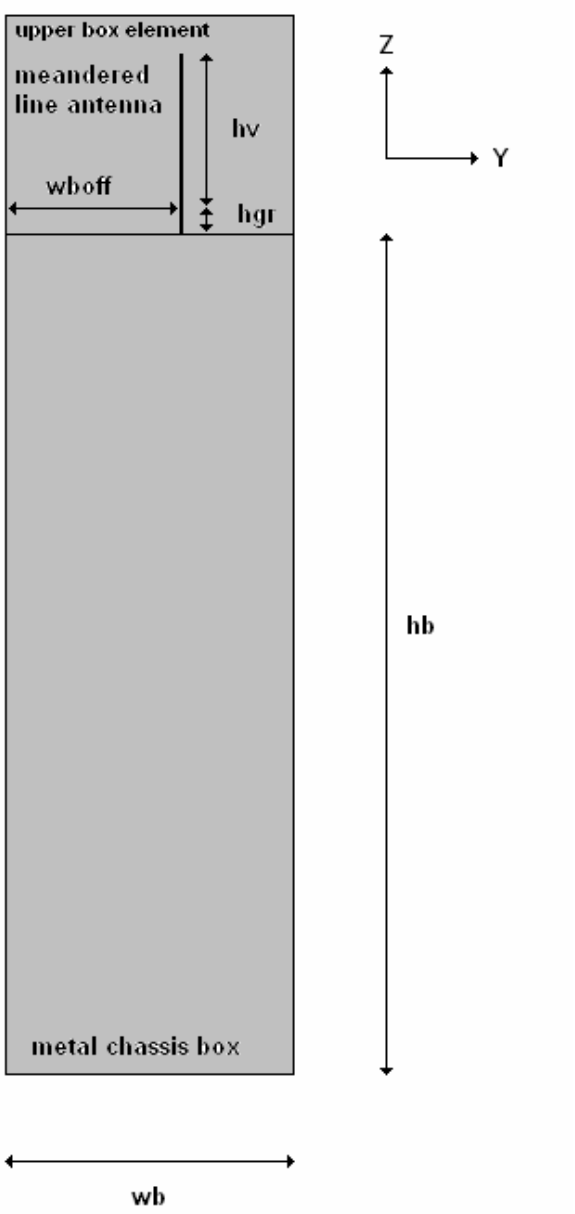

Figure 5.69: Antenna geometry in the YZ plane.

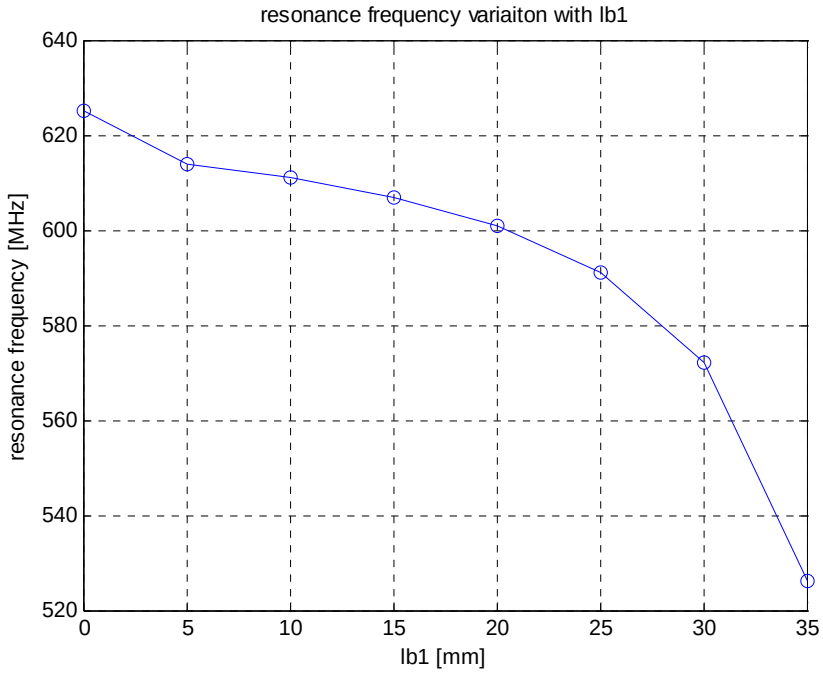

Figure 5.70: resonance frequency variation with lb1

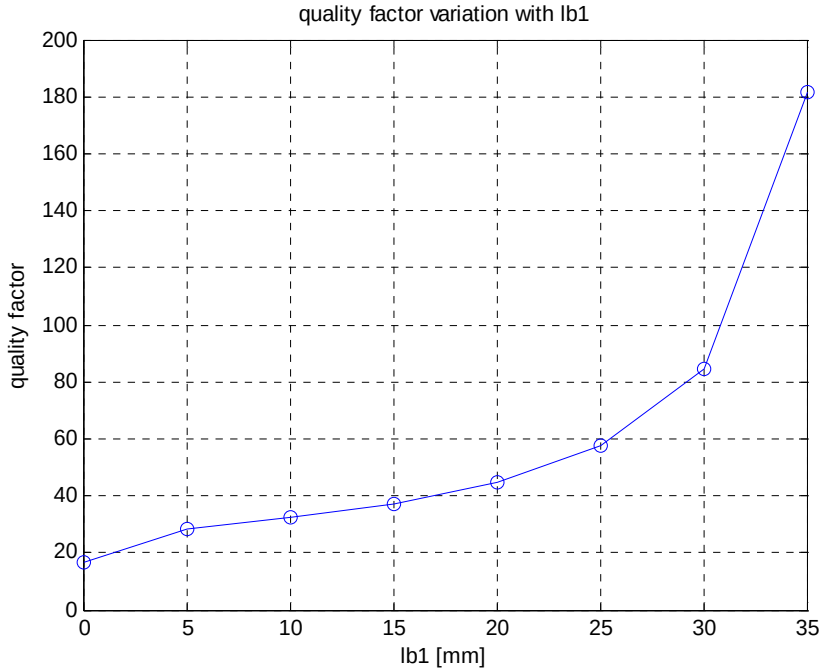

Figure 5.71: quality factor variation with lb1

As we can see from fig. 5.70, the resonance frequency decreases as the upper box element is larger, that corresponds to a higher coupling effect.
This may be explained by the fact that when the coupling is higher, the antenna looks electrically longer, that corresponds in a decrease in the resonance frequency.
Fig. 5.71 shows the behaviour of the quality factor, that grows dramatically with lb1, corresponding to a smaller relative bandwidth. As before the coupling may affect the quality factor, that we want to keep small in order to design a large bandwidth antenna.
This suggests a compromise choice between quality factor and antenna volume, that accounts also for the free space to be left in order to reduce the effects of coupling.
Looking at fig. 5.71 we choose lb1 = 4mm, because a smaller length will correspond to a smaller quality factor gain difference.

5.7.3: Tuning investigations.

Now we investigate the effect of a lumped capacitor placed at the end of the meander, between the meander and the metal chassis box, when lb1 = 20mm and when lb1 = 0mm.
The capacitor will vary between 0.1pF and 1pF.

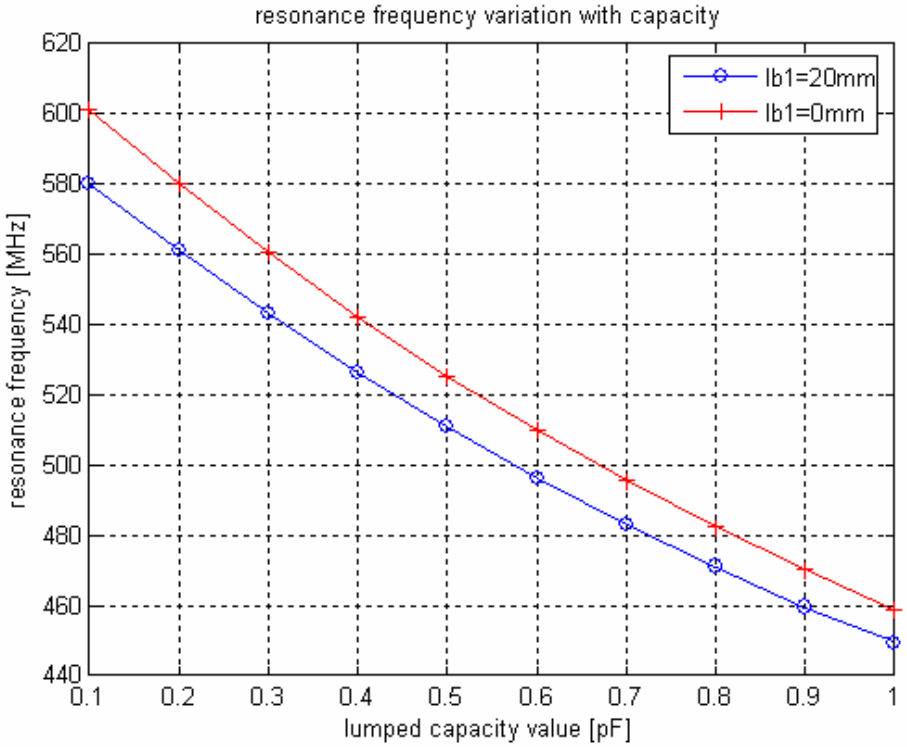

Figure 5.72: resonance frequency variation with capacity.

Fig.5.72 shows a linear decrease in the resonance frequency with capacity, in both cases.
This tuning capability is possible by the fact that varying the capacity value we are modifying the inherent electrical length of the meandered antenna.

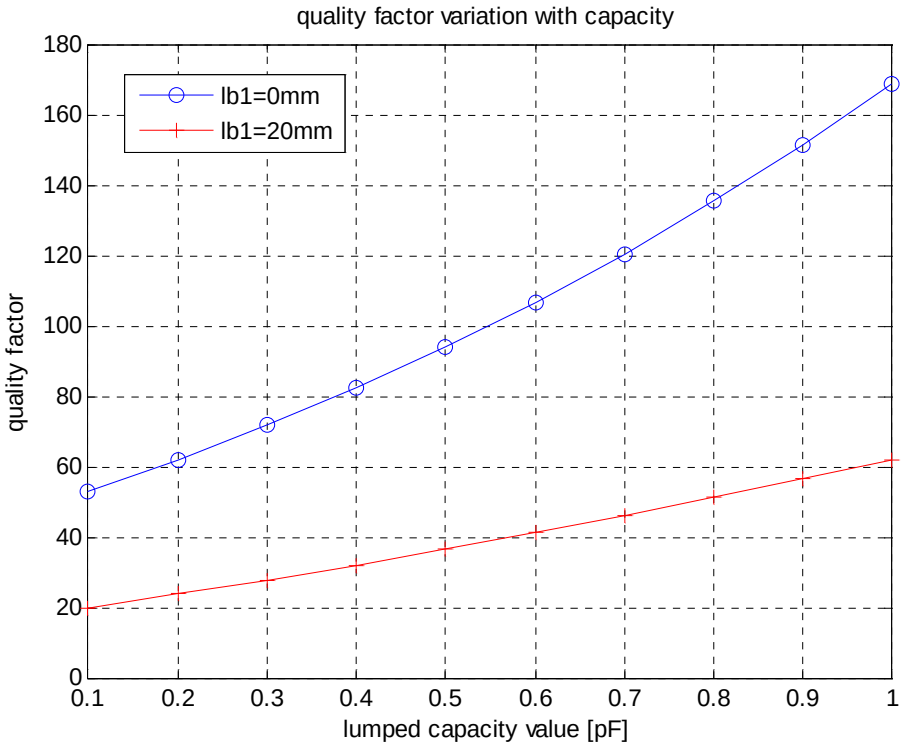

Figure 5.73: quality factor variation with capacity

As we can see from figure 5.73, the quality factor increases to much when we tune the resonance frequency varying the capacity in the presence of the upper box element.
When the meander is in free space on the top of the chassis (lb1 = 0mm), the quality factor variation is reduced respect to the case of lb1 = 4mm.
Also here we have to consider a performance trade-off, but it seems difficult to have a wide tuning range with small Q values when the meander is internal.
So we have to address to other antenna configurations, trying in the next to place the meandered antenna on the top of the chassis in another way.

5.8: Top meandered monopole antenna design.

5.8.1: Introduction.

Here we present a possible antenna configuration to fulfill the impedance bandwidth requirements of DVB-H standard in the frequency range 470MHz-702MHz.
We remind here that we defined the impedance bandwidth that frequency range in which the absolute value of the reflection coefficient S11 is smaller than 0.7 in natural value or equivalently -3 in dB.
We suppose to have at our disposal a varactor that can provide a capacity range at least between 1pF and 15 pF.
Keeping in mind the investigations carried out before in the report, we suggest a configuration in which the maximum antenna height over the chassis box is obtained through a proper meandering.
Because of the fact that the chassis box typically acts as the main radiator, we place the antenna where the chassis is longer respect to other dimensions.
The antenna is thought to be internal, which means that all the remaining volume not occupied by the antenna itself needs to remain empty, in order to avoid undesired capacitive coupling effect that would decrease the antenna performances.
Various configuration were tried, but if we go below certain values of antenna height over the chassis box (that acts as ground plane), we are no more able to satisfy the DVB-H specified requirements.
This height will be 20mm, with a total antenna volume of:
$70mm \times 20mm \times 20mm = 28cm^3$

We define the following parameters:

- lb [mm]: length of the metal chassis box.
- wb [mm]: width of the metal chassis box.
- hb [mm]: length of the metal chassis box.
- los [mm]: length of meander horizontal section.
- lvs [mm]: length of meander vertical section.
- hme [mm]: height of the meander over the chassis.
- off1 [mm]: y-oriented feed offset.
- off2 [mm]: x-oriented feed offset.

5.8.2: Simulation.

We will place a varactor between two sections of the meandered antenna, as we can see in fig.1, so that we can vary the electrical length of the antenna.
We simulate this varactor with the introduction of a lumped element in the FDTD algorithm, that will act as a variable capacitor ranging from 1pF to 15pF.

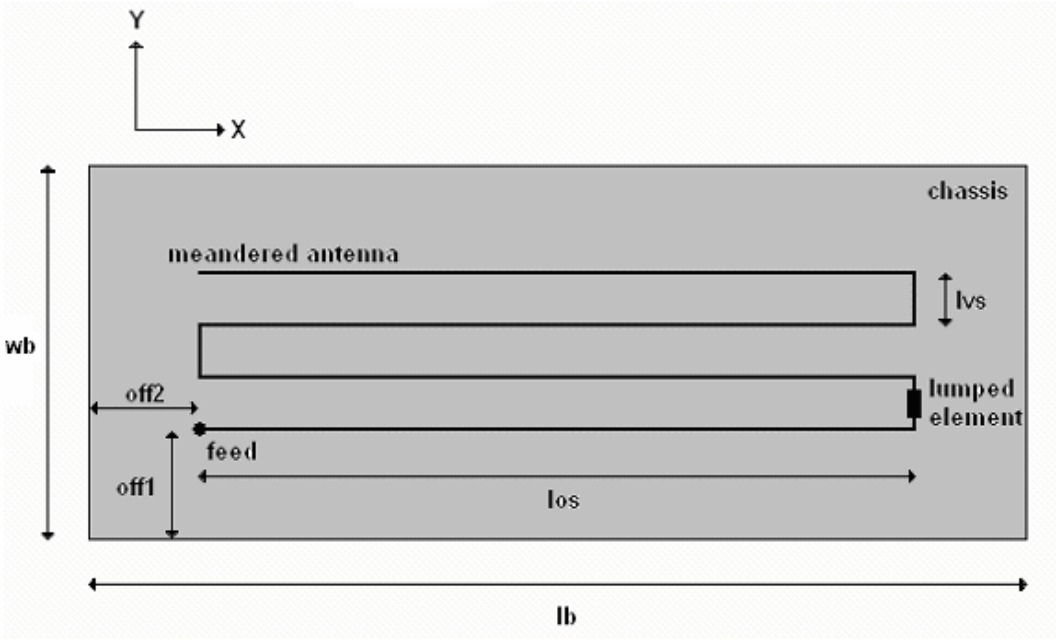

Figure 5.74: meandered antenna in the XY plane.

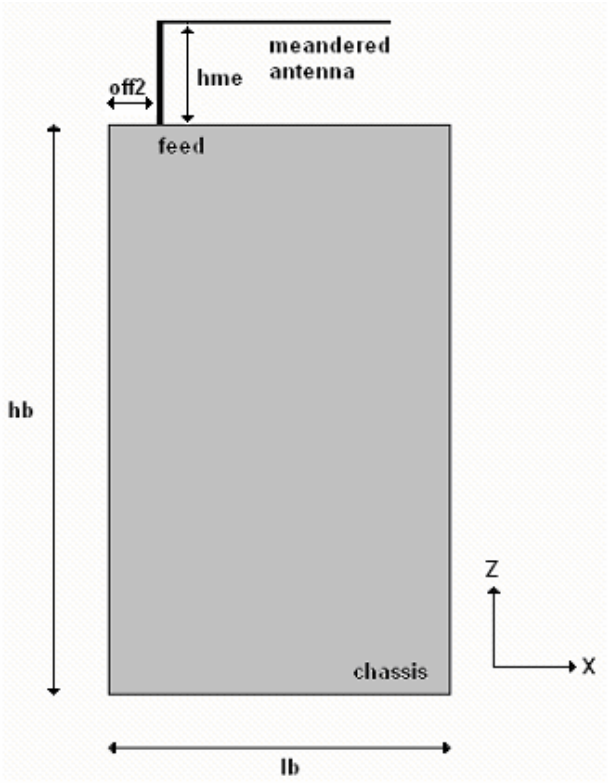

Figure 5.75: meandered antenna in the XZ plane.

In the following table we summarize the antenna geometric features:

lb [mm]	wb [mm]	hb [mm]	hme [mm]
70	20	100	20
los [mm]	lvs [mm]	off1[mm]	off2 [mm]
65	5	5	5

Table 5.12: meandered antenna geometric features.

Now we proceed to show the simulation results.
As we can see in fig. 5.76, the resonance frequency decreases as the capacity increases, because of the fact that the antenna appears electrically longer.
Fig. 5.77 shows that the antenna quality factor experiences a saturation as the capacity grows, confirmed by the correspondent behaviour of the impedance bandwidth in fig.5.79.

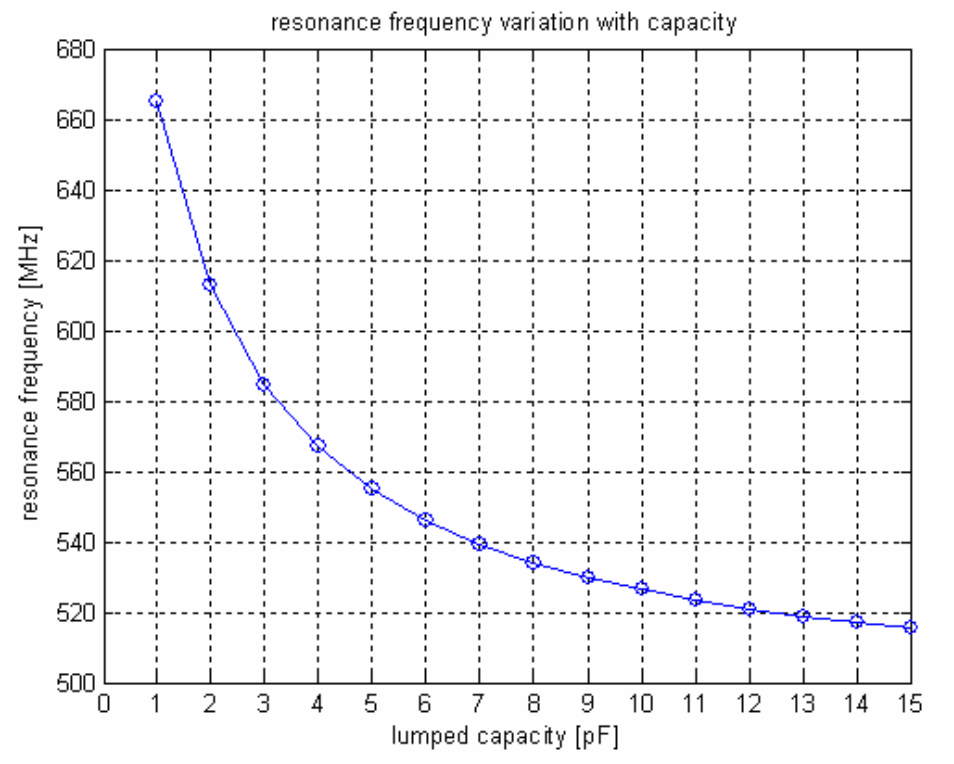

Figure 5.76: resonance frequency variation with capacity.

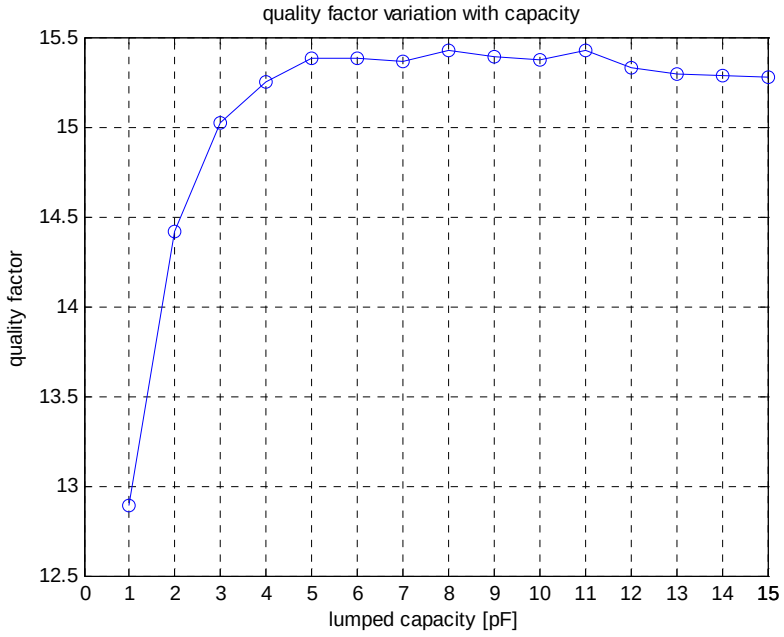

Figure 5.77: quality factor variation with capacity.

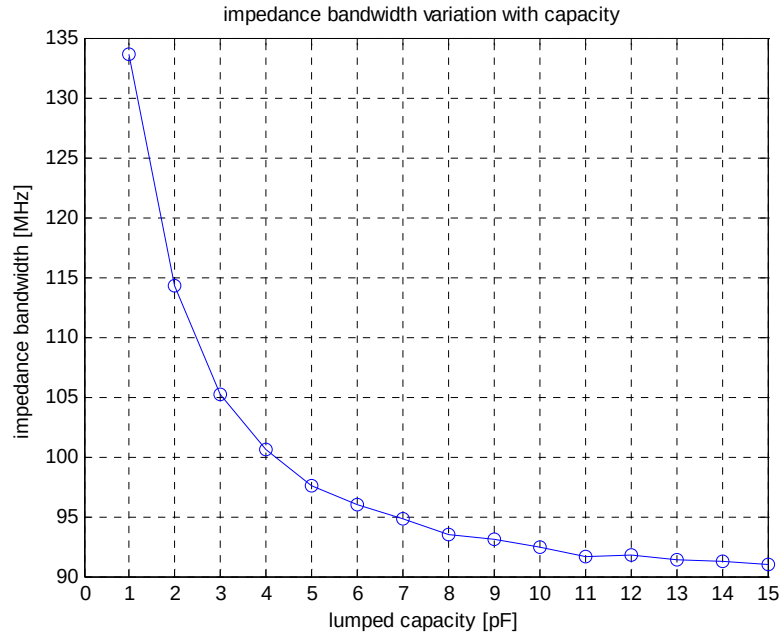

Figure 5.78: impedance bandwidth variation with capacity.

Finally we show the behaviour of the reflection coefficient S11 that allows the tuning over the desired frequency range.
As we can see in fig. 5.79, the tuneability is verified, with a correspondent relative impedance bandwidth of more than 40%.

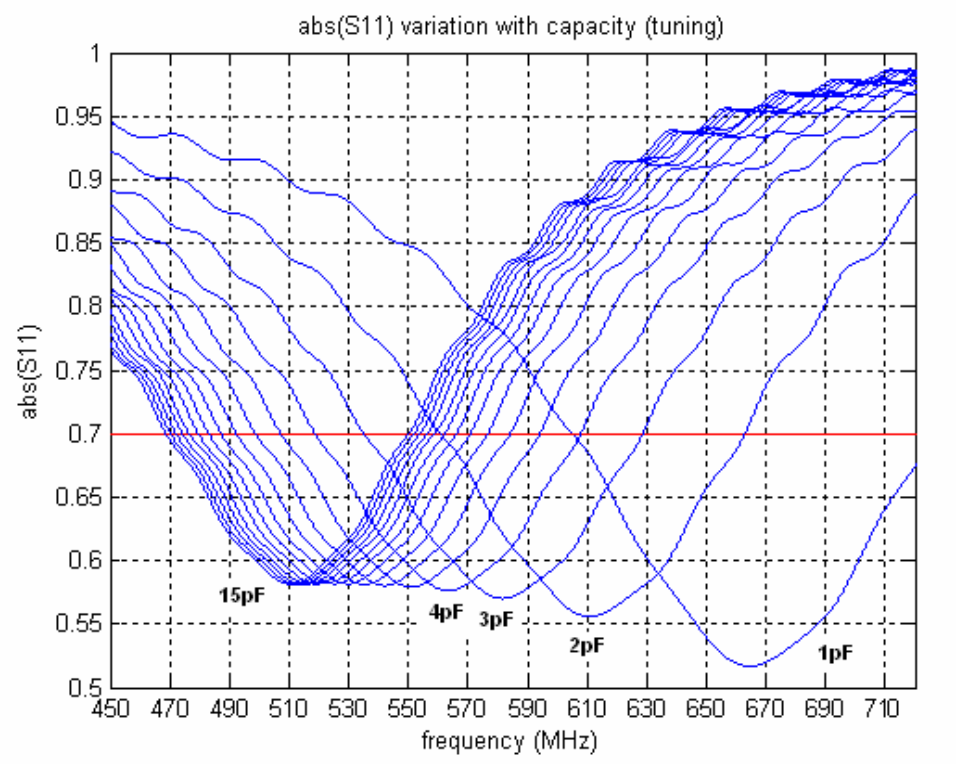

Figure 5.79: abs(S11) variation with capacity (tuning).

In the following we show the Smith chart for each tuning step, that reveals the limits of our implementation, because of the need of a better impedance matching.

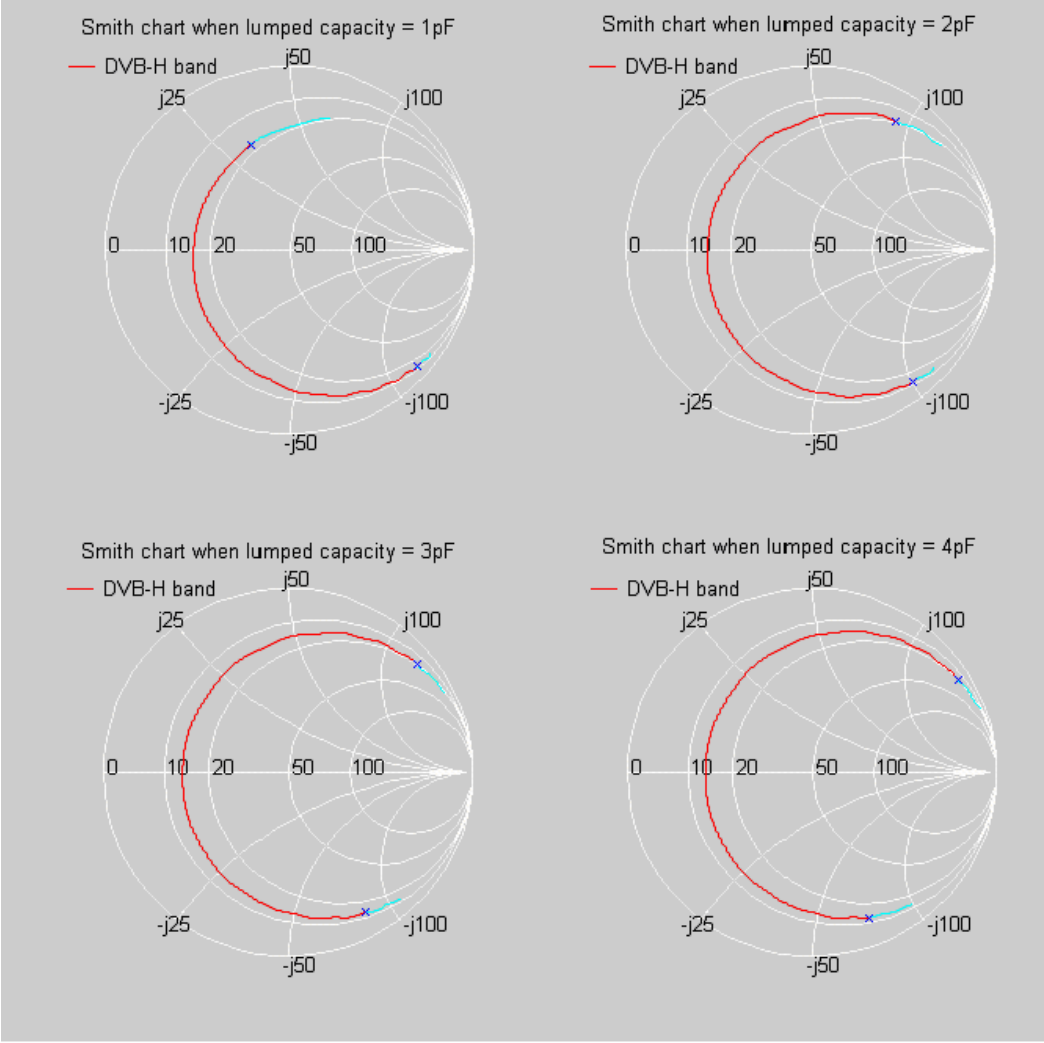

Figure 5.80: Smith charts corresponding to the top meandered monopole antenna with lumped capacity (1pF-4pF).

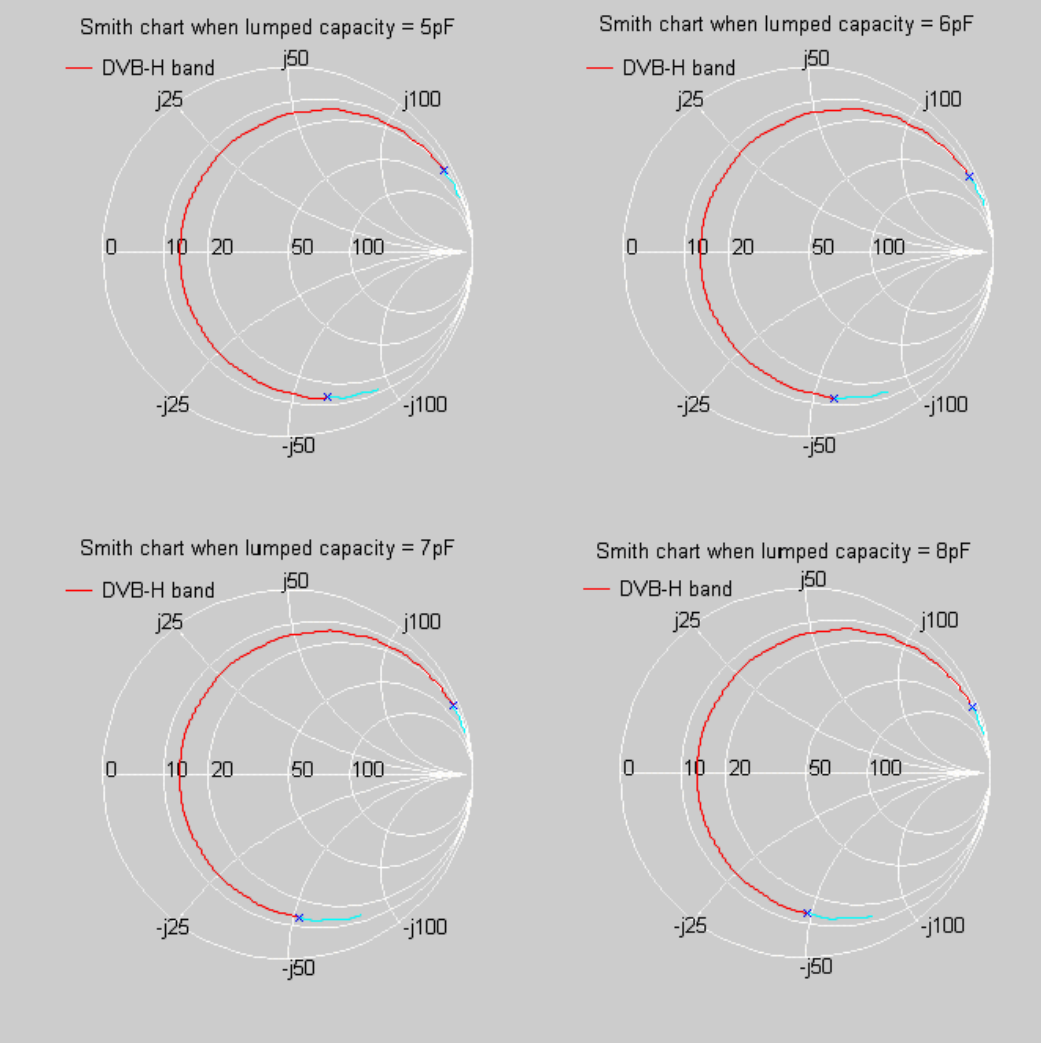

Figure 5.81: Smith charts corresponding to the top meandered monopole antenna with lumped capacity (5pF-8pF).

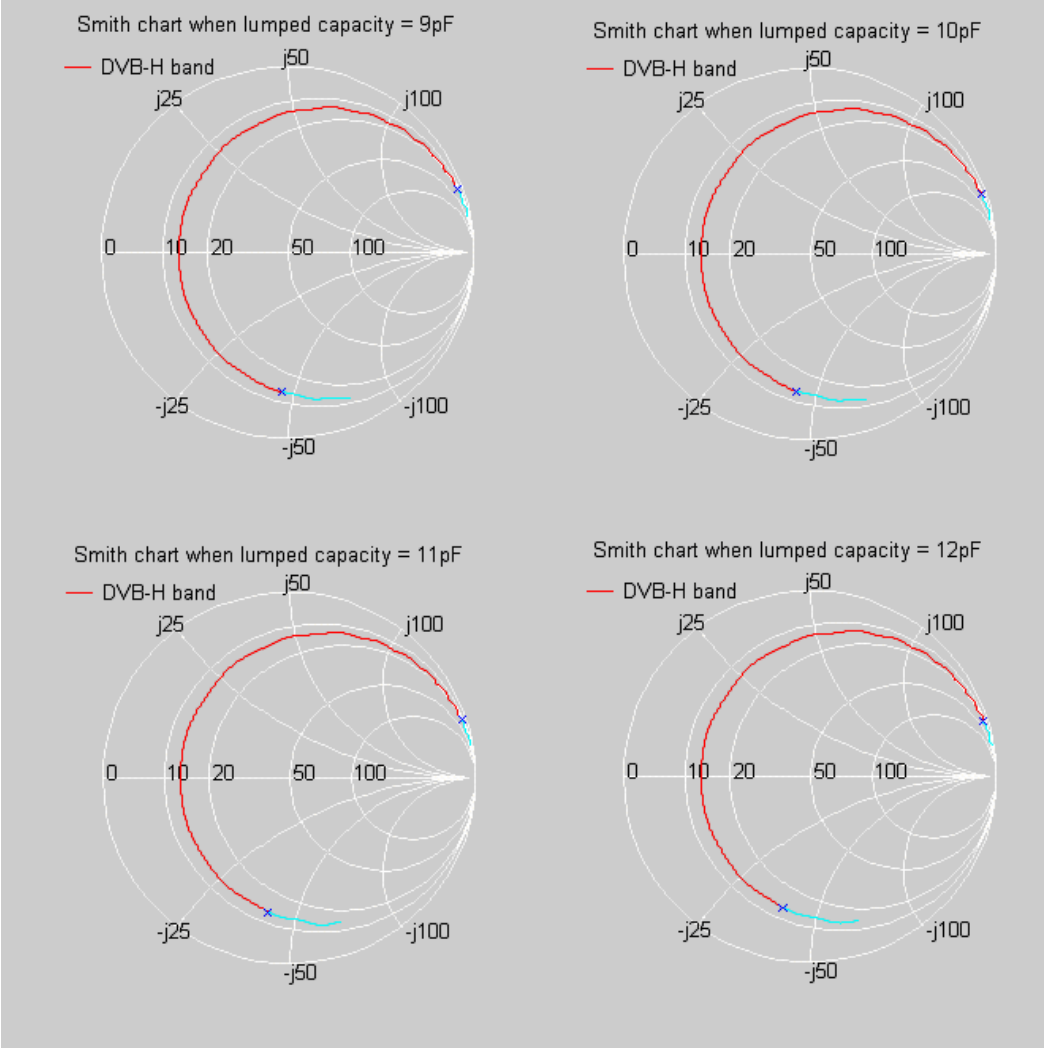

Figure 5.82: Smith charts corresponding to the top meandered monopole antenna with lumped capacity (9pF-12pF).

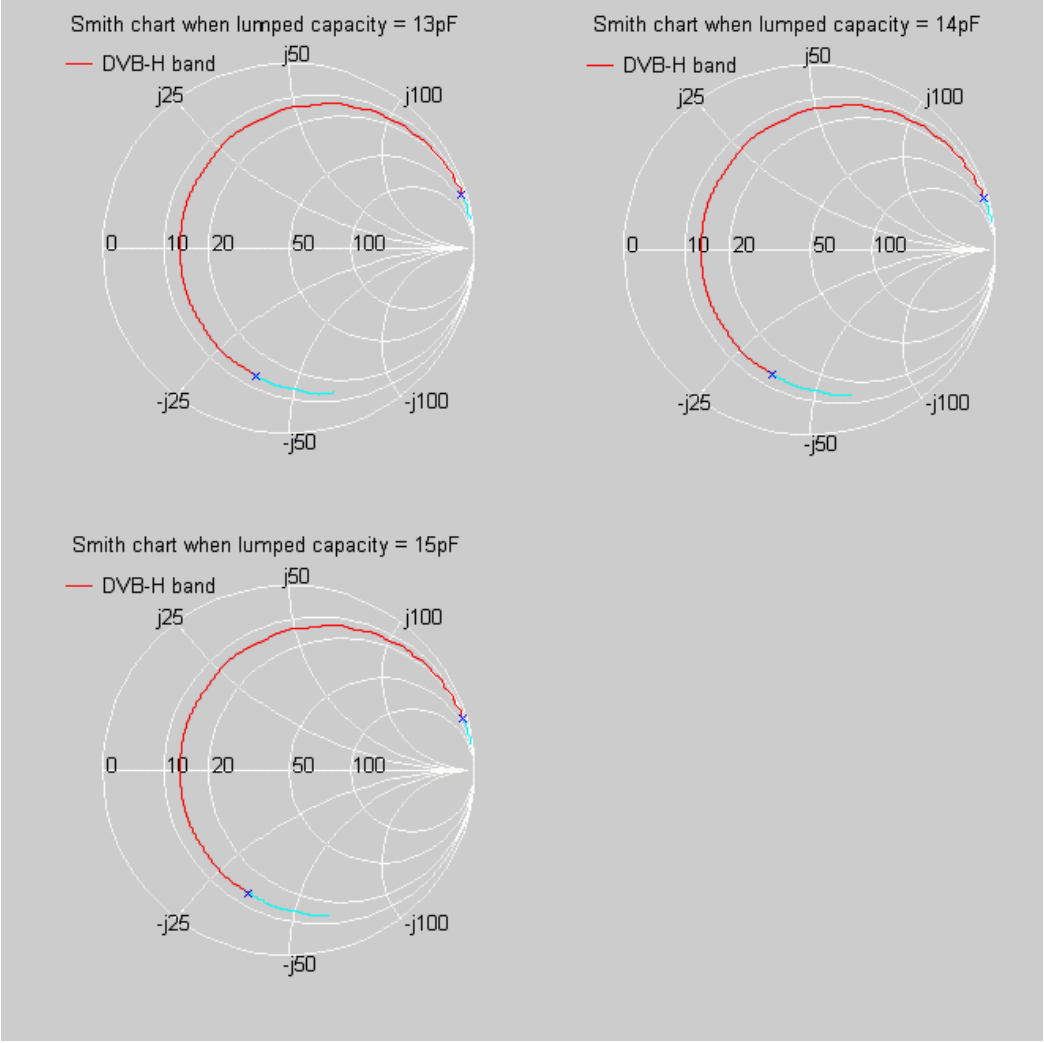

Figure 5.83: Smith chart corresponding to the top meandered monopole antenna with lumped capacity (13pF-15pF).

5.8.3: Effects of antenna volume reduction.

Now we modify slightly the antenna geometry, changing only the parater "hme", that is the height of the meandered antenna over the chassis box.

So we choose hme = 10mm reducing the antenna volume to $14cm^3$.

We expect worst performances respect to before, where hme was equal to 20mm.

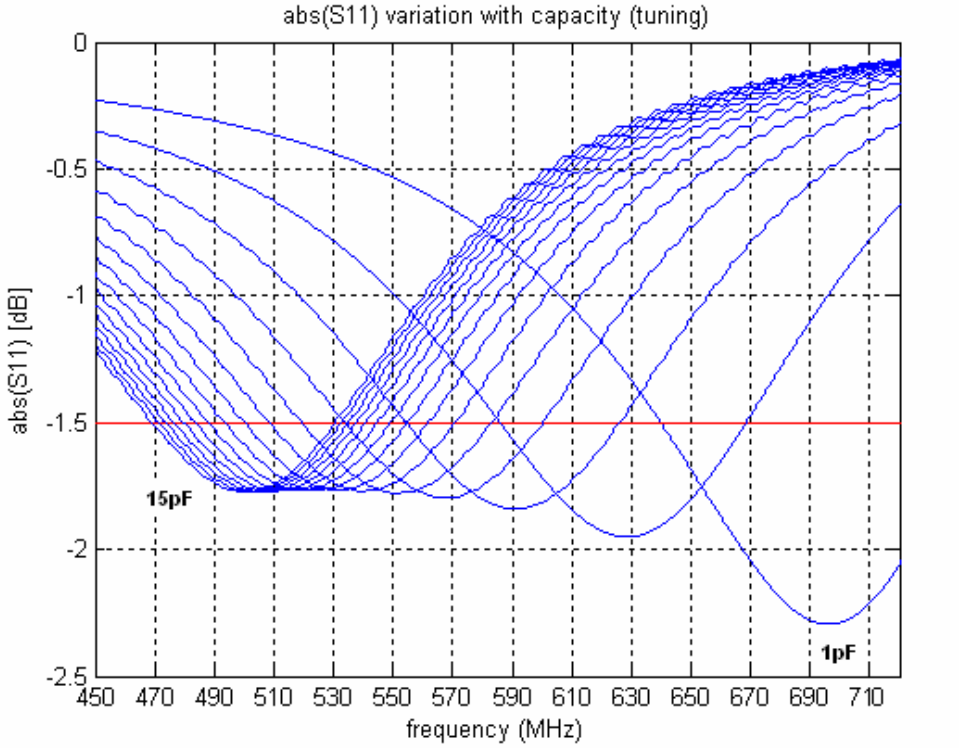

Figure 5.84: abs(S11) variation with capacity (tuning).

As we can see from fig. 6.84, we cannot satisfy our requirements.

In fact we defined the impedance bandwidth that frequency range in which the absolute value of the reflection coefficient S11 is smaller than -3 dB, but here we loose other 1.5 dB. Too much power is reflected back and then wasted.

If we want a better design solution for a smaller antenna, we have to change perspective, introducing for example a switched antenna, which input impedance can be matched progressively in different sub-bandwidths; in the next section we provide one example.

5.9: Top meandered switched monopole antenna.

5.9.1: Introduction.

Now we modify the meandered antenna studied before in section 5.8, reducing the height of the meander over the chassis (hme) to 10mm, and using only two sections for the meandering, as we can see in fig. 5.85.
In fact we are no more using lumped elements, but we will use several matching circuit to cover our bandwidth of interest (470MHz-702MHz).
This can be done with RF-switches, that select each time the needed matching circuit.
We will use simple L-section matching circuits (App. B), in order to reduce at minimum the number of reactive components to use. However, this is an ideal case, because of the fact we need to include the resistive parasitic losses in all the reactive elements we use.
Moreover we know that also the switches include losses, so that we should understand the advantages and the drawbacks of this choice.

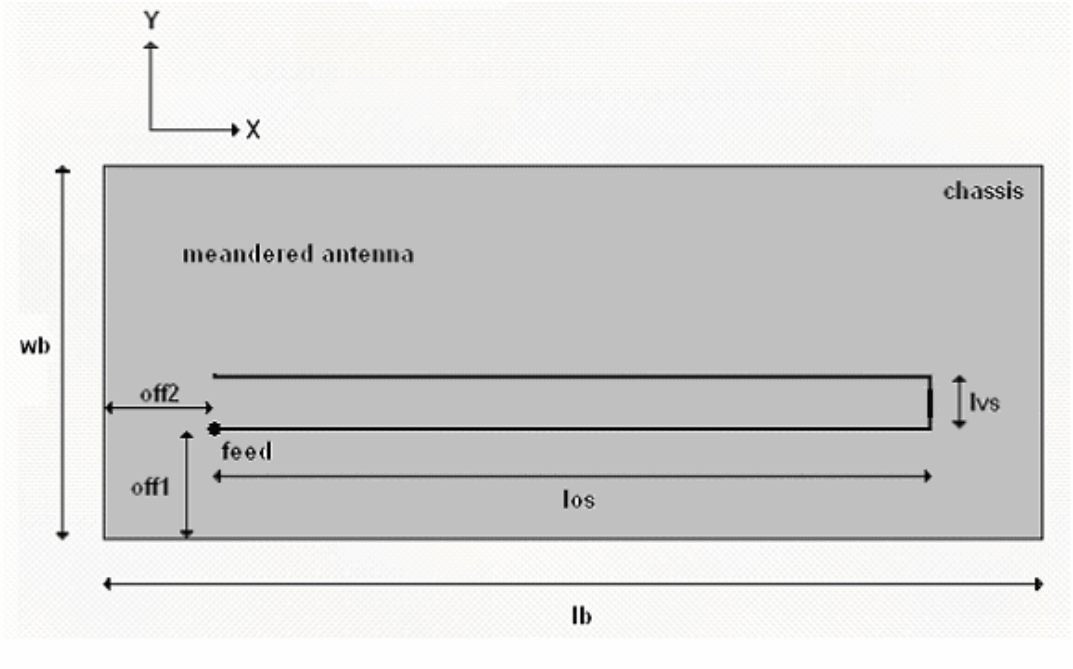

Figure 5.85: meandered monopole antenna view in the XY plane.

lb [mm]	wb [mm]	hb [mm]	hme [mm]
70	20	100	10
los [mm]	lvs [mm]	off1[mm]	off2 [mm]
65	5	5	5

Table5.13: geometric parameters of the simulated antenna.

5.9.2: Simulation.

As we can see from fig. 5.86, we need seven matching circuits to cover the whole bandwidth of interest, so that in each sub-bandwidth the antenna is matched to 50Ω.
In the next we show the Smith chart relative to each single matching circuit.
However, this is possible at the expense of both complexity and losses in our design.

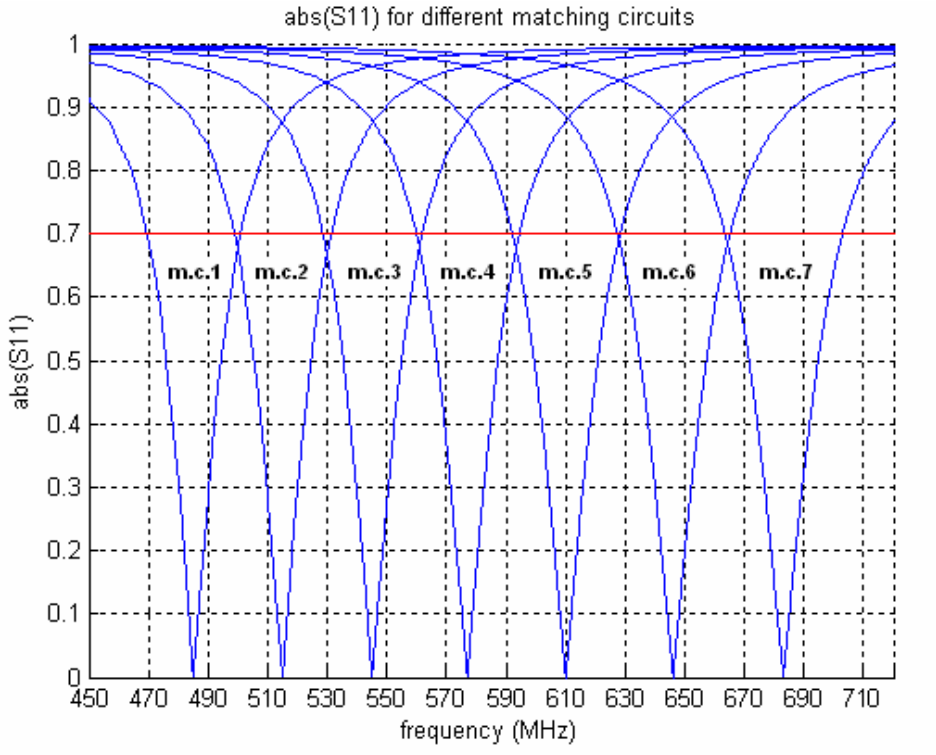

Figure 5.86: abs(S11) for different matching circuits (m.c.1-m.c.7).

matching circuit (m.c.)	m.c.1	m.c.2	m.c.3	m.c.4	m.c.5	m.c.6	m.c.7
Z1: capacity [pF]	20.71	19.6	18.71	17.51	16.21	14.87	13.49
Z2: inductance [nH]	35.34	28.13	21.84	16.1	10.9	5.85	1.16

Table5.14: values of the reactive elements in the matching circuits 1-7.

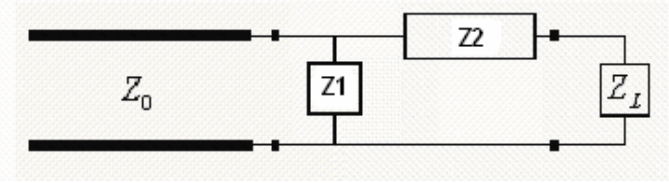

Figure 5.87: matching circuit topology.

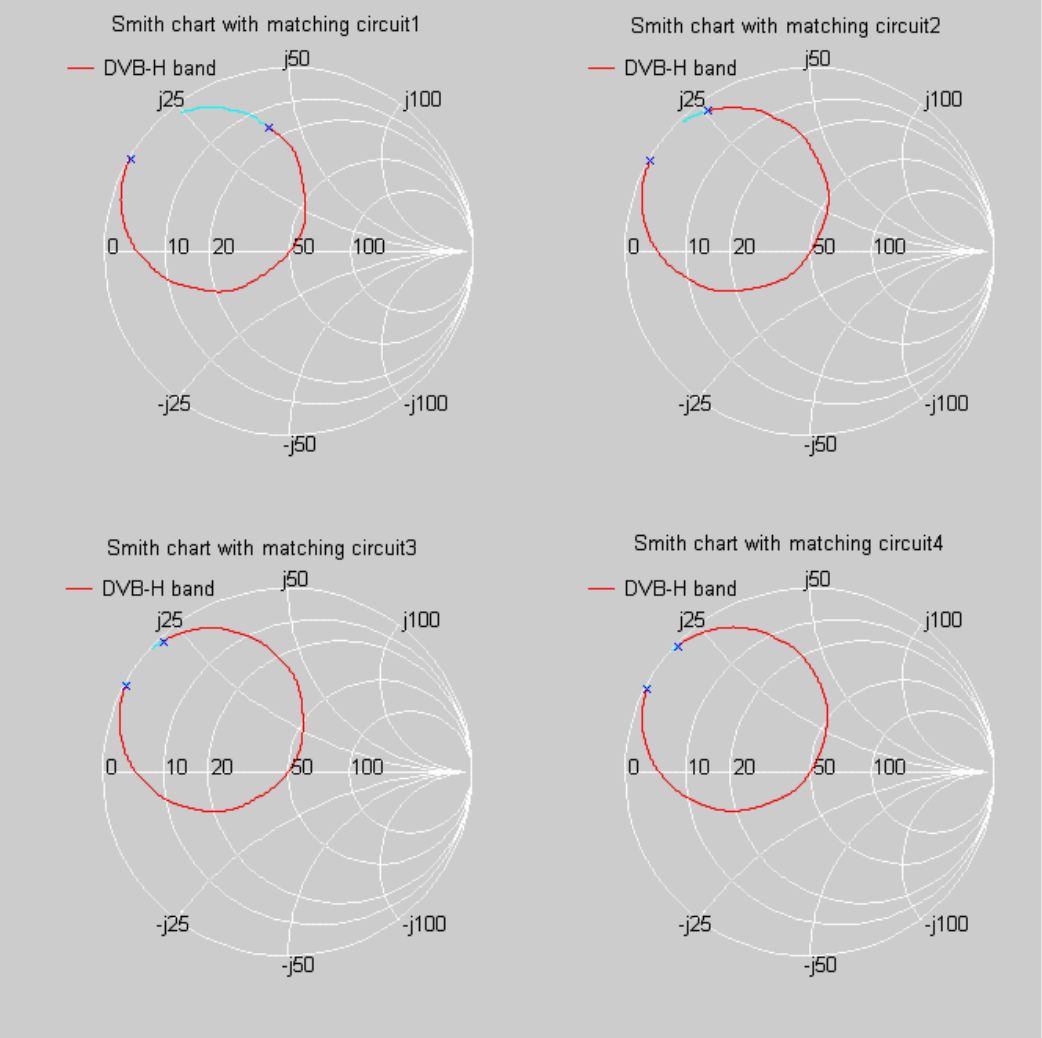

Figure 5.88: Smith charts for matching circuits 1-4.

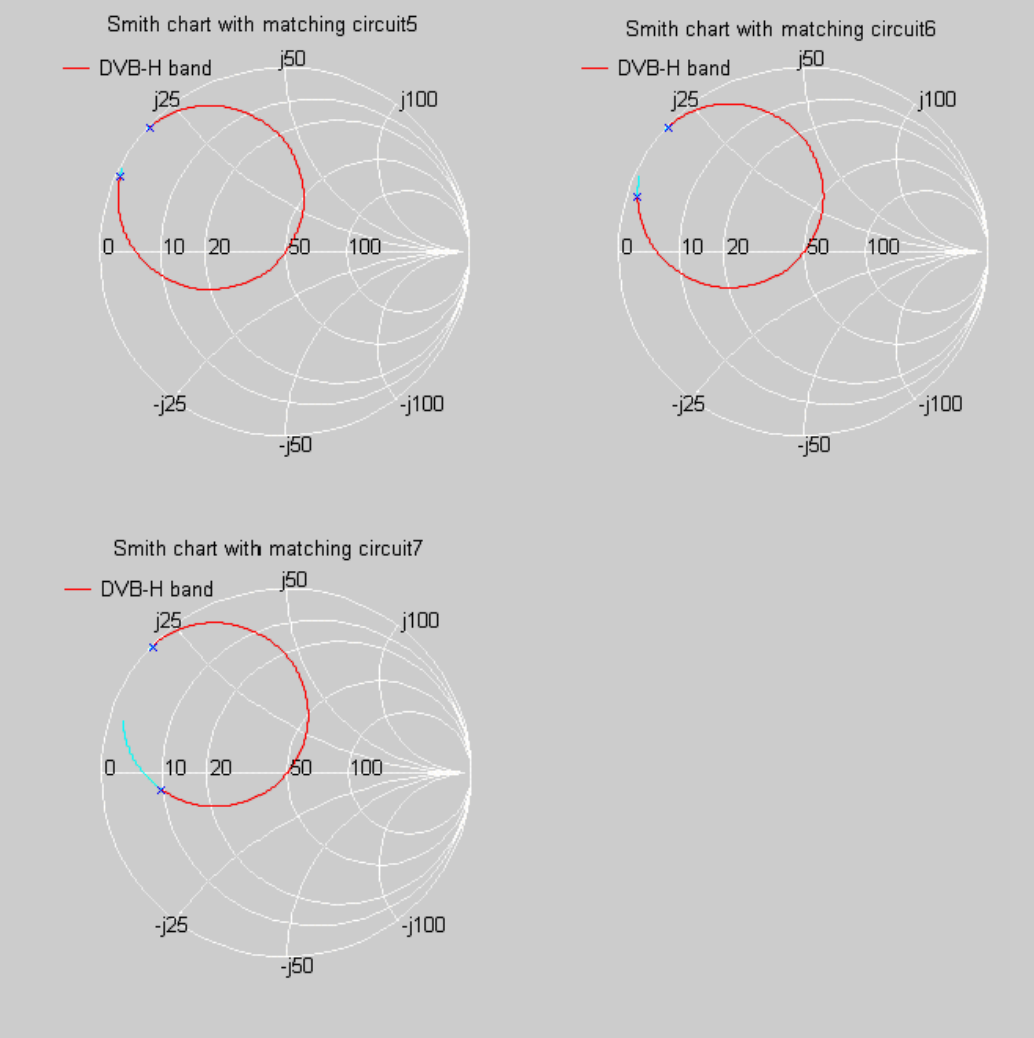

Figure 5.89: Smith charts for matching circuits 5-7.

5.9.3: Optimum impedance matching.

Because of the fact that with the L-sections we have a perfect match only at a single frequency, we tried to find a compromise between impedance bandwidth and the absolute value of the reflection coefficient S11 in each sub-bandwidth.
We did this keeping the same matching network topology, made up by two reactive elements as before (fig.5.87).
Thanks to a proper sweep of the values of these reactive elements, we found an optimum, that corresponds to the highest impedance bandwidth possible keeping S11 less than 0.7.
As we can see from fig. 5.90, now we need only five matching circuits, that makes easier the design because of the reduced number of components implied.
Even if the wide bandwidth matching theory would suggest the use of more reactive elements for each single matching circuit, this is the best solution we found with only two reactive components.

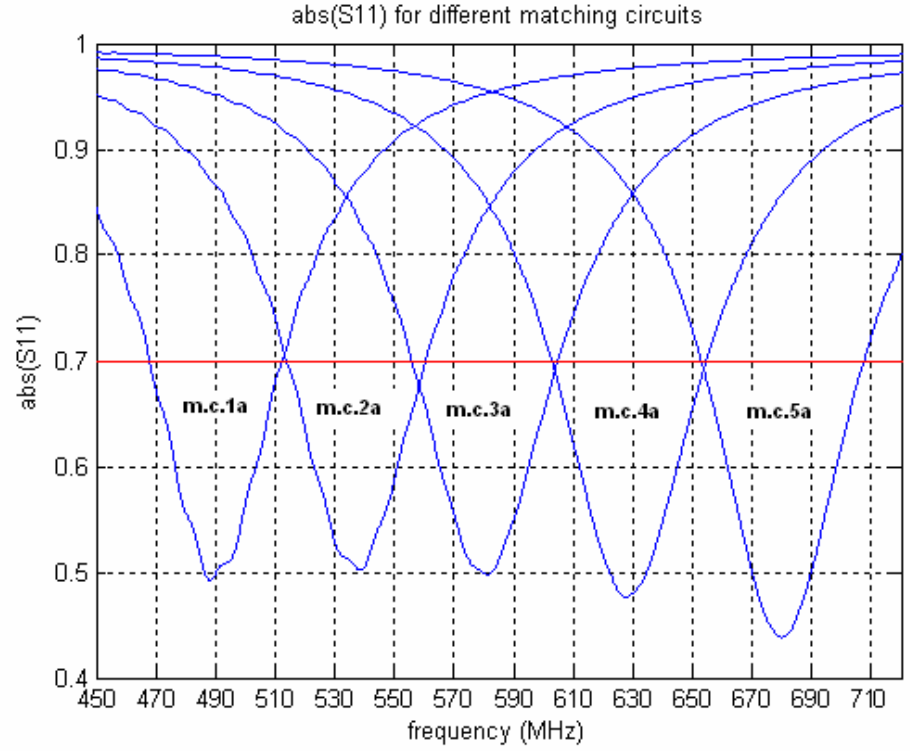

Figure 5.90: abs(S11) for different matching circuits (m.c.1a-m.c.5a).

matching circuit (m.c.)	m.c. 1a	m.c.2a	m.c.3a	m.c.4a	m.c.5a
Z1: capacity [pF]	10.14	10.48	8.78	8.47	7.51
Z2: inductance [nH]	36.73	25.77	17.72	9.96	3.22

Table5.15: values of the reactive elements in the matching circuits 1a-5a.

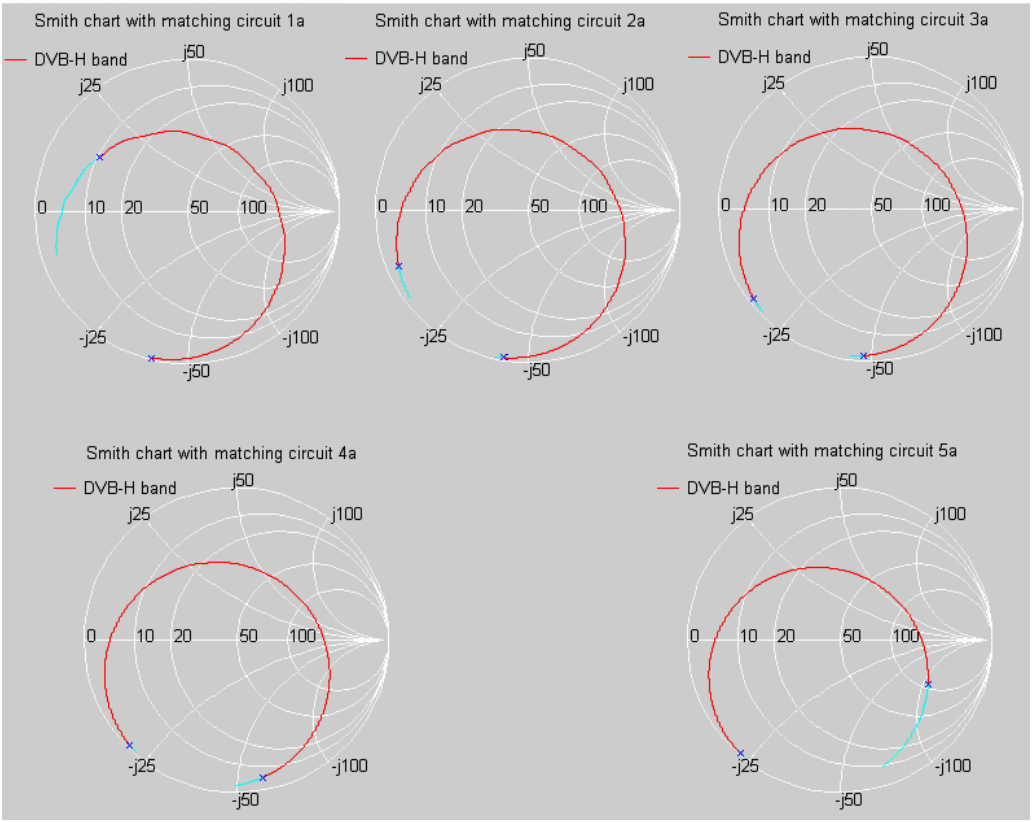

Figure 5.91: Smith charts for matching circuits 1a-5a.

5.9.4: Simulations and impedance matching with a smaller volume antenna.

In the next we show the limit of this approach, considering the same antenna as before but changing only the height "hme" from 10mm to 5mm.
Now we expect a narrower bandwidth in each sub-bandwidth, so that we will need more matching circuits to cover our frequency range (470MHz-702MHz).
As we can see in fig.5.92, now we need 24 matching circuits, and this number seems to be too high.

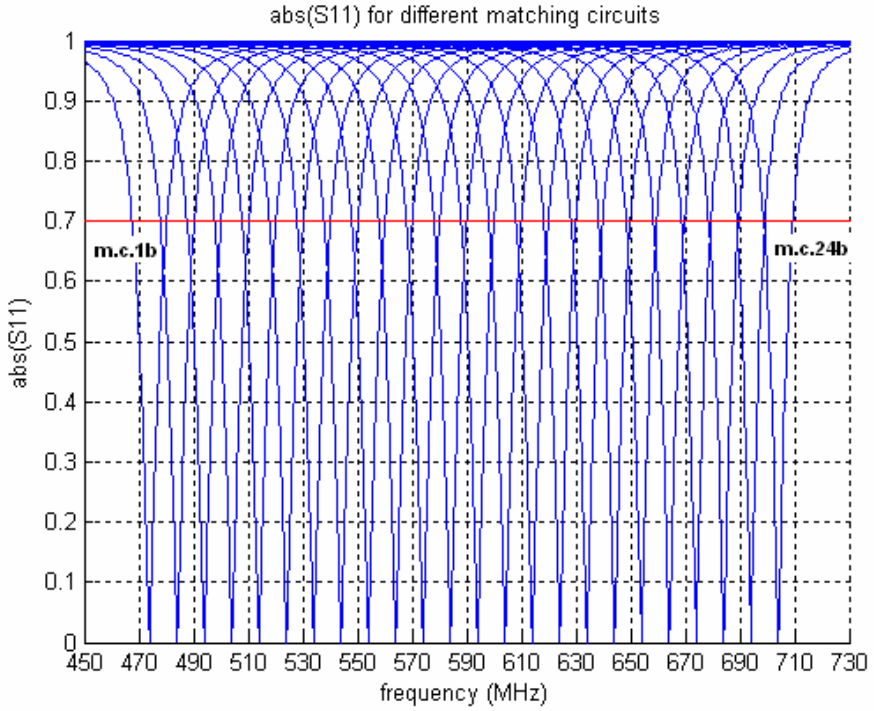

Figure 5.92: abs(S11) for different matching circuits (m.c.1b-m.c.24b).

matching circuit (m.c.)	m.c. 1b	m.c.2b	m.c.3b	m.c.4b	m.c.5b	m.c.6b
Z1: capacity [pF]	39.39	39.11	38.47	37.74	37.4	36.46
Z2: inductance [nH]	16.55	14.73	13.06	11.43	9.89	8.42
matching circuit (m.c.)	m.c.7b	m.c.8b	m.c.9b	m.c.10b	m.c.11b	m.c.12b
Z1: capacity [pF]	36.19	35.26	34.85	34.09	33.46	32.87
Z2: inductance [nH]	6.99	5.63	4.3	3.04	1.8	0.59
matching circuit (m.c.)	m.c. 13b	m.c.14b	m.c.15b	m.c.16b	m.c.17b	m.c.18b
Z1: capacity [pF]	32.08	31.57	30.77	30.15	29.55	28.64
Z2: capacity [nF]	0.58	1.75	2.86	3.99	5.08	6.18
matching circuit (m.c.)	m.c.19b	m.c.20b	m.c.21b	m.c.22b	m.c.23b	m.c.24b
Z1: capacity [pF]	28.41	27.09	27.31	25.59	26.2	24.2
Z2: capacity [nF]	7.29	8.35	9.5	10.55	11.77	12.82

Table5.16: values of the reactive elements in the matching circuits 1b-2.

So we tried as before to reduce the number of matching circuits.
We found an optimum configuration in which 15 matching circuits instead of 24 are needed, even if also this number seems to be high.

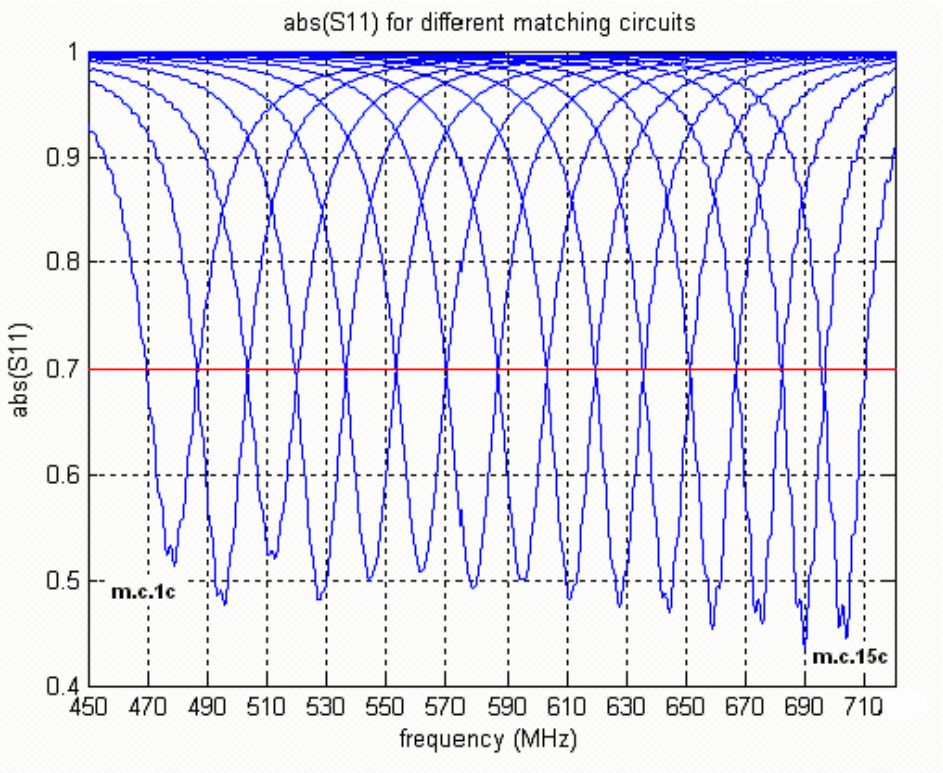

Figure 5.93: abs(S11) for different matching circuits (m.c.1c-m.c.15c).

matching circuit (m.c.)	m.c.1c	m.c.2c	m.c.3c	m.c.4c
Z1: capacity [pF]	21.36	22.11	20.3	20.97
Z2: inductance [nF]	17.71	14.53	12.02	9.41
matching circuit (m.c.)	m.c.5c	m.c.6c	m.c.7c	m.c.8c
Z1: capacity [pF]	19.82	19.01	18.81	18.03
Z2: inductance [nF]	7.14	4.88	2.73	0.76
matching circuit (m.c.)	m.c.9c	m.c.10c	m.c.11c	m.c.12c
Z1: capacity [pF]	17.8	17.19	16.72	16.33
Z2: capacity [nF]	1.18	3.03	4.82	6.56
matchingcircuit (m.c.)	m.c.13c	m.c.14c	m.c.15c	
Z1: capacity [pF]	15.71	15.41	14.86	
Z2: capacity [nF]	8.28	10	11.54	

Table5.17: values of the reactive elements in the matching circuits 1c-15b.

Conclusions

In this Master Thesis, we modified the 2nd generation FDTD program created by the Center for Person Kommunikation (CPK) at Aalborg University, in order to include lumped components in our simulations (App. A, C). It was then possible to simulate resistors, capacitors and inductors.
We found a fair agreement between our lumped components modellization and the commercial software CST Microwave Studio (5.4, 5.5).
We derived simple tendencies for all the antennas we simulated.
The antenna quality factor of a PIFA is more sensitive to the height of the top plate over the ground plane, even if also the ratio between the top plate dimensions has to be considered (5.2).
Even if the quality factor dramatically decreases as this height increases, we always need to make the antenna as small as possible, so that a large height is not acceptable.
The ground plane size is very important when we want characterize the behaviour of one antenna. In fact we found that the antenna input impedance starts to converge only when the ground plane size is comparable with one wavelength (5.3).
We derived similar tendencies for the antenna quality factor and for the resonance frequency.
However every time we need to establish a proper trade-off between accuracy of results and computational resources.
In order to simulate more realistic antennas, we replaced the ground plane with a metal chassis box, which approximate dimensions are dictated by our reference handheld device (5.4).
To gain more impedance bandwidth, we addressed our attention on tuneable antennas.
The first configuration we studied was not so promising, in fact when we simulate a varactor between the pifa top plate and the metal chassis box that acts as the ground plane, we are not able to satisfy our requirements (5.4).
In fact in this case we were not able to cover all our bandwidth of interest with an acceptable mismatch loss.
Then we introduced a new antenna structure: the meandered pifa antenna (5.5).
This antenna is made up by two meandered plates properly connected by a varactor, and varying progressively its capacity value, we are able to have a full tuning over our band of interest (470MHz, 702MHz), with a mismatch loss criterium of -3dB.
When we include a series resistor to model the varactor, we experience a lower radiation efficiency, even if we need a smaller varactor tuning range thanks to a wider impedance bandwidth.
Because of the need of smaller volume antennas, we changed antenna geometry introducing the meandered monopole antenna (5.6, 5.7).
We found that when we increase the number of the meandering sections, the capacitive coupling between the subsequent sections makes the antenna electrically shorter.
We tried different configurations, and the most promising was the tuneable meandered monopole, that allowed us to satisfy our requirements with a reduced varactor tuning range (5.8).

However the height of the meandering over the chassis metal box was still to high, so that we tried to provide more compact solutions.
In the last investigations we introduced a switched meandered monopole antenna, that thanks to several matching circuits provided a satisfactory impedance bandwidth in a limited volume (5.9).
We conclude that each solution we found has his advantages and drawbacks, and that only a combined tuneable-switchable antenna would dramatically decrease the antenna volume, at the expense of both antenna complexity and losses increase.

Future work

One of the missing parts in this report is the measurement test, that would lead to a deeper understanding of the the simulated antenna design solutions.
In fact the lumped components we included in our simulations, can only give an overall idea of the real behaviour of components like varactors or switches once they are manufactured in real antennas.
More study is needed to reduce further the antenna volume, trying to find hybrid solutions such as a combined tuneable-switchable antenna.

APPENDIX A: FDTD lumped components documentation.

A.1: Documentation.

Here we show the modifications that have been made to the FDTD program developed at Aalborg University to include lumped components.
We found the theoretical background for this implementation mainly in Taflove [A.1], and we modified properly the FDTD algorithm developed at Aalborg University in Fortan77.
We decided to model capacitors, resistors and inductors, even if in some commercial software we can find also more complicate components such as diodes, MOSFET and so on.
However in those implementation, the FDTD package includes a direct link to programs such PSPICE, that make easier to model in the FDTD code very complicated structures.
We thought to have the capability to directly include the definition of the lumped components in the "filename.adf" file, in order to be consistent with the first will of the algorithm designer to give to the final user a user-friendly way to set up a simulation in short time.
The main idea is to specify in the lowest number of parameters the characteristics of the lumped components we want to include in the FDTD algorithm.
First of all we have to specify where this lumped component has to be placed in the FDTD lattice.
In order to do this we choose three spatial coordinates that will specify the single FDTD cell, respectively in the x, y and z direction.
The next step is to specify the orientation of this component, that is its alignment respectively with the x, y or z axis.
Now we specify the type of the component and after its impedance value, that will be set automatically depending on the type specified respectively in Farads, Ohms or Henries.
We can have in the algorithm as much lumped components we want, depending on our needs.
The lumped components definition is organized in arrays, so that the user has more control to the whole implementation.
The first thing to do when we set up the simulation is to define the proper values in the file "static.h", where takes place the static allocation of all the arrays the algorithm needs.
In our case we will simply add information about the max number of lumped components we want to use in our simulation.

Now we show more details of this implementation:

- lum: it is a binary variable to enable or disable the lumped components:
  1. lum = 1: the lumped component algorithm is enabled.
  2. lum = 0: the lumped component algorithm is disabled.

- lumax: it is the max number of lumped components used in the simulation, and it has to be specified in the file "static.h" for the allocation of the corresponding arrays.

- index: it is a dummy index to describe the elements of the lumped components arrays.

- lumx(index) for index = 1, 2, 3, . . . , lumax is the x location of the cell corresponding to the $(index)^{th}$ lumped component.

- lumy(index) for index = 1, 2, 3, . . . , lumax is the y location of the cell corresponding to the $(index)^{th}$ lumped component.

- lumz(index) for index = 1, 2, 3, . . . , lumax is the z location of the cell corresponding to the $(index)^{th}$ lumped component.

- lumdir(index) for index = 1, 2, 3, . . ., lumax is the orientation of the cell corresponding to the $(index)^{th}$ lumped component:
  1. lumdir(index) = -1 set the $(index)^{th}$ lumped component oriented along the x axis.
  2. lumdir(index) = 0 set the $(index)^{th}$ lumped component oriented along the y axis.
  3. lumdir(index) = 1 set the $(index)^{th}$ lumped component oriented along the z axis.

- lumtype(index) for index = 1, 2, 3, . . ., lumax is the type of the $(index)^{th}$ lumped component:
    1. lumtype(index) = 1 set the $(index)^{th}$ lumped component as a capacitor.
    2. lumtype(index) = 2 set the $(index)^{th}$ lumped component as a resistor.
    3. lumtype(index) = 3 set the $(index)^{th}$ lumped component as an inductor.

- lumimped(index) for index = 1, 2, 3, . . ., lumax define the value of the impedance of the $(index)^{th}$ lumped component: this value will be automatically set as a capacity [F], resistance [Ohm], or inductance [H] depending on the type of component in that specific lattice location.

In order to make working this lumped components algorithm, we had to modify the following files:

1. statich.h
2. define.h
3. define.f
4. filename.adf
5. writepar.f
6. parameters.h
7. maxwell.h
8. maxwell.f

A.2: Example.

All the previous statements summarize simply in the following example.
Supposing we want to place a lumped capacitor of 1pF in the FDTD location $cell_{x,y,z}(10,15,20)$ oriented along the z axis, a lumped resistor of 50.7 Ohm in the FDTD location $cell_{x,y,z}(18,23,35)$ oriented along the y axis, and finally a lumped inductor of 231.5 nH in the FDTD location $cell_{x,y,z}(11,22,32)$ oriented along the x axis, we simply do the following:

1. First we set in the "static.h" file lumax = 3, because of the fact we have a total number of three lumped components.

2. Now we define in the "filename.adf " the following parameters:

   lum =1

   lumx(1) = 10
   lumy(1) = 15
   lumz(1) = 20
   lumdir(1) = 1
   lumtype(1) = 1
   lumimped(1) = 1e-12

   lumx(2) = 18
   lumy(2) = 23
   lumz(2) = 35
   lumdir(2) = 1
   lumtype(2) = 2
   lumimped(2) = 50.7

   lumx(3) = 11
   lumy(3) = 22
   lumz(3) = 32
   lumdir(3) = -1
   lumtype(3) = 3
   lumimped(3) = 231.5e-9

3. Now we can continue the simulation set up as usual.

Appendix B: Impedance matching theory.

B.1: Impedance matching.

When the impedance of the antenna Z_L is different from the characteristic impedance of the feeding network Z_0, part of the voltage will be reflected from the antenna, corresponding to a loss of the power delivered to the antenna [B.1].
We can calculate the reflection coefficient as [B.2]:

$$\Gamma = \frac{Z_L - Z_0}{Z_L + Z_0} \tag{B.1}$$

When the antenna is perfectly matched to the feeding transmission line, no reflection will occur, so the Γ will be zero.
We don't desiderate a high reflection coefficient, because this corresponds in a waste of power in both cases of transmitting and receiving antenna.
However we have to accept a small mismatch to achieve good antenna performances, in order to have a fair matching on the whole band of operation of the antenna.
When we deal with transmission lines, we know that in the general case in each section there are two waves propagating in opposite directions, that create the so called standing wave pattern. So there will be a correspondent voltage at each point of the transmission line, result of the sum of the aforementioned two waves.
If we define a ratio between the maximum and the minimum value of this sum, we obtain the so called voltage standing wave ratio (VSWR) [B.3]:

$$VSWR = \frac{1+|\Gamma|}{1-|\Gamma|} \tag{B.2}$$

There are alternative ways to define a mismatching metric, such as the reflection loss (L_{refl}), that in other words is the power loss due to reflection [4]:

$$L_{refl} = 10 \cdot \log \frac{1}{1-|\Gamma|^2} \tag{B.3}$$

The return loss (L_{retn}) is useful to describe the ratio the propagated and reflected power:

$$L_{retn} = 10 \cdot \log \frac{1}{|\Gamma|^2} \tag{B.4}$$

The impedance bandwidth of one antenna stands for that frequency band over which a defined criterion can be fulfilled [B.1].
Typically the impedance bandwidth is defined in term of the absolute value of Γ, so for example the relation $|\Gamma|$ = 6 dB means that this criterium has to be maintained over the whole band of interests.
The previous relation corresponds equivalently to a L_{retn} = 6dB or VSWR< 3.01.

B.2: L-section impedance matching.

A very simple matching network is the L-section, made up by two reactive components, that can match an arbitrary load impedance to a transmission line.
These two elements are inductors or capacitors.
This topology is mainly attractive for its simplicity, because of the need of matching circuits with a limited number of elements, that introduce both parasitic resistive losses and manufacturing complexity.
There are two possible configurations for this matching network, depending on the value of the load impedance.
If we call with R_L the resistive part of the load impedance Z_L, and with Z_0 the characteristic impedance of the transmission line, we have the following analytic solutions:

1. $R_L > Z_0$

The impedance seen looking into the network made up by the cascade of the matching circuit and the load impedance must be equal to Z_0 (fig. B.1):

$$Z_0 = jX + \frac{1}{jB + \frac{1}{(R_L + jX_L)}} \tag{B.5}$$

Solving the previous equation separating real and imaginary parts we have [B.4]:

$$B = \frac{X_L \pm \sqrt{\frac{R_L}{Z_0} \cdot \left(R_L^2 + X_L^2 - Z_0 R_L\right)}}{R_L^2 + X_L^2} \tag{B.6}$$

$$X = \frac{1}{B} + \frac{X_L Z_0}{R_L} - \frac{Z_0}{B R_L} \tag{B.7}$$

Two physically realizable solutions are then possible

- if X is positive we have an inductor.
- if X is negative we have a capacitor.
- If B is positive we have a capacitor.
- If B is negative we have a capacitor.

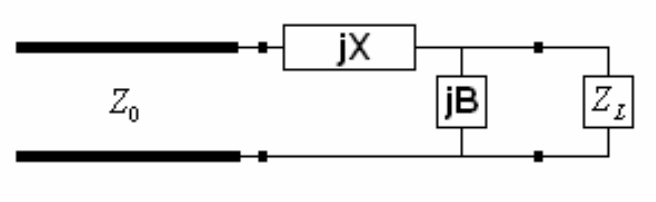

Figure B.1: Matching network for case 1.

2. $R_L < Z_0$

The impedance seen looking into the network made up by the cascade of the matching circuit and the load impedance must be equal to Z_0 (fig. B.2):

$$Z_0 = \frac{1}{jB + \frac{1}{R_L + j(X + X_L)}} \tag{B.8}$$

Solving the previous equation separating real and imaginary parts we have [B.4]:

$$X = \pm\sqrt{R_L \cdot (Z_0 - R_L)} - X_L \tag{B.9}$$

$$B = \pm\frac{1}{Z_0}\sqrt{\frac{(Z_0 - R_L)}{R_L}} \tag{B.10}$$

Four physically realizable solutions are then possible.

- if X is positive we have an inductor.
- if X is negative we have a capacitor.
- If B is positive we have a capacitor.
- If B is negative we have a capacitor.

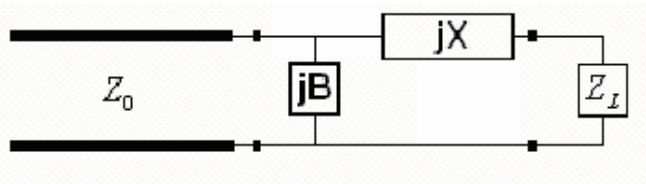

Figure B.2: Matching network for case 2.

Appendix C: Fotran77 code for the lumped components modelling in the FDTD Algorithm developed at Aalborg University.

C.1: static.h

```
*~~~~~~~~~~~~~~~~~~~~~~~~~~~~~~~~~~~~~~~~~~~~~~~~~~~~~~~~~~~~~~~~~~~~-*-fortran-*-~~~~~~~~~~
* DEFINITION OF GLOBAL PARAMETERS
* ------------------------------
* mats   : Maximum number of materials inclusive basic media. Note,
*          that mats >= 1!
* maxant : Maximum number of unit cell of media different from basic.
* maxze  : Maximum number of E-field components that are zeroed.
* mnotdp : Maximum number of time domain points output.
* mnos   : Maximum number of sources.
* mnoi   : Maximum number of impedance points
* mnonfb : Maximum number of near field boxes
*~~~~~~~~~~~~~~~~~~~~~~~~~~~~~~~~~~~~~~~~~~~~~~~~~~~~~~~~~~~~~~~~~~~~~~~~~~~~~~~~~~~~~~~~~~~~
~~~
      integer mats,maxant,maxze,mnotdp,mnos,mnoi,mnonfb,mnotw,lumax

      parameter ( mats=3, maxant=300000,maxze=20000,mnotdp=8,mnos=1,
     -      mnoi=1, mnonfb=3,mnotw=1,lumax=3)
```

C.2: define.h

```
 * -*-fortran-*-
*********************************************************************
* define.h                    * 2nd Generation FDTD Program   *
* Contains type declarations for    * Aalborg University, CPK       *
* main define and ADF.              * Compiled by kvs 01-96         *
*********************************************************************

* local
      integer l

*~~~~~~~~~~~~~~~~~~~~~~~~~~~~~~~~~~~~~~~~~~~~~~~~~~~~~~~~~~~~~~~~~~~~~~~~
~~~
* DEFINITION OF GLOBAL PARAMETERS
* ------------------------------
* pi     : pi
* d2r    : degree->radian conversion
* r2d    : radian->degree conversion
*~~~~~~~~~~~~~~~~~~~~~~~~~~~~~~~~~~~~~~~~~~~~~~~~~~~~~~~~~~~~~~~~~~~~~~~~
~~~
      real pi,r2d,d2r

      parameter (pi=3.14159265, d2r=pi/180.0, r2d=180.0/pi)

*~~~~~~~~~~~~~~~~~~~~~~~~~~~~~~~~~~~~~~~~~~~~~~~~~~~~~~~~~~~~~~~~~~~~~~~~
~~~
* OTHER SYMBOLIC CONSTANTS AND TYPE DECLARATIONS
* ---------------------------------------------
* xdir,ydir,zdir are used when building the FDTD space.
*~~~~~~~~~~~~~~~~~~~~~~~~~~~~~~~~~~~~~~~~~~~~~~~~~~~~~~~~~~~~~~~~~~~~~~~~
~~~
      integer xdir,ydir,zdir
      parameter(xdir=-1,ydir=0,zdir=1)



*~~~~~~~~~~~~~~~~~~~~~~~~~~~~~~~~~~~~~~~~~~~~~~~~~~~~~~~~~~~~~~~~~~~~~~~~
~~~
* TYPE DECLARATION OF VARIABLES USED IN ASCII DEFINITION FILE
(ADF)
* all variables are explained in the ADF.
*~~~~~~~~~~~~~~~~~~~~~~~~~~~~~~~~~~~~~~~~~~~~~~~~~~~~~~~~~~~~~~~~~~~~~~~~
~~~
```

```
* PARAMETERS FOR SIMULATION IDENTIFICATION
* ----------------------------------------
      character*60 titel
      character*12 fname
      parameter(fname ='indata')
      integer sid

* PARAMETERS FOR SIMULATION OUTPUTS AND CONTROLS
* ----------------------------------------------
      character*24  outfile1,outfile2,outfile3,outfile4,
     -      outfile5,outfile6,outfile7,outfile8,outfile9,
     -      logfil,infile
      character*12 template
      logical timedo,eqcur,fraeqcur,nefi,farfi,fsamp,patch,imped,
     -      inputpow,rpow,h_source,e_source

* PARAMETERS FOR FUNDAMENTAL FDTD SETTINGS
* ----------------------------------------

      integer xo,yo,zo
      integer lb,hb,wb,hsc,wsc,L1p,L2p,soff
      integer ibx,iby,ibz,lbx,lby,lbz,mg

      integer maxx,maxy,maxz
      real resol

* PARAMETERS FOR GENERATING THE ADF FILE
* --------------------------------------
      integer l1,l2,l3,l4,l5

* PARAMETERS FOR ELECTRICAL FIELD SOURCE
* --------------------------------------
      logical impuls
      integer anos, timoff, nmax
      real freq,sigmaf
      integer xs(mnos),ys(mnos),zs(mnos),
     -      nspx(mnos),nspy(mnos),nspz(mnos),
     -      apts(mnos)
      real tau,spread
      real ssd(mnos),phoff(mnos)
* PARAMETERS FOR IMPEDANCE
* ------------------------
      integer ximp(mnoi),yimp(mnoi),zimp(mnoi),nipx(mnoi),
     -      nipy(mnoi),nipz(mnoi),dioi(mnoi),anoi
      integer fsteps,imloop
      real BW
```

```
      logical mutadm
* PARAMETERS FOR NEARFIELD AND FARFIELD
* --------------------------------------
      integer minbx,minby,minbz,maxbx,maxby,maxbz
      integer nearbegx(mnonfb),nearbegy(mnonfb),nearbegz(mnonfb)
     -      ,nearendx(mnonfb),nearendy(mnonfb),nearendz(mnonfb)
      integer nfcode,anonfb
      real omega1,freq1

* PARAMETERS FOR INPUT POWER SETTINGS
* ------------------------------------
      integer pinx,piny,pinz,pinextx,pinexty,pinextz


* PARAMETERS FOR THINWIRE
* -----------------------
      integer anotw,thx(mnotw),thy(mnotw),thz(mnotw),thl(mnotw)
     -      ,thdir(mnotw)
      real thr(mnotw)
      logical thw


* PARAMETERS FOR TIME DOMAIN FIELDS AND STEADY STATE TEST-
POINT
* ---------------------------------------------------------------
      integer xtp,ytp,ztp
      integer anotdp
      integer xtim(mnotdp),ytim(mnotdp),ztim(mnotdp),fcomp(mnotdp)
      real criterion

* PARAMETERS FOR NF2FF-TRANSFORMATION
* ------------------------------------
      integer noang
      real alfa,beta,alfas,betas,thstart,thstop,deltath,deltaphi

* PARAMETERS FOR PATCH-CURRENT
*
~~~~~~~~~~~~~~~~~~~~~~~~~~~~~~~~~~~~~~~~~~~~~~~~~~~~~~~~~~~~~~~~~~~~~~~~~~~~~~
~~
      integer ixp1,ixp2,iyp1,iyp2,izp2
      real epsint,sigint

* PARAMETERS FOR MATERIALS
* ------------------------
      integer matno
      real epsi(mats),my(mats),sigma(mats)
```

```
* PARAMETERS FOR GENERATING AUTOCAD SCRIPT-FILE
* ---------------------------------------------
      logical acad

* SPACE SETTINGS
* --------------
      real deltax,deltay,deltaz,deltat


*~~~~~~~~~~~~~~~~~~~~~~~~~~~~~~~~~~~~~~~~~~~~~~~~~~~~~~~~~~~~~~~~~~~~~~~~~~~~~~~~
~~~
* VARIABLES FOR MATERIAL LOCATIONS
* --------------------------------
* matant = Number of unit cells with material specified by index
* x,y,z  = Coordiantes of unit cells with mateiral specified by
*          'mats' index.
*~~~~~~~~~~~~~~~~~~~~~~~~~~~~~~~~~~~~~~~~~~~~~~~~~~~~~~~~~~~~~~~~~~~~~~~~~~~~~~~~
~~~~
      integer matant(mats),x(maxant,mats),
     -      y(maxant,mats), z(maxant,mats),
     -      zxx(maxze), zxy(maxze), zxz(maxze),
     -      zyx(maxze), zyy(maxze), zyz(maxze),
     -      zzx(maxze), zzy(maxze), zzz(maxze)

      integer ix,iy,iz,lx,ly,lz,inx,iny,inz

* PARAMETERS FOR LUMPED ELEMENTS


      integer lumx(lumax)

      integer lumy(lumax)

      integer lumz(lumax)

      integer lumdir(lumax)

      integer lum

      integer lumtype(lumax)

       real lumimped(lumax)
```

```
*~~~~~~~~~~~~~~~~~~~~~~~~~~~~~~~~~~~~~~~~~~~~~~~~~~~~~~~~~~~~~~~~~~~~~~~~~~~~
~~~
* COMPLETELY DUMM VARIABLES!
* -------------------------
* The following variables are used to "convert" parameters to data
* statements. In the Ascii Definition File, some variables, which are
* supposed to be entered in a common area, are declared as parameters.
* Thus, these varibles must be changed to data statements in order to
* be put in a common area. This is done through the dummies.
*~~~~~~~~~~~~~~~~~~~~~~~~~~~~~~~~~~~~~~~~~~~~~~~~~~~~~~~~~~~~~~~~~~~~~~~~~~~~
~~~
      integer dmaxx, dmaxy, dmaxz
      integer dminbx, dminby, dminbz
      integer dmaxbx, dmaxby, dmaxbz

*  COMMON STATEMENTS
        common /sub1/ zxx,zxy,zxz,zyx,zyy,zyz,zzx,zzy,zzz,ix,iy,iz,
    -              lx,ly,lz,inx,iny,inz

        common /sub2/ x,y,z,matant

        common /lattice/ dmaxx,dmaxy,dmaxz,dmaxbx,dmaxby,dmaxbz,
    -       dminbx,dminby,dminbz

        common /anglepar/ noang,alfa,beta,alfas,betas,thstart,thstop,
    -                  deltath,deltaphi
        common /source/ anos,xs,ys,zs,nspx,nspy,nspz,apts,phoff,ssd
        common /impedance/ anoi,ximp,yimp,zimp,nipx,nipy,nipz,dioi
        common /logicimp/ imped
        common /nearfield/ anonfb,nearbegx,nearendx,nearbegy,
    -       nearendy,nearbegz,nearendz
        common /pin_par/ pinx,piny,pinz,pinextx,pinexty,
    -       pinextz,inputpow
        common /acadvar/ acad
        common /matnumber/ matno
        common /testpoint/ xtp,ytp,ztp
        common /tdpoint/ anotdp,xtim,ytim,ztim,fcomp
**********************************************************************
* LOCALS
* ------
**********************************************************************
      integer i,j,k
      integer nozex,nozey,nozez
      integer nftotl
```

C.3: define.f

```
*~~~~~~~~~~~~~~~~~~~~~~~~~~~~~~~~~~~~~~~~~~~~~~~~~~~~~~~~~~~~~~~~~~~~~~~~*
*                   FINITE DIFFERENCE TIME DOMAIN                       *
*                   for numerical calculations of                       *
*                        Maxwell's Equations                            *
*                      DEFINITION DESCRIPTION                           *
*                                                                       *
*               2nd Generation FDTD program by Ole Nørklit,             *
*               Gert Frølund Pedersen, and Kasper Vork Steffensen       *
*                                                                       *
*               This is the 2nd generation FDTD program                 *
*               developed at Aalborg University, at                     *
*               Center for Personkommunikation. This                    *
*               program is a revision and optimization of               *
*               the FDTD program developed by                           *
*               Sten Naae Hornsleth, Morten Damgaard,                   *
*               and Henrik Simonsen with contributions from             *
*               Henrik Kuhl, Jan Elling, Morten Gentsch,                *
*               Jørn Toftgaard, Ole Nørklit, Gert F Pedersen,           *
*               and Kasper V Steffensen.                                *
*                                                                       *
*               Aalborg University, Center for Personkommunikation      *
*               Denmark, fall 1995                                      *
*                                                                       *
*               Author: kvs, 11-95                                      *
*~~~~~~~~~~~~~~~~~~~~~~~~~~~~~~~~~~~~~~~~~~~~~~~~~~~~~~~~~~~~~~~~~~~~~~~~*

***********************************************************************
* Generates an binary definition     * 2nd Generation FDTD Program     *
* file (BDF) and optionally an       * Aalborg University, CPK         *
* Autocad 12 script file.            * Compiled by kvs 01-96           *
***********************************************************************

      program define
      implicit none

      include 'static.h'
      include 'define.h'

* INCLUDE ASCII DEFINITION FILE (ADF)
      include  'filename.adf'


* EVALUATION OF ADF DATA
      if(acad) then
         close(2, status='keep')
      end if

      omega1=freq1*2*pi          ! NF Fourier Transform Frequency

      if(impuls) then
         spread=2*pi*sigmaf      ! Angular spread
         tau=real(timoff)/spread ! Time offset
      else
         BW=0                    ! If sine, BW=0 and fsteps=1
```

```
         fsteps=1
      end if

      if(imloop.lt.0) imloop=0

      deltax=(1/sqrt(epsi(1)*my(1)))/(resol*freq)
      deltay=(1/sqrt(epsi(1)*my(1)))/(resol*freq)
      deltaz=(1/sqrt(epsi(1)*my(1)))/(resol*freq)
      deltat=deltax/(2*(1/sqrt(epsi(1)*my(1))))

      print*,'Frequency  =',freq
      print*,'resolution = ',resol
      print*,'Delta X    = ',deltax
      print*,'Delta T    = ',deltat

      alfa=alfa*d2r             ! Converting degress to radians
      beta=beta*d2r             ! for NF2FF calculations.
      alfas=alfas*d2r         ! rettet 25-09-96 gfp
      betas=betas*d2r
      thstart=thstart*d2r
      thstop=thstop*d2r
      deltath=deltath*d2r
      deltaphi=deltaphi*d2r

      do 300 i=1,anos
         phoff(i)=phoff(i)*d2r
 300  continue

      j=12
      do 400 i=1,12
         if(template(i:i).eq.' ') then
            if(i.lt.j) j=i
         end if
 400  continue

      outfile1=template(:j-1)//'.Timedom'       ! Timedomain fields
      outfile2=template(:j-1)//'.Eqcur'         ! Equivalent current
      infile  =template(:j-1)//'.EqcurIN'       ! READ Eqcur-file
      outfile3=template(:j-1)//'.Nearfi'        ! Nearfields
      outfile4=template(:j-1)//'.Farfi'         ! Farfields
      outfile5=template(:j-1)//'.Fsamp'         ! farfields
      outfile6=template(:j-1)//'.Patch'         ! patch current
      outfile7=template(:j-1)//'.Imped'         ! Impedance
      outfile8=template(:j-1)//'.Pin'           ! Input power
      outfile9=template(:j-1)//'.Radpow'        ! Radiated power
      logfil = template(:j-1)//'.LOGFILE'        ! LOGFILE


* STARTING TO WRITE BDF
      nozex = inx-1
      nozey = iny-1
      nozez = inz-1
      print*,'Number of Ex=0 ',nozex
      print*,'Number of Ey=0 ',nozey
      print*,'Number of Ez=0 ',nozez

      do 500 i=1,matno
```

```
         print*,'Number of cells for material ',i,' ',matant(i)
 500  continue


********** OPENING BINARY DEFINITION FILE (BDF) *************
*************************************************************
      open(1, file=fname, status='new', access='sequential',
     -      form='unformatted')

      write(1,err=8000)sid
      write(1,err=8000)titel
      write(1,err=8000)logfil
* WRITES SPECIFICATIONS AND SPECIAL PARAMETERS FOR SIMULATION
      write(1,err=8000)impuls
      write(1,err=8000)eqcur
      write(1,err=8000)farfi
      write(1,err=8000)fsamp
      write(1,err=8000)imped
      write(1,err=8000)nefi
      write(1,err=8000)rpow
      write(1,err=8000)timedo
      write(1,err=8000)inputpow
      write(1,err=8000)patch
      write(1,err=8000)h_source
      write(1,err=8000)e_source
      write(1,err=8000)fraeqcur
      write(1,err=8000)thw

* WRITES PARAMETERS FOR TEST POINT
      write(1,err=8000)xtp
      write(1,err=8000)ytp
      write(1,err=8000)ztp

      if(timedo) then
         write(1,err=8000)anotdp
         print*,'tdp=',anotdp
         do 600 i=1, anotdp
            write(1,err=8000)xtim(i)
            write(1,err=8000)ytim(i)
            write(1,err=8000)ztim(i)
            write(1,err=8000)fcomp(i)
 600     continue
         write(1,err=8000)outfile1
      end if

      if(eqcur) then
         write(1,err=8000)outfile2
         write(1,err=8000)infile
      end if


      if(nefi) then
         write(1,err=8000)outfile3
         write(1,err=8000)nfcode
         write(1,err=8000)omega1
         write(1,err=8000)anonfb
         do 650 i=1,anonfb
```

```
            write(1,err=8000)nearbegx(i)
            write(1,err=8000)nearendx(i)
            write(1,err=8000)nearbegy(i)
            write(1,err=8000)nearendy(i)
            write(1,err=8000)nearbegz(i)
            write(1,err=8000)nearendz(i)
650      continue
      end if

      if(farfi)then
         write(1,err=8000)noang
         write(1,err=8000)alfa
         write(1,err=8000)beta
         write(1,err=8000)outfile4
      end if
      if(fsamp)then
         write(1,err=8000)alfas
         write(1,err=8000)betas
         write(1,err=8000)thstart
         write(1,err=8000)thstop
         write(1,err=8000)deltath
         write(1,err=8000)deltaphi
         write(1,err=8000)outfile5
      end if

      if(patch) then
         write(1,err=8000)ixp1
         write(1,err=8000)ixp2
         write(1,err=8000)iyp1
         write(1,err=8000)iyp2
         write(1,err=8000)izp2
         write(1,err=8000)epsint
         write(1,err=8000)sigint
         write(1,err=8000)outfile6
      end if
      if (imped) then
         write(1,err=8000)outfile7
         write(1,err=8000)imloop
      end if
      if (inputpow) then
         write(1,err=8000)outfile8
         write(1,err=8000)pinx
         write(1,err=8000)piny
         write(1,err=8000)pinz
         write(1,err=8000)pinextx
         write(1,err=8000)pinexty
         write(1,err=8000)pinextz
      end if

       if(thw) then
          write(1,err=8000)anotw
          do 670 i=1,anotw
             write(1,err=8000)thx(i)
             write(1,err=8000)thy(i)
             write(1,err=8000)thz(i)
             write(1,err=8000)thdir(i)
             write(1,err=8000)thl(i)
```

```
            write(1,err=8000)thr(i)
 670       continue
       end if


      if (rpow) write(1,err=8000)outfile9

      write(1,err=8000)criterion
* WRITES PARAMETERS FOR 3 DIMENSIONS

      write(1,err=8000)maxx
      write(1,err=8000)maxy
      write(1,err=8000)maxz
      write(1,err=8000)maxbx
      write(1,err=8000)maxby
      write(1,err=8000)maxbz
      write(1,err=8000)minbx
      write(1,err=8000)minby
      write(1,err=8000)minbz
      write(1,err=8000)deltax
      write(1,err=8000)deltay
      write(1,err=8000)deltaz
      write(1,err=8000)deltat
      write(1,err=8000)freq
      write(1,err=8000)nmax
      write(1,err=8000)matno

* WRITES PARAMETERS FOR SOURCE LOCATION
      write(1,err=8000)anos
      do 700 i=1,anos
         write(1,err=8000)xs(i)
         write(1,err=8000)ys(i)
         write(1,err=8000)zs(i)
         write(1,err=8000)nspx(i)
         write(1,err=8000)nspy(i)
         write(1,err=8000)nspz(i)
         write(1,err=8000)apts(i)
         write(1,err=8000)ssd(i)
         write(1,err=8000)phoff(i)
 700  continue
* WRITES PARAMETERS FOR SOURCE SIGNAL
      write(1,err=8000)tau
      write(1,err=8000)spread

* WRITES PARAMETERS FOR IMPEDANCE POINTS
      write(1,err=8000)anoi
      do 800 i=1,anoi
         write(1,err=8000)ximp(i)
         write(1,err=8000)yimp(i)
         write(1,err=8000)zimp(i)
         write(1,err=8000)nipx(i)
         write(1,err=8000)nipy(i)
         write(1,err=8000)nipz(i)
         write(1,err=8000)dioi(i)
 800  continue
      write(1,err=8000)mutadm
      write(1,err=8000)BW
```

```
      write(1,err=8000)fsteps


* WRITES MATERIAL CONSTANTS FOR OTHER MATERIALS. Note that epsi(1),
* my(1), and sigma(1) is basic material!

      do 1000 i = 1,matno
         write(1,err=8000)epsi(i)
         write(1,err=8000)my(i)
         write(1,err=8000)sigma(i)
 1000 continue

* WRITES POSITIONS FOR OTHER MATERIALS
      do 2000 i = 2,matno
         write(1,err=8000)matant(i)
         do 2000 k = 1,matant(i)
            write(1,err=8000)x(k,i)
            write(1,err=8000)y(k,i)
            write(1,err=8000)z(k,i)
 2000    continue

* WRITES WHERE Ex IS SET TO ZERO
      write(1,err=8000)nozex
      do 3000 i = 1,nozex
         write(1,err=8000)zxx(i)
         write(1,err=8000)zxy(i)
         write(1,err=8000)zxz(i)
 3000 continue

* WRITES WHERE Ey IS SET TO ZERO
      write(1,err=8000)nozey
      do 4000 j = 1,nozey
         write(1,err=8000)zyx(j)
         write(1,err=8000)zyy(j)
         write(1,err=8000)zyz(j)
 4000 continue

* WRITES WHERE Ez IS SET TO ZERO
      write(1,err=8000)nozez
      do 5000 k = 1,nozez
         write(1,err=8000)zzx(k)
         write(1,err=8000)zzy(k)
         write(1,err=8000)zzz(k)
 5000 continue
      write(1,err=8000)int(707)
      close(1, status='keep')

* Finds maximum length of nearfield vector.
      nftotl=0
      do 6000 i=1,anonfb
         nftotl=nftotl+( (nearendx(i)-nearbegx(i)+1)*
     -         (nearendy(i)-nearbegy(i)+1)*(nearendz(i)-nearbegz(i)+1))
 6000 continue


* PREPARE THIN WIRE SETTINGS
      l=0
```

```
      if(thw) then
         do 6100 i=1,anotw
            if(thl(i).gt.l) l=thl(i)
 6100    continue
      else
         anotw=1
         l=1
      end if



**********************************************
* Writing parameters.h for the FDTD compilation *
**********************************************
      call writepar(sid,maxx,maxy,maxz,matno,noang,anonfb,
     -      nftotl,fsteps,anos,
     -      anoi,anotdp,nozex,nozey,nozez,pinextx+1,
     -      pinexty+1,pinextz+1,anotw,l,
     -      lumx,lumy,lumz,lumdir,lumtype,lum,lumax,lumimped)

      goto 9000

 8000 close(1, status='delete')
      print*,'**** ERROR WHILE WRITING - NO FILE IS SAVED ****'

 9000 stop
      end


      BLOCK DATA varini
**********************************************************************
* INITIALIZATION OF VARIABLES FOR ZERO E-FIELD AND MATERIALS          *
**********************************************************************
      include 'static.h'

      integer dummy(2)

      integer ix,iy,iz,lx,ly,lz,inx,iny,inz
      integer temp
      parameter(temp=maxant*mats)
      integer matant(mats),x(maxant,mats),y(maxant,mats),
     -      z(maxant,mats),
     -      zxx(maxze), zxy(maxze), zxz(maxze),
     -      zyx(maxze), zyy(maxze), zyz(maxze),
     -      zzx(maxze), zzy(maxze), zzz(maxze)

      common /sub1/ zxx,zxy,zxz,zyx,zyy,zyz,zzx,zzy,zzz,ix,iy,iz,
     -      lx,ly,lz,inx,iny,inz

      common /sub2/ x,y,z,matant

* INITIALIZATION OF VARIABLES FOR ZERO E-FIELD SPECIFICATION
      data  zxx /maxze*0/,
     -      zxy /maxze*0/,
     -      zxz /maxze*0/

      data  zyx /maxze*0/,
```

```
-      zyy /maxze*0/,
-      zyz /maxze*0/

 data  zzx /maxze*0/,
-      zzy /maxze*0/,
-      zzz /maxze*0/

 data ix,iy,iz /1,1,1/
 data lx,ly,lz /0,0,0/
 data inx,iny,inz /1,1,1/

 data  x /temp*0/,
-      y /temp*0/,
-      z /temp*0/,
-      matant /mats*0/

 data dummy /mnotdp,mnos/
 end
```

C.4 filename.adf

```
* -*-fortran-*-
*~~~~~~~~~~~~~~~~~~~~~~~~~~~~~~~~~~~~~~~~~~~~~~~~~~~~~~~~~~~~~~~~~~~~~~~~*
*                   FINITE DIFFERENCE TIME DOMAIN                       *
*                   for numerical calculations of                       *
*                        Maxwell's Equations                            *
*                                                                       *
*                       2nd Generation FDTD program by                 *
*                 Gert Frølund Pedersen, and Kasper Vork Steffensen     *
*                                                                       *
*               Aalborg University, Center for Personkommunikation      *
*               Denmark, fall 1996                                      *
*                                                                       *

*~~~~~~~~~~~~~~~~~~~~~~~~~~~~~~~~~~~~~~~~~~~~~~~~~~~~~~~~~~~~~~~~~~~~~~~~*

**********************************************************************
* ASCII DEFINITION FILE (ADF).       * 2nd Generation FDTD Program   *
* This file contains all relevant    * Aalborg University, CPK       *
* information for an FDTD            * Compiled by gfp 11-96         *
* simulation. This file must not be  **********************************
* mistaken for the BINARY DEFINITION FILE (BDF) which is generated   *
* from this ascii file.                                              *
**********************************************************************
*~~~~~~~~~~~~~~~~~~~~~~~~~~~~~~~~~~~~~~~~~~~~~~~~~~~~~~~~~~~~~~~~~~~~~~~~
* PARAMETERS FOR SIMULATION IDENTIFICATION
* ---------------------------------------
*     titel    : The title of the FDTD simulation. Is written in the
head
*                of the binary definition file.
*     template : This string variable is concatenated on all output
*                files from the FDTD program. Max 12 characters.
*     sid      : Simulation Identification number. The integer
counterpart
*                of 'titel'.
*~~~~~~~~~~~~~~~~~~~~~~~~~~~~~~~~~~~~~~~~~~~~~~~~~~~~~~~~~~~~~~~~~~~~~~~~
      data titel /'filename
     -Mauro Pelosi 31-04-06'/
      data template /'filename'/
      data sid /3104001/



*~~~~~~~~~~~~~~~~~~~~~~~~~~~~~~~~~~~~~~~~~~~~~~~~~~~~~~~~~~~~~~~~~~~~~~~~
* PARAMETERS FOR SIMULATION OUTPUTS AND CONTROLS
* ---------------------------------------------
*     timedo -> e_source : Logicals that states which jobs to run.
*~~~~~~~~~~~~~~~~~~~~~~~~~~~~~~~~~~~~~~~~~~~~~~~~~~~~~~~~~~~~~~~~~~~~~~~~
      data timedo /.TRUE./              ! Time domain fields.
      data eqcur /.FALSE./              ! Equivalent currents.
      data fraeqcur /.FALSE./           ! Fraeqcur read file.
      data nefi /.TRUE./                ! Frequency domain nearfields.
      data farfi /.TRUE./              ! Frequency domain farfields.
      data fsamp /.FALSE./              ! Farfield samples.
      data patch /.FALSE./              ! Patch currents.
```

```
      data imped /.TRUE./               ! Impedance.
      data inputpow /.TRUE./           ! Input power.
      data rpow /.TRUE./               ! Radiated power.
      data h_source /.FALSE./           ! Magnetic field source.
      data e_source /.TRUE./            ! Electric field source.
```

```
*~~~~~~~~~~~~~~~~~~~~~~~~~~~~~~~~~~~~~~~~~~~~~~~~~~~~~~~~~~~~~~~~~~~~~~~~~~~~
* PARAMETERS FOR FUNDAMENTAL FDTD SETTINGS
* ----------------------------------------
* xo    -> zo    : An arbitrary offset point for specs.
* resol          : Resolution. deltax /lambda/resol
* maxx  -> maxz  : Total FDTD space (incl. boundary)
*~~~~~~~~~~~~~~~~~~~~~~~~~~~~~~~~~~~~~~~~~~~~~~~~~~~~~~~~~~~~~~~~~~~~~~~~~~~~
      parameter(xo=10,yo=10,zo=10)
      parameter(hsc=15/5)
      parameter(lb=100/5,wb=20/5,hb=70/5)
      parameter(resol=30000/293)
      parameter(maxx=2*xo+lb,maxy=2*yo+wb,maxz=2*zo+hb+1+hsc)
```

```
*~~~~~~~~~~~~~~~~~~~~~~~~~~~~~~~~~~~~~~~~~~~~~~~~~~~~~~~~~~~~~~~~~~~~~~~~~~~~~~
~
* PARAMETERS FOR FARFIELD
* -----------------------------------
* minbx -> minbz : Determines lower limit of the NF2FF boundary.
* maxbx -> maxbz : Determines upper limit of the NF2FF boundary.
*~~~~~~~~~~~~~~~~~~~~~~~~~~~~~~~~~~~~~~~~~~~~~~~~~~~~~~~~~~~~~~~~~~~~~~~~~~~~~~
~
      parameter (minbx=4, minby=4, minbz=4)
      parameter (maxbx=maxx-4, maxby=maxy-4, maxbz=maxz-4)
```

```
*~~~~~~~~~~~~~~~~~~~~~~~~~~~~~~~~~~~~~~~~~~~~~~~~~~~~~~~~~~~~~~~~~~~~~~~~~~~~
* PARAMETERS FOR ELECTRICAL FIELD SOURCE (Remember to set e_source!)
* ----------------------------------
* impuls    : Logical which selects either sine or gauss excitation.
*             (TRUE=gauss, FALSE=sine)
* freq      : Center frequency
* sigmaf    : Selects frequency domain spread of Gaussian pulse.
* timoff    : Sets the time offset tau of the Gaussian pulse in terms
of
*             time spread as (tau=timeoff*time_spread), where the time_
*             spread is calculated from the frequency spread of the
pulse.
*             Normally, timeoff=4
* nmax      : Maximum number of time steps.
* anos      : Actual number of e-field sources.
*             Note, that anos<mnos specified in PARENT
```

```
* xs - zs   : One dimensional array of 'anos' denoting the coordinate
*             of the i'th source. i=1:1:anos.
* nspx-nspz : 1D array of anos denoting the extention of the i'th
*             source in each direction.
* apts      : 1D array of 'anos' denoting which field component to
*             excite: (-1=Ex, 0=Ey, 1=Ez).
* ssd       : 1D array of 'anos' denoting the amplitude of the excited
*             signal. See DOCUMENTATION on delta gap field excitation!
* phoff     : 1D array of 'anos' denoting the phase offset in DEGREES
of
*             the i'th source.
*~~~~~~~~~~~~~~~~~~~~~~~~~~~~~~~~~~~~~~~~~~~~~~~~~~~~~~~~~~~~~~~~~~~~~~~~
      data impuls /.TRUE./
      data freq /586e6/
      data sigmaf /300e6/
      data timoff /4/
      data nmax /75000/
      data anos /1/
      xs(1)=xo+1
      ys(1)=yo+1
      zs(1)=zo+hb
      nspx(1)=1
      nspy(1)=1
      nspz(1)=hsc
      apts(1)=1
      ssd(1)=1.0
      phoff(1)=0.0



*~~~~~~~~~~~~~~~~~~~~~~~~~~~~~~~~~~~~~~~~~~~~~~~~~~~~~~~~~~~~~~~~~~~~~~~~
~
* PARAMETERS FOR NEARFIELD
* ------------------------
* nfcode : Specifies which nearfield components are output.
* freq1  : Specifies the frequency for the nearfield Fourier transform.
* anonfb : Actual number of near-field boxes. Note: anonfb<=mnonfb.
* nearbegx -> nearbegz : Lower limit of nearfield boundary.
* nearendx -> nearendz : Upper limit of nearfield boundary.
*~~~~~~~~~~~~~~~~~~~~~~~~~~~~~~~~~~~~~~~~~~~~~~~~~~~~~~~~~~~~~~~~~~~~~~~~
~

      data nfcode /63/
      data freq1 /586e6/
      data anonfb /1/


      nearbegx(1)=xo
      nearbegy(1)=yo
      nearbegz(1)=zo
      nearendx(1)=xo+lb
      nearendy(1)=yo+wb
      nearendz(1)=zo+hb+hsc+1
```

```
*~~~~~~~~~~~~~~~~~~~~~~~~~~~~~~~~~~~~~~~~~~~~~~~~~~~~~~~~~~~~~~~~~~~~~~~~~~~~
~
* PARAMETERS FOR IMPEDANCE
* ------------------------
* BW     : Bandwith of which the impedance response os wanted.
* fsteps : Number of impedance samples in BW.
* imloop : Size of the loop for H-field integration. If imloop=0, the
*          smallest loop is used. If imloop=1, the integration loop is
*          1 cell outside the smallest loop etc.
* anoi   : Actual number of impedance points. anoi<=mnoi
* ximp   : 1D array of anoi. Contain all x-coordinates of the imp-
points
* yimp   : 1D array of anoi. Contain all y-coordinates of the imp-
points
* zimp   : 1D array of anoi. Contain all z-coordinates of the imp-
points
* nipx - nipz : 1D arrays of anoi. Denotes the extention of the
impedance
*               point. Works as nspx-nspy for the source.
* dioi   : 1D array of anoi. Denotes the direction of the impedance
point.
*          Similar to apts() for the source.
* mutadm : If this logical is .TRUE. the FDTD program will calculate
the
*          mutual admittance Y21. That is, Y21=I2/V1, when V2=0
*                                          ===================
*          The Y21 can be transformed into Z12 by a proper formula
*          (see  Pozar p.235). When using mutadm YOU are in charge of:
*               --> USING TWO SOURCES.
*               --> SOURCE #1 IS EXCITED AS DESIRED.
*               --> THE AMPLITUDE OF SOURCE #2 EQUALS 0.0 {ssd(2)=0.0}
*          If YOU do not do this right, garbage will be output.
*~~~~~~~~~~~~~~~~~~~~~~~~~~~~~~~~~~~~~~~~~~~~~~~~~~~~~~~~~~~~~~~~~~~~~~~~~~~~
~
      data BW /300e6/
      data fsteps /3000/
      data imloop /0/
      data anoi /1/
      data mutadm /.FALSE./

      ximp(1)=xs(1)
      yimp(1)=ys(1)
      zimp(1)=zs(1)
      nipx(1)=nspx(1)
      nipy(1)=nspy(1)
      nipz(1)=nspz(1)
      dioi(1)=apts(1)




*~~~~~~~~~~~~~~~~~~~~~~~~~~~~~~~~~~~~~~~~~~~~~~~~~~~~~~~~~~~~~~~~~~~~~~~~~~~~
~
* PARAMETERS FOR INPUT POWER SETTINGS
* -----------------------------------
```

```
* pin?       : Locates the lower corner of a box on which the net
*              power flow if calculated.
* pinext?    : Indicates the extention of the box in the three
*              firections.
*~~~~~~~~~~~~~~~~~~~~~~~~~~~~~~~~~~~~~~~~~~~~~~~~~~~~~~~~~~~~~~~~~~~~~~~~~~~~
~
      pinx = xo
      piny = yo
      pinz = zo
      pinextx=lb
      pinexty=wb
      pinextz=hb+hsc+1




*~~~~~~~~~~~~~~~~~~~~~~~~~~~~~~~~~~~~~~~~~~~~~~~~~~~~~~~~~~~~~~~~~~~~~~~~~~~~
~
* PARAMETERS FOR THINWIRE
* -----------------------
* thw         : Logical. If true, the thinwire algorithm is enables
* anotw       : The actual number of thin wires set in the FDTD space
* thx,thy,thz : Lower fix point of thin wire
* thdir       : Orientation of thin wire (-1=X  0=Y  1=Z)
* thl         : Extention of thin wire
* thr         : Radius of wire in terms of wavelength
*~~~~~~~~~~~~~~~~~~~~~~~~~~~~~~~~~~~~~~~~~~~~~~~~~~~~~~~~~~~~~~~~~~~~~~~~~~~~
~
      thw=.FALSE.
      anotw=0



*~~~~~~~~~~~~~~~~~~~~~~~~~~~~~~~~~~~~~~~~~~~~~~~~~~~~~~~~~~~~~~~~~~~~~~~~~~~~
~
* PARAMETERS FOR TIME DOMAIN FIELDS AND STEADY STATE TEST-POINT
* ------------------------------------------------------------
* xtp -> ztp : Test point for evaluating steady state.
* criterion  : The fraction of maximum value for valid steady state.
* anotdp     : Number of desired time domain field points.
*              Note, that anotdp <=mnotdp (specified in PARENT file).
* xtim(anotdp) -> ytim(anotdp) : Array holding the coordinate of the
*                                specific field point.
* fcomp(anotdp) : Array holding which field component (1-6) to output.
*                 (1=Ex, 2=Ey, 3=Ez, 4=Hx, 5=Hy, 6=Hz)
*~~~~~~~~~~~~~~~~~~~~~~~~~~~~~~~~~~~~~~~~~~~~~~~~~~~~~~~~~~~~~~~~~~~~~~~~~~~~
~
      xtp=xo+lb+2
      ytp=yo+wb+2
      ztp=zo+hb+2
      data criterion /0.001/

      data anotdp /1/

      xtim(1)=xtp
```

```
      ytim(1)=ytp
      ztim(1)=ztp
      data fcomp(1) /1/



*~~~~~~~~~~~~~~~~~~~~~~~~~~~~~~~~~~~~~~~~~~~~~~~~~~~~~~~~~~~~~~~~~~~~~~~~~~~~
* PARAMETERS FOR NF2FF-TRANSFORMATION
* ---------------------------------
* noang   : Number of angle steps in radiation pattern
* alfa    : Elevation angle from Y- towards Z-axis in deg. in farfield
*           pattern.
* beta    : Elevation angle from Y- towards Z-axis in deg. in
coordinate
*           system.
* alfas   : Elevation angle from Y- towards Z-axis for sampling the
farfield.
*           In degrees.
* betas   : Angle of the coordinatesystem, from Y- towards Z-axis for
*           sampling the farfield, in deg.
* thstart : Start angle for sampling in theta
* thstop  : Stop angle for sampling in theta
* deltath : Resolution in theta in deg.
* deltaphi: Resolution in phi in deg.
*~~~~~~~~~~~~~~~~~~~~~~~~~~~~~~~~~~~~~~~~~~~~~~~~~~~~~~~~~~~~~~~~~~~~~~~~~~~~
      data noang /360/
      data alfa /0.0/
      data beta /0.0/
      data alfas /0.0/
      data betas /0.0/
      data thstart /0.0/
      data thstop /180.0/
      data deltath /5.0/
      data deltaphi /5.0/



*~~~~~~~~~~~~~~~~~~~~~~~~~~~~~~~~~~~~~~~~~~~~~~~~~~~~~~~~~~~~~~~~~~~~~~~~~~~~
* PARAMETERS FOR PATCH-CURRENT
*~~~~~~~~~~~~~~~~~~~~~~~~~~~~~~~~~~~~~~~~~~~~~~~~~~~~~~~~~~~~~~~~~~~~~~~~~~~~
****epsint brugt som ipz1!!
      data ixp1,ixp2,iyp1,iyp2,izp2,epsint,
     -        sigint /16,16,16,20,20,20.,0./



*~~~~~~~~~~~~~~~~~~~~~~~~~~~~~~~~~~~~~~~~~~~~~~~~~~~~~~~~~~~~~~~~~~~~~~~~~~~~
* PARAMETERS FOR MATERIALS
* ------------------------
* matno  : Actual number of materials inclusive the basic material.
```

```
*          Note, that matno<=mats specified in static.h! ALso

* epsi() : Permittivity. Note that epsi(1) is treated as the basic
*          material!
* my()   : Permeability. Note that my(1) is treated as the basic
*          material!
* sigma(): Conductivity. Note that sigma(1) is treated as the basic
*          material!

*~~~~~~~~~~~~~~~~~~~~~~~~~~~~~~~~~~~~~~~~~~~~~~~~~~~~~~~~~~~~~~~~~~~~~~~~~~~~
      data matno /2/

      epsi(1)=8.854e-12         ! Vacuum permittivity
      my(1)=1.25664e-6          ! Vacuum permeability
      sigma(1)=0.0              ! Vacuum (?) conductivity


** Antenna plast
      epsi(2)=2.30*epsi(1)
      my(2)=my(1)
      sigma(2)=0.0
* Print
*      epsi(2)=5.0*epsi(1)
*      my(2)=my(1)
*      sigma(2)=0.01

* muscle  at 900MHz
      epsi(2)=41.5*epsi(1)
      my(2)=my(1)
      sigma(2)=0.76

* muscle at 1800
*      epsi(3)=32.5*epsi(1)
*      my(3)=my(1)
*      sigma(3)=1.72


*********************************************
**********LUMPED ELEMENTS PARAMETERS***********
*********************************************


*enable the lumped elememement routine
*     lum=0 lumped element not enebled
*     lum=1 lumped element enabled



*we have array with "lumax" number of elements,
*corresponding to the number of lumped components we need.
*REMEMBER TO DEFINE "LUMAX" IN THE FILE STATIC.H!!!!

*lumx(index) for index=1,2,3,... lumax
*is the x location of the cell corresponding to
*the (index)th lumped component

*lumy(index) for index=1,2,3,... lumax
```

```
*is the y location of the cell corresponding to
*the (index)th lumped component

*lumz(index) for index=1,2,3,... lumax
*is the z location of the cell corresponding to
*the (index)th lumped component


*lumdir(index) for index=1,2,3,... lumax
*is the orientation of the cell corresponding to
*the (index)th lumped component:

*lumdir(index)=-1 set the (index)th lumped component
*oriented along the x axis

*lumdir(index)=0 set the (index)th lumped component
*oriented along the y axis

*lumdir(index)=1 set the (index)th lumped component
*oriented along the z axis


*lumtype(index) for index=1,2,3,... lumax
*is the type of the (index)th lumped component:

*lumtype(index)=1 set the index(th) lumped component
*is a capacitor

*lumtype(index)=2 set the index(th) lumped component
*is a resistor

*lumtype(index)=2 set the index(th) lumped component
*is an inductor


*lumimped(index) for index=1,2,3,... lumax
*define the value of the impedance
*of the (index)th lumped component:
*this value will be automatically set
*as a capacity [F],resitance [Ohm],or inductance [H]
*depending to the type of component
*in that specific location

**********************************************************

*here it is possible to specify the input parameters of
*the lumped components.

      lum=1

      lumx(1)=xo+12
      lumy(1)=yo+2
      lumz(1)=zo+hb
      lumdir(1)=1
      lumtype(1)=3
      lumimped(1)=1e-12
```

```
      lumx(2)=xo+12
      lumy(2)=yo+2
      lumz(2)=zo+hb+1
      lumdir(2)=1
      lumtype(2)=2
      lumimped(2)=10

      lumx(3)=xo+12
      lumy(3)=yo+2
      lumz(3)=zo+hb+2
      lumdir(3)=1
      lumtype(3)=3
      lumimped(3)=10e-9

***********************************************************************
*****
***********************************************************************
*****
***********************************************************************
*****
* DO NOT TOUCH THE FOLLOWING 3 DATA DECLARATIONS!
*
* ~~~~~~~~~~~~~~~~~~~~~~~~~~~~~~~~~~~~~~~~~~~~~~~~
*
*     COMPLETELY DUMM VARIABLES!
*
*     -------------------------
*
*     The following variables are used to "convert" parameters to data
*
*     statements. In the Ascii Definition File, some variables, which
are  *
*     supposed to be entered in a common area, are declared as
parameters. *
*     Thus, these varibles must be changed to data statements in order
to  *
*     be put in a common area. This is done through the dummies.
*
***********************************************************************
*****
***********************************************************************
*****
      data dmaxx, dmaxy, dmaxz /maxx,maxy,maxz/
      data dminbx, dminby, dminbz /minbx,minby,minbz/
      data dmaxbx, dmaxby, dmaxbz /maxbx,maxby,maxbz/



*~~~~~~~~~~~~~~~~~~~~~~~~~~~~~~~~~~~~~~~~~~~~~~~~~~~~~~~~~~~~~~~~~~~~~~~~
* PARAMETERS FOR GENERATING AUTOCAD SCRIPT-FILE
* ------------------------------------------
* acad  : If true, generates an Autocad 12 script file
*~~~~~~~~~~~~~~~~~~~~~~~~~~~~~~~~~~~~~~~~~~~~~~~~~~~~~~~~~~~~~~~~~~~~~~~~
      data acad /.TRUE./

      if(acad) then
      j=12
```

```
      do 1 i=1,12
         if(template(i:i).eq.' ') then
            if(i.lt.j) j=i
         end if
 1    continue

      open(2, file=template(:j-1)//'.scr', status ='new',
     -      access='sequential',form='formatted')
      call acadgen
      end if


*~~~~~~~~~~~~~~~~~~~~~~~~~~~~~~~~~~~~~~~~~~~~~~~~~~~~~~~~~~~~~~~~~~~~~~~~~~~~
* SUBROUTINE CALLS FOR DESIGNING STRUCTURE
*~~~~~~~~~~~~~~~~~~~~~~~~~~~~~~~~~~~~~~~~~~~~~~~~~~~~~~~~~~~~~~~~~~~~~~~~~~~~


      call box(xo,yo,zo,lb,wb,hb)

      call plate(xo,yo,zo+hb+hsc,16,wb,0)

      call linz(xo,yo,zo+hb,hsc,1)
```

C.5: writepar.f

```
************************************************************************
* Writes the parameters.h file for the FDTD compilation                *
************************************************************************
      subroutine writepar(sid,maxx,maxy,maxz,maxmat,maxang,anonfb,
     -      nftotl,impsteps,mnos,mnoi,mnotdp,a,b,c,
     -      xpin,ypin,zpin,mnotw,thwl,lumx,
     -      lumy,lumz,lumdir,lumtype,lum,lumax,lumimped)
      implicit none
      integer sid,maxx,maxy,maxz,maxmat,maxang,nftotl,
     -      impsteps,mnos,mnoi,mnotdp,a,b,c,maxze
      integer temp,anonfb,xpin,ypin,zpin,mnotw,thwl,lumax

      integer lum,prin
      integer lumx(lumax),lumy(lumax),lumz(lumax)
      integer lumdir(lumax),lumtype(lumax)
      real lumimped(lumax)
      maxze=b
      if(a.gt.b) maxze=a
      if(c.gt.maxze) maxze=c



      open(1,file='parameters.h', status='new',
     -      err=1000,form='formatted')
      write(1,'(A,A)',err=1000)'******** Header for parameters *******'
     -      ,'* -*-fortran-*-'
      write(1,'(A,A)',err=1000)'*************************************'
     -      ,'***************'
      write(1,'(A,A)',err=1000)'*    Automitically written by DEFINE '
     -      ,'   /kvs 2-96   *'
      write(1,'(A,A)',err=1000)'*************************************'
     -      ,'***************'
      write(1,'(A,I7,A)',err=1000)
     -      '*    This header is written for FDTD SID=',sid,'    *'
      write(1,'(A,A)',err=1000)'*************************************'
     -      ,'***************'


      write(1,'(A)',err=1000)' '

      write(1,'(A)',err=1000)'* FDTD space parameters'
      write(1,'(A)',err=1000)'      integer sizx,sizy,sizz'
      write(1,'(A,I3,A,I3,A,I3,A)',err=1000)
     -      '      parameter (sizx=',maxx,',sizy=',maxy,
     -      ',sizz=',maxz,')'
      write(1,'(A)',err=1000)

      write(1,'(A)',err=1000)'* Max. number of materials'
      write(1,'(A)',err=1000)'      integer maxmat'
      write(1,'(A,I2,A)',err=1000)'      parameter(maxmat=',maxmat,')'
      write(1,'(A)',err=1000)' '

      write(1,'(A)',err=1000)'* Max. number of angles for NF2FF'
```

```
      write(1,'(A)',err=1000)'      integer maxang'
      write(1,'(A,I3,A)',err=1000)'      parameter (maxang=',maxang,
     -      ')'
      write(1,'(A)',err=1000)' '

      write(1,'(A)',err=1000)'* Max. nearfield vector length'
      write(1,'(A)',err=1000)'      integer nftotl,mnonfb'
      write(1,'(A,I6,A,I3,A)',err=1000)
     -      '      parameter (nftotl=',nftotl,', mnonfb=',anonfb,')'
      write(1,'(A)',err=1000)' '

      write(1,'(A)',err=1000)'* Max. input power box dimension'
      write(1,'(A)',err=1000)'      integer xpin,ypin,zpin'
      write(1,'(A,I3,A,I3,A,I3,A,)',err=1000)
     -      '      parameter (xpin=',xpin,',ypin=',ypin,
     -      ',zpin=',zpin,')'
      write(1,'(A)',err=1000)' '

      write(1,'(A,A)',err=1000)'* Number of frequency steps for',
     -      ' impedance routine'
      write(1,'(A)',err=1000)'      integer impsteps'
      write(1,'(A,I4,A)',err=1000)'      parameter(impsteps=',impsteps,
     -      ')'
      write(1,'(A)',err=1000)' '



      write(1,'(A)',err=1000)'* Max. number of sources'
      write(1,'(A)',err=1000)'      integer mnos'
      write(1,'(A,I2,A)',err=1000)'      parameter(mnos=',mnos,')'
      write(1,'(A)',err=1000)' '

      write(1,'(A)',err=1000)'* Max. number of Impedance points'
      write(1,'(A)',err=1000)'      integer mnoi'
      write(1,'(A,I2,A)',err=1000)'      parameter(mnoi=',mnoi,')'
      write(1,'(A)',err=1000)' '

      write(1,'(A)',err=1000)'* Max. number of Timedomain points'
      write(1,'(A)',err=1000)'      integer mnotdp'
      write(1,'(A,I2,A)',err=1000)'      parameter(mnotdp=',mnotdp,')'

      write(1,'(A)',err=1000)' '
      write(1,'(A)',err=1000)'* Max. number of zeroed E-fields'
      write(1,'(A)',err=1000)'      integer maxze'
      temp=3*maxze+1
      write(1,'(A,I6,A)',err=1000)'      parameter(maxze=',temp,')'
      write(1,'(A)',err=1000)' '

      write(1,'(A)',err=1000)'* Max. number of thin wires'
      write(1,'(A)',err=1000)'      integer mnotw'
      write(1,'(A,I3,A)',err=1000)'      parameter(mnotw=',mnotw,')'
      write(1,'(A)',err=1000)' '

      write(1,'(A)',err=1000)'* Max. length of thin wire(s)'
      write(1,'(A)',err=1000)'      integer thwl'
      write(1,'(A,I3,A)',err=1000)'      parameter(thwl=',thwl,')'
      write(1,'(A)',err=1000)' '
```

```
      write(1,'(A)',err=1000)'* lumx'
      write(1,'(A,I3,A)',err=1000)'           integer lumx(',lumax,')'


      write(1,'(A)',err=1000)
     -    '        data lumx /  '
      do 1266 prin = 1,lumax

      if(prin.eq.1)then
      write(1,'(A,I,A)',err=1000)'     - '       ,lumx(prin),''
      else
      write(1,'(A,I,A)',err=1000)'     - ,'      ,lumx(prin),''
      end if
1266  continue
      write(1,'(A)',err=1000)'     -       /'
      write(1,'(A)',err=1000)' '









      write(1,'(A)',err=1000)'* lumy'
      write(1,'(A,I3,A)',err=1000)'       integer lumy(',lumax,')'


      write(1,'(A)',err=1000)
     -    '       data lumy /  '
      do 1267 prin = 1,lumax

      if(prin.eq.1)then
      write(1,'(A,I,A)',err=1000)'     - ',      lumy(prin),''
      else
      write(1,'(A,I,A)',err=1000)'     - ,',     lumy(prin),''
      end if
1267  continue
      write(1,'(A)',err=1000)'     -       /'
      write(1,'(A)',err=1000)' '
```

```
      write(1,'(A)',err=1000)'* lumz'
      write(1,'(A,I3,A)',err=1000)'        integer lumz(',lumax,')'


      write(1,'(A)',err=1000)
     -    '        data lumz /  '
      do 1268 prin = 1,lumax

      if(prin.eq.1)then
      write(1,'(A,I,A)',err=1000)'     -      ',lumz(prin),''
      else
      write(1,'(A,I,A)',err=1000)'     -      ,',lumz(prin),''
      end if
 1268 continue
      write(1,'(A)',err=1000)'     -  /'
      write(1,'(A)',err=1000)' '









      write(1,'(A)',err=1000)'* lumtype'
      write(1,'(A,I3,A)',err=1000)'       integer lumtype(',lumax,')'


      write(1,'(A)',err=1000)
     -    '        data lumtype /  '
      do 1269 prin = 1,lumax

      if(prin.eq.1)then
      write(1,'(A,I,A)',err=1000)'     -      ',lumtype(prin),''
      else
      write(1,'(A,I,A)',err=1000)'     -     ,',lumtype(prin),''
      end if
 1269 continue
      write(1,'(A)',err=1000)'     -       /'
      write(1,'(A)',err=1000)' '









      write(1,'(A)',err=1000)'* lumdir'
      write(1,'(A,I3,A)',err=1000)'        integer lumdir(',lumax,')'


      write(1,'(A)',err=1000)
     -    '       data lumdir /  '
      do 1270 prin = 1,lumax
```

```
      if(prin.eq.1)then
      write(1,'(A,I,A)',err=1000)'     -      ',lumdir(prin),''
      else
      write(1,'(A,I,A)',err=1000)'     -      ,',lumdir(prin),''
      end if
 1270 continue
      write(1,'(A)',err=1000)'     -        /'
      write(1,'(A)',err=1000)' '


      write(1,'(A)',err=1000)'* lumimped'
      write(1,'(A,I3,A)',err=1000)'        real lumimped(',lumax,')'


      write(1,'(A)',err=1000)
     -    '       data lumimped /  '
      do 1271 prin = 1,lumax

      if(prin.eq.1)then
      write(1,'(A,E,A)',err=1000)'     -      ',lumimped(prin),''
      else
      write(1,'(A,E,A)',err=1000)'     -      ,',lumimped(prin),''
      end if
 1271 continue
      write(1,'(A)',err=1000)'     -        /'
      write(1,'(A)',err=1000)' '



      write(1,'(A)',err=1000)'* Max. length of thin wire(s)'
      write(1,'(A)',err=1000)'      integer lum'
      write(1,'(A,I3,A)',err=1000)'      parameter(lum=',lum,')'
      write(1,'(A)',err=1000)' '
      write(1,'(A)',err=1000)' '

      write(1,'(A)',err=1000)'* lumax'
      write(1,'(A)',err=1000)'      integer lumax'
      write(1,'(A,I3,A)',err=1000)'      parameter(lumax=',lumax,')'
      write(1,'(A)',err=1000)' '
      write(1,'(A)',err=1000)' '


      close(1,status='keep')

      goto 2000
 1000 print*,'File "parameters.h" exist. Remove it and restart the',
     -      ' DEFINE program.'
      print*,'This file is needed in the compilation of the FDTD',
     -      ' program.'
      close(1,status='delete')

 2000 continue

      return
      end
```

C.6: parameters.h

```
******** Header for parameters ******** -*-fortran-*-
*****************************************************
*    Automitically written by DEFINE    /kvs 2-96    *
*****************************************************
*    This header is written for FDTD SID=3104001     *
*****************************************************

* FDTD space parameters
      integer sizx,sizy,sizz
      parameter (sizx= 40,sizy= 24,sizz= 38)

* Max. number of materials
      integer maxmat
      parameter(maxmat= 2)

* Max. number of angles for NF2FF
      integer maxang
      parameter (maxang=360)

* Max. nearfield vector length
      integer nftotl,mnonfb
      parameter (nftotl=  1995, mnonfb=  1)

* Max. input power box dimension
      integer xpin,ypin,zpin
      parameter (xpin= 21,ypin=  5,zpin= 19)

* Number of frequency steps for impedance routine
      integer impsteps
      parameter(impsteps=3000)

* Max. number of sources
      integer mnos
      parameter(mnos= 1)

* Max. number of Impedance points
      integer mnoi
      parameter(mnoi= 1)

* Max. number of Timedomain points
      integer mnotdp
      parameter(mnotdp= 1)

* Max. number of zeroed E-fields
      integer maxze
      parameter(maxze=  2401)

* Max. number of thin wires
      integer mnotw
      parameter(mnotw=  1)

* Max. length of thin wire(s)
      integer thwl
      parameter(thwl=  1)
```

```
* lumx
          integer lumx(  3)
        data lumx /
     -                       22
     - ,                      22
     - ,                      22
     -       /

* lumy
       integer lumy(  3)
       data lumy /
     -                       12
     - ,                      12
     - ,                      12
     -       /

* lumz
        integer lumz(  3)
        data lumz /
     -                              24
     -      ,                        25
     -      ,                        26
     -  /

* lumtype
       integer lumtype(  3)
        data lumtype /
     -                              3
     -     ,                        2
     -     ,                        3
     -       /

* lumdir
        integer lumdir(  3)
       data lumdir /
     -                              1
     -      ,                        1
     -      ,                        1
     -        /

* lumimped
        real lumimped(  3)
       data lumimped /
     -         0.10000000000000000E-11
     -      ,   0.10000000000000000E+02
     -      ,   0.10000000000000000E-07
     -        /

* Max. length of thin wire(s)
      integer lum
      parameter(lum=  1)


* lumax
      integer lumax
      parameter(lumax=  3)
```

C.7: Maxwell.h

```
* -*-fortran-*-
*********************************
******* Header for maxwell *******
*********************************

* LOCALS
      integer i,j,k,temp,tempint
      real temp1,temp2
      logical iscap
      integer in
      logical flag




* GLOBALS

      integer maxx,maxy,maxz,maxbx,maxby,maxbz,minbx,minby,minbz
*      integer zeroex(sizx,sizy,sizz), zeroey(sizx,sizy,sizz),
*     -        zeroez(sizx,sizy,sizz)
      integer zerox(maxze),zeroy(maxze),zeroz(maxze)
      integer mat(sizx,sizy,sizz),matno,nozex,nozey,nozez
*     integer lumx(lumax),lumy(lumax),lumz(lumax),lumtype(lumax)
*     integer lumdir(lumax)
*     real lumimped(lumax)

      real deltax,deltay,deltaz,deltat,freq
      real ex(sizx,sizy,sizz), ey(sizx,sizy,sizz),
     -     ez(sizx,sizy,sizz), hx(sizx,sizy,sizz),
     -     hy(sizx,sizy,sizz), hz(sizx,sizy,sizz)
      real epsi(maxmat),my(maxmat),sigma(maxmat),c,eta,omega,pi,
     -     consta,constb,constc,cap,invepsi(maxmat),tdxdepsi(maxmat),
     -      efmatpar(maxmat)



      common /param/ maxx,maxy,maxz,maxbx,maxby,maxbz,
     -     minbx,minby,minbz,deltax,deltay,deltaz,
     -     deltat,freq
      common /h_fields/ hx, hy, hz
      common /e_fields/ ex, ey, ez
      common /matrix/ mat
      common /mat/ matno,epsi,my,sigma,invepsi,tdxdepsi,efmatpar
      common /zeroe/ zerox,zeroy,zeroz,nozex,nozey,nozez
      common /naturconst/ c,eta,omega,pi,consta,constb
```

C.8: maxwell.f

```
************************************************************************
* H and E field update.              * 2nd Generation FDTD Program     *
* E-field is updated via an entry    * Aalborg University, CPK         *
* statement.                         * Compiled by kvs 11-95           *
************************************************************************
* This source file is optimized for memory and speed on both single    *
* and multi-processor systems. 01-96 gfp & kvs.                        *
************************************************************************

       subroutine h_update
       implicit none
       include 'parameters.h'
       include 'maxwell.h'

*************************************************************
*initialization of the parameters of the lumped components

       real constlum1(lumax)
       real constlum2(lumax)
       real constlum3(lumax)
       real constr(lumax)
       real constr1(lumax)
       real constr2(lumax)
       real induef(lumax)


       do 1777 in = 1,lumax


       constlum1(in)=0
       constlum2(in)=0
       constlum3(in)=0
       constr(in)=0
       constr1(in)=0
       constr2(in)=0

 1777 continue




       do 1888 in = 1,lumax

       if(lumtype(in).eq.1)then
       constlum1(in)=1
       constlum2(in)=((deltax)/(2*c*(epsi(1)*deltax+lumimped(in))))
       else if(lumtype(in).eq.2)then

       constr(in)=1.0/(4*c*lumimped(in)*epsi(1))


       constlum1(in)=(1.0-constr(in))/(1.0+constr(in))
```

```
       constlum2(in)=1.0/(2*c*epsi(1)*(1+constr(in)))

       else if(lumtype(in).eq.3)then

       constlum1(in)=1.0/(2*c*epsi(1))
       constlum2(in)= -(deltax/(4*c*c*epsi(1)*lumimped(in)))

       else

       constlum3(in)=1

       end if

 1888 continue

*************************************************************



* H-FIELDS IS CALCULATED IN INTERIOR AT TIME N+1/2

end if

       do 100 k = 1,maxz-2
          do 100 j = 1,maxy-2
             do 100 i = 1,maxx-2
                hx(i,j,k)=hx(i,j,k) + consta*
     -              (ey(i+1,j,k+1)-ey(i+1,j,k)
     -              + ez(i+1,j,k)-ez(i+1,j+1,k))

                hy(i,j,k)=hy(i,j,k) + consta*
     -               (ez(i+1,j+1,k)-ez(i,j+1,k)
     -               + ex(i,j+1,k)-ex(i,j+1,k+1))

                hz(i,j,k)=hz(i,j,k) + consta*
     -               (ex(i,j+1,k+1)-ex(i,j,k+1)
     -               + ey(i,j,k+1)-ey(i+1,j,k+1))


 100  continue
* x1
      k=maxz-1
      do 200 j=1,maxy-1
         do 200 i=1,maxx-2
            hx(i,j,k)=hx(i,j,k) + consta*
     -           (ey(i+1,j,k+1)-ey(i+1,j,k)
     -           + ez(i+1,j,k)-ez(i+1,j+1,k))
 200        continue

* x2
      j=maxy-1
      do 250 k=1,maxz-2
         do 250 i=1,maxx-2
            hx(i,j,k)=hx(i,j,k) + consta*
     -           (ey(i+1,j,k+1)-ey(i+1,j,k)
     -           + ez(i+1,j,k)-ez(i+1,j+1,k))
```

```
 250        continue


* y1
      k=maxz-1
      do 300 j=1,maxy-2
         do 300 i=1,maxx-2
            hy(i,j,k)=hy(i,j,k) + consta*
     -           (ez(i+1,j+1,k)-ez(i,j+1,k)
     -           + ex(i,j+1,k)-ex(i,j+1,k+1))
 300        continue

* y2
      i=maxx-1
      do 350 k=1,maxz-1
         do 350 j=1,maxy-2
            hy(i,j,k)=hy(i,j,k) + consta*
     -           (ez(i+1,j+1,k)-ez(i,j+1,k)
     -           + ex(i,j+1,k)-ex(i,j+1,k+1))
 350        continue


* x1
      i=maxx-1
      do 400 k=1,maxz-2
         do 400 j=1,maxy-1
            hz(i,j,k)=hz(i,j,k) + consta*
     -           (ex(i,j+1,k+1)-ex(i,j,k+1)
     -           + ey(i,j,k+1)-ey(i+1,j,k+1))
 400     continue

* x2
      j=maxy-1
      do 450 k=1,maxz-2
         do 450 i=1,maxx-2
            hz(i,j,k)=hz(i,j,k) + consta*
     -           (ex(i,j+1,k+1)-ex(i,j,k+1)
     -           + ey(i,j,k+1)-ey(i+1,j,k+1))
 450        continue




         return



         entry e_update

****************************************
**lum=1 enable the lumped components ***
****************************************

         if(lum.eq.1)then
```

```
* E-FIELDS IS CALCULATED IN INTERIOR AT TIME N+1
*
* The following compiler directive is suited for a SGI PowerCHALLENGE
* multi-processor system.
*
*C$ DOACROSS share(maxz,maxy,maxx,ex,consta,mat,efmatpar,tdxdepsi,hz
*C$&  ,hy,ey,hx,ez) local(k,j,i,temp,temp1,temp2)
         do 500 k = 2,maxz-1
          do 500 j = 2,maxy-1
           do 500 i = 2,maxx-1
              temp=mat(i,j,k)
              temp1=tdxdepsi(temp)
              temp2=efmatpar(temp)



              do 1265 in = 1,lumax
        if(i.eq.lumx(in).and.j.eq.lumy(in).and.k.eq.lumz(in)
     -      .and.lumdir(in).eq.-1.and.lumtype(in).ne.3)then


              flag=.true.




          ex(i,j,k)= constlum1(in)*ex(i,j,k) +
     -       constlum2(in)*((hz(i,j,k-1)-hz(i,j-1,k-1))
     -             + (hy(i,j-1,k-1)-hy(i,j-1,k)))



        else if(i.eq.lumx(in).and.j.eq.lumy(in).and.k.eq.lumz(in)
     -     .and.lumdir(in).eq.-1.and.lumtype(in).eq.3)then
           induef(in)=induef(in)+ex(i,j,k)

                 ex(i,j,k)= ex(i,j,k) +
     -       constlum1(in)*((hz(i,j,k-1)-hz(i,j-1,k-1))
     -             + (hy(i,j-1,k-1)-hy(i,j-1,k)))+
     -             +  constlum2(in)*induef(in)

        flag=.true.

        end if

 1265 continue
```

```
      if(flag.eqv..false.)then

      ex(i,j,k)= temp2*ex(i,j,k) +
-       temp1*((hz(i,j,k-1)-hz(i,j-1,k-1))
-            + (hy(i,j-1,k-1)-hy(i,j-1,k)))

    else if(flag.eqv..true.)then
    flag=.false.

    end if




         do 1365 in = 1,lumax
    if(i.eq.lumx(in).and.j.eq.lumy(in).and.k.eq.lumz(in)
-      .and.lumdir(in).eq.0.and.lumtype(in).ne.3)then


         flag=.true.


      ey(i,j,k)= constlum1(in)*ey(i,j,k) +
-       constlum2(in)*((hx(i-1,j,k)-hx(i-1,j,k-1))
-          + (hz(i-1,j,k-1)-hz(i,j,k-1)))






   else if(i.eq.lumx(in).and.j.eq.lumy(in).and.k.eq.lumz(in)
-     .and.lumdir(in).eq.0.and.lumtype(in).eq.3)then



  induef(in)=induef(in)+ey(i,j,k)


       ey(i,j,k)= ey(i,j,k) +
-       constlum2(in)*((hx(i-1,j,k)-hx(i-1,j,k-1))
-          + (hz(i-1,j,k-1)-hz(i,j,k-1)))+
-           + constlum2(in)*induef(in)




       flag=.true.

       end if

1365 continue
```

```
    if(flag.eqv..false.)then



      ey(i,j,k)= temp2*ey(i,j,k) +
-       temp1*((hx(i-1,j,k)-hx(i-1,j,k-1))
-          + (hz(i-1,j,k-1)-hz(i,j,k-1)))


    else if(flag.eqv..true.)then
    flag=.false.

    end if




       do 1465 in = 1,lumax
  if(i.eq.lumx(in).and.j.eq.lumy(in).and.k.eq.lumz(in)
-      .and.lumdir(in).eq.1.and.lumtype(in).ne.3)then


         flag=.true.




      ez(i,j,k)= constlum1(in)*ez(i,j,k) +
-       constlum2(in)*((hy(i,j-1,k)-hy(i-1,j-1,k))
-          + (hx(i-1,j-1,k)-hx(i-1,j,k)))




    else if(i.eq.lumx(in).and.j.eq.lumy(in).and.k.eq.lumz(in)
-     .and.lumdir(in).eq.1.and.lumtype(in).eq.3)then

               induef(in)=induef(in)+ez(i,j,k)

             ez(i,j,k)= ez(i,j,k) +
-       constlum1(in)*((hy(i,j-1,k)-hy(i-1,j-1,k))
-          + (hx(i-1,j-1,k)-hx(i-1,j,k)))+
-            constlum2(in)*induef(in)
```

```
        flag=.true.

        end if

1465 continue




        if(flag.eqv..false.)then


          ez(i,j,k)= temp2*ez(i,j,k) +
     -       temp1*((hy(i,j-1,k)-hy(i-1,j-1,k))
     -          + (hx(i-1,j-1,k)-hx(i-1,j,k)))


        else if(flag.eqv..true.)then
        flag=.false.

        end if



500    continue


           do 600 k = 2,maxz-1
            do 600 j = 2,maxy-1
               temp=mat(1,j,k)
               temp1=tdxdepsi(temp)
               temp2=efmatpar(temp)

               ex(1,j,k)= temp2*ex(1,j,k) +
     -              temp1*((hz(1,j,k-1)-hz(1,j-1,k-1))
     -              + (hy(1,j-1,k-1)-hy(1,j-1,k)))


600  continue
           do 700 k = 2,maxz-1
            do 700 i = 2,maxx-1
               temp=mat(i,1,k)
               temp1=tdxdepsi(temp)
               temp2=efmatpar(temp)

               ey(i,1,k)= temp2*ey(i,1,k) +
     -               temp1*((hx(i-1,1,k)-hx(i-1,1,k-1))
     -               + (hz(i-1,1,k-1)-hz(i,1,k-1)))
```

```
 700  continue

            do 800 j = 2,maxy-1
             do 800 i = 2,maxx-1
                temp=mat(i,j,1)
                temp1=tdxdepsi(temp)
                temp2=efmatpar(temp)

                ez(i,j,1)=temp2*ez(i,j,1) +
     -               temp1*((hy(i,j-1,1)-hy(i-1,j-1,1))
     -               + (hx(i-1,j-1,1)-hx(i-1,j,1)))

 800  continue


      k=nozez*3-2
      do 900 tempint=1,k,3
         ez(zeroz(tempint),zeroz(tempint+1),zeroz(tempint+2))=0.
 900  continue

      j=nozey*3-2
      do 1000 tempint=1,j,3
         ey(zeroy(tempint),zeroy(tempint+1),zeroy(tempint+2))=0.
 1000  continue

      i=nozex*3-2
      do 1100 tempint=1,i,3
         ex(zerox(tempint),zerox(tempint+1),zerox(tempint+2))=0.
 1100  continue



       else

*  E-FIELDS IS CALCULATED IN INTERIOR AT TIME N+1
*
*  The following compiler directive is suited for a SGI PowerCHALLENGE
*  multi-processor system.
*
*C$ DOACROSS share(maxz,maxy,maxx,ex,consta,mat,efmatpar,tdxdepsi,hz
*C$&  ,hy,ey,hx,ez) local(k,j,i,temp,temp1,temp2)
         do 501 k = 2,maxz-1
          do 501 j = 2,maxy-1
           do 501 i = 2,maxx-1
              temp=mat(i,j,k)
              temp1=tdxdepsi(temp)
              temp2=efmatpar(temp)

           ex(i,j,k)= temp2*ex(i,j,k) +
     -       temp1*((hz(i,j,k-1)-hz(i,j-1,k-1))
     -             + (hy(i,j-1,k-1)-hy(i,j-1,k)))


           ey(i,j,k)= temp2*ey(i,j,k) +
     -       temp1*((hx(i-1,j,k)-hx(i-1,j,k-1))
     -          + (hz(i-1,j,k-1)-hz(i,j,k-1)))
```

```
           ez(i,j,k)= temp2*ez(i,j,k) +
     -       temp1*((hy(i,j-1,k)-hy(i-1,j-1,k))
     -          + (hx(i-1,j-1,k)-hx(i-1,j,k)))

501   continue

            do 601 k = 2,maxz-1
             do 601 j = 2,maxy-1
                temp=mat(1,j,k)
                temp1=tdxdepsi(temp)
                temp2=efmatpar(temp)

                ex(1,j,k)= temp2*ex(1,j,k) +
     -               temp1*((hz(1,j,k-1)-hz(1,j-1,k-1))
     -               + (hy(1,j-1,k-1)-hy(1,j-1,k)))

601  continue
            do 701 k = 2,maxz-1
             do 701 i = 2,maxx-1
                temp=mat(i,1,k)
                temp1=tdxdepsi(temp)
                temp2=efmatpar(temp)

                ey(i,1,k)= temp2*ey(i,1,k) +
     -                temp1*((hx(i-1,1,k)-hx(i-1,1,k-1))
     -                + (hz(i-1,1,k-1)-hz(i,1,k-1)))
701  continue

            do 801 j = 2,maxy-1
             do 801 i = 2,maxx-1
                temp=mat(i,j,1)
                temp1=tdxdepsi(temp)
                temp2=efmatpar(temp)

                ez(i,j,1)=temp2*ez(i,j,1) +
     -                temp1*((hy(i,j-1,1)-hy(i-1,j-1,1))
     -                + (hx(i-1,j-1,1)-hx(i-1,j,1)))
801  continue
     k=nozez*3-2
     do 901 tempint=1,k,3
        ez(zeroz(tempint),zeroz(tempint+1),zeroz(tempint+2))=0.
901  continue

     j=nozey*3-2
     do 1001 tempint=1,j,3
        ey(zeroy(tempint),zeroy(tempint+1),zeroy(tempint+2))=0.
1001 continue

     i=nozex*3-2
     do 1101 tempint=1,i,3
        ex(zerox(tempint),zerox(tempint+1),zerox(tempint+2))=0.
1101  continue

     end if
     return
     end
```

POST PHATA RESURGO